Induced Pluripotent Stem (iPS) Cells for Cell Replacement Therapy in Huntington's Disease (HD).

January 2015

Narawadee Choompoo

Supervisors

Prof. Anne E. Rosser

Dr. Claire M. Kelly

Dedicated to the memory of my beloved Mother,

For the endless love, inspiration, and belief.

DECLARATION

APPENDIX 1:
Specimen layout for Thesis Summary and Declaration/Statements page to be included in a Thesis

DECLARATION

This work has not been submitted in substance for any other degree or award at this or any other university or place of learning, nor is being submitted concurrently in candidature for any degree or other award.

Signed …… (candidate) Date ……

STATEMENT 1

This thesis is being submitted in partial fulfillment of the requirements for the degree of ……(insert MCh, MD, MPhil, PhD etc, as appropriate)

Signed …… (candidate) Date ……

STATEMENT 2

This thesis is the result of my own independent work/investigation, except where otherwise stated.
Other sources are acknowledged by explicit references. The views expressed are my own.

Signed …… (candidate) Date ……

STATEMENT 3

I hereby give consent for my thesis, if accepted, to be available online in the University's Open Access repository and for inter-library loan, and for the title and summary to be made available to outside organisations.

Signed …… (candidate) Date ……

STATEMENT 4: PREVIOUSLY APPROVED BAR ON ACCESS

I hereby give consent for my thesis, if accepted, to be available online in the University's Open Access repository and for inter-library loans **after expiry of a bar on access previously approved by the Academic Standards & Quality Committee.**

Signed …… (candidate) Date ……

Summary

The research presented in this thesis focuses on the differentiation of medium spiny neurons (MSNs) from iPS cells derived from human primary fetal cells with an aim to provide genuine DARPP32 positive MSNs for cell transplantation in Huntington's disease (HD). iPS cell lines were generated from various human embryonic tissues, with further neural induction, regional specification, and maturation using my modified protocol to directly differentiate the pluripotent stem cells (PSCs) towards a neural lineage, specifically lateral ganglionic eminence (LGE) precursors and eventually MSNs. Subsequent neuronal differentiation of LGE precursors or early post mitotic MSNs was assessed both *in vitro* and *in vivo*.

Chapter 3 focussed on an alternative approach to that used in chapter 3. Here the *piggyBac* transposon system was used. In this method 5 reprogramming factors were incorporated into the plasmid OSKML (Oct4, Sox2, Klf4, c-Myc, Lin28). As a result 5 iPS cell lines were successfully established from human embryonic primary whole ganglionic eminence (WGE) and fetal fibroblasts. It is noteworthy, that a reprogramming efficiency was 6-14 folds higher when using human WGE as a starting material in comparison to cortex tissue and fibroblast. In addition, more rapid kinetic in pluripotency conversion was recognised in human WGE which was 7-10 times faster in human WGE comparing to cortex and fibroblast. Various strategies were applied to investigate and characterize the pluripotency of the established iPS cell lines such as morphological appearance, *in vitro* differentiation, teratoma formation and RT-PCR of pluripotent gene expression.

Chapter 4 looked to take the cell lines generated in chapter 4 and take the cells through the process of neural differentiation and subsequent directed differentiation to generate DARPP32 positive MSNs. In this chapter the human ES cell line (H9) was introduced and used as a control for the iPS cell cultures. In the first instance, one iPS cell line (iPS WGE623 C9) was taken through neural differentiation, using EBs-based method with the Arber et al protocol (submitted). Unfortunately, this iPS cell line was unsuccessful at reaching a state of mature neuronal differentiation. As a result it was decided to modify the protocol, and the modified protocol was developed and used on the 5 iPS cell lines. In summary, 3 out of 5 iPS cell lines produced MSNs like cells confirmed by gene expression profile and immunocytochemistry against a hallmark of neural and MSNs markers, especially DARPP32 expression. 1 iPS cell line originating from human fibroblasts (iPS HEF 962) was unable to be terminally differentiated to DARPP32 expressing neurons due to unexpected infection occurring, however, it appeared to be differentiating towards a striatal MSNs phenotype as a similar pattern and LGE precursors were identified by FoxP1 and FoxP2 markers. Another iPS cell line (iPS WGE623 C9) was unable to fully differentiate to MSNs as pluripotent cells expressing Oct4 and Tra-1-60 were persistently appearing in culture. This may in fact be related to the method used, the *piggyBac* transposon

system as it would appear there are issues with complete removal of the transposons from the cells following reprogramming. Finally, the cells were validated *in vivo* following transplantation into a lesion induced rodent model of HD. iPS cell line WGE 928 and the human ES (H9) cell line were used in the transplantation studies. Surviving grafts were identified in
all animals receiving the iPS derived cell grafts; however, there were 7 out of 20 animals that exhibited tumour-like formation at 7 weeks post-surgery. In addition the H9 derived grafts had similar findings with 3 out of 6 animals presenting with tumour-like structures. However, when this protocol was applied to the H9 cell line using a monolayer based method, there was an absence of tumours in all transplanted animals post transplantation at 7 weeks.

Acknowledgements

Firstly, I would like to extend my sincere gratitude to Professor Anne E. Rosser for all your help, understanding and endless support throughout my PhD. Thank you for your encouragement, commitment and guidance directing me to do better research and improve my critical thinking. I really appreciate it.

Thank you for all members of the Brain Repair Group, past and present, for being such as great team. Especially a big thank you to the AER group; Anne, Rike, Claire, Sophie, Ngoc Nga, Amy, Vicky, Radha, and Susannah for your constant support and encouragement along the way. This thesis would not have been possible if it was not for the help and support of so many people.

Claire, I cannot thank you enough for your help and support. This thesis would not be possible without you. Thank you for pushing me toward the end and keeping me on track when everything seemed to go wrong.

A big thank you to the Thai Stem Cell Network, especially Bass and Tuempong, for all your invaluable suggestions and expertise. An enormous thanks to the stem cell networks and the many collaborations with scientists in various institutes (especially Sanger Institute and Centre of Stem Cells Biology, Sheffield) who make science move forwards.

To all my friends at home in Thailand and my friend who is sitting next to me helping to put this thesis together, Natta Borisoot. Thank you for being such a good friend since we met in high school. Good luck with your Masters.

To my father and sisters, I am nearly there. It won't be long. Thank you for your endless love and support. I could never thank you enough for all that you do for me.

Last but definitely not least, my beloved mother Nittaya Choompoo. My first teacher who taught me about life and gave me a lesson on how much family means. Sorry to keep you waiting for so long. But no worry, I will live a full life not only for me but for you too. Whenever we meet again, I will have an interesting life to share with you. See you when I see you.

Abbreviations

AP	Alkaline phosphatase
A/P	Anterior-posterior
AFP	Alpha Feto Protein
BDNF	Brain-derived neurotrophic factor
BFCNs	Basal forebrain cholinergic neurons
BMP	Bone morphogenetic protein
BrdU	Bromodeoxyuridine
BRG	Brain repair group
BSA	Bovine serum albumin
cAMP	Cyclic adenosine monophosphate
CDM	Chemically defined medium
CNS	Central nervous system
CPP	Cell penetrating protein
Cpu	Caudate-Putamen
CRL	Crown Rump Length
CsA	Cyclosporin A
CTIP2	COUP TF1-interacting protein 2
CTX	Cortex
DA	Dopamine
DAB	Diaminobenzidine
DARPP-32	Dopamine and adenosine 3’ 5’- monophosphate regulated phosphprotein
DCX	Doublecortin
DKK-1	Dickkopf-related protein 1
DMEM	Dulbecco’s Modified Eagle’s Medium
DMSO	Dimethyl sulfoxide
DNase	Deoxyribonuclease
DP	Dorsal pallium
D/V	Dorsal/Ventral
E	Embryonic day
E. coli	*Escherichia coli*
EBs	Embryoid body
EDTA	Ethylene diamine tetra acetic acid
EGF	Epidermal growth factor
ES	Embryonic stem cell

FACs	Fluorescence activated cell sorting
FBS	Foetal Bovine serum
FGF	Fibroblast growth factor
FIAU	1-2'-deoxy-2'-fluoro-ß-D-arabinofuranosyl-5-iodouracil
GABA	Gamma-amino butyric acid
GABAergic In.	GABAergic interneurons
GAD	Glutamate decarboxylase
GDNF	Glial cell derived neurotrophic factor
GFAP	Glial fibrillary acidic protein
Glut. N.	Glutametegic neurons
GMP	Good manufacturing practice
GP	Globus pallidus
GPe	Globus Pallidus (external segment)
GPi	Globus Pallidus (internal segment)
GSH2	Glutathione synthetase
HBSS	Hanks buffered saline solution
HDAC	Histone deacetylase
HD	Huntington's disease
HEF	Human embryonic fibroblasts
HPs	Hematopoietic progenitors
HTT	Huntingtin
ICM	Inner cell mass
IGF	Insulin-like growth factor
i.p.	Intra-peritonal
iPS	Induced pluripotent stem
KSR	'Knock-out' serum replacement
LGE	Lateral ganglionic eminence
LIF	Leukaemia inhibitory factor
LP	Lateral pallium
MAP2	Microtubule-associated protein 2
mDA	Midbrain dopaminergic neurons
MEF	Mouse embryonic fibroblasts
MEM	Non-essential amino acids
MGE	Medial ganglionic eminence
MNs	Motor neurons
MP	Medial pallium
MSNs	Medium-sized spiny neurons

NE	Neuroepithelial cells
NEAA	Non-essential amino acid
NEPs	Neural epithelial cells
NeuN	Neuronal nuclei
NGS	Normal Goat Serum
NI	Neural induction
NPC	Neural precursor cells
NSCs	Neural stem cells
P	Passage
PBS	Phosphate Buffered Saline
PGCs	Primordial germ cells
PD	Parkinson's disease
PFA	Paraformaldehyde
PLL	Poly-L-lysine
PNS	Peripheral nervous system
POL	Poly-L-Ornithine
PS	Penicillin/Streptomycin
PSCs	Pluripotent stem cells
QA	Quinolinic acid
Q-PCR	Semi-quantitative RT-PCR
RA	Retinoic acid
RG	Radial glia
R-NSCs	Rosette neural stem cells
RT-PCR	Reverse transcription polymerase chain reaction
SCNT	Somatic cell nuclear transfer
SEM	Standard error of the mean
Se V	Sendai virus
SHH	Sonic hedgehog
SN	Substantia nigra
STN	Subthalamic nucleus
SVZ	Sub-ventricular zone
SWIFT	South Wales initiative for Fetal Transplantation
TBS	TRIS buffered saline
TH	Tyrosine hydroxylase
TNS	TRIS non-saline
TRIS	Trizma base
TS-Se V	Temperature-sensitive Sendai virus

TTFs	Tail tip fibroblasts
TX-TBS	Triton X-100 TBS
VM	Ventral mesencephalon
VZ	Ventricular zone
WGE	Whole ganglionic eminence
Wnt	Wingless
ZO-1	Zonula occludens-1

Contents

Table of figures

Chapter 4: Human iPS cell derived GABAergic MSNs-liked cells using EBs-Based Method.

Appendix A: Neural induction Monolayer-Based Method

Table of tables

Chapter 1

Introduction

1.1 Pluripotent Stem Cells

The study of pluripotent stem cells contributes to a broader understanding of cell development and differentiation, and presents many opportunities for medical science, such as cell transplantation for degenerative diseases, drug screening and drug toxicology.

1.1.1 Embryonal Carcinoma cells

Embryonal carcinoma (EC) cells were first identified in the 1950s in the mouse through the study of teratocarcinoma (Stevens L.C. and Little C.C, 1954). This cancer comprises both undifferentiated and differentiated cells of the three germ layers: endoderm, mesoderm, and ectoderm (Kleinsmith and Pierce, 1964). The pluripotent properties of EC cells and their capacity for (at least theoretically) unlimited self-renewal were presented in 1964 (Kleinsmith and Pierce, 1964). In the 1970s, mouse EC cell lines were first produced for use in scientific study, such as developmental characterisation (Kahan and Ephrussi, 1970). It was reported that some EC cells can generate a wide range of somatic cells (Brainster, 1974), although in the same year Atkin et al 1974, reported that they have a limited developmental potential due to the genetic alterations arising during the development of the teratocarcinoma (Atkin et al, 1974). EC cells show some similarities of protein and antigen expression with those cells of the inner cell mass (ICM) (Gachelin et al., 1977; Solter et al., 1978). A human EC cell line was successfully produced in 1977 (Hogan et al, 1977), but these cells had a restricted differentiation potential largely due to their aneuploid nature, thus limiting their usefulness as an in vitro model of human development. Hence, the usefulness of EC cells as a possible cell source for therapeutic application is limited.

1.1.2 Embryonic germ cells

Mouse embryonic germ (EG) cells were first generated from primordial germ cells (PGCs) in 1992 (Matsui et al, 1992; Resnick et al, 1992). EG cells expressed some of the same markers as ES cells (such as SSEA1 and 3, Oct4) and are morphologically indistinguishable from ES cells in culture (Matsui et al., 1992; Resnick et al., 1992). In addition, chimeras could be generated when EG cells were injected into blastocysts (Labosky et al., 1994; Stewart et al., 1994). However, EG cells still retain some characteristics of primordial germ cells (PGCs) and have genetic alterations which likely reflect the developmental stage at which they were originally taken (Labosky et al, 1994; Tada et al, 1997). The derivation of human EG cells was first reported in 1998 (Shamblott et al., 1998), but human EG cell applications have been restricted by their limited long-term proliferative capacity (Turnpenny et al, 2003). To date, no stable EG cell line has been reported to generate teratomas with differentiation into all three germ lines (reviewed in Yu and Thomson, 2008).

1.1.3 Embryonic stem cells

In 1970, Stevens and Solter showed that transferring early mouse embryos to the adult mouse kidney or testicular capsule lead to development of teratocarcinomas (Stevens L.C., 1970; Solter et al., 1970), demonstrating the pluripotent capacity of some cells of the embryo, and thus advancing attempts to produce pluripotent cells in vitro. Embryonic stem (ES) cells are generated from the ICM of the blastocyst and can give rise to trophectoderm and all three layers of the embryo (Evans and Kaufman, 1981; Martin 1981) avoiding the need to develop carcinomas as seen with EC cells. ES cells have the ability to proliferate extensively whilst maintaining their pluripotency (Martin, 1981). The first mouse ES cell line was derived in 1981, using the same culture medium as that used for mouse EC cells (Evans and Kaufman, 1981; Martin 1981). ES cells are able to differentiate into all cell types of the three germ layers - ectoderm, mesoderm, and endoderm in vitro and when transplanted, are capable of germline transmission to generate chimeric animals, which is in contrast to EC cells (Bradley et al, 1984). Thus, ES cells can be used to generate models of disease and to understand developmental pathways by introducing modifications into the mouse germline. Initially, a feeder cell layer (mouse embryonic fibroblast, MEFs) was used to

culture ES cells, but over time there has been a move away from this method to a feeder free system that is more adaptable for clinical application (specifically for GMP (good manufacturing practice) manufacture of these cells). As well as the feeder system there have been many modifications to the culture system as a whole with, for example, changes to the culture media where this has been replaced by medium taken from co-culture with other cells that will nourish the ES cells (Smith et al, 1988; Williams et al, 1988). Different ES cell lines are cultured optimally under different conditions with adaptations to the feeder layer, substrate, and culture medium.

Human ES cells were first derived in 1998, originally using the previously reported mouse ES cell co-culture medium and MEFs (Thomson et al, 1998), and were also shown to have the potential to differentiate into cells of all three germ layers (Amit et al, 2000). However, the conditions used for optimal culture of mouse and human ES cells are different in that human ES cells do not survive in leukemia inhibitory factor (LIF)-containing media, a prerequisite for mouse ES cell culture (Daheron et al, 2004; Humphrey et al, 2004). In addition, mouse and human ES cells require different feeder cells or substrates for culture, and the human ES cells are more susceptible to cell death during dissociation procedures (Daheron et al, 2004; Humphrey et al, 2004). Human ES cells have been adapted over time to feeder free GMP grade cell lines. ES cells offer a potentially unlimited supply of cells for use in transplantation, drug screening, and generation of disease models. However, use of ES cells is associated with a number of ethical and moral issues, and there is also an issue of immune rejection following transplantation. These are both important barriers to the use of ES cells as a cell source for study and for regenerative medicine applications, and thus it is important to continue to explore other cell sources that may circumvent these problems (Figure 1.1).

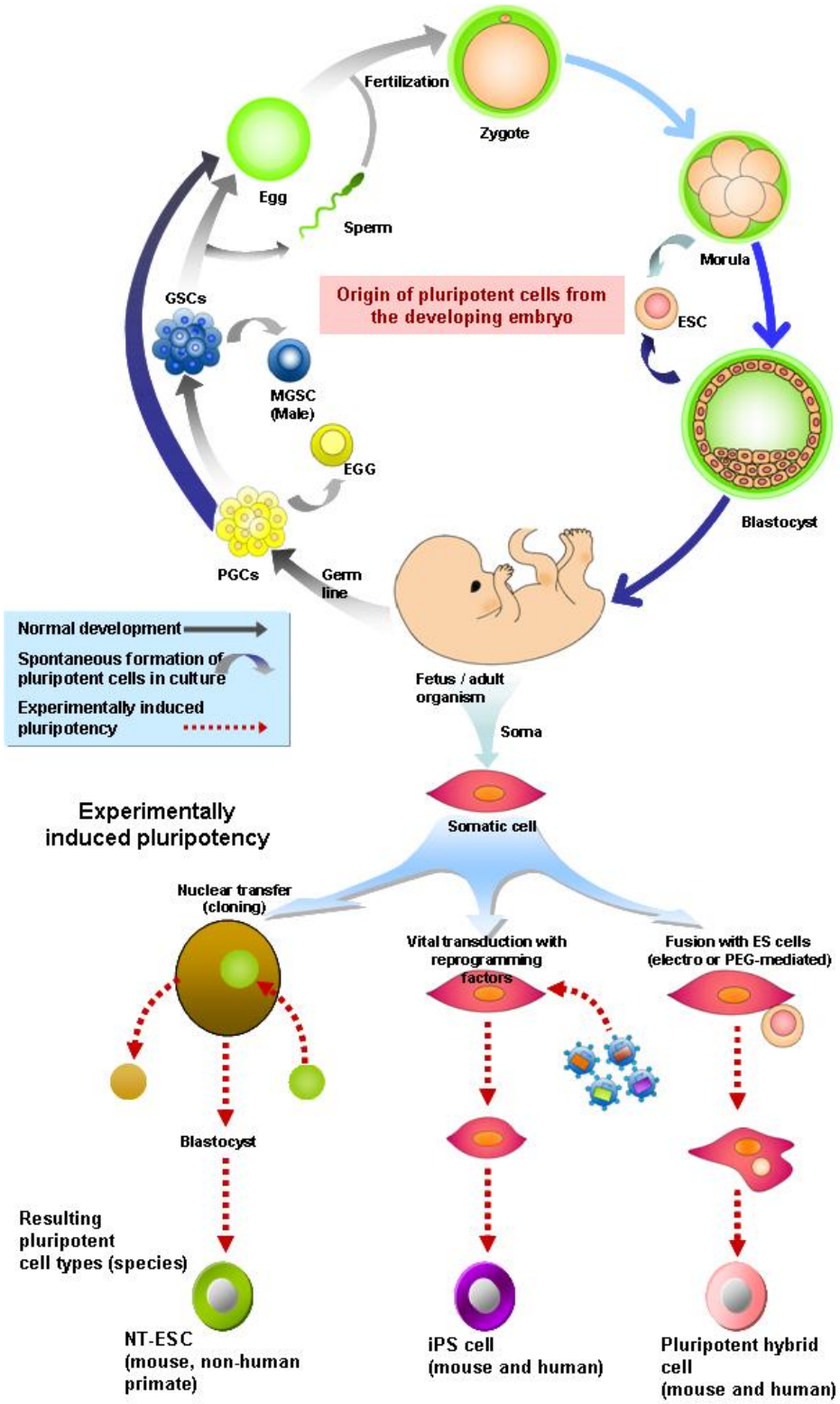

Figure 1.1 Schematic of the origin of pluripotent cells from the developing embryo; three reprogramming strategies for induced pluripotent cells. (Adapted from Christopher Lengner and Rudolf Jaenisch, 2008)

1.1.4 Induced pluripotent stem (iPS) cells

One aim of generating pluripotent stem cells from adult somatic cells is to produce donor cells for transplantation that have the potential to circumvent the supply and demand problems of human fetal cells and the ethical and immunological issues associated with both human fetal and human ES cells. Miller and co-workers used a cell-cell fusion technique to generate pluripotent cells between thymus and EC cells, which resulted in cells that could generate teratocarcinomas in syngeneic mice (Miller et al., 1976). Furthermore, the largely successful work by Ian Wilmut to clone 'Dolly the sheep' in 1997, changed the prospect for developmental studies (Wilmut et al., 1997). This experiment ignited the idea of using somatic cell nuclear transfer (SCNT) as a method for generation of pluripotent stem cells (Wilmut et al., 1997). In addition, however, SCNT and cell-cell fusion techniques did not clarify the essential factors needed for somatic cell reprogramming (reviewed in Yu and Thomson, 2008).

1.1.4.1 Generation of mouse induced pluripotent stem (iPS) cells

Induced pluripotent stem cells were first described in 2006 by Yamanaka's group (Takahashi and Yamanaka, 2006). By introducing four exogenous transcription factors in a retrovirus to differentiated cells and nurturing those cells in an embryonic environment, they were able to directly reprogram them to pluripotent cells. Yamanaka and Takahashi reported that 24 genes are involved in reprogramming mouse somatic cells to cells which are similar in appearance to mouse ES cells. The potential inducing pluripotent factors were divided into three categories. The first division composed of the transcription agents that are highly expressed in ES cells such as Oct4, Nanog, UTF1, Sall4, Sox15, Rex1 and Sox2. The second category comprised of genes having a key role in ES cells and related to tumour generation for example c-Myc, Klf4, β-catenin, Grb2, TCL1, ERas and Stat3. The final group was the factors particularly expressed in ES cells such as ECAT1, Fbx15, ESG1, DNMT3L, ECAT8, ECAT15-1, ECAT15-2, Fthl17, Stella, and GDF3; however, the function of the third group of factors remains unclear (Takahashi and Yamanaka, 2006). From a series of combinations they concluded that the four factors-- Oct4, Sox2, c-Myc, and Klf4, which are present in high levels

in ES cells, are sufficient to transform mouse fibroblasts into cells which mimic ES cells. (See Figure 1.2).

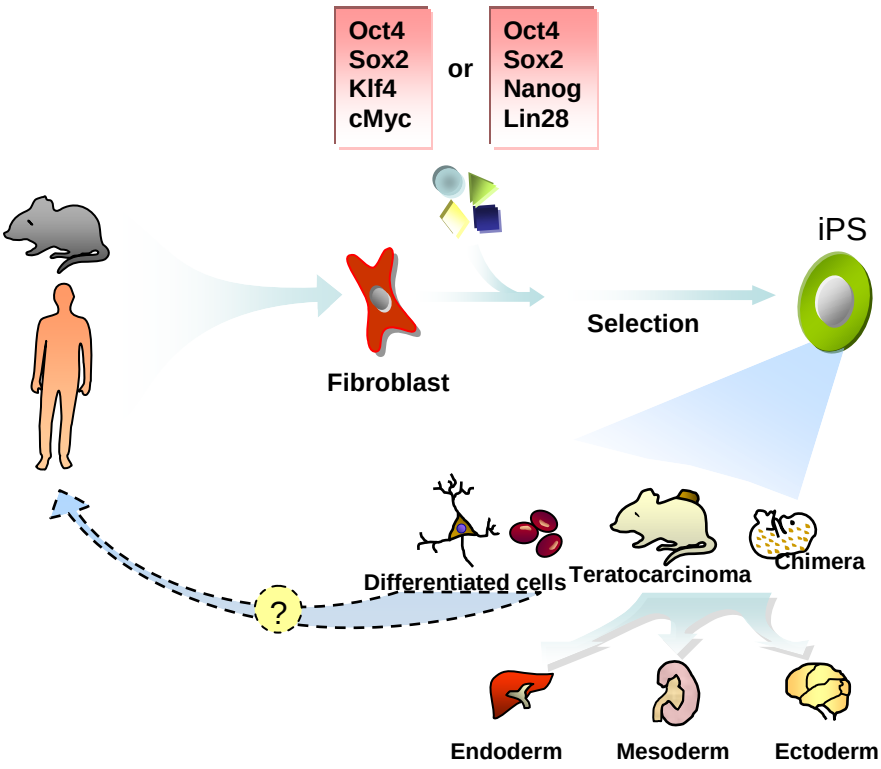

Figure 1.2 Schematic demonstrates direct reprogramming mouse and human fibroblasts to iPS cells with five defined factors Oct4, Sox2, Klf4, c-Myc, and Lin28. After selection, iPS cells are derived. These cells could differentiate into all cell types within three germ layers as assayed by teratoma formation and developmental contribution. (Adapted from Welstead Grant et al., 2008)

Subsequently, there have been many reports strengthening this finding (Maherali et al., 2007; Meissner et al., 2007; Okita et al. 2007; Takahashi et al., 2007; Wernig et al., 2007; Yu et al., 2007; Wernig et al., 2008; Nakagawa et al., 2008; Stadfeld et al., 2008; Yamanaka et al., 2008; Brambrink et al., 2008; Woltein et al., 2009; Kaji et al., 2009).

Interestingly, mouse iPS cells derived by the Yamanaka group, in which Fbx15 was used as a selection marker, were unable to generate germline cells in chimeras, even though they were otherwise found to present the same characteristics as mouse ES cells (Takahashi and Yamanaka, 2006). Global gene expression was used to distinguish the pattern between the Fbx15-derived iPS cells and mouse ES cells; it demonstrated that the promoter areas of Oct4 and Nanog still remain methylated in the resulting iPS cells (Takahashi and Yamanaka, 2006). Yamanaka and Takahashi mentioned that Oct4 and Sox2 play an important role in determining a cells destination, either to a tumour cell or resembling an ES cell (Takahashi and Yamanaka, 2006), whereas, c-Myc

facilitates Oct4 and Sox2 by unwinding its chromatin structure (Knoepfler et al., 2006), thus paving the way for both transcription factors to bind to their target gene (Nakatake et al., 2006).

Many previous studies, suggested that disturbance of Nanog expression leads to loss of pluripotency, thus deriving an endoderm cell line, for example Mitsui et al., 2003, and Silva (2006) found that Nanog helps to enhance somatic cell reprogramming in the cell-cell fusion method. Thus, much pointed to Nanog as a selective marker for the derivation of iPS cells. Selecting iPS cells based upon their ability to reactivate Oct4 and Nanog promoters resulted in iPS cells that more closely resembled mouse ES cells with respect to epigenetic status and gene expression; and the ability to produce all three germ lines in adult chimeric mice (Maherali et al., 2007; Okita et al., 2007; Wernig et al., 2007). In addition, compared to Fbx15 iPS cells, Nanog iPS cells could maintain stable ES cell markers expression for prolonged periods in culture (Okita et al., 2007). Moreover, Nanog expressing mouse iPS cells presented the same pattern of gene expression as mouse ES cells in response to LIF and retinoic acid compared to Fbx15 iPS cells (Okita et al., 2007), which were dissimilar in gene expression profile under the same conditions. However, one consideration that needs to be made is with respect to the use of c-Myc, as it was reported that iPS cells generated under the same conditions as those described above resulted in tumour formation in mouse chimeric pups (20% of pups presented with tumours) (Okita, 2007).

Wernig (2007) also generated iPS cells using four defined factors with retroviral vector delivery to reprogram MEFs and tail-tip fibroblast (TTFs). Oct4 or Nanog were used as selective markers to pick the reprogrammed colonies. The Oct4- and Nanog- iPS cells demonstrated similar epigenetic status, and protein levels of Oct4, Sox2, and Nanog were the same as ES cells. Moreover, these reprogrammed pluripotent stem cells could produce teratocarcinomas as well as all three germlines in chimaeras (Wernig et al., 2007). Wernig and colleagues reported that the pluripotent property strictly associated with the activity of the Oct4 locus, rather than the Nanog- locus. A major hope is that iPS cell technology will allow transplantation therapy using patients' somatic cells as an individual resource, to circumvent ethical and immune rejection issues. In an effort to overcome this, Sommer and colleagues introduced a lentiviral vector with

transduction of 4 defined-reprogramming factors as a transgene set 'STEMCCA' (Sommer et al., 2009). They claimed that with this transfection method only 1-3 copies of the viral vector would be integrated into the host genome, compared to at least 15 copies with a similar method using a retrovirus reported by Takahashi and Wernig in 2007. Sommer suggested that this novel method produced higher reprogramming efficiency (0.5%) compared to the relatively low efficiency (0.1%) reported in the previous studies as well as avoiding genomic alteration and viral reactivation (Sommer et al., 2009; Takahashi et al., 2007; Okita et al., 2007, Wernig et al., 2007). (See Table 1.1 for summary of mouse iPS cell generation).

1.1.4.2 Generation of human induced pluripotent stem cells

Takahasi et al in 2007 reported the generation of human iPS cells using the same cocktail of transcription factors as used in the murine studies (Takahashi et al., 2007) and following from this Yu et al also reported successful iPS cell generation however, in this instance there was a modification to the transcription factor cocktail used with Klf4 and c-Myc being substituted with Nanog and Lin8 (Yu et al., 2007). Following on from this Park et al reported the successful generation of human iPS cells from various origins (differentiated-, neonatal-, primary foetal-, and adult- fibroblasts) using retroviral infection method, and selecting ES cell like colonies by morphological appearance (Park et al., 2008). Oct4 and Sox2 were essential to initiate the reprogramming process; without the expression of both transcription factors, iPS colonies were unable to be generated (Yu et al., 2007; Park et al., 2008), while either Klf4 or c-Myc elimination led to a decrease in the number of ES cell-like colonies as previously presented in mouse iPS cell production (Wernig et al., 2008; Nakagawa et al., 2008; Stadtfeld et al., 2008).

Therefore, it could be said that three factors are sufficient to reprogram somatic cells to pluripotent cells (Park et al., 2008). The iPS cells produced from Park's lab showed pluripotent properties in both *in vivo* and *in vitro* studies, for example expressing human ES cell surface markers (SSEA3, SSEA4, TRA-1-81, and TRA-1-60), showing pluripotent gene expression comparable to human ES cells (Oct4, Sox2, Rex1, GDF3), generating teratomas with all three germ lines in nude mice, and displaying similar epigenetic pattern as in human ES cells (Park et al., 2007). More mature differentiated cells, such as mesenchymal stem cells,

neonatal foreskin fibroblasts, and adult fibroblasts, require the addition of more factors (hTRAT and SV40 large T) in order to obtain reprogrammed-cell colonies (Park et al., 2008). However, Park reported that both hTRAT and SV40 large T gene expression were undetectable; therefore his explanation of this event is that hTRAT and SV40 large T are nothing to do with reprogramming initiation but help to improve the efficiency of iPS cell generation (Park et al., 2008).

At the same time, Yu also derived $CD45^+$ hematopoietic cells, IMR90 fetal fibroblasts, and human foreskin fibroblasts through the application of different factors (Oct4, Sox2, Nanog, and LIN28) using lentiviral vectors (Yu et al., 2007). The iPS cells obtained from 3 different origins met the pluripotent standard of ES cells; for example a morphological appearance similar to ES cells, genes- and typical cell surface marker expression comparable to human ES cells, and teratoma and Embryoid body (EB) production (Yu et al., 2007). However, foreskin iPS cells showed variable teratoma production specifically in terms of the germline differentiation within the teratoma with some clones producing more ectoderm than others (Yu et al., 2007). Again Oct4 and Sox2 were mentioned as crucial factors for reprogramming, while Nanog and Lin28 may help to improve the efficiency and frequency of direct reprogramming mechanisms (Yu et al., 2007; Park et al., 2007).

One year later, human iPS cells were successfully reprogrammed with three factors in the absence of c-Myc (Nakagawa et al., 2008). As mentioned above c-myc brought about high rates of tumerogenicity in descendants caused by reactivation of this gene (Okita et al., 2007, Yu et al., 2007).

However, the efficiency of clone generation from human dermal fibroblasts was lower with c-Myc omission, at 0.001% (Nakagawa et al., 2008). The iPS cells produced in this study showed a similarity with human ES cells in terms of cell morphology, specific cell surface markers (SSEA3,4, TRA-1-60,-80, Nanog), gene expression (Oct4, Sox2, Nanog, Rex1), teratoma and chimera production (Nakagawa et al., 2008). Thus, it was recognized that additional molecules were needed in order to improve the efficiency. In the meantime, Lowry performed a transduction experiment using 5 reprogramming genes Oct 4, Sox2, Klf4, Lin28 and Nanog (OSKLN) in a retroviral vector in order to transform human neonatal dermal fibroblasts to a pluripotent state (Lowry et al., 2008). The colonies emerged around day 14, but gene expression analysis showed them to be partially

reprogrammed, and they failed to generate EBs. However, after day 21, ES cell like-colonies were identified, that expressed a full range of pluripotent genes, and generated cells from all three embryo germ layers (See Table 1.2).

Table 1.1 Mouse iPS cells generation.

Studies	Cell source	Factors	Methods	Finding
Takahashi and Yamanaka, 2006	-Mouse Embryonic fibroblast	Oct4, Sox2, c-Myc, Klf4	- Retrovirus-mediated transfection - Fbx15 selection marker	- similar morphology, proliferation as ES cells - cannot contribute to adult chimeric mice - different DNA methylation pattern and gene expression to ES cells
Okita et al, 2007	-Mouse Embryonic fibroblast	Oct4, Sox2, c-Myc, Klf4	- Retrovirus-mediated transfection - Nanog selection marker - mutant c-Myc (T58A) - GFP-TRES-PURO cassette	- similar morphology, proliferation and gene expression as ES cells - tumours formation with 3 germ lines - efficiency less than 0.1% - 20% tumour development in offspring
Wernig et al, 2007	-Mouse Embryonic fibroblast - Tail tip fibroblast (TTFs)	Oct4, Sox2, c-Myc, Klf4	- Moloney-based retroviral vector pLIB - Nanog or Oct4 selection marker - Oct4-IRES-GFPneo or Nanog-neo	- normal Oct4, Sox2, Nanog RNA and protein levels - epigeneticly identical to ES cells - able to generate viable chimeras with 3 germ lines
Meissner et al, 2007	-Mouse Embryonic Fibroblast -TTFs	Oct4, Sox2, c-Myc, Klf4	- MEFs carried IRES-EGFP at Oct4 loci - retrovirus encoded four factors - Morphological selection by directly picking the colony or whole plate passaging	- Could generate adult chimeras and teratomas when injected into nude mice - Efficiency: overall efficiency is about 0.5% - Reprogramming is a slow and gradual process
Okita et al, 2008	-Mouse embryonic fibroblast	Oct4, Sox2, c-Myc, Klf4	- an adenovirus mediated gene system - pcCX-OKS-2A and pCX-cMyc	- generate teratoma with 3 germ layers when transplant to nude mice - produce adult chimeric mice - similar morphology, proliferation and gene expression as ES cells - the efficiency is lower than transduction with viral vector methods - Southern blot: no plasmid DNA integration was observed
Nakagawa et al, 2008	-Mouse Embryonic fibroblast -TTFs - Human fibroblast	4 factors and 3 factors without c-Myc	- GFP-IRES-Puro - Nanog selection marker - Fbx15 with βgeo - DsRed retrovirus	- day 14 and 21 GFP+ colonies - ES cell-like marker genes - produce adult chimeric mice - significantly reduced tumourigenic risk - less efficient, but more specific induction of iPS cells

Studies	Cell source	Factors	Methods	Finding
Mikkelsen et al, 2008	-Mouse embryonic fibroblast - B lymphocyte	Oct4, Sox2, c-Myc, Klf4	-inducible lentiviral vectors with Nanog-GFP	- similar morphology, proliferation and gene expression as ES cells - pluripotentiality of iPS cells line was shown by teratoma formation
Brambrink et al, 2008	-Mouse embryonic fibroblast	Oct4, Sox2, Klf4, c-Myc	- doxycycline (dox)-inducible lentiviral vector	- need at least 12 days to see the iPS cell colonies
Wernig et al, 2008	-Mouse embryonic fibroblast	4 factors and 3 factors without c-Myc	- Retroviral vector - Oct4 neo and Nanog neo mice	- reprogramming process was substantially delayed -produce chimeric mice and tumours with 3 germ lines - morphologically and functionally the same as 4 factors iPS cells
Stadtfeld et al, 2008	- Oct^{IND} mouse TTFs - Oct^{IND} hepatocytes - Oct^{IND} fetal liver cells	3 factors Sox2, Klf4, and c-Myc	- adenovirus transduction - using $OCT4^{IND}$ instead of Oct4 viral expression	- **Oct^{IND} fetal liver cells:** at 24-30 days 9 iPS cells like colonies recognized expressing Sox2, SSEA-1 - **Oct^{IND} TTFs**: a single colony - **Oct^{IND} Hepatocytes:** 3 colonies which expressed Oct4, SSEA-1, indistinguishable from ES cell markers - form teratomas with all three germ layers - able to generate adult chimeras - efficiency was extremely low: less than 0.0001%-0.001%
Stadtfeld et al, 2008	-Mouse embryonic fibroblast	Oct4, Sox2, Klf4, c-Myc	-inducible vectors	- show pluripotent properties and could generate chimeras - 0.016% efficiency when introduced to exogenous factors for 8-9 days - 0.06% efficiency when exposed to pluripotent transcription factors for more than 10 days - inducing reprogramming using pluripotent transcription factors is gradual processes
Eminli et al, 2008	-Mouse neural progenitor cells (NPCs)	3 factors Oct4, Klf4, and c-Myc	- Lentiviral vector	- the reprogramming efficiency is about 28% - in the human experiment, similar results were obtained

Studies	Cell source	Factors	Methods	Finding
Kaji et al, 2009	-Mouse and human embryonic fibroblast	Oct4, Sox2, c-Myc, Klf4	- a single multiprotein expression vector (pCAG2LMKOSimO) - pCAG2LMKOSimO with a *piggyBac transposon*	- similar morphology, proliferation and gene expression as ES cells - tumour development comprising 3 germ layers - able to generate adult chimeric mouse
Woltjen et al, 2009	- Mouse and human embryonic fibroblast	Oct4, Klf4, Sox2, c-Myc	- *piggyBac transposon* deliver doxycycline transcription factors - rtTA –MEFs	- contribute to teratoma with 3 embryonic germ layers - could generate adult chimeras - expressed pluripotent cells markers at a similar level to ES cells - PB insertion could be removed from iPS cells by seamless excision
Sommer et al, 2009	-TTFs	OSKM as 'STEMCCA' cassette	- Lentivirus with 4 definded factors - GFP –R26-M2rtTA in Sox2 loci	- at day 6 (with EFI promoter), morphology similar to ES cells; day 6-8 (with TetO promoter) no colony in an absences of doxycycline - can generate teratoma formation with all germ layears - the reprogramming efficiency is 0.5% (10-fold higher than the similar method previously reported)

OSKM = Oct4, Sox2, Klf4, c-Myc; $OCT4^{IND}$ = a doxycycline-inducible Oct4 allele driven by a reverse-tetracycline–dependent transactivator (rtTA) present in the ROSA26 locus; rtTA= a reverse-tetracycline–dependent transactivator; hES= human ES

Table 1.2 Human iPS cells generation.

Studies	Cell source	Factors	Methods	Finding
Takahashi et al, 2007	-Adult human dermal fibroblast	Oct4, Sox2, c-Myc, Klf4	- Retroviral deliver system	-morphology, proliferation, surface antigens, gene expression, epigenetic status and telomerase activity similar to human ES cell -*in vitro* and *in vivo* differentiation to all 3 germ layers
Yu et al, 2007	- Derived $CD45^+$ hematopoietic cells - IMR90 fetal fibroblast - Human newborn foreskin fibroblast	Oct4, Sox2, Nanog, LIN28	- Gentamicin selection for derived $CD45^+$ hematopoietic cells - Morphology selection for IMR90 fetal fibroblasts - Lentiviral vectors transduction	- all resulting iPS cells from different sources had ES cell characteristics,,telomerase re-activation, pluripotent markers (SSEA3, SSEA4, Tra-1-80, Tra-1-60), and epigenetic profile - generated teratomas with all three germ layers in adult mice - iPS cells differentiated from foreskin showed variations in teratoma formations
Nakagawa et al, 2008	- Human dermal fibroblast	3 factors Oct4, Sox2, Klf4	- Retroviral deliver system	- iPS cells were similar to hES cells in terms of cell morphology, cell surface markers (SSEA3,4, TRA-1-60,-80, Nanog), gene expression (Oct4, Sox2, Nanog, Rex1), teratomas and chimera production
Huangfu et al, 2008	- Primary human fibroblast: BJ and NHDF	3 factors Oct4, Sox2, Klf4 and VPA treatment	Molony murine leukemia retrovirus transduction - ES cells like forms selective method	- after 30 days, reprogrammed colonies - morphology, gene expression, epigenetic profile, and pluripotent properties were comparable to human ES cells
Kim et al, 2009	- Human fibroblast	Oct4, Klf4, Sox2, and c-Myc	Cell penetrating peptide (CPP) with 9 arginine residing amino acid	- protein induced iPS cells with pluripotent, morphology, gene expression, pluripotent specific markers. - epigenetic status comparable to hES cells - Efficiency was low - 0.001% of input cells - slow method

Studies	Cell source	Factors	Methods	Finding
Kim JB et al, 2009	- Human fetal neural stem cells	1 factor: Oct4	Retroviral transduction	- iPS cells resembled ES cells in terms of morphology, genes and pluripotent cell surface marker expression, epigenetic patterns - generated teratomas and adult chimeras - the efficiency is about 0.004%
Zhou et al, 2009	- Human embryonic fibroblast (IMR90)	Oct4, Klf4, Sox2, and c-Myc	Adenoviral deliver system	- efficiency very low 0.0002% - morphology and pluripotent features similar to ES cells - an absence of vector genome detection
Yu et al, 2009	- Human foreskin fibroblasts	4 factors: Oct4, Sox2, Nanog, Lin28 -6 factors: add c-Myc, and Klf4 -6 factors: add Klf4, SV40LT	Non integrating episomal vectors Orip/EBNA1 - IRES co-expressed with reprogramming factors - vectors could be removed using drug selection	- iPS cells revealed hES cell like morphological appearance, gene expression profiles, epigenetic status, teratomas formation with all three germ lines - four factors: efficiency 0.1% - added c-Myc and Klf4: efficiency 1% - free from transgenes and vectors DNA integration - reprogramming does not require chromosomal integration or continuous expression of exogenous pluripotent factors
Fusaki et al, 2009	- Human fibroblasts	4 factors: Oct4, Sox2, Klf4, c-Myc	Sendai virus	- ES like morphology - *in vivo* and *in vitro* differentiation demonstrated 3 germ layers - Oct4 and Nanog promoters were demethylated
Warren et al, 2010	- Human epidermal keratinocytes and murine embryonic fibroblasts	4 factors: Oct4, Sox2, Klf4, c-Myc; -5 factors: Oct4, Sox2, Klf4, c-Myc, Lin28 In low-oxygen condition (5% O_2)	Synthetic mRNA modified	- ES like morphology - *in vivo* and *in vitro* differentiation demonstrated 3 germ layers - additional of VPA made no different in reprogramming efficiency - five factors: efficiency 2% - five factors in low Oxygen condition: efficiency 4.4%

Studies	Cell source	Factors	Methods	Finding
Ban et al, 2011	-Human fibroblasts -CD34+-CB cells	Oct4, Sox2, Klf4, and c-Myc	Sendai virus	- expression of human ES marker SSEA4, TRA-1-60, TRA-1-81, Nanog, and Oct4 - *in vitro* and *in vivo* differentiation: EBs and teratomas with all 3 germ layers - the reprogramming efficiency >0.1% - the vectors do not reactivate or are detectable in the established-iPS cells at the late passage or after the temperature shifting procedure
Okita et al, 2011	- Human dermal fibroblast	Different combination factors of: Oct3/4, Sox2, Klf4, c-Myc, L-Myc, Lin28, Nanog, p53 shRNA, SV40-LT	Episomal plasmid vector	- a cellular morphology similar to human ES colonies - Karyotypically normal - RT-PCR expressed pluripotent stem cell markers - Global gene expression profiles were similar to ES cells - DNA methylation levels of CpG sites in promotor region of Nanog were low in pla-iPS (plasmid vector derived iPS cells) comparing to human dermal fibroblast
Ono et al, 2012	- Human nasal epithelial cells	Oct4, Sox2, Klf4, and c-Myc	Sendai virus	- reprogramming efficiency 0.075%-0.1% - using a temperature-sensitive mutant Sendai virus to shut off transgene by temperature shift - similar level of endogenous Oct4, Sox2, Klf4, c-Myc to hES cells - no expression of vector genome by RT-PCR - *in vitro* and *in vivo* differentiation: EBs and teratomas

1.1.4.3 Efficiency improvement of iPS cell strategies

Numerous studies have shown integration of transgenes and vector DNA into host DNA using retroviral and lentiviral transduction (Yu et al., 2009; Zhou et al., 2009). Using the viral transduction method up to 10-20 integration sites were reported in the resulting clones (Takahashi et al., 2008; Aoi et al., 2008;); these alterations in the host genome resulted in; abnormal gene transcription (Zhou et al., 2009; Yu et al., 2009), 20% tumour formation found in the descendants (Okita et al., 2007), and 18 out of 36 chimeric mice generated from iPS cell mosaics were killed by cancer, which has been rarely observed from ES cell chimeras (Wernig et al., 2008). Therefore, many research groups have attempted to improve the delivery methods required for reprogramming, not only to avoid genomic alteration and tumour formation, but also to improve the quality and clinical application potential of iPS cells (Kim et al., 2009, Ban et al., 2011; Ono et al., 2012).

In 2009, Yu and co-workers applied internal ribosome entry site 2 (IRES2) co-expression with four and six reprogramming factors using non integrative episomal vectors—Epstein-Barr nuclear antigen-1 (OriP/EBNA1) (Yu et al., 2009). Yu claimed that using this delivery system, exogenous reprogramming genes and viral vector DNA were undetectable by PCR and southern blot analysis of the resulting iPS cell clones (Yu et al., 2009). The pluripotent properties and the developmental direction of the resulting iPS cells showed ES cell like features including morphology, pluripotent gene profiles, specific human ES cell surface markers, teratomas with all three germ layers —ectoderm, mesoderm, and endoderm, and an epigenetic status showing highly demethylated Oct4 and Nanog promoters (Yu et al., 2009). However, the efficiency was low: just 3-6 ES cell like colonies were identified from $1x10^6$ infected fibroblasts (Yu et al., 2009).

In the meantime, human fetal fibroblasts were successfully dedifferentiated back into pluripotent cells without vector DNA integration by adenoviral gene transduction with four factors Oct4, Sox2, Klf4, and c-Myc (Zhou et al., 2009). These cells showed human ES cell like characteristics in terms of morphology, pluripotent gene expression (SSEA3, SSEA4, TRA-1-81, TRA-1-60, Oct4, Nanog), comparable ES cell surface markers, and generation of teratomas (with 3 germ layers). However, the adenoviral

delivery strategy resulted in low efficiency of around 0.0002% (Zhou et al., 2009). Interestingly from the point of view of this thesis, Zhou claimed successful differentiation of dopaminergic neurons from these cells despite the low efficiency (Zhou et al., 2009) raising the possibility that MSNs could also then be generated following specific directed differentation.

Cell penetrating protein (CPP) are small peptides rich in positively charged amino acids such as arginine or lysine which are able to move across the cell membrane (Ziegler et al., 2005; EI-Sayed et al., 2009). Their cell penetrating ability was used to deliver four reprogramming factors (Oct4, Sox2, Klf4, and c-Myc) in order to induce somatic cells to a pluripotent state (Kim et al., 2009). Each defined factor was fused with a 9 arginine peptide (9R) and transfected into HEK293 cells to generate the stable HEK cell line expressing each reprogramming factor separately (Kim et al., 2009). Human fibroblasts cultured in ES cell conditions were subjected to a protein treatment with the extracted protein from the four HEK cell lines over a period of 6 days for 16 hours each day (Kim et al., 2009). Eight weeks later ES cell like colonies were identified with alkaline phosphatase (AP) positive staining and morphological selection (Kim et al., 2009). Protein induced iPS cells demonstrated pluripotent abilities by formation of teratomas when injected into nude mice, and also generated EBs which were able to differentiate into cell types from all three germ layers (Kim et al., 2009). Furthermore, the resulting iPS cells exhibited similar gene expression profiles (Oct4, Nanog, Sox2, Rex1, Gdf3, and hTERT), pluripotent markers (Oct4, Nanog, SSEA3, SSEA4, TRA-1-60), and epigenetic profiles (demethylated at Oct4 and Nanog promoters) to human ES cells; even though, the derivative efficiency of iPS cell production was also reported to be very low, 0.001% of input cells (Kim et al., 2009).

To date there have been many attempts to improve the reprogramming efficiency and to generate vector-free iPS cells. One such reprogramming technology is the Sendai virus vector (Se V) mediated- iPS cells which was introduced by Fusaki and co-workers in 2009 (Fusaki et al., 2009). Se V is an enveloped-RNA genome virus vector of the Paramyxovirdae family (reviewed in Ban et al, 2011). It was claimed to replicate only in the cytoplasm of transfected cells, transfect with high efficiency in a wide range of cell types

and species, and more importantly has also been applied as a gene therapy in many areas such as AIDS, ischemia, and cystic fibrosis (Fusaki et al., 2009; Ban et al., 2011; Ono et al., 2012). The major advantage of Se V vector is that it is a RNA virus therefore it does not go through a DNA phase nor integrate into the host genome. A simple method to remove the vector from the genome can be carried out by changing the temperature (Ban et al., 2011; Ono et al., 2012) or by applying anti-Se V-HN antibody (Fusaki et al, 2009). The reprogramming efficiency was reported to be about 0.75±0.1% (Fusaki et al., 2009; Ono et al., 2012). More recently, the temperature-sensitive Sendai virus (TS-Se V) vector was innovated as an effective transduction method in order to produce iPS cells that are safe enough for clinical usage (0.08-0.1% efficiency) (Ban et al., 2011; Ono et al., 2012).

Various methods have been developed to improve the efficiency and to avoid genetic manipulation. Kaji introduced a single multiprotein expression vector which combined four reprogramming factors MKOS (c-Myc, KLF4, Oct4, and Sox2) and 2A peptides in order to induce mouse and human fibroblasts to a pluripotent like state (Kaji et al., 2009). Kaji claimed that the reprogramming efficiency was 2.5%, although the efficiency was calculated differently to that used in the viral studies described above (about 0.01-0.1%). High expression of c-Myc and Klf4 and similar expression of Oct4 and Sox2 were found in all 8 iPS cell lines generated from the 12 colonies identified. In addition, the protein levels of all four defined factors were comparable to the ES cells. Using Cre transfection, Kaji et al claimed to eliminate all four exogenous reprogramming factors from the resulting iPS cells. In the same period, the *piggyBac* transposon system was developed to successfully deliver doxycycline inducible transcription factors in mouse and human somatic cell reprogramming (Woltjen et al., 2009). In this study, *piggyBac* was reported as a simple and effective transduction method, suitable for use in a wide range of cell types, along with removable exogenous pluripotent factors.

1.1.4.4 Safety concerns about reprogrammed cell generation and usage.

The concept of using iPS cells as a donor cell source for neurodegenerative diseases is currently hindered by safety concerns. To improve the practical quality of iPS cells and avoid tumour development after transplantation, Wernig and his team reprogrammed mouse fibroblasts using three factors Oct4, Sox2, and Klf4, rather than the previous four defined factors (Wernig et al., 2008). The results showed that mouse fibroblasts could be reprogrammed in the absence of c-Myc. In the experiment, Oct4 or Nanog were used as selection markers both with and without neomycin selection. Wernig reported that removal of the drug selection element does not affect the rate of reprogramming of somatic cells and as such it remains a slow and gradual process (Meissner et al., 2007; Wernig et al., 2007). The conclusion was that three factors Oct4, Sox2, and Klf4 are sufficient to completely reprogram differentiated cells to pluripotent cells over a prolonged culture period. Similarities in morphology and function are reported for three and four factor iPS cells derivation, and these iPS cells could produce mature chimaeras, and developed three germ line tumours when injected into nude mice. However, the number of drug-resistant colonies was dramatically reduced in the absence of c- Myc and neomycin-resistant iPS colonies were only detected approximately 30-70 days after infection with three factor retroviruses (Wernig et al, 2008). Wernig (2008) concluded that c-Myc increases the propensity of iPS colonies and speeds up the processes of cell reprogramming.

At the same time the Nakagawa group published a paper supporting the idea of using three key factors, without c-Myc, in both mouse and human fibroblasts (Nakagawa et al., 2008). Nakagawa reported that the iPS cells maintained good quality with fewer cells of a non-iPS background (Nakagawa et al., 2008). As expected, the omission of c-Myc resulted in a significant reduction of tumorigenicity in chimeras and their progeny (Nakagawa et al., 2008). In addition, the results from this study further emphasized that without reactivation of c-Myc retroviruses the reprogramming process was delayed and fewer iPS colonies were obtained (Nakagawa et al., 2008).

In spite of the safety concerns about tumour development after transplantation, viral transduction has been considered for clinical application.

Meissner et al in 2007 reported a strategy to generate unmodified genetic iPS cells based on a morphologically distinctive strategy that did not require the use of drug selection (Meissner et al., 2007). This resulted in a 5 fold increase in the reprogramming efficiency of MEFs compared to other viral approaches (0.1% efficiency). Moreover, Meissner reported that stable iPS cell lines could be produced from 5 out of 6 directly selected colonies and also presented pluripotent abilities by generating adult chimeras and teratomas when injected into nude mice. He also supported the notion that direct reprogramming is a slow and gradual method which is also indeterminate and results in biological differences in each yield. (See Figure 1.3).

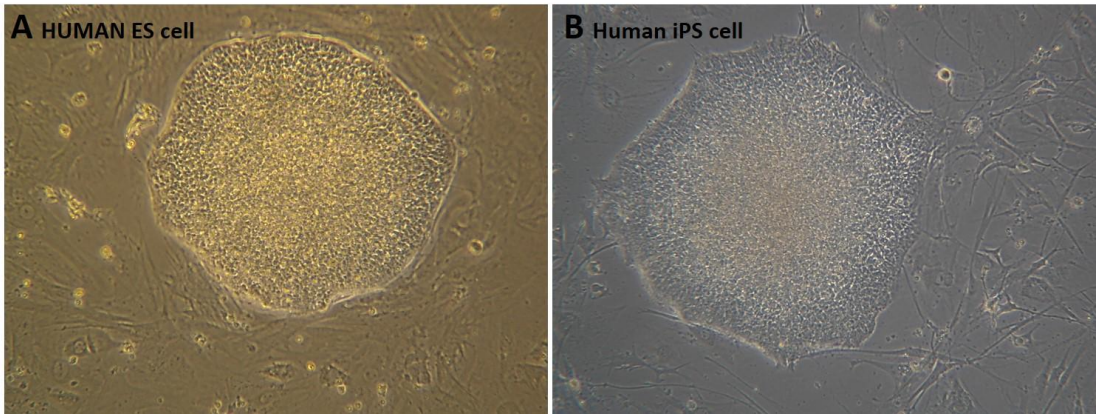

Figure 1.3 Two colonies of pluripotent stem cells – one of human ES cells (A) and one of human iPS cells, derived from reprogrammed adult cells (B). It is clear from the photomicrographs that both cell populations form colonies that share similarities in morphology in vitro.

In 2008, Stadtfeld and his colleagues introduced an adenovirus transduction system to deliver three defined factors Sox2, Klf4, and c-Myc into Oct^{IND} mouse TTFs hepatocytes, and fetal liver cells (where the Oct4 has been modified using a doxycycline-inducible Oct4 allele present in the ROSA26 locus that is driven by a reverse-tetracycline–dependent transactivator (rtTA)), instead of using retroviral method therefore avoiding DNA integration from viral vectors to the host genomic DNA (Stadtfeld et al., 2008).

However, the efficiency was very low at about 0.0001%-0.001%, whereas retroviral usage gave 0.01%-0.1% effectiveness. According to southern blot and PCR studies, plasmid DNA integration could not be detected in the adeno-iPS colonies and it was not possible to amplify the

vector DNA. Okita and coworkers also published a paper in 2008 in which mouse iPS cells were produced without viral vectors. In this paper, a pCX-OKS-2A vector, which identifies the importance of the order in which the transcription factors were placed in the vector (Oct4, Klf4, Sox2 respectively), and a pCX-c-Myc plasmid were transfected into MEFs. The resulting iPS cells not only exhibited morphology indistinguishable from ES cells, but also expressed similar levels of pluripotent markers as ES cells. From examinations for the unification between host genome and plasmid DNA, Okita claimed that the iPS cells generated from plasmid vector appeared to be free from the DNA integration. The efficiency of iPS cells generated by the Okita group was lower than the viral transfection method, as in Stadtfeld group (Stadtfeld et al., 2008; Okita et al., 2008).

1.1.4.5 Molecular changes and mechanisms of reprogramming process.

The molecular mechanisms of somatic cell reprogramming are still unclear. The variability with which iPS colonies appear in the different systems (ranging from 10 days to 8 weeks) makes is more difficult to pinpoint these molecular mechanisms and their mode of action. The epigenetic events during the reprogramming process and the up-regulation or down-regulation of involved pluripotent genes are still a mystery (see Figure 1.4 and 1.5). It is not known whether the reprogramming of somatic cells to pluripotent cells is a timed sequential process or if it is a random process, but what is important is that more studies are needed in order to understand the molecular processes before such cells are to be used in any clinical application.

In 2008, Brambrink and his colleagues attempted to clarify the activation pattern of known ES cell markers over the reprogramming period of iPS cells. They suggested that AP was activated before SSEA-1, and after the cells were completely reprogrammed and Oct4 and Nanog expression were exhibited. In addition, in this reprogramming process at least 12 days was required after the transduction of the four factor lentivirus before the first iPS colonies could be recognised. This finding was emphasized by Stadtfeld's discovery in the same year where it took more than 8 days of inducing exogenous transcription factors expression in order to obtain iPS cell colonies that were stabilized to maintain their pluripotent status (after day 20)

(Stadtfeld et al, 2008). In addition, Thy1 (highly expressed in differentiated cells and fibroblasts) was found to be down regulated contrasting with SSEA-1 (ES cell marker), which increased after this time point. Stadtfeld claimed that Thy1 down regulation not only occurred before the expression of SSEA-1, but also induced the expression of SSEA-1. Moreover, the results from this study supported the previous findings that to be successful in cell reprogramming the endogenous pluripotent genes—Oct4, Sox2 and telomerase (Stadtfeld et al., 2008) need to be reactivated, whereas the X chromosome was kept silent (Maherali et al., 2007; Okita et al., 2007; Wernig et al., 2007).

All these steps were found at the late process of reprogramming as the cells became independent from the expression of four defined factors (Stadtfeld et al., 2008). However, Stadtfeld pinpointed that the silencing of the four exogenous transgenes (Oct4, Sox2, Klf4, and c-Myc) using retroviral vectors occurred gradually from the early stage and was complete by the late stage of the reprogramming process, corresponding to epigenetic modifications and pluripotent gene regulation.

This finding contrasted with the previous suggestion that incompletely reprogrammed cells still displayed imperfect silencing of viral vectors (Takahashi and Yamanaka, 2006). Interestingly in his study, he also found that Fbx15 was reactivated at the early stage of reprogramming (day 3 after exogenous factors transduction) before Nanog and Oct4 genes were expressed. Incompletely reprogrammed iPS cells using Fbx15 as a selective maker may be explained by this phenomena (Stadtfeld et al., 2008; Mikkelsen et al., 2008). In another major study, Mikkelsen and co-workers discovered a similar epigenetic profile between Fbx15 iPS cells and 3 lines of partial reprogramming cells in his experiments (Mikkelsen et al., 2008). Partial reprogramming could be explained by several factors such as activation of anti-pluripotent genes triggered by proliferative stress, failing to activate or suppress endogenous/exogenous reprogramming factors (Mikkelsen et al., 2008). He also suggested that to facilitate and improve successful reprogramming strategies the application of DNA methyl-transferase inhibitors could be considered (Mikkelsen et al., 2008). (Figure 1.4 and1.5).

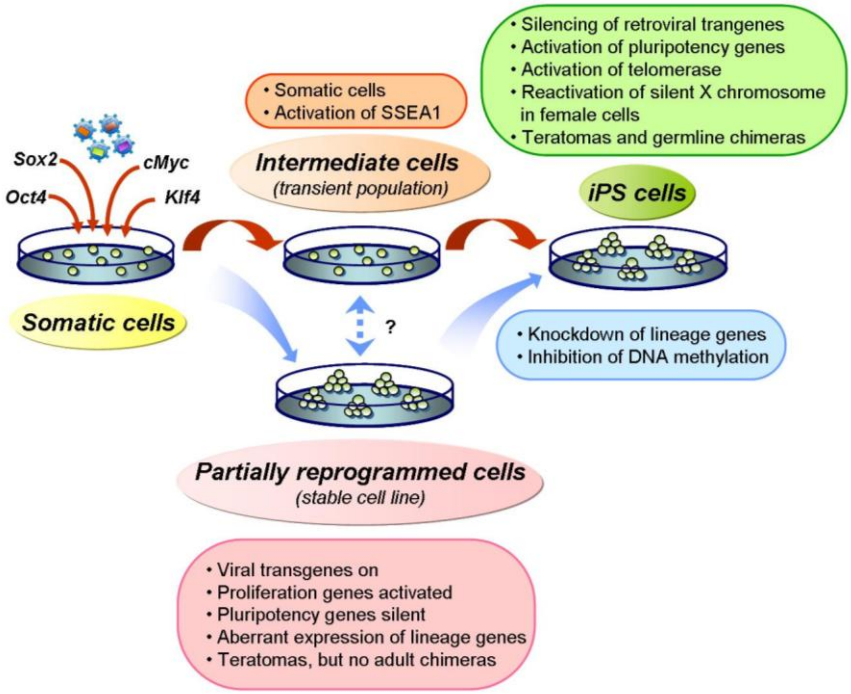

Figure 1.4 Schematic illustrations of direct reprogramming processes to a pluripotent cell state. Direct reprogramming as illustrated here comprises 3 steps which are the starting, intermediate, and end stages. Pluripotent properties start to be able to recognized by the 'intermediate stage' and further conversion to iPS cells occurs through DNA methylation and knock down of lineage-specific genes. Partial reprogramming may stem from transient intermediate cells. (Adapted from Hochedlinger and Plath, 2009).

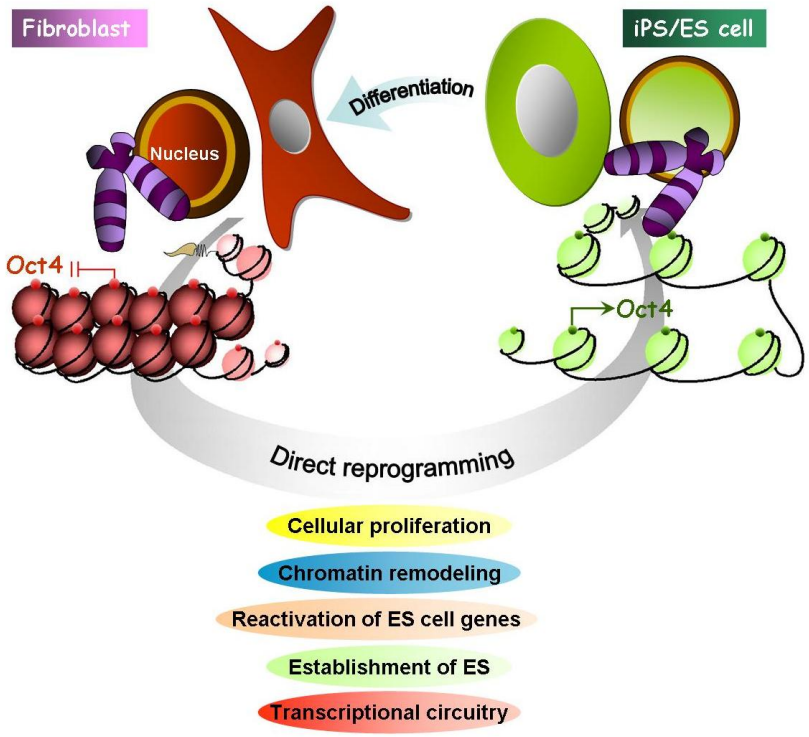

Figure 1.5 Schematic showing rewiring of epigenetic regulation to change cell fate with two opposing processes – differentiation and direct reprogramming. The transition from one cell state to another appears to depending on cellular proliferation, chromatin remodeling, and reactivation of pluripotent genes. Therefore, global gene expression pattern will change from fibroblast to ES like state. (Adapted from Welstead Grant et al., 2008)

1.1.4.6 Therapeutic potential of human induced pluripotent stem cells

The promise of iPS cells as a novel donor cell source for cell therapy in degenerative diseases, their implementation to understand normal development and cell lineage differentiation, and their application in disease modeling for various human diseases including cancer, have attracted the attention of many research groups around the world where multiple attempts have already been made to generate human iPS cells.

In fact nuclear reprogramming in human cells was achieved in 2005 using fusion of human somatic cells with human ES cells (Cowan et al., 2005). Cowan and colleagues found that there were similarities in morphological structure, antigen expression profiles, and genetic profiles such as DNA methylation pattern, specific gene expression, reporter gene stimulation between reprogrammed- and ES cells. Moreover, Cowan claimed that these hybrid cells also show ES like pluripotency by producing EBs in culture and teratomas in nude mice. One year later, the capacity of myeloid precursors to be reprogrammed using cell-cell fusion model with human ES cells was reported (Yu et al., 2006). Yu highlighted that surprisingly the hybrid cells could differentiate back to their original cell type (myeloid precursors) with an efficiency similar to ES cells. Yu was also concerned about the differences between species and how the reprogramming process may differ; the factors that promote self-renewal of human ES cells are distinctively different from mouse ES cells. However, the controversy of destroying human embryos and immune rejection hinder the use of ES cells for clinical application. Thus, iPS cells are an attractive alternative cell source to explore as they overcome many of these issues.

1.1.4.7 Safety concerns in human iPS cell usage.

Two major hurdles for the clinical application of iPS cells is the efficiency of generation, and the involvement of the oncogenes c-Myc and Klf4 which may alter the host cells genome (Huangfu et al., 2008). One approach that is working towards addressing these issues was reported by Kim et al 2008. In this study adult stem cells containing high levels of essential reprogramming factors such as Sox2 (in adult neuronal stem cells) were used as the original cell source, and were successfully turned to a totipotent state with fewer transcription factors used for induction (Oct4 with either Klf4 or c-Myc) (Kim et al., 2008).

The ability to generate iPS cell colonies in the absence of c-Myc identifies a move towards the generation of clinically useable cells. In addition, small molecules such as histone deacetylase (HDAC) and DNA methyltransferase were used as the enhancers to improve the efficiency of somatic cell reprogramming, because these molecules do not alter the genomic structure of host cells (Huangfu et al 2008). Huangfu reported that two primary human fibroblast lines (BJ and NHDF) achieved a pluripotent state after being infected with three transcription factors (Oct4, Sox2, and Klf4), and an additional 1-2 weeks of valproic acid (VPA) treatment; the efficiency of reprogramming method was claimed on the basis of Oct4-GFP positive cell production as 2%, and as 1% based on the number of iPS colonies (Huangfu et al., 2008).

Although, the 3 factor-induced iPS clones met all the criteria to resemble human ES cells, infected cells needed to be cultured for up to 30 days in order to identify ES cell-like forms (Huangfu et al., 2008). After succeeding in three factor reprogramming, Hangfu also induced BJ and NHDF using two core reprogramming factors (Oct4 and Sox2) and VPA treatment (Huangfu et al., 2008). Although, the two factor reprogramming strategy showed a significant decrease in efficiency compared to three factors; the iPS cells generated by only two factors showed pluripotent characteristics, gene expression profiles, and epigenetic patterns comparable not only to iPS cells produced by three factors but also comparable to human ES cells (Huangfu et al., 2008). Huangfu concluded from his study that Oct4 and Sox2 are the essential factors in direct reprogramming method, whereas Klf4 is a non-essential factor, but plays a role as the facilitator. Moreover, two factors with small molecule--VPA are sufficient to reprogram primary neonatal fibroblasts (that have low levels of reprogramming factor expression) (Huangfu et al., 2008).

After several attempts to reduce the exogenous transcription factors used in reprogramming differentiated cells, in 2009 Kim and his co-workers claimed that introduction of Oct4 alone is adequate to induce human foetal neural stem cells to a totipotent state (Kim et al., 2009). To obtain the iPS cell colonies, the transfected cells were cultured in human ES cell conditions for 10-11 weeks. Single factor induced iPS cells shared similarities in morphological appearance and epigenetic patterns to human ES cells (Kim et al., 2009). In addition, epigenetic remodelling in the resulting iPS cells were confirmed with demethylated Oct4 and Nanog

promoters as presented in pluripotent cells (Kim et al., 2009). These iPS cells also exhibited the pluripotent characteristics in both in vivo and in vitro examinations (Kim et al., 2009). However, the efficiency of using only Oct4 to reprogram somatic cells was very low at 0.004%, therefore the finding of novel small molecules to improve the efficiency or even replace all the reprogramming factors could be an ideal strategy to generate safe and practical iPS cells as a cell source for regenerative medicine (Kim et al., 2009).

The ultimate goal of iPS cell derivation for degenerative diseases is to provide transplantable patient-specific cell sources which overcome ethical and immune rejection difficulties as found with other donor cell sources. Hematopoietic progenitors (HPs) derived from iPS cells were reported to successfully rescue and improve all aspects of pathology in a mouse sickle cell anemia model (Hanna et al., 2007). Sickle cell anemia mice were transplanted with iPS cell derived HPs to examine “proof of principle” and functional therapeutic potential in the iPS cell usage (Hanna et al., 2007).

Interestingly, one year later, Wernig reported functional benefit and behavioral improvement using iPS cell derived neural stem cells (NSCs) transplanted into a Parkinson’s disease (PD) rat model (Wernig et al., 2008). Wernig claimed that *in vitro* NSCs generated from iPS cells were able to differentiate into all neural cell types (β-III tubulin (neuronal maker), GFAP (glial marker), O4 (oligodendrocyte marker) positive staining) including dopaminergic neurons after delivery of patterning factors (FGF8 and sonic hedgehog) (Wernig et al., 2008). In addition, migration of NSCs from iPS cells was observed in various brain regions such as the striatum, midbrain, and hypothalamus after injection to the striatum (Wernig et al., 2008). Furthermore, functional restoration and behavioral improvement were confirmed by electrophysiological demonstration of action potentials, synaptophysin expression, and bias movement reduction in amphetamine induced rotations up to 8 weeks post transplantation (Wernig et al., 2008). The previously mentioned studies provide evidence that iPS cells have the potential to be a donor cell source for cell replacement in regenerative medicine.

1.2 Huntington's disease

Huntington's disease (HD) was first described by George Huntington who detailed the classic features of this neurodegenerative disease in his now well-known paper of 1872 (Huntington G., 1872). The CAG trinucleotide repeat expansion of the huntingtin gene (HTT) encodes mutant protein huntingtin (mHtt) which has an abnormally long polyglutamine tract. This mutation is responsible for HD (The Huntington's disease collaborative research group, 1993). The gain of function toxicity caused by mHtt may disturb normal activities (Imariso et al., 2008). It is clear that the major effects of mHtt are due to toxic gain of function, although there is controversy about the extent to which loss of function is important in the pathogenesis of HD.

HD pathology affects increasingly widespread areas of the brain, although the predominant pathology in HD is loss of MSNs in the striatum, which results in compensatory ventricular enlargement. Due to the widespread connections of the striatum with brain regions subserving many different functions, damage to the striatum results in impairment of cognition, motor dysfunction and also leads to psychiatric impairments in HD patients. As the disease progresses, more widespread areas of brain are affected with shrinkage/degeneration of the cortex (Meynert et al., 1877; Jelgersma et al., 1907) (Figure 1.6).

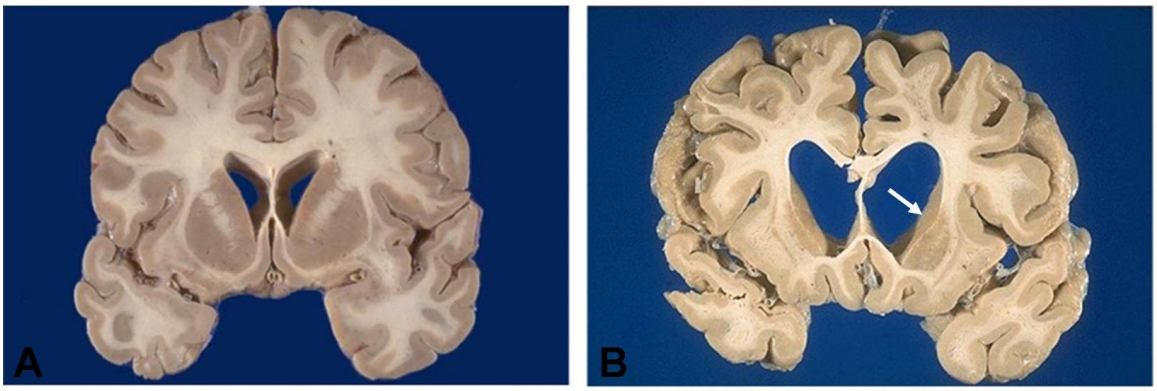

Figure 1.6 Coronal section through normal brain (A) and HD brain (B). The arrow shows atrophy of the striatum, due largely to loss of medium spiny neurons. (Picture from http://marcora.caltech.edu/science.htm)

After the initial discovery of the HTT gene in 1993, understanding HD in terms of biology, genetic, and therapeutic potential have gone much further, however there is no disease-modifying treatment in clinical usage (Thomson et al., 2002; Kim SD and Fung VS, 2014; Zielonka et al., 2015) and a clear understanding of the mechanism of disease is still unknown. Therapeutic treatment in HD is limited compared to some other neurodegenerative diseases such as PD (Kelly et al., 2009); most drugs or treatments available at this moment are only able to relieve the symptoms rather than cure the disease (Thomson et al., 2002). One potential therapy that has shown promise is the transplantation of primary fetal striatal tissue in HD, where there is “proof of principle” in both animal models (Dunnett et al., 1998; Armstrong et al., 2000), and HD patients (Bachoud-Levi et al., 2000; Rosser et al., 2002; Bachoud-Levi et al., 2006). However, human fetal tissue usage brings controversial ethical issues, limitations in tissue supply, accuracy and reliability of dissection following retrieval of tissue, and there is also the issue of immune rejection following transplantation (Kelly et al., 2009). Therefore, alternative donor cell sources need to be explored and generated. The most likely alternatives to replace primary fetal tissue as a donor cell source are neurons derived from stem cells.

Human pluripotent stem cells such as human ES/iPS cells also hold promise as a powerful tool for drug screening, toxicology, developmental studies, and study and of neurodegenerative disease mechanisms (Aubry et al., 2008, Gaspard and Vanderhaeghen, 2010; Ma et al., 2012; Delli Carri et al., 2013). The reason being is that human ES/iPS cells can self-renew and differentiate to almost all kinds of desired-cell phenotypes.

However, for most of these uses it is important to be able to differentiate stem cells towards specific differentiated phenotypes – which for HD is the medium spiny neuron. The extent to which the phenotype needs to be “authentic” is not clear for all applications, but for cell replacement therapy in the brain, it is clear from animal work that the cells for transplantation must be authentic for full functional recovery (Dunnett SB. and Rosser AE., 2011; Rosser, A. E. and Svendsen, 2014). There have been a number of attempts to persuade human ES/iPS cells toward an MSN phenotype (Aubry et al., 2008; Shin et al., 2011, Ma et al., 2012; Delli Carri et al., 2013), described in more detail below.

1.2.1 Directed differentiation of pluripotent stem cells (PSCs) towards a striatal MSN phenotype

The nervous system derives originally from the ectoderm layer. The inner cell mass give rises to epiblasts, from which 3 germ layers arise: ectoderm, endoderm and mesoderm. The neuroectoderm or neuroepithelium forms the so-called 'neural plate' by the second week of gestation, which then forms a neural tube and eventually an entire central nerous system (CNS) (Pankratz et al, 2007). Regional specification to forebrain, midbrain, hindbrain and spinal cord is a fine-tuning process requiring different signals directing the differentiation of distinct neural subtypes (Pankratz et al, 2007). Nervous system development consists of 3 main processes of neural induction, neurulation, and nervous system patterning (Rubenstein et al., 1998; Evans et al., 2012). (Figure 1.7)

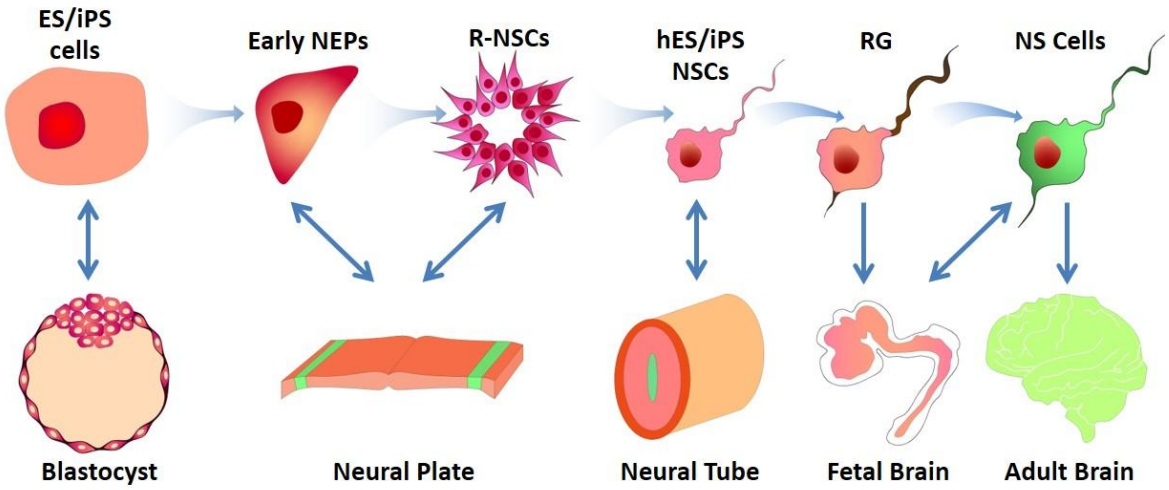

Figure 1.7 Schematic of how stage specific nervous system development *in vivo* corresponds to distinctive neural cell populations' *in vitro* differentiation. ES cells from the blastocyst stage or reprogrammed cells such as iPS cells differentiate to early neural epithelial cells (NEPs) which give rise to all neural cells similar to the neural plate. Soon after neural induction, NEPs display a neural rosette structure (R-NSCs) which mimics neural tube formation in development, following which they then differentiate further to human ES/iPS derived neural stem/precursor cells (human ES/iPS NSCs). Regional patterning *in vitro* by exposure to chemical combinations in culture can represent antero-posterior (A/P) axis and dorsal-ventral (D/V) patterning *in vivo*. Human ES/iPS NSCs transform to another transitory stem cell type, radial glia (RG), which are the majority of the progenitor population in late development and the early post natal stages, They then maturate further to neural cells in vitro and in development. (Adapted from Casarisa et al., 2013; http://www.intechopen.com/books/neural-stem-cells-new-perspectives/systems-for-ex-vivo-isolation-and-culturing-of-neural-stem-cells)

Initiation of primitive ectoderm occurs when the pluripotent stem cells from the inner cell mass (ICM) undergo a series of changes associated with up and down regulation of various genes. A decrease in *Oct4* expression coupled with

upregulation of *Sox1* and *Gbx2* were observed during neural plate configuration. Undifferentiated neural progenitors within the neural tube were defined by the presence of *Sox1, Sox2, Nestin, Mash1,* and *N-CAM*. At the gastrulation stage, the neural plate, which lines the anterior axis of the embryo, folds to generate the neural tube and finally creates both CNS and peripheral nervous system (PNS). The orchestra of genes, molecular signals, and transcription factors such as FGF, bone morphogenic protein (BMP), retinoic acid (RA), sonic hedgehog (SHH), and Wnts result in development of the designated cellular and molecular identities and positional specification (Manel et al., 2010; Evans et al., 2012).

The positional arrangement of the antero-posterior and dorso-ventral axes appear to be triggered by the concentration gradient of Shh and BMP4 from the surrounding cells (Reviewed in Lang et al., 2004). SHH has been reported to induce the expression of ventral forebrain genes including *Nkx2.1, Gsh2*, and *PAX6* (reviewed in Evans et al., 2012). Retinoic acid (RA) has long been known to play a crucial role in neural development and maintenance of a neural phenotype (Schwartz H. P. et al., 2008). In addition, RA is also known as a caudal restricted inducer, which controls dorsoventral identification *in vitro* (Zhang SC. 2006, Schwartz H. P. et al., 2008, Erceg S. Et al, 2008). In contrast to Shh, this signalling molecule plays an important role in ventral neural tube patterning of the telencephalon and spinal cord via the homeobox gene-Nkx family (Yun K. Et al., 2000; Schwartz H. P. et al., 2008). (Figure 1.8)

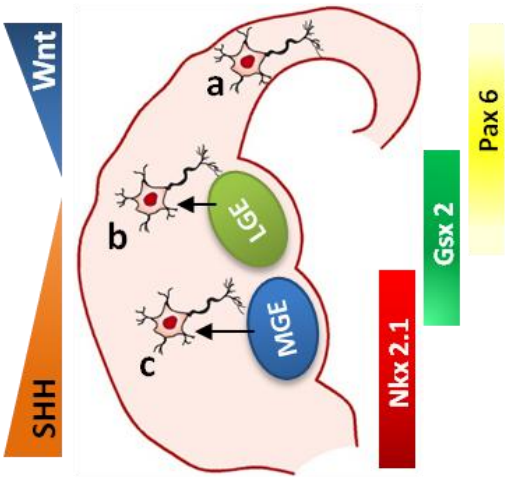

Figure 1.8. An illustration of the molecular gradient between SHH and Wnt signalling within the developing cortex accompanied by gene expression resulting from this gradient. Progenitors in these domains mainly generate glutamatergic neurons (a), GABAergic projection neurons (b), and basal forebrain cholinergic neurons (BFCNs) (c), respectively. (Adapted from Liu et al., 2011) SHH= Sonic hedgehog, Wnt= Winless, MGE= medial ganglionic eminence, LGE= lateral ganglionic eminence, Nkx2.1= NK2 homeobox 1, Gsx2= glycogen synthase kinase, Pax6= paired box 6.

The pattern of gene expression varied in different regions. *Nkx6.1* and *Olig2* indicate the ventral axes whereas the dorsal axis was marked by the appearance of by *Dbx1, Irx3,* and *Pax6*.

The cerebral cortex and basal ganglia develop from the telencephalon which is formed by the invagination of the rostral forebrain (Yun K. et al., 2000; Schuuemans C. and Guillemot F., 2002). The telencephalon is subdivided into its dorsal (pallial) and ventral (subpallial) regions with each region expressing different combinations of transcription factors (Yun K. et al., 2000). Glutamatergic projection neurons are the main cell population of the pallium compartment. In contrast, the subpallium is largely made up of GABAergic neurons (Stoykova et al., 1996; Yun K. et al., 2000). The expression of *Pax6, Ngn1/2* and *Emx1/2* are associated with the dorsal telencephalon whilst *Gsx1, Gsx2, Gad67, Dlx1, Dlx2* and *Six3* are detectable in the subpallium compartment (Stoykova et al., 1996; Yun K. et al., 2000). Thus the development of the telencephalon is tightly regulated by various combinations of transcription factors together with small molecules such as Shh, Notch and BMP (Schuurmans C. and Guillemol F., 2002, Campbell K., 2003). Furthermore there is much evidence to indicate that the molecularly defined regional subdivisions and basic organization of the developing

telencephalon among vertebrate species has been conserved (Smith-Fernandez et al., 1998; Puelles et al., 2000, Yun K. et al., 2000).

Arising from the ventral telencephalon is the septum and the MGE and LGE, collectively referred to as the whole ganglionic eminence (WGE). The MGE and LGE give rise to the adult striatum. The LGE is further divided into 2 compartments of which the dorsal LGE (dLGE) expresses *Pax6, Gsx2* and *ER81* and the larger ventral LGE (vLGE) expresses *Gsx1, Gsx2* and *Pax6* (Yun K. et al 2000; Campbell K., 2003). Surrounding the developing telencephalon are two proliferative zones the subventricular zone (SVZ) and the ventral zone VZ and it is here where the projection neurons and interneurons are born and from where they then migrate to populate areas of the adult striatum and the cortex respectively (Eisenstat DD. et al., 1999; Campbell et al., 2003; Evans et al., 2012; Campbell et al., 1995; Anderson et al., 1997; Olsson et al., 1998; Evans et al., 2012). (Figure 1.9)

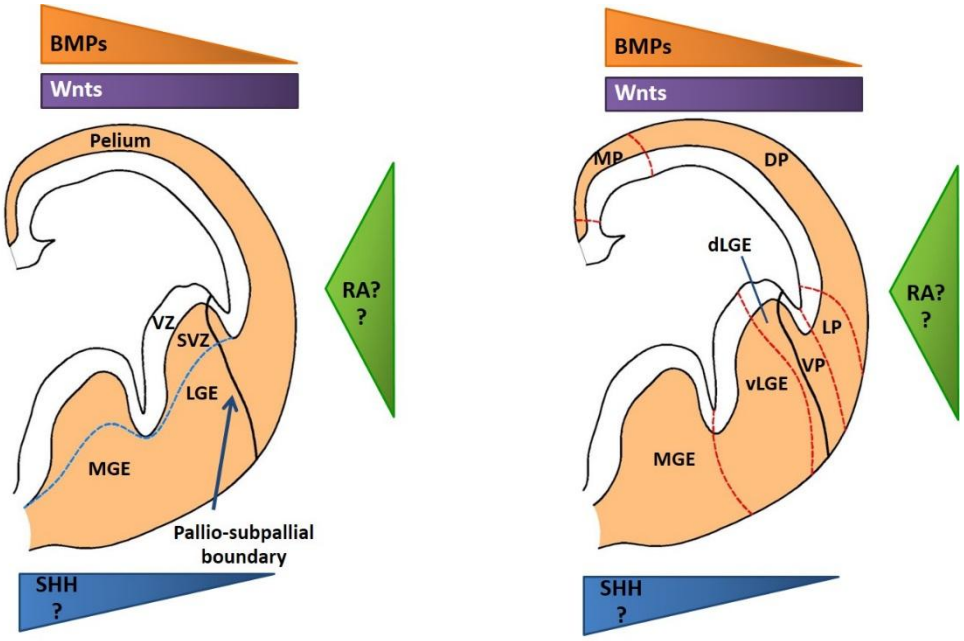

Figure 1.9 A schematic to show the relation between molecular gradients and morphological structures in a coronal hemisection of mouse telencephalon at E12.5. The ventricular zone (VZ), which is a proliferative area of neuronal progenitors, extends along the D/V axis.The subventricular zone (SVZ), which is a special characteristic of telencephalon, also contains neuronal precursor cells (presenting by the blue dashed line). Neural progenitors migrate from VZ and SVZ to populate particular areas of the brain. The red dashed lines demonstrate the approximate boundaries between distinct telencephalon progenitor domains. Abbreviations: MGE/LGE= medial/lateral ganglionic eminence; MP= medial pallium, DP= dorsal pallium, LP= lateral pallium, VP= ventral pallium. (Adapted from Olsson et al., 1995).

1.2.2 Pluripotent stem cells and establishment of neuronal linage differentiation *in vitro*.

An ability to differentiate into any type of cell with almost unlimited expansion of cells' progeny make iPS cells an attractive cell source for developmental studies, cell therapy, drug screening, and toxicology. Neural precursors derived from pluripotent stem cells were reported to share similar characteristics to cells differentiating from primary brain tissue with subsequent differentiation into neurons and glial cells. There have been many attempts to manipulate PSCs cells towards desired phenotypes in order to pave the way for therapeutic utilization in regenerative medicine (Figure 1.10). Generally speaking, there are several processes involved in neural lineage conversion, for example unleashing pluripotentiality, inducing neural lineage identities, and specifying cells' fate restriction. To initiate a neural lineage, different methods are available such as aggregation of multicellular EBs, direct differentiation from a monolayer adherent system, co-culture with neural inducing cells or membranes and genetically engineered-PSC lines (involving the use of nuclease mediated novel gene targeting technologies) (reviewed in Schwartz P. H., et al, 2008).(Table 1.3)

.

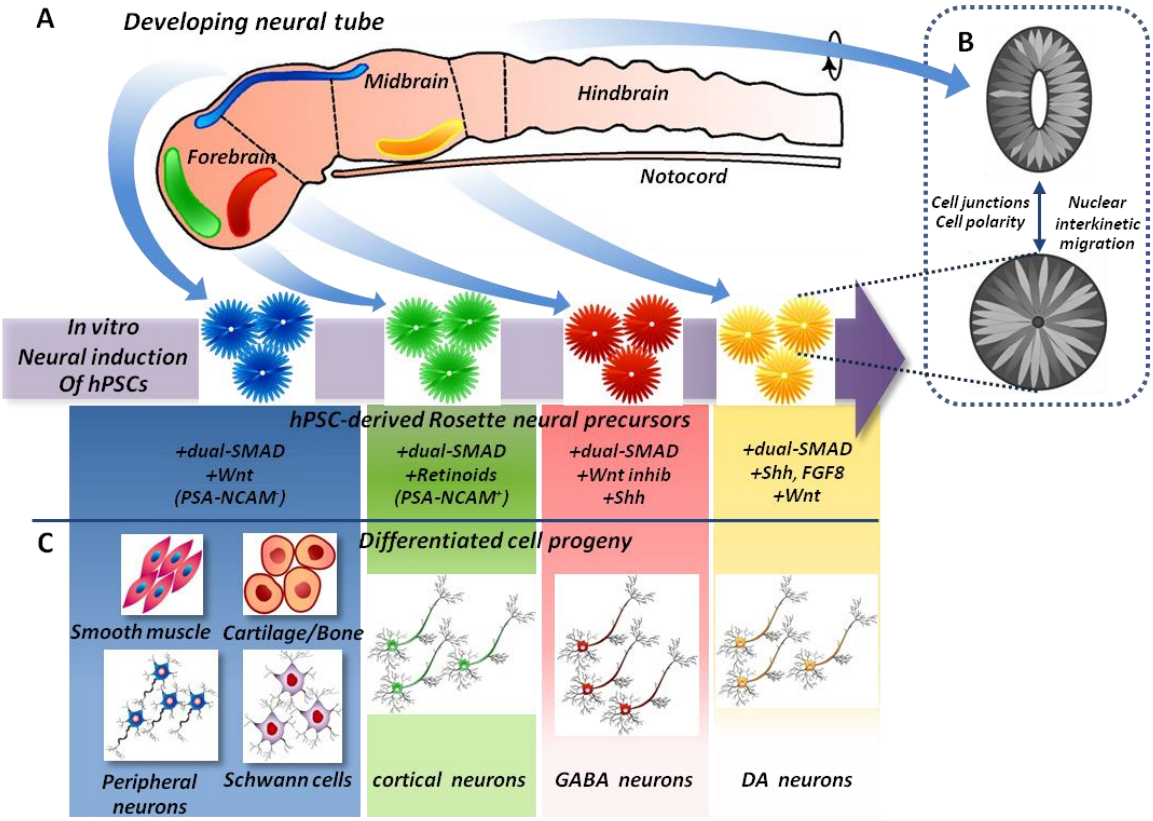

Figure 1.10. A schematic of in vitro neural induction and conversion of PSC generate NPCs. A distinctive combination of signalling regulators can direct the differentiation of PSCs to positionally restricted neural rosette precursors along the developing neural tube **(A).** Rosette formation *in vitro* shares similar spatial organization of cell junctions and cell polarization with neural tube development *in vivo* **(B).** With regional specific commitment, distinct neuronal subtypes were generated **(C).** (Adapted from Broccoli et al., 2014)

Table 1.3 Pluripotent stem cells and establishment of neuronal linage differentiation.

Author	Cell	Method	Result
Fraichard et al. 1995	Mouse ES cells	- EBs for 2 DIV in a presence of retinoic acid 1 µM. - Aggregated ES cells were re-plated and cultured in ES medium up to 20 DIV.	- Nestin positive staining at 3-4 DIV. - GFAP and O4 positive cells were recognised at 9 DIV. - Map2 (a+b), Map5, NF200 positive cells were observed and synaptophysin was also identified at 10 DIV. The pattern of expression was similar to primary E16 mouse cortex differentiation *in vitro*. - 8 DIV, AchE and GAD were expressed among neuronal-like cells.
Bain et al. 1995	Mouse ES cells	- EB formation Day 0-4 without RA, and RA supplement 0.5 µM on Day 4-8 VS control group no RA addition	- Strong up-regulation of neuronal genes such as MASH1, Wnt-1, NF-M, NF-L. - Strongly repressed mesodermal genes such as Brachyury, cardiac actin, zeta-globin.
Okabe et al. 1996	Mouse ES cells	- EB formation from day 0-4. -Re-plated on coated culture disk and incubate with ITSFn medium.	- Highest proliferation of neuronal precursors was found when culturing with 3N3FL medium. ->80% of the NPCs were Nestin+ while 10% of the population was MAP2+. -90% of BrdU+ cells were Nestin+ cells.
Li et al. 1998	Mouse ES cells	- EBs with RA supplement. - Bifunctional selection system of βgeo tagged to Sox2 gene by homologous recombination and further selective by G418 (200 µg/ml) application.	-50% were positively stained for neuronal markers: NF-L, NF-M, MAP2, Tau, β-III tubullin while 20% became immunopositive for GFAP. -Fresh plated cells were 100% nestin positive and within these cultures were 40-50% Sox1 and Sox2 +ve expression. -90% β-galactocidase expressing cells were obtained.

Author	Cell	Method	Result
Zhang SC. et al. 2001	hES cells: H1, H9, H9.2 lines	- 4 DIV as EBs and further differentiation as adherent aggregated cells in defined medium. - On FGF2 addition for 5 days and start neural induction by withdrawal of FGF2. -Special selection of neuro epithelial cells using Dispase and expanding neuronal precursors as free floating aggregations/neurospheres.	- By 7 DIV neural rosettes appeared which were immunoreactive for Nestin and Mash1. - After re-plating as adhered EBs; there was Map2ab and β-III tubulin expression at 7 to 10 DIV and around 10 to 14 DIV there was NF positivity. - No tumour generation in transplantation recipients. The hES derived neural precursors could be differentiated into various types of neurons and glia.
Perrier L. A. et al. 2004	hES cells: H1, H9, HES-3; Rhesus monkey line: R366; Cynomolgus parthenogenetic line: Cyno1	- 28 DIV onto MS5, MS5-Wnt, or S2 stroma cells in serum replacement medium and N2 modified medium respectively. - Neural rosettes were mechanically triturated and re-plated onto POL/Laminin coated plate in N2 medium supplement with Shh, FGF8, AA, BDNF for 7-9 DIV. - Withdrawal of Shh and FGF8 and further differentiate cells in N2 medium with BDNF, GDNF, dcAMP, TGFβ3, and AA.	- At 2 weeks, neural rosettes form edon MS5 or MS5-Wnt and expressed neural markers, nestin, Pax6, NCAM, and Sox1. - Semiquantitative RT-PCR revealed a decrease in gene expression of Oct4 and nanog associated with increase in Pax6 and Map2 markers. - 3 fold increase in TH positive neurons but no expression of other midbrain dopaminergic neuron markers (28 DIV). - After P2 (50 DIV) of the 30-50% Tuj1+ expression cells 64-79% expressed TH. Astrocytes were observed in long term culture (70 DIV).

Author	Cell	Method	Result
Gerrard et al. 2005	hES cells: H1, H7, H9	- Adherent culture system - Plate down hES as small clump onto matrigel or PLL/Laminin coated plate. - Using BMP antagonist: noggin/ follistatin supplemented in N2B27 medium.	- After 10 DIV, neuro- progenitor like-cells were clearly identified in noggin supplement whereas in follistatin they appeared to be fibroblast-like. - RT-PCR: down regulation of GATA6 and Id protein. - No AFP expression at 6 DIV in both control and noggin supplement conditions. - After 13 DIV, AFP positive expression was highly expressed in control groups. 30 DIV typical neural rosette formation emerged and expressed nestin, musashi, PSA-NCAM (neural progenitor markers). - GFAP+ was found from 80 DIV. - 60 DIV: mostly expressed GABA and GAD65 positive neurons, few TH neurons and no glutamatergic neurons.
Ueno et al. 2006	mES and hES cells	- Amniotic membrane matrix-based ES cells differentiation (AMED) with serum free medium system. - Mouse ES cells cultured on gelatin-coated hAM. - hES cells cultured on laminin-coated hAM.	- In mouse ES: 7 DIV 90% were nestin+, NCAM+. - No gene expression for mesoderm (Brachyury) and endoderm (AFP, SOX17) markers. Less proliferation and less efficient (around 60-70%) neural differentiation when ES cells were cultured on other matrix such as gelatin, collagen IV, laminin or fibronectin. - 9 DIV: 62% of TuJ1+ and around 39% TH+ neurons were detected by 13 DIV. In hES: 15 DIV >85% nestin+, rosette formation appearance. 30 DIV TuJ+ expressing neurons were present, of which ~31% co-expressed with TH+ later on at day40-42.

Author	Cell	Method	Result
Joannides J. A. et al. 2007	hES :H9, HUES9 (P30-60)	-hES colonies were cultured on MEFs before the ES colonies were dissected into small fragments and further grown as free-floating spheres in human neuralizing medium (HNM) to generate hES-NSCs. -hES-NSCs were terminally differentiated by adhering onto PDL/laminin-coated plates and cultured in DMEM/F12+ 2%B27, w/ or w/o FBS for up to 4 weeks and were transplanted at $1x10^5$-$2.5x10^5$ cells/µl.	-D25 immature neuronal markers expressed Nestin+, Masashi1+,Sox1+,Sox2+,Pax6+, NCAM+. -14 DIV further differentiation in the presence of B27 and FBS neuronal population increased but no O4+, or GFAP+ expression. -D45 onwards, hES-NSCs exhibited O2+ but not GFAP+ with a high proliferation rate. -with terminal differentiation neurons, gila and oligodendrocytes population were generated which confirmed the NSC properties.
Pankratz et al. 2007	- hES: H1, H9 - Rhesus monkey ES: R366.4	- A chemical defined monolayer neural differentiation system. - ES cells were grown as EBs for 4 days and transferred to defined medium for a further 2 DIV before being attached to culture dish. - 14-16DIV neuroepithelial cells were cultured as aggregates for several days before being dissociated and re-plated onto POL/laminin coated vessel in defined medium+ BDNF, GDNF, AA, cAMP, laminin.	- After 8-10 DIV, columnar morphology of neuroectoderm and neural markers with anterior regional profile were found. - After 6 DIV neuroectodermal markers Sox1, NCAD, Sox3, Zic1, Churchill were expressed, whereas Sox1 were present until 15 DIV by RT-PCR analysis which co-responding to down regulation of pluripotent markers which eventually undetectable after10-11 DIV. - 54% of PAX6+ expression at 8 DIV - this became 95% by 11 days. At 14-16 DIV neural tube-liked rosette structure emerged. - PAX6, Lhx2, BF1, Otx2 expression were observed in almost all of columnar cells whereas posterior regional markers were not recognized.

Author	Cell	Method	Result
Erceg et al. 2008	- hES: H1, H9	- hES cells grow onto human foreskin fibroblasts in ES medium. - hES cells were transferred onto human matrix coated plate and cultured in modified TeSR1 for 7 days. - 7-14 DIV culture in GRM medium and re-plated the cells at day 14 on to POL/laminin coated plate with additional GRM/bFGF in culture medium.	- Neural rosette appeared on day 2 after being cultured on plates coated with human collagen IV, vitronectin, and fibronectin - Neural progenitor marker-nestin was expressed from day 2, whereas PAX6+ was expressed within rosette structures from day 5. - At 14 DIV cells expressed nestin, PAX6, BLBP, RC2, - At 28 DIV cells were positive for Musashi1, A2B5, MAP2. TUJ1 expressing neurons were increased from 20% to 62% at 42 DIV (with 46%GABA+, 43% glutamate+, 7% serotonin+, 14%GFAP+, 23%O4+ in here). RT-PCR showed loss of pluripotent expression and gain of a more neuronal profile.
Li X. et al. 2008	hES: H1, H9 (P19-42)	-4 DIV as EBs then as adherent aggregated cells in defined medium. At day 10 RA was added into chemical defined medium. neural rosettes were collected D14 and cultured in free floating manner for 1 week -After 24 DIV BDNF,GDNF, IGF1, purmorphamine were supplemented to culture condition. -Around 45 DIV cells were dissociate and re-plated onto POL/laminin with a presence of BDNF, GDNF, IGF1, B27, RA for 3-5 day before co-culture with C2C12 myoblasts.	-Neuroepithelial cells (NE) emerged at 8-10DIV of differentiation processes which demonstrating of primitive anterior NE by positive expression of Otx2 and Pax6. -Hoxb4, the start to exibit when supplementing with RA for 1 week.

1.2.3 Human PS cell derived GABAergic projection neurons (MSNs).

In recent years there have been a number of reports of protocols to more accurately and more efficiently generate functional GABAergic MSN-like cells from PSCs suitable for cell replacement therapy in HD. In comparison to the PD literature where there is ample reports generating dopamine neurons from both ES and iPS cell lines, the field in relation to HD is relatively in its infancy with only a small body of literature reported to date. The initial studies carried out in ES cells have shown great potential, however, there is still the need for further investigations to be carried out to optimise protocols.

The first study was carried out by Aubry et al (2008) and using a multistep protocol they reported the ability to obtain 56% DARRP32 positive neurons (out of a total of 36% GABAergic neurons in the culture) using two human ES cell lines H1 and H9. This protocol involved an element of patterning by the addition of SHH, DKK-1 (a Wnt signalling inhibitor), and BDNF; and finally, terminal differentiation to post mitotic GABAergic MSNs-like cells was achieved by adding valproic acid and dbcAMP. However, these human ES derived MSN-like cells overgrew post transplantation into the rat quinolinic acid (QA)-lesioned striatum. By week 8 post transplantation, the animals exhibited weight loss and disturbance of balance and movement. The brains were taken and analysed at 13, 15-16, and 17 weeks post transplantation. Histological analysis revealed that there was graft survival in all brains accompanied by overgrowth and disruption of the striatum, even though there was negative staining of the pluripotent marker-Nanog in the graft.

In 2012, Ma and colleagues claimed that with 93% of human ES derived (H1 and H9 lines) β-III tubullin positive cells, they could achieve up to 80% DARRP-32 expression if they induced human ES cells to a primitive neuro-epithelial phenotype as suspension EBs for 10-12 days to persuade them to ventral neural progenitors. As with Aubry et al (2008) the cells were subjected to patterning with the addition of SHH/purmorphamine in order to regionalise the cells toward a ventral telencephalon fate. Subsequently neural precursor cells were cultured in the presence of BDNF, glial cell derived neurotrophic factor (GDNF), insulin-like growth factor (IGF) and cyclic adenosine monophosphate (cAMP) to generate mature MSNs. 4 months post transplantation into the QA-lesioned

mouse striatum, they found 86% β-III tubulin positive neurons of which 58% were DARRP32 positive. In addition, grafted animals showed improvement in locomotor deficits on the rotarod and open field tests, as well as on the Treadscan analysis. Ma highlighted that the effective production of authentic MSNs needed a defined concentration of morphogens during the appropriate time window (Ma et al, 2012). Although not specifically reported, the images presented in the manuscript would suggest the appearance of overgrowth in these grafted animals.

More recently, Delli Carri et al reported the generation of so-called 'authentic striatal projection neurons' from iPS- and human ES cells. Dual SMAD inhibition - SB431542 and Noggin (from Chambers et al., 2009), was applied to a monolayer of human ES/iPS cells to initiate the equivalent to 'gastrulation stage' *in vivo*. Again, Shh and DKK-1 were used to pattern the cells thus generating LGE specific like cells that were immunopositive for FOXG1 (58%) and GSX2 (64%) in vitro, along with RT-PCR analysis indicating DLX5, DLX6, and ISL1 expression. Finally, the cells were cultured in a neuronal differentiation environment using N2 medium supplementing with B27 and BDNF up to 80 DIV that resulted in 20% DARPP-32 positive neurons being generated. Subsequent transplantation of these cells into the QA lesioned rat brain showed some evidence of functional improvement on rotational analysis. However, this was based on a very small number of animals and a short period of time post transplantation. Furthermore, there was clear evidence of graft overgrowth in these animals.

In each of these studies, whilst positive data is presented in terms of the ability to generate DARPP-32 positive neurons from PSCs, there is clearly further work required to modify these protocols so as to address the issues of overgrowth in vivo. Also, in each of these studies the in vitro culture period was relatively prolonged ranging from 47 to 80 days before MSN like cells were identified. The current gold standard marker for mature MSNs is DARPP-32, but other more immature markers have been identified that may be important in road mapping the progress of these protocols such as FoxP1 and Ctip2 (Tamura et al., 2004; Arlotta et al., 2008). (Table 1.4)

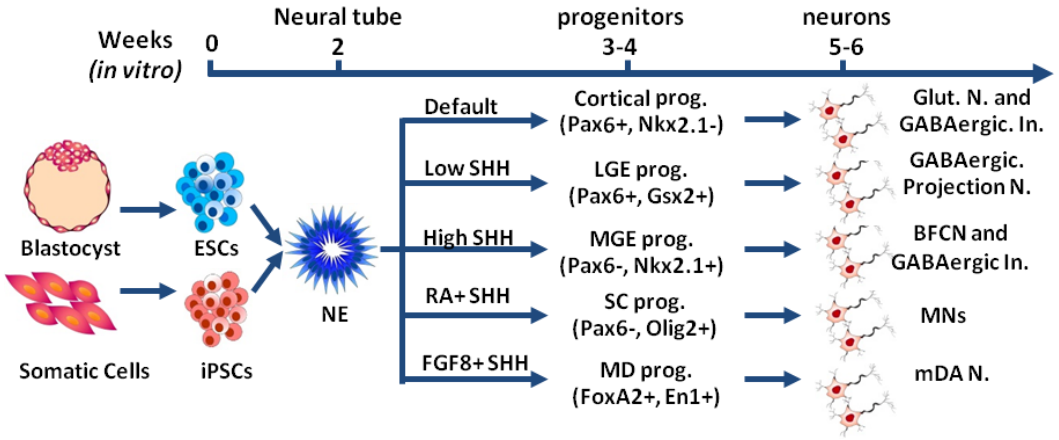

Figure 1.11. A schematic representing the pathway for generating specific neuronal phenotypes from PSCs utilising the information gained through understanding the developmental pathways and the gene expression profiles of these cells. ES/iPS cells differentiate toward primitive neuroepithelial cells. In the absence of exogenous signalling, glutamatergic neurons and GABAergic interneurons are subsequently derived by default from the neuroepithelial cells (NE). With the addition of low concentration of SHH, the NE cells differentiate to Gsx positive cells/LGE progenitors which later on in culture express DARPP32. In the presence of high concentration SHH, MGE progenitors will be generated which produce BFCN and GABAergic interneurons. With RA, NE become Olig2 positive progenitors in supplement with SHH and later generate motor neurons. Under FGF8 and SHH, NE are specified to ventral midbrain progenitors, which then produce midbrain dopaminergic neurons. NE= neruepithelial; Glut. N. = glutametegic neurons; GABAergic In. = GABAergic interneurons; MNs= motor neurons; mDA= midbrain dopaminergic neurons (Adapted from Liu et al., 2011).

Table 1.4 Human PS cell derived GABAergic projection neurons (MSNs).

Author	Cell lines	Methods	Results
Aubry Laetitia et al 2008, PNAS	hES (H1 and H9)	- 3 steps: 1. Neural induction by co-culture with MS5. 2. Regional commitment by mechanically isolated neural rosettes and cultured in N2 medium with BDNF; ventral telencephalic patterning by adding SHH and DKK1. 3. Neuronal maturation by adding VPA and dbcAMP in low density conditions.	- In vitro: ICC and Q-PCR from 0 -60 DIV; rosette formation appeared around 21-23 DIV in contrast the Oct4 and Nanog which disappeared. - DIV 29-30 Nestin+, PAX6+, and Ki67+; BF1+ expression reached a plateau. GSH2 and DLX2 peaked with the addition of BDNF, SHH, and DKK-1. - DIV 46-59 to DIV62-72: within the Map2+ population were found ~36% GABA+, 53% DARRP32+, 10% calbindin+, 55% calretinin, ≤2% TH+, persistent expression of Nestin+ and PAX6+; Q-PCR showed increased expression of DARRP32, GAD67, and calbindin. -Overgrowth of surviving graft.
Ma et al 2012, Cell	hES (H1 and H9)	- 3 steps: 1. Neural induction: hES cells were differentiated to NE for 10-12 days in NI medium.- 2. Induced ventral progenitors by adding SHH 200 ng/ml or purmorphamine 0.65 µM from day 12-26. To generate spinal GABA neurons, RA 0.1 µM was added from day 10-23. 3. Neural differentiation: NPCs were dissociated with accutase and re-plated onto coated coverslips at day 26 in neurobasal medium supplemented with BDNF 20 ng/ml, GDNF 10 ng/ml, IGF 10 ng/ml, and cAMP 1 µM.	-In vitro: 32 DIV 93% were neurons based on phase contrast and β-II tubullin+ analysis. 90% of these cells were GABA+ of which 89% also express DARRP32. - HPLC revealed that the GABA+ neurons responded to high-potassium solution (which depolarizes neuron) gave rise to 6 times increasing of GABA- level release. -70 DIV whole cell patch-clamp: 16 out of 18 GABA expressing neurons present active neuron characteristic firing action potentials - Transplantation into QA-lesioned mice: 4 mth after transplantation forebrain neurons (FBN) and spinal neurons (SBN) grafts did not overgrow. 62%-80% of the FBN and SBN grafts respectively were GABA+ neurons. Only FBN grafts expressed Meis2+, Ctip2+ and DARRP32+ (the latter comprising 58.6%± 3% of total graft cells)

Author	Cell lines	Methods	Results
Delli Carri et al. 2013, Stem cell Rev and Rep 2013, Development and Stem cells	hES/iPS cells	3 steps -inhibit the TGF-β/BMP pathway for neural induction - patterning: SHH and DKK1 for ventral telencephalic specification - Human PS cells have been exposed to DUAL-SMAD inhibitor Noggin (interchangeable with BMP inhibitor--Dorsomorphin/ Noggin analog--LDN193189) and SB. - Neural induction by Dual-SMAD inhibitor and also attain FOXG1+ and OTX+. - Ventral telencephalon introduction by applying SHH with WNT signalling modulation pathway- DKK-1. - Terminal differentiation uses the increasing concentration of BDNF from 30 - 50 ng/ml.	ICC- Day15-25: FOXG1+, GSX2+ -Day 45: Ctip2+, FoxP1+, FoxP2+ -maturation: GABA+,Map2+ -Day 80: 20% co-expressing with DARRP32 and Ctip2 (D2 and A2a receptor); 80% GABA+ Ctip2+, Calbindin+ - Electrophysiological properties: 57% exhibited repetitive firing, 30% elicited a single action potential, 13% not respond - FOXP1+/FOXP2+/CTIP2+/calbindin+/DARRP32+ MSNs - TX cells differentiated to DARRP32+ and restoration of apomorphine-induced rotation behaviour in QA lesion rats - Within MAP2+ population: contain 78% GABAergic cells, CTIP2+/calbindin+; 20% DARPP32 and Ctip2 co-expression.

The Project Aim:

The ultimate aim of this study is to explore an alternative cell source which is suitable in term of practical and ethical usage with a potential to be a donor cell source for cell therapy in HD. An iPS cell line has been considered as an attractive cell source for degenerative and regenerative medicine after the first recovery in 2006. Therefore, we aim to generate a clinical safe iPS cell line and explore various fetal tissues as a suitable originated cell source. The source material used to generate the iPS cells was human fetal derived and two sorts of lines were generated: one from human fetal WGE (developing striatum), and one from fetal fibroblasts. This has allowed comparisons to be drawn between the two sources in terms of their ability to generate iPS cell lines and differentiate into mature MSNs. As highlighted above there are a number of options available in terms of protocols to generate these cells. Here I explore two of these protocols and highlight the advantages of using the *piggyBac transposon* deliver system over the plasmid DNA approach. From an early time point it was clear that the plasmid DNA approach was not going to be a viable route and hence the emphasis of this thesis is on the *piggyBac* method. The iPS cells generated using this approach were also compared with human ES cells in terms of morphology, pluripotent marker expression, gene expression profiles, *in vitro* and *in vivo* differentiation.

In term of ES/iPS cells derived MSNs, there are only few protocols available with the low efficiency to generate functional MSN. I report a novel protocol which has been improved to increase the efficiency of MSNs conversion with less time expense *in vitro* differentiation base on previous published papers. I show that these ES/iPS cells can differentiate to a desired MSN phenotype with a typical of DARPP32 positive expression. In addition, the ES/iPS cells derived MSN can survive transplantation, further differentiate, and maturate in a QA-lesioned HD model rat brain.

Chapter 2
Materials and Methods

2.1 In vitro Methods.

Mouse and Human Embryonic Fibroblasts (MEFs and HEFs) Maintenance methods.

2.1.1 Derivation of mouse embryonic fibroblasts (MEFs).

MF1 pregnant mice were sacrificed by cervical dislocation on embryonic day E13.5. The abdomen was cleaned with 70% alcohol and a cut through the skin and peritoneum was made to expose the uterine horn. The uterine horn was removed and placed onto an untreated bacteriological grade petri dish (Sterilin®, Newport, UK) containing Hank's Balanced Salt Solution (HBSS, Life Technologies®, Paisley, Scotland, UK). The embryonic sac was cut and the embryos were removed from the sac. The embryos were de-capitated and visceral organs removed. The remaining carcases were washed in Dulbecco's Modified Eagle Medium: Nutrient Mixture F-12 (DMEM/F12, Life Technologies®), placed in a clean petri dish, and then minced with a sterile scalpel blade. 0.05% Trypsin:EDTA (Life Technologies), 2 ml, was added to the tissue and incubated for 20 minutes at 37°C. DMEM/F12, 5 ml, was added to the petri dish and the tissue suspension was transferred to a 15 ml centrifuge tube and centrifuged at 86.64 g for 3 minutes. The supernatant was removed; the tissue was manually triturated in 400 µl DMEM/F12 using a 200 µl pipette until a quasi-single cell suspension was obtained. 1ml cell suspension was added to each 140 mm Nunc™ cell culture petri-dish (Thermo Scientific™,Bishop Meadow Road, Loughborough) followed by 19 ml of MEF media (DMEM high glucose (GE Healthcare Life Science, Buckinghamshire, UK) 450 ml, 10% Fetal Bovine Serum (FBS, Life Technologies®), 1% Penicillin and Streptomycin (PS, Life Technologies®), 1% L-Glutamine (Life Technologies®) and placed in the incubator at 37°C overnight. Next day, the spent medium was taken off to remove the floating cellular debris and replaced with fresh MEF media. MEFs were allowed to proliferate with a change in medium every other day until the MEFs reached 70-90% confluence.

Maintenance and Passaging of MEFs.

MEFs were cultured in MEF medium. Once the MEFs reached 80-90% confluency, they were washed once with 1X phosphase buffer saline (PBS) (Life Technologies). Trypsin:EDTA, 1 ml, was added to the culture plate and swirled to ensure that all the plate was covered. The plate was then incubated 37˚C for 5 minutes. 10 ml of MEF media was added to the plate to inactivate the Trypsin:EDTA reaction and a pipette was used to triturate and dislodge any remaining cells. The MEFs suspension was transferred to a 50 ml centrifuge tube and centrifuged at 86.64 g for 3 minutes. The supernatant was aspirated off before the pellet of cells was dispersed by gently flicking the bottom of the falcon tube. The MEFs were split 1:4 with 1 ml of MEF cell suspension added to 19 ml MEF medium in a 140 mm cell culture treated petri dish. The MEFs were well distributed over the culture plate and incubated in 5%CO_2 at 37˚C.

Freezing MEFs

The spent culture medium was removed from the culture plate and washed once with 5 ml 1XPBS. Trypsin:EDTA, 1 ml, was added to the culture plate and incubated at 37°C for 5 minutes. Gentle tapping was used to help dislodge the MEFs from the dish. DMEM/FBS 9 ml, was loaded onto the plate to wash and remove the MEF from the culture dish. The cell suspension was then transferred to a 15 ml centrifuge tube and centrifuged at 86.64 g for 3 minutes. The supernatant was removed before the cell pellet was dispersed by gently flicking the tube. The pellet was re-suspended in 500 µl ice-cold MEF freezing medium (10% Dimethyl Sulfoxide (DMSO, Sigma, Gillingham, Dorset, UK) in MEF medium) and then transferred to a cryovial (Thermo Scientific™). Cryovials were packed into a freezing container and kept in the -80˚C freezer. The cryovials were transferred to liquid nitrogen the next day for long term storage.

Thawing MEFs.

The cryovial cap was loosened to release the trapped nitrogen after removing the cryovial from the liquid nitrogen. The bottom half of the cryovial was placed in a water bath at 37°C until a small ice crystal could be observed. The cells were gently transferred to 10 ml MEF medium in a 15 ml centrifuge tube and

obtain centrifuged at 86.64 g for 3 minutes. The cell pellet was re-suspended in 10 ml MEF medium before being transferred to a 10 cm culture dish and incubated at 5% CO_2 and 37°C.

MEFs Irradiation.

MEFs were irradiated after 3 passages in culture. MEF media was aspirated off from the culture plates, and 10 ml of 1XPBS was flooded onto the plate to wash off the old medium. 1 ml 0.05%Trypsin:EDTA was added and swirled around the plates after removing the PBS. After 5 minutes or until the cells started to separate from the plates, 5 ml MEF media was added to stop the trypsin reaction. All media and cells were pipetted into a 50 ml centrifuge tube and centrifuged at 86.64 g for 3 minutes. The supernatant was aspirated off; 20 ml MEF media was added and a Gilson pipette was used to thoroughly mix the cell suspension. 10 µl of suspension was mixed with 10 µl trypan blue (Life Technologies®) and then cells were counted using a haemocytometer with Countess® Automated Cell Counter (Life Technologies®). Cells were irradiated for 30 minutes at 216 Rads/minute for total exposure of 6480 Rads. Irradiated cells were centrifuged for 3 minutes at 86.64 g, re-suspended with MEF freezing media, and aliquoted cells into prepared cryovials ($1x10^6$ cells per vial in 1 ml) before placing in a cyrobox at room temperature. The vials were placed in the -80˚C for 24 hours before transfer to liquid nitrogen for long-term storage.

2.1.2 Derivation of human embryonic fibroblasts (HEFs).

Human fetal tissue was collected according to Kelly et al., 2011, following local research ethics committee approval (02/4446 post mortem human fetal tissue for neural transplantation in HD (and PD)) and under the guidelines of the Polkinghorne report (Polkinghorne, 1989) and the UK Department of Health (Department of Health, 1995), with full ethical consent from the maternal donor, under the South Wales initiative for transplantation in HD (SWIFT-HD) program. The embryo was washed once with 1XPBS, de-capitated and the visceral organs removed into a DMEM/F12 filled-culture dish. The torso was placed onto the sterile petri dish and minced with a sterile blade. Human fibroblasts were obtained by adding DMEM/F12 to re-suspend the cells before transferring to a 15 ml tube.

The tube was centrifuged at 86.64 g for 3 minutes in order to collect the fibroblasts' pellet. The supernatant was aspirated off and the pellet was re-suspended in 10 ml HEF medium (Minimum Essential Media- GlutaMAX™-I (MEMα, Life Technologies®), 20% FBS, 1% PS, 1% MEM Non-Essential Amino Acids Solution (Non-essential Amino Acid (NEAA), Life Technologies®)). HEFs were transferred to a 10 cm 0.1%gelatin-coated culture plate and were allowed to expand at 37°C. HEF medium was changed the next day to get rid of debris and dead cells.

Maintenance and Passaging of HEFs.

HEFs were maintained in HEF medium. At 80-90% confluency, HEFs were washed once with 1XPBS, incubated at 37˚C for 5 minutes in 0.05%Trypsin:EDTA, harvested from the culture dishes following addition of HEF medium and centrifuged at 86.64 g for 3 minutes. The supernatant was aspirated off and the resulting pellet was re-suspended in 4 ml HEF medium. The cell suspension, 1 ml, was re-seeded onto gelatin-treated tissue culture petri-dishes filled with 9 ml HEF medium and incubated at 37°C.

Freezing HEFs.

HEFs were frozen as per the protocol described above for MEFs.

Thawing HEFs.

HEFs were thawed as per the protocol described above for MEFs.

Primary Human Fetal Cell Maintenance methods.

2.1.3 Human Neural Stem Cell.

Dissection and preparation of human primary fetal cells.

Human fetal tissue was collected according to Kelly et al., 2011. WGE, cortex and skin tissue were dissected by a member of the brain repair group (BRG). Each donor sample is referred to by its SWIFT (South Wales Initiative for Fetal Transplantation) number (a unique identifier used for anonymity), however clone C9 referred to throughout the text is in fact derived from SWIFT 623, all other clones are referred to by their SWIFT number. The cortex and ganglionic

eminences were dissected according to Dunnett and Bjorklund (1992) (Figure 2.1 and 2.2). Dissected tissue pieces were collected using a Pasteur pipette and left to descend in 15 ml Hibernate®-E CTS™ medium (Life Technologies®). The Hibernate®-E CTS™ medium was removed and 400 µl DMEM/F-12 plus 1% PS was added to wash the tissue 2 times. 400 µl 0.1% trypsin (Worthington) was added to the tissue and incubated at 37°C for 20 minutes. 0.05% DNAse (Sigma) was then added to the tissue. The tissue was again incubated at 37°C for a further 5 minutes.

To dilute the enzymes, 10 ml DMEM/F-12 with 1% PS was added to the tissue and centrifuged at 86.64 g for 3 minutes. The media was aspirated off; the remaining pellet was re-suspended in 400 µl DMEM/F-12 and manually triturated using a 200 µl Gilson pipette (10-15 strokes). To assess cell viability, 10 µl cell suspension was taken and counted using 0.4% trypan blue exclusion assay and a disposable haemocytometer with Countess® Automated Cell Counter (Life Technologies®). Cell number was calculated according to the formula (live cells counted/1000 (as data is given per ml)/10 x dilution factor = cells/µl cell suspension). Total number of cells can be determined based on final volume.

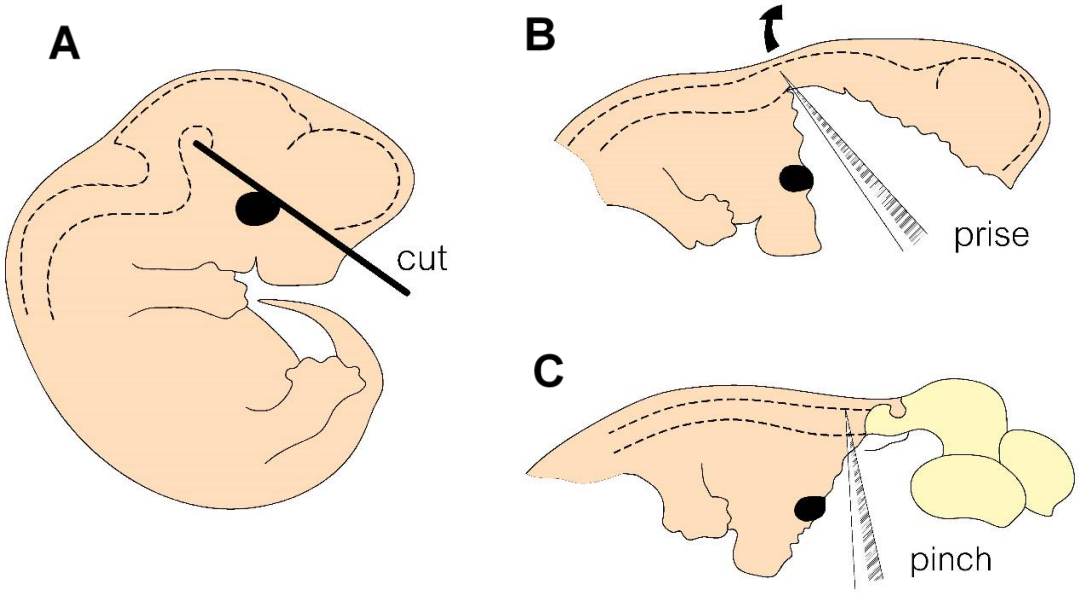

Figure 2.1 the brain removal: The embryo is cut from the front above the eye and the ventral mesencephalic flexure. A fine forcep is used to peel off the skin and meninges which covering the whole brain (B). The brain is pinched and pulled gently away from the body (C) (Adapted from Dunnett and Bjorklund, 1992).

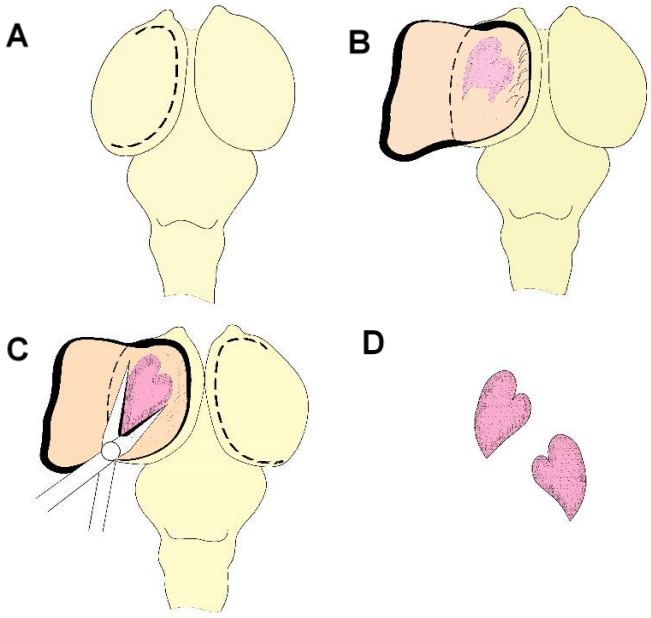

Figure 2.2 Dissection of the striatal and cortical eminences: the medial cortex is cut in a longitudinal line (A), the striatum is then exposed at the area on the floor of the lateral ventricle (B). Iridectomy scissors are used to cut and gently remove the striatum from both hemispheres (C, D). (Adapted from Dunnett and Bjorklund, 1992).

Neuronal differentiation culture.

Sterile 13 mm glass cover slips (Appleton Woods, Birmingham) were placed into each well of a 24 well Nunc™ cell-culture treated multidishes (Thermo scientific) 500 µl Poly-L-Lysine hydrobromide solutions (PLL) (100 µg/ml, Sigma) was added to each well. The plate was left in the fridge at 4°C overnight. PLL was aspirated off and the coverslips washed 3 times with sterile water, and then left to dry under the UV light for 45 minutes.

For neuronal differentiation culture, cells were plated at 100,000 cells per coverslip in 30 µl of neuronal differentiation medium (DMEM/F12, 1% FBS, 1% PS, 2% B-27® Supplements (Life Technologies®)). The cells were allowed to settle on the PLL coated coverslips for at least three hours at 37°C, and then 500 µl neuronal differentiation medium was gently added to each well. Cells were incubated at 37°C in humidified 5%, CO_2, 95% atmospheric air, and were left to

differentiate for 7-14 days. 500µl of fresh differentiation medium was replaced in each well every 2-3 days.

Proliferation of human primary fetal neural stem cells.

To culture neural cells (neurospheres), 200 cells per µl were added to T25 flasks (Thermo Scientific™) with 10 ml proliferation medium (DMEM/F12, 1% PS, 2% B-27®, 20 ng/ml FGF2 (R&D), 20 ng/ml epidermal growth factor (EGF) (Sigma) and were maintained at 37°C. Fresh proliferation medium 5 ml, with 2 times concentration of growth factors, replaced 5ml of old medium every 2-3 days.

Passaging of primary human fetal expanded cells.

Passaging of neurospheres was undertaken when the spheres increased 2-3 folds in size with more packed and dense cells inside, approximately 14 days in the case of human tissue. Neurospheres and their medium were taken up into a 15 ml centrifuge tube and centrifuged at 86.64 g for 3 minutes. The medium was aspirated off and the pellets were re-suspended by adding 400 µl of trypsin and kept in the incubator at 37°C for 20 minutes. 400 µl DNAse was added and the pellets were returned to the incubator at 37°C for further 5 minutes. DMEM/F12 10 ml was added into the centrifuge tube. The tube was centrifuged at 86.64 g for 3 minutes, the media aspirated off and 400 µl DMEM/F12 plus 1% PS was added to the cells that were manually dissociated using a 200 µl Gilson pipette (10-15 strokes) into a quasi single cell suspension. Trypan blue was used with the countess cell counter to assess cell viability as explained above. Cells were plated into 24 well plates, as described above, or expanded in 10 ml of proliferation medium at the concentration of $2x10^6$ cells per T25 flask.

Pluripotent Stem Cell (PSC) Maintenance and differentiation.

2.1.4 Human ES and iPS cell Methods.

Thawing human ES and iPS cell.

A vial of human ES/iPS cells was removed from liquid nitrogen and immediately placed on ice. The lid was slowly loosened to emit the trapped nitrogen. The lower half of the cryovial was then immersed and swirled around in a water bath at 37°C until the cells' solution was defrosted. The content was gently

transferred to a 15 ml centrifuge tube containing 10 ml of pre-warmed human ES/iPS medium in a drop by drop fashion and centrifuged at 21.66 g for 3 minutes. The supernatant was aspirated; the cell pellet was dispersed by gently flicking the tube. 5 ml human ES/iPS (Knock out DMEM/F12 (Life Technologies®), 20% Knock out serum replacement (KSR, Life Technologies®), 1% L-Glutamine/β-mercaptoethanol solution (Life Technologies®), 1% NEAA, 0.8 ng/µl bFGF (R&D systems, Abingdon, Oxfordshire, UK) media was added to the cell pellet and then transferred to a MEF feeder plate which had been washed once with 1XPBS. Cells were cultured in the CO_2 incubator at 37˚C, and fed once every day, by removal of old medium and addition of fresh medium.

Maintenance and Passaging of human ES/iPS cell culture.

Once human ES/iPS cell reached confluence, 5 ml human ES/iPS cell media was replaced with fresh human ES/iPS medium 2-3 hours before passaging to nurture the cells. After discarding the culture medium and washing with 5 ml of PBS. Collagenase IV medium (1% Collagenase IV (Life Technologies®) in K/O DMEM), 2 ml, was added to the cells; the plate was then returned to the incubator for 20 minutes until the edges of the human ES/iPS colonies start to curl. The collagenase was removed and cells were washed once in 1XPBS before addition of 3 ml human ES/iPS media to the cells. The ES/iPS colonies were manually picked using a sterile pulled glass pipette to cut around the edges of human ES/iPS colonies as well as cut the ES/iPS colonies into smaller pieces. Floating colonies were collected in a 15 ml centrifuge tube and centrifuged at 21.66 g for 3 minutes. The media was aspirated off and replaced with 5 ml ES/iPS cell medium then transferred to a fresh 1xPBS pre-washed plate of MEFs in ES/iPS medium and incubated.

Freezing human ES/iPS cell.

Three days after passaging, human ES/iPS cells were flooded with fresh human ES/iPS medium 2-4 hours before freezing down. The culture medium was removed from the culture petri dish and washed once with 1XPBS. PBS was removed from the culture petri dish and 2 ml 1%collagenase IV was added to the plate. The plate was returned to the incubator at 37°C for 20 minutes or until the

edges of human ES/iPS colonies started to curl. The collagenase IV medium was aspirated off from the culture plate and 5 ml of ES/iPS medium was added to the culture plate. The colonies were manually cut around the edges and separated from the MEFs using a sterile needle. The ES/iPS cells were transferred to cryovial with 200 µl freezing medium (10% DMSO in human ES medium). Cells from 1 well of a 6 well plate were distributed to 3 cryovials. The cryovials were then placed into a freezing container and kept in -80°C. The day after, cryovials were moved to liquid nitrogen for the long term storage.

2.1.5 PSC derived neuronal cells.

Neural induction EB-Based Method (Figure 2.3).

The human ES/iPS colonies were lifted from feeder cells using collagenase type IV medium, manually cut to smaller pieces and picked. Human ES/iPS colonies were cultured as free-floating EBs in untreated bacteriological grade petri dishes in human ES/iPS medium without bFGF supplement for 2 days. For initiation of the neural induction protocol EBs were harvested and transferred into KSR medium (K/O DMEM/F12, 10% KSR, 1% L-Glutamine/β-mercaptoethanol, 1% NEAA, 1% PS) with addition of 10 µM SB431542 (Tocris Bioscience, Bristol, UK), 200 ng/ml Noggin (R&D systems), 200 nM Dorsomorphin (Tocris), 100 ng/ml SHH (R&D systems) and 100 ng/ml Dickkopf-related protein 1 (DKK-1, R&D systems). Medium was changed every other day for 5 days. The EBs were harvested and transferred to N2B27 medium (1:1 ratio Neurobasal medium to Dulbecco's Modified Eagle Medium/Ham's F-12 (Advanced DMEM/F12, 1% N-2 supplement, 1% B-27®, 0.5% PS, 0.5% Glutamax™ (all from Life Technologies®)) with addition of the previously described supplements for further 5 days. At day 10, EBs were harvested and re-attached onto Corning® Matrigel® Basement Membrane Matrix (Matrigel®, USA) in N2B27 medium, which was subsequently changed every other day.

Around day 12-16, neural rosette structures were recognized and these were passaged (passage 1) between days 16-22 by incubating with Accutase® (Sigma) for 5-7 minutes at 37°C and dissociating as a single cell suspension. Then DMEM/F12 10 ml was added and cells were centrifuged at 86.64 g for 3 minutes. After aspirating off the supernatant, cells were re-suspended in 400 µl

N2B27 medium with ROCK inhibitor 10 µM (Y-27632, MERCK Millipore). Cells were counted and re-plated onto PLL/POL/Laminin (Poly-L-Ornithine, Sigma; laminine, PeproTech) pre-treated coverslips at 100,000 cells/coverslip in 24 well-plate and $1x10^6$ cells/well of a 6-well tissue culture plate in previous mentioned supplement. The media was changed every other day and an additional 25 ng/ml recombination human Activin A (PrepoTech) was added to culture medium around day 20.

Cells were subsequently passaged (passage 2) and re-plated onto PLL-POL-Laminin pre-coated plate/coverslips 9 days later with afore described method and culture medium.

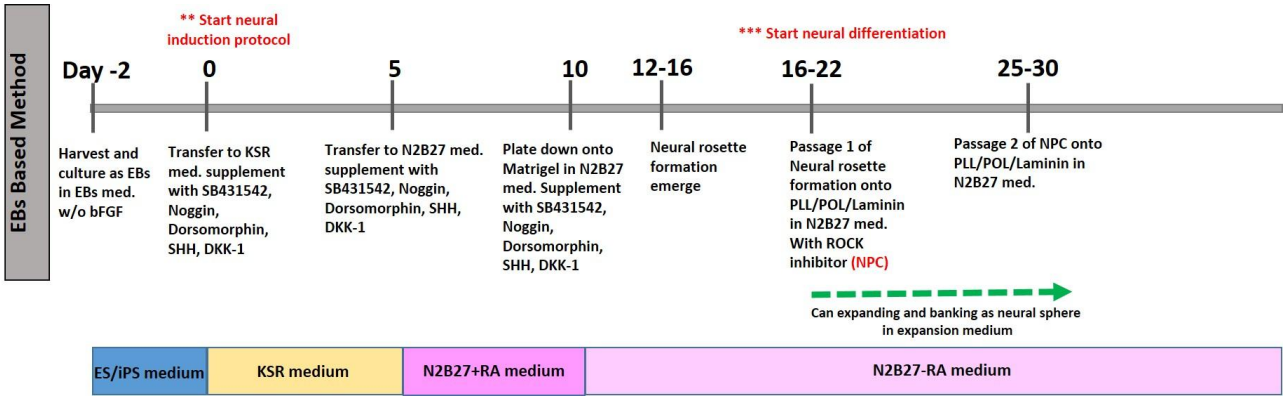

Figure 2.3 Time line of neural induction from PSC using EBs-Based method which is described in section above. (EB= embryoid body, NI medium= neural induction medium, NPC= neural precursor cell)

Neural induction Monolayer-Based Method.

Human ES/iPS cells at 70-80% confluency were passaged as cell clumps and distributed from 1 well of a 6 well-plate in 1:3 ratio (~20-25% each well). Cells were re-attached onto 9 mg/ml Geltrax® matrix (Life Technologies®) coated 6 well-plate and cultured in ES/iPS medium. The day after, medium was changed to neural induction medium (NI medium, Gibco®, Paisley, Scotland, UK). Full medium changing was performed every other day for 7 days until the cells reached 80-90% confluence. Cells were passaged (passage 1) as a single cell suspension by incubating with 1 ml Accutase® for 5-7 minutes. NI medium 9 ml was added; cells were passed through the cell strainer and centrifuged at 86.64 g for 3 minutes. Cells were cultured in NI medium and adhered onto Geltrax® coated tissue culture dish at $2.5\text{-}3.0x10^5$ cells/well of 6-well plate. Between days 10-14, cells were dissociated again (passage 2) (using the previously described method). Cells were

passaged again (passage 3) between days 16-22, when they were plated onto PLL-POL-Laminin pre-treated tissue culture plates/coverslips in neural expansion medium (1:1 ration NI medium and Advanced™ DMEM/F12). From this stage cells were be able to be expanded and banked as NPCs (Figure 2.4).

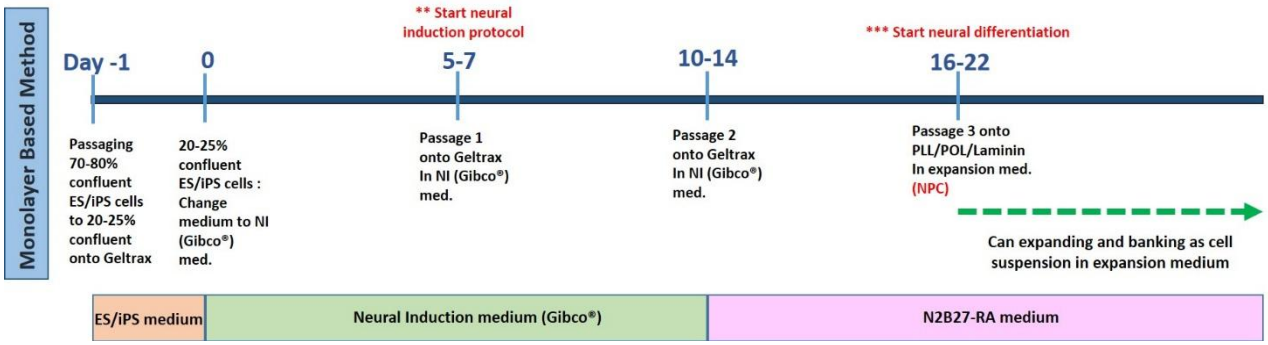

Figure 2.4 time line of neural induction from PSCs using Monolayer-based method which described in section above.

Neuronal Differentiation.

NPCs were maintained in N2B27 medium (1:1 ratio Neurobasal medium to Advanced™ DMEM/F12, 1% N-2, 1% B-27®, 0.5% PS, 0.5% Glutamax™) with change in the combination of neurotrophic factors, small molecules, and growth factors at different days, (Figure 2.5). The differentiation protocol to derive MSN-like cells is further described in detail in Chapter 5.

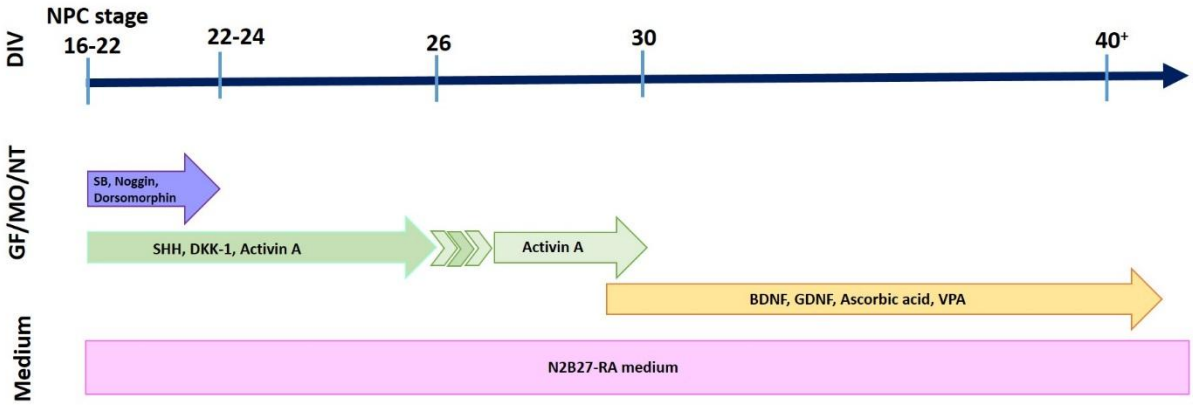

Figure 2.5 Time line of PSC differentiation toward MSN liked-phenotype.

Immunocytochemistry and Microscopy.

2.1.6 Cell Fixation and Immunocytochemistry.

After 7-14 days of neuronal differentiation, cells were washed for 3 minutes using 1x PBS. Cells were fixed with 4% paraformaldehyde (PFA) for 20 minutes;

then washed with PBS three times for three minutes each. Ethanol 100%, was added to permeabilise the cells for 2 minutes and then followed by 3 washes in PBS for 3 minutes each. Cells were submerged in 300 µl blocking serum (1% Bovine Serum Albumin (BSA) (life technologies®) in 1XPBS, 2% appropriate normal serum) to prevent non-specific antigen binding for one hour. Blocking solution was replaced by primary antibodies (isolated and raised from different species to the blocking serum) which were made up in blocking solution at the appropriate concentrations (Appendix C). The cells were incubated overnight in primary antibody at 4°C for double labelling, it is essential that the primary antibodies were raised within different species.

The primary antibody was removed and cells were washed 3X3 minutes with PBS. Secondary antibody (Alexa-Fluor fluorescent labels anti mouse 594 (Red) and anti-rabbit 488 (Green) (Life Technologies®)) was made up in the same blocking solution as primary antibody and added at the concentration of 1:200. Cells were left in the dark by covering the plate with aluminium foil at room temperature for two hours. The secondary antibody was removed and the cells were washed 3 times with 1x PBS. 300 µl Hoechst (Sigma) nuclear staining solution was added for 5 minutes followed by rinsing 3 X 3 minutes with 1X PBS. The coverslips were gently placed onto a glass slide in mountant (PBS: Glycerol, 1:1) and kept at 4°C overnight. The coverslips were sealed with clear nail varnish at the edge of each coverslip; all slides were stored in the dark at 4°C in order to protect from photo bleaching.

2.1.7 Microscopy.

Leica DMRBE Microscope was used to visualize cultured cells under different UV fluorescence wave length (red= 594 nm, green= 488 nm, blue= 346 nm). Photos were taken using Leica image software program.

2.2 Molecular methods.

2.2.1 RNA Extraction and Quality check

The Qiagen RNAeasy mini kit and QiaShredder (both Qiagen, Skelton House Lloyd Street North, Manchester) were used to do the RNA extraction following the manufacturer's protocol. The concentration of RNA was determined using NanoDrop® ND-1000 Spectrophotometer (Thermo Scientific™) (Appendix E).

2.2.2 cDNA synthesis

cDNA synthesis was performed using 1 µg RNA and SuperScript® Reverse Transcriptase II (Life Technologies®) following the manufacturer's protocol from Invitrogen (Appendix E).

2.2.3 Polymerase Chain Reaction (PCR)

The PCR reaction was carried out using a PTC-100™ programmable thermal controller (MJ Research, Inc.). The primer sequences used to generate reprogramming factors and CPP are shown below, according to Kim et al (2009). The optimized RT-PCR programmes are shown in table 2.2.

Primers	Primer sequences
Hu Oct4 F	GGATCCGAATTCATGGCGGGACACCTGGCTTCAG
Hu Oct4-9R R	AAAAAAGTCGACGCGGCGTCTGCGTCTGCGGCGTCTGCGGTTTGAATGCATGGGAGAGCC
Hu Oct4-9R R XhoI	AAAAAACTCGAGGCGGCGTCTGCGTCTGCGGCGTCTGCGGTTTGAATGCATGGGAGAGCC
Hu Sox2 F	GGATCCGAATTCATGTACAACATGATGGAGACGG
Hu Sox2 9R R	AAAAAACTCGAGGCGGCGTCTGCGTCTGCGGCGTCTGCGCATGTGTGAGAGGGGCAGTG
Hu Klf4 F	GGATCCGAATTCATGGCTGTCAGCGACGCGCTGC
Hu Klf4 9R R	AAAAAACTCGAGGCGGCGTCTGCGTCTGCGGCGTCTGCGAAAGTGCCTCTTCATGTGTAAGGC
Hu c-Myc F	GGATCCGAATTCATGCCCCTCAACGTTAGCTTCAC
Hu c-Myc 9R R	AAAAAACTCGAGGCGGCGTCTGCGTCTGCGGCGTCTGCGCGCACAAGAGTTCCGTAGCTGTTC
RFP F	AATGACCTCGAGATGGCCTCCTCCGAGGACGTCAT
RFP R	GAAAACCTCGAGTTACAGGAACAGGTGGTGGCGGCCCTC
RFP 9R F	AATGACCTCGAGATGGCCTCCTCCGAGGACGTCAT
RFP 9R R	GAAAACCTCGAGGCGGCGTCTGCGTCTGCGGCGTCTGCGCAGGAACAGGTGGTGGCGGCCCTC
Hu Oct4- R	AAAAAAGTCGACGTTTGAATGCATGGGAGAGCC
Hu Oct4- R XhoI	AAAAAACTCGAGGTTTGAATGCATGGGAGAGCC
Hu Sox2 R	AAAAAACTCGAGCATGTGTGAGAGGGGCAGTG
Hu Klf4 R	AAAAAACTCGAGAAATGCCTCTTCATGTGTAAGGC
Hu c-Myc R	AAAAAACTCGAGCGCACAAGAGTTCCGTAGCTGTTC

Table 2.1 Primer sequences for PCR programme for amplification of the reprogramming factors Oct4, Sox2, Klf4, cMyc, as well as RFP and CPP.

Step	RFP		RFP-9R		OCT4		Nanog	
	Temp. (°C)	Time	Temp. (°C)	Time	Temp. (°C)	Time	Temp. (°C)	Time
1. Primary denature	98	60 sec	98	60 sec	94	2 min	94	2 min
2. Cycle denature	98	15 sec	98	15 sec	94	15 sec	94	30 sec
3. Primer annealing	75	90 sec	72	90 sec	55	20 sec	58	30 sec
4. Primer elongation	72	5 min	72	5 min	72	1 min	72	30 sec
5. Go to step 2 x amount of cycles (times)	75	23	72	19	72	30	72	30

Step	Sox2		Lin28		cMyc		Klf4	
	Temp. (°C)	Time	Temp. (°C)	Time	Temp. (°C)	Time	Temp. (°C)	Time
1. Primary denature	94	2 min	94	2 min	94	2 min	94	2 min
2. Cycle denature	94	15 sec	94	30 sec	94	15 sec	94	30 sec
3. Primer annealing	50	20 sec	58	30 sec	55	20 sec	58	30 sec
4. Primer elongation	72	1 min	72	30 sec	72	1 min	72	30 sec
5. Go to step 2 x amount of cycles (times)	72	34	72	30	72	30	72	30

Table 2.2 Table presenting an optimized RT-PCR programme for amplification of PCR product.

2.2.4 PCR Product Purification Protocol using Microcentrifuge.

PCR product was cleaned of any remaining buffers and salt using the PCR purification kit (Qiagen). The protocol was carried out as per the manufacturer's guide. All products were eluted in 30 µl H_2O and stored at -20^{0}C (Appendix E).

Reagents	Volume added (µl)
1. Buffer PBI	1x volume of PCR reaction
2. Buffer PE	750
3. Buffer EB or water	30-50

Typical reaction using the Qiagen PCR clean up kit.

2.2.5 DNA Extraction from Agarose gel

Linearised vector was purified by running on a 1% agarose gel at 110 volt for 1 hour, on confirmation of size, the DNA fragments were excised from the gel with a clean sharp scalpel and purified according to gel purification kit (Qiagen). DNA was eluted in 30 µl H_2O and stored at -20^0.

Reagents	Volume added (µl)
1. Buffer QG	3x volume of gel slice
2. Isopropanol	1x volume of gel slice
3. Buffer QG	500
4. Buffer PE	700
5. Buffer EB	30-50

Typical reaction using the Qiagen gel purification kit.

2.2.6 Subcloning pcDNA 3.1 myc-His A with RFP/RFP-9R/Oct4 reprograming gene.

The reactions as described in the table below were prepared on ice at all times.

Reactions	Volume added (µl)	
	Insert DNA (RFP/RFP-9R/Oct4)	VECTOR
1. Nuclease free water	6	6
2. 10X Buffer D	2	2
3. Insert DNA product	10 (33 ng)	-
4. pcDNA 3.1 myc- His1	-	10(100 ng)
5. XhoI restriction enzyme	2	2
6. BSA	0.2	0.2
Total Volume	20	20

Reaction of insert DNA product and plasmid vector pre-treated before sub-cloning.

All solutions were added, thoroughly mixed in microcentrifuge tubes, and immediately incubated at 37°C for 2 hours and then at 65°C for a further 15 minutes in the heat block to denature the restriction enzyme. The tubes were centrifuged to collect all DNA solution; the inserted DNA was stored at -20°C.

The vector was further treated as the following described with shrimp alkaline phosphatase (SAP) so as to avoid re-circulisation. 100 ng of plasmid DNA

was added to the master mix solution (10x SAP Buffer 5 µl, nuclease free water 13 µl, SAP 2 µl). The tubes were centrifuged at 18603.52 g for 10-15 seconds and then incubated at 65^0C for 15 minutes.

The gene of interest was sub-cloned into plasmid vector as the following describes. DNA concentrations of an insert product and vector were determined using a NanoDrop® spectrophotometer. The values were inserted into the formula below.

$$\frac{\text{100 ng of vector x size of insert}}{\text{size of vector}} \times \frac{\text{insert 3 (ratios)}}{\text{vector1}} = \text{X ng of insert}$$

Solutions (µl)	Ligation reaction	Vector (control)	Insert (control)
1. Insert DNA	6	-	7
2. Plasmid DNA	1	7	-
3. Nuclease free water	1	1	1
4.10X T4 Buffer	1	1	1
5.T4 ligase	1	1	1
Total volume	10	10	10

Reaction of vector to insert DNA ligation.

2.2.7 Transformation and inoculation of plasmid DNA

The ligated plasmids were transformed into chemically competent TOP10 (Invitrogen) *Escherichia. coli* (E.coli) by heat shocking the bacteria from ice then transferred into sterile bacteriological tubes (Falcon, Becton Dickinson Labware, New Jersey, USA) containing pre-warmed SOC media (Invitrogen). Bacteria were incubated in a 4.54 g shaking oven at 37˚C for 1 hour. After cultivation, 50 µl of bacteria was plated onto ampicillin (100 µg/ml) LB (Luria-Bertani (DIFCO; Becton Dickinson)) selection agar plate. The remaining solution was transferred to 1.5 ml microcentrifuge tube and centrifuged at 4650.88 g for 3 minutes. 150 µl of supernatant was taken off and discarded; the pellet was re-suspended in the remaining medium and plated. The plates were incubated at 37˚C overnight. After this step, an individual colony was picked using an inoculation loop, and transferred to the tubes containing 5 ml LB medium containing ampicillin. The tubes were returned back to the incubator at 37°C for 12-16 hours on the shaker at 4.54 g (as per the protocol from Invitrogen) (Appendix E).

2.2.8 Purification of DNA (Plasmid Mini-prep (Qiagen))

The bacteria suspension was centrifuged at 1816.75 g for 3 minutes; the supernatant was poured off. DNA was purified using plasmid Mini-prep kit (Qiagen) following the manufacturer's instructions (Appendix E). DNA was eluted in 50 µl EB buffer and stored at -20^{0}C.

2.2.9 DNA digestion

The obtained DNA was digested for an analytical check by incubation with restriction enzyme, Xho I, 10x buffer D (Promega, Southampton, UK), and 10X BSA. Nuclease free water was added to make up the total volume to 10 µl. The solution was incubated at 37°C for 2 hours before heating the tubes at 65°C for a further 15 minutes. DNA was run for 1 hour at 110 volt on a 1% agarose gel plus SafeView nucleic acid stain to check the existence of inserted DNA by visualising against undigested DNA and DNA fragments.

To confirm the direction of the inserted DNA, the obtained DNA was cut by restriction enzyme Age I and AhD I. The reactions as presented in the table below were mixed on ice in microcentrifuge tubes. They were incubated at 37˚C for 2 hours and then a further 15 minutes at 65˚C. To examine the molecular weight of interested DNA, an appropriate amount and concentration of loading dye was mixed with the DNA, loaded on 1% agarose gel (added with SafeView) and run for 1 hour at 110 volt. The gel was viewed under UV light comparing 100 bp and 1 kb DNA ladder.

Typical reaction: Age I and AhD I Digest the pcDNA3.1-Myc/His A –RFP checking for the orientation of inserted DNA.

Solutions	**Volume (µl)**
1. DNA	4
2. Multicore Buffer	1
3. BSA	0.1
4. Water	2.9
5. Age I restriction enzyme	1
6. AhD I restriction enzyme	1
Total volume	10

2.2.10 Expanding *piggyBac* transposon (pPB-CAG.OSKML-puΔtk) and transposase (pCyL43/ pCyL50)

LB medium, 5 ml, and 150 µg/ml Ampicillin were added into 3 falcon tubes. The tubes were incubated at 37˚C for 1 hour before each agarose gel with samples were cut into small pieces and put into each falcon tube. The tubes were returned to the incubator and further incubated at 37˚C on maximum speed shaker for an hour. The medium were poured into each flask which contained 100 ml LB medium and 150 µg/ml Ampicillin, 100 µl. The flasks were incubated overnight at 37˚C on a maximum speed shaker (4.54 g).

2.2.11 Purification of DNA (Plasmid Midi-prep (Qiagen))

The bacterial suspension was harvested into a 50 ml falcon tube. The tube was placed into the Centrifuge 5810 R (eppendorf) at 4˚C to spin at 2616.12 g for 15 minutes. DNA was purified using the plasmid Midi-prep kit (Qiagen) following the manufacturer's instructions (Appendix E).

2.2.12 Transfection of human primary tissues using Lipofectamine®.

The day before transfection, human primary tissue or human cell line were plated into 6 well-culture plates at 500,000 cells each well. The cells were incubated at 37˚C in differentiation medium as mentioned without PS. The following day, 1 µg plasmid DNA was gently mixed with 100µl Opti-MEM® I reduced serum (life technologies®). Lipofectamine® was used according to manufacturer's instructions. Briefly, Lipofectamine® was prepared with Opti-MEM® (using 1:3 ratio of DNA: Lipofectamine®), and then stored at room temperature for 5 minutes. Both DNA and Lipofectamine® solutions were mixed and allowed to stand at room temperature for 30 minutes.

The differentiation medium was aspirated off cells and 1500 µl of the mixed DNA and Lipofectamine® solution was applied. The 6 wells plate were then incubated at 37˚C for 6 hours; and then, 1500 µl Opti-MEM® I reduced serum was added to each well for 24 hours.

2.3 In vivo methods.

2.3.1 Animal care, anaesthesia, and immunosuppression

All animal experiments were performed in compliance with local ethical guidelines and approved animal care according to the UK Animals (Scientific Procedure) Act 1986 and its subsequent amendments. Adult female Sprague-Dawley rats weighing 200-250 gm (Harlan, UK) were housed in cages of up to 4 animals in a natural light-dark cycle with access to food and water ad libitum.

All surgeries were performed under isoflurane anaesthesia which was induced in an induction chamber with 5% isoflurane and 0.8 L/minute oxygen. Passive inhalation of isoflurance 1-2 L/minute in a mixture of oxygen 0.8 L/minute and nitrous oxide 0.4 L/minute was maintained to keep anaesthesia during surgical procedures. Animals were recovered in 38°C recovery chamber and received analgesia by subcutaneous injection with 30 µl Metacam and 5 ml of 0.09% saline glucose. Animals were returned to their cages and monitored for weight and health for 3 days after surgery.

In xenograft transplantation experiments, animals received intra-peritoneal injection (i.p.) with immunosuppressant Cyclosporin A (CsA, Sandimmun, 10 mg/kg; Novartis, Hampshire, UK) the day before surgery and daily for the duration of the experiment.

2.3.2 Quinolinic acid (QA) lesion of the rat striatum

QA was dissolved in 0.1 M phosphate-buffer to make a 15 mg/ml (90 mM) solution and pH adjusted to 7.4. Animals received a unilateral injection of QA to the right striatum. Prior to surgery, animals were injected with 30 µl Metacam into the scruff. Then the skull was exposed and small burr holes drilled above the right striatum. QA 0.75 µl was injected via a cannula attached to a 10 µl Hamilton syringe driven by a mechanical pump at 2 sites for 3 minutes per site and 1.5 minutes each at 2 heights. The stereotaxic coordinates from bregma were -3.5/-2.8 mm medial-lateral (ML), -0.4/+1.0 mm AP, and -5.0/4.0 mm DV below dura mater. The syringe needle was left in place for 3 minutes at the lesion site following the infusion. After withdrawal of the needle, the incision was cleaned and

sutured. Animals received a 150 µl intramuscular injection of diazepam for sedative effect to prevent post lesion seizure.

2.3.3 Unilateral striatal transplantation

For cell transplantation into the adult rat striatum, 500,000 cells in 2 µl of neuronal differentiation medium (250,000 cells/µl) were administered at 2 depths using a Hamilton syringe with a bore diameter of 0.25 mm. Cells were injected into the lesioned right striatum using stereotaxic coordinates +0.7 mm (AP) and -3.1 mm (ML) from bregma and -4.5 mm and -3.5 mm (DV) for 1 minute at each site and the needle was left *in situ* for a further 3 minutes to minimize reflux of grafts along the needle tract. After the needle was withdrawn, the wound was sutured.

2.3.4 Perfusions and tissue sectioning

Animals were terminally anaesthetised by intra-peritoneal injection of sodium pentobarbital (Euthatal, Merial) and transcardially perfused with a prewash solution (PBS at pH 7.3) for 2 minutes followed by 4% PFA solution at pH 7.3 for 5 minutes. The brains were removed and transferred into 4% PFA overnight shaking at room temperature. The following day, the brains were placed into 25% sucrose in prewash solution until they sank. Brains were sectioned coronally at 40 µm thickness using a freezing-stage microtome. Sections were stored in 48-well plates in anti-freezing solution at -20°C.

2.3.5 Haematoxylin and Eosin (H&E)

The brain sections (1 in 12 series) were mounted onto glass microscope slides (coated with 1% gelatin) and air-dried overnight at 37°C. The sections were dehydrated and rehydrated in increasing levels of alcohol before being placed in xylene for 1 hour. Sections were then placed in 1% haematoxylin for 20 minutes followed by acid alcohol for 3 minutes and 1% eosin for around 20-45 seconds before being dehydrated in increasing concentrations of alcohol. The slides were placed in xylene before coverslipping with DPX mountant.

2.3.6 Immunohistochemistry on free-floating tissue sections with DAB.

1 in 12 series of brain sections were washed thoroughly in Tris buffered saline (TBS) (pH 7.4) quenched with 10% hydrogen peroxide and 10% methanol in distilled water for 5 minutes followed by 3 times washing in TBS for 5 minutes each wash. The sections were incubated in blocking solution (3% normal serum in 0.5% triton X-100 in TBS (Tx-TBS)). After discarding the blocking solution, primary antibodies were added at the appropriate concentration in 1% serum in Tx-TBS and incubated overnight at 4°C. Sections were washed 3 times for 10 minutes in TBS before addition of biotinylated secondary antibodies at 1:200 dilution in 1% serum in TBS for 2 hours and followed by another round of 3x10 minutes washes in TBS. Primary and secondary antibodies are listed in appendix C. Streptavidin ABC (A and B both at 1:200 dilution in 1% serum in TBS which prepared 30 minutes before use) was added for a further 2 hours. The sections were washed 3x10 minutes in TBS and rinsed with 0.05 M Tris non saline (TNS) pH 7.4 and positive staining was visualized using diaminobenzidine (DAB) staining at 0.5 mg/ml in fresh TNS with 12 µl hydrogen peroxide (brown). Finally, sections were washed twice in TNS before mounting on gelatin coated glass microscope slides. Sections were allowed to air dry and then dehydrated in increasing levels of alcohol, cleared in xylene and coverslips were mounted using DPX mountant.

For double staining with Vector® SG, the SK-4700 kit (Vector, USA) was used by mixing 10 ml TNS with 3 drops Chromogen and 3 drops hydrogen peroxide. The sections were washed in TNS buffer and incubated in Vector® SG solution until the desired level of staining is achieved (5-15 minutes). Sections were rinsed with TNS for 1 minute followed by washing in TBS 3 times for 5 minutes/wash. Free floating sections were mounted on slides and dried overnight before dehydration, clearing, and mounting as described above.

2.3.7 Immunofluorescence on free-floating tissue sections

The brain sections 1 in 12 series were washed with 1X Tx-PBS 0.5% (pH 7.4) thoroughly for 10 minutes x 3 times. The section were then permeated with 100% ethanol for 2 minutes and immediately washed with 1X Tx-PBS 0.5% 3 times for 5 minutes each time. After discarding the Tx-PBS 0.5%, blocking medium (1%BSA in Tx-PBS 0.5% and 2% normal serum) was added onto the sections and incubated at the room temperature for 1 hour on the shaker. Primary antibody was supplemented in the previously described blocking medium and added to the brain sections. The sections were then place at 4℃ and incubated overnight.

After overnight incubation, the sections were placed on the shaker for 1 hour at room temperature. The sections were washed 3 times for 10 minutes in PBS before addition of Alexafluor secondary antibodies at 1:200 dilution in blocking medium for 2 hours at room temperature followed by another round of 3x10 minutes washes in PBS. Hoechst (1:10,000 in 1XPBS) was added for 5 minutes and sections were rinsed twice with 1XPBS for 10 minutes/wash before mounting with fluorescence mounting medium (Dako) and coverslipped.

Chapter 3

Generation of iPS cells derived from primary human fetal tissue by direct reprogramming using *piggyBac transposon*.

3.1 Introduction

Several methods for the generation of iPS cells have been reported in the literature as outlined in the introduction to this thesis. Using primary fetal neural tissue from the developing striatum as the source material for the generation of such iPS cells and following on from the failures of the CPP method described in chapter 3, we chose to explore an alternative approach, the *piggyBac transposon* method. *piggyBac* transposon has been introduced as a highly effective gene transportation method. The *piggyBac transposons* take advantage of the fact that it can contain a large insertion, up to 10 kb, there is no genomic alteration in the host genome and there can be complete excision of the cargo with no footprint being left behind, resulting in generation of vector-free iPS cell lines (Kaji et al., 2009, Yusa et al., 2009; Woltjen et al., 2009). In addition, the *piggyBac transposon* has been reported to be highly active in mammalian and mouse cells (Cary et al., 1989; Yusa et al, 2009).

The resulting iPS cell-lines generated from MEFs have been indistinguishable from ES cells in terms of their pluripotent properties, proliferation and the production of chimeras (Yusa et al., 2009). In addition, the reprogramming efficiency was improved overall up to 1%, similar to the viral transfection method (Yusa et al., 2009).

Similarly, Woltjen et al, 2009 reported the generation iPS cell colonies using fibroblast cells as the starting material using the same approach; the *piggyBac transposon*. The resulting iPS cell-lines ticked all the boxes based on differentiation evaluations such as teratoma formation, production of chimeras and pluripotent marker expression (Woltjen et al., 2009; Yusa et al., 2009).

Here I report on a study carried out using the *piggyBac Transposon* method. iPS cell lines were generated from primary human primary fetal neural cells, fetal neurospheres and skin fibroblasts. The pluripotency of the cell lines was verified using a range of methods in vitro and compared to that of human ES cells.

3.2 Aims

The aim was to propagate a viral-free iPS cell line appropriate for transplantation in HD using the *piggyBac transposon* strategy. Specifically human fetal derived tissues were used as the starting material given the local availability of this tissue. The hypothesis behind this experiment was based on the notion that iPS cells generated from a specific starting material, in this case developing striatal tissue may be more readily able to differentiate back to this cells of this tissue type during neural induction and differentiation, thereby facilitating the process of generating specific neuronal cell types from the iPS cells; i.e. it was hoped that the pluripotent cells would retain an “epigenetic memory” that would allow this process to be more efficient. Thus, human primary fetal cells derived from the developing striatum or cortex, and fetal skin fibroblasts were used; the latter two acting as controls for the hypothesis being tested. The iPS cell lines generated were rigorously evaluated in terms of morphological appearance, pluripotent properties, teratoma formation, cell-specific markers, and gene expression profiles. Chapter 5 goes on to investigate the neural differentiation *in vitro* and and following transplantation of these cells.

3.3 Experimental design

To begin with, prior to transfection, the human fetal tissues were prepared accordingly; the neural cells were prepared as either primary cell cultures or expanded as neurospheres for up to 7 days and both were then dissociated as single cells onto PLL and laminin coated tissue culture plates; HEFs were dissociated as single cells and re-attached onto gelatin coated tissue culture dishes in differentiation medium. The next stage involved a series of steps over a number of days. Firstly, the cells were transfected with *piggyBac transposon* and transposase (pPB-CAG.OSKML-puΔtk and pCLy43) using Lipofectamine® for up to 24 hours (Figure 3.1). The transfection solution was then replaced by differentiation medium and after 48 hours the transfected cells were separated and re-plated on a MEF feeder layer, cultured in differentiation medium for a further 24 hours and then ES cell medium was added. The ES medium was fully changed every day until iPS cell colonies appeared (Figure 3.2).

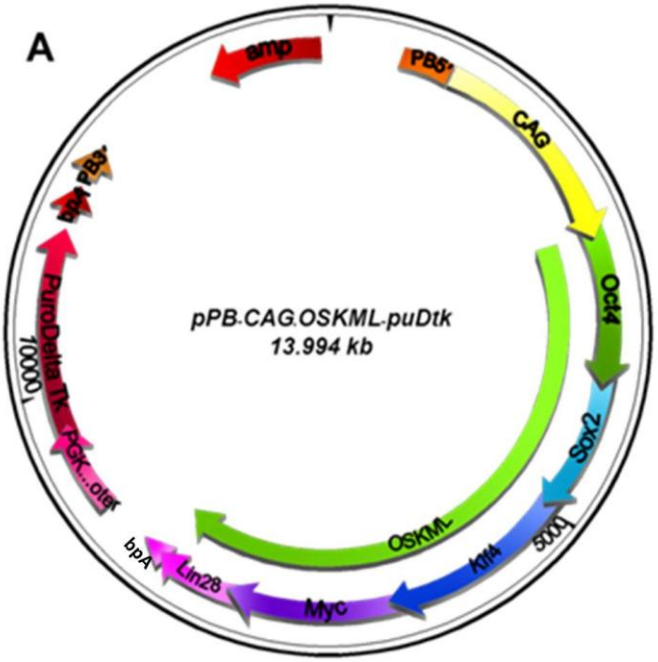

Figure 3.1 The schematic of *piggyBac Transposon* (pPB.CAG.OSKML-puDtk) construction for iPS cell generation. The transposon is used as a gene delivery vector system which contains 5'UTR situated between the CAG promoter and Oct4 sequences. The reprogramming genes Oct4, Sox2, Klf4, c-Myc, and Lin28 (OSKML) were linked by 2A peptides. 3'UTR sequence (bpA= bovine growth hormone polyadenylation signal) is after Lin28 sequences. A continuous CAG promoter drives the reprogramming transcription with each gene linked by 2A peptides, which mediated continuously, transcribe of the five factors OSKML. The PGK promoter drived-*puΔtk* works as a negative selection marker after removing the transposon from the iPS cells (Adapted from Yusa et al, 2009).

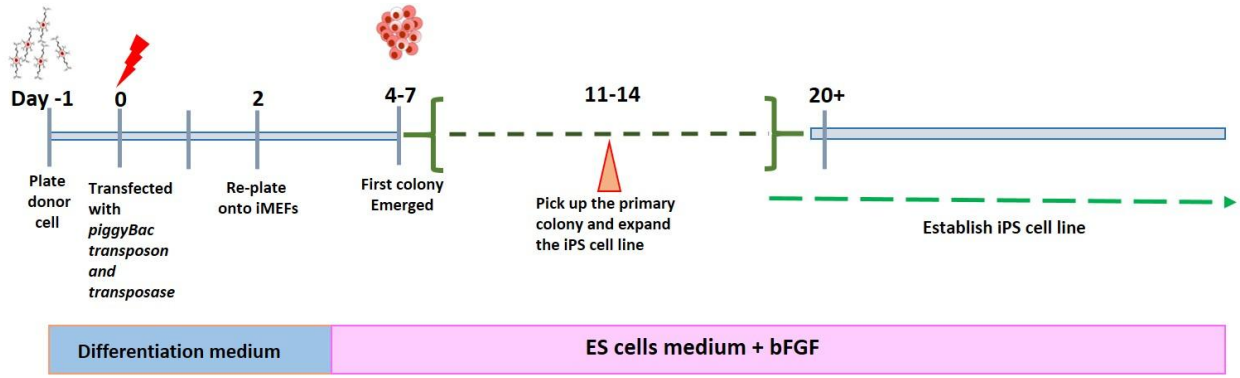

Figure 3.2 Timeline of transposon mediated-reprogramming of iPS cells. Human neural cells (WGE/cortex) and HEFs were plated down and differentiated for 1 day prior to the transposon transfection. Day 0, pPB.CAG.OSKML-puDtk and pCyL43 were transfected into the donors in addition with Lipofectamine® transfection reagent. The transposon was allowed to cooperate with the host genome and alter gene expression for 2 days after infection in differentiation medium before the cells were dislodged and re-attached onto iMEFs. ES medium with bFGF supplement was added and the media changed daily. The first colony emerged around 2-4 days after re-plating and culturing in the ES cell condition. Primary colonies were selected and expanded around day 11 as the morphology showed similarities to ES colony.

3.4 Methods

3.4.1 Reprogramming of human primary fetal neural cells and HEFs using transposon vectors.

The day before transfection, human primary fetal neural cells and HEFs, $5x10^5$ cells, were plated down as single cells onto a 6-well plate coated with PLL and laminin. The cells were cultured with differentiation medium without antibiotic overnight (day -1). The next day (day 0), cells were transfected under various conditions as per table (Table 3.1) using Lipofectamine® transfection reagent. Lipofectamine® was incubated in Optimem®, 50 µl, at room temperature for 5 minutes. The *piggyBac* DNA and transposase were added into Optimem, 50 µl, and the solution was mixed with the Lipofectamine® solution. The reprogramming cocktail was incubated at room temperature for 25 minutes. 900 µl Optimem® was added to the cocktail and gently mixed by pipetting up and down. The differentiation medium was aspirated off from each well and then the mixture was added onto the cells in each well. 500 µl Optimem® was added to obtain the total volume of 1500 µl. The 6-well plate was then incubated at 37˚C for 6 hours before 1.5 ml of warm, fresh differentiation medium without PS was added to each well (total volume 3 ml) and incubated further at 37˚C.

Condition Ratio	pPB-CAG.OSKML-puΔtk (1μg = 1μl)	pCyL43 (1μg = 1μl)	Lipofectamine (μl)
1:3	0.5	0.5	3
2:6	1.0	1.0	6
3:9	1.5	1.5	9
4:12	2.0	2.0	12

Table 3.1 Conditional ratios of vector DNA (*piggyBac transposon*--pPB-CAG.OSKML-puΔtk (μg) and transposase-- pCyL43 (μg)) with the volume of Lipofectamine® (μl).

3.4.2 Re-plating the transfected human primary fetal neural cells and HEFs onto MEFs feeder layer.

The day after transfection (day 1), the transfected HEFs and human FNPs were dissociated using Accutase®. DMEM/F12 was added to the dissociated cells, and the cell suspension was collected in a 15 ml centrifuge tube. The tube was spun at 86.64 g for 3 minutes. The supernatant was aspirated off; 200-250 μl of differentiation medium was added to the pellet before triturating 25-30 times to break up the clump. The MEFs feeder plate was prepared beforehand by washing with 1XPBS and culturing with 2 ml fresh and warm differentiation medium. The transfected cells were re-plated onto MEFs feeder layer and cultured at 37˚C.

3.4.3 Culturing and passaging the iPS colonies.

On day 3, ES cell medium was added to the transfected cells and the culture medium was changed every day until iPS cell colonies were identified. Each iPS cell colony was separated, picked up, and transferred onto MEFs feeder layer in a 24-well plate. The colony was cultured until it was large in size or dense enough to passage. Passaging was carried out using collagenase IV solution for 8-10 minutes until the edge of the colony was lifting off the culture plate and then fresh ES cell medium was added. A flame pulled glass pipette was used to cut the colony into small pieces, which were collected and transferred to the 15 ml centrifuge tube. The plate was then washed again with ES cell medium to collect all the colony fragments. The cells were spun at 13.86 g for 3 minutes; then the supernatant was aspirated. The cells were re-suspended in the ES cell medium and placed onto new MEFs feeder plate for further expansion, maintaining a frozen stock for characterization of these cells.

3.4.4 Transgene excision by transposase enzyme in reprogrammed iPS cells

iPS cells were detached from the feeders as small clumps using collagenase IV as described previously. Preparing transposase (pCyL43), Lipofectamine® 3 µl was incubated in 50 µl Optimem® for 5 minutes at room temperature. The cells were rinsed with warm 1XPBS and centrifuged at 13.86 g for 3 minutes before the supernatant was aspirated. The transposase was then gently mixed with 1.5 ml Optimem® and applied to the cells in non-attachment Sterilin culture dish for 6 hours at 37°C. iPS cells were collected and centrifuged at 13.86 g for 3 minutes. Supernatant was aspirated and the cell pellet was re-suspended in ES cell medium before re-plating onto iMEFs. ES cell medium was fully replaced every day for additional 2-3 days. 200 ng/ml 1-2'-deoxy-2'-fluoro-ß-D-arabinofuranosyl-5-iodouracil (FIAU) was supplemented into ES cell medium to select the transgene free iPS colonies. Surviving iPS cell colonies were picked and further expanded as individual colonies.

3.4.5 Detection of transgene integration within the iPS cell lines

Transgene integration and transposon structure can detect by RT-PCR using the primers listed below.

Region	Primers to detect transgene integration	Primer sequences
1. Oct4-Sox2 junction	Primer F in Oct4 region Primer R in Sox2 region	CCTCTGTTCCCGTCACTGCTCTG GAACAGCCCGGACCGCGT
2. Sox2-Klf4 region	Primer F in Sox2 region Primer R in Klf4 region	GCACATGGCCCAGCACTACC GAGAAGACACTGCGTCCAGCAGG
3. Klf4-Myc region	Primer F in Klf4 region Primer R in Myc region	TCAGTGCCAGAAGTGTGACAGG TATCACCAGCAACAGCAGAGCGAG
4. Myc-Lin28 region	Primer F in Myc region Primer R in Lin 28 region	TCCATTCAAGCAGACGAGCACAAG GGAGAAGGCGCCAGAGGAGG
5. Lin28-3'UTR junction	Primer F in Lin28 region Primer R in 3'UTR bpA region	CCAGCAGGGCCCCAGTTCTC AGGACAGCAAGGGGGAGGATT
6. Transposon 2 (PGK promoter)	Primer F Primer R	GCGTCGACCGACTGTGCCTTCTAGTTGCCAGCC GTTGGCGCCTACCGGTGGATGTGGAATGTG
7. Endogenous control	Primer F Primer R	GGGGCCTTCTGGGGGTAAAGTTCAGAACAC TGGCTGCCTGAGGGCAAGAGGGAAAGAATC

Table 3.2 Primers list for exogenous transgene integration.

3.4.6 Teratoma formation

iPS cell colonies were detached from feeders using collagenase IV. The colonies were cut into small clumps using a sterile needle and the cells were transferred to a 15 ml centrifuge tube. ES cell medium was added to a total volume 10 ml. Cells were centrifuged at 13.86 g for 3 minutes before the supernatant was aspirated off. Cell clumps were re-suspended and gently triturated in ES cell medium. The cells, approximately $1x10^6$ iPS cells, were mixed with Matrigel in a 1:1 ratio to enable them to clump and stay localized following injection subcutaneously into dorsal flanks of immune compromised-mice recipients. Around 8-10 weeks later, tumours were dissected, processed, and analysed by histological applications. The work was done by Dr. Susan Hunter, School of Bioscience, Cardiff University.

3.5 Results

The *piggyBac Transposon* method was applied to a number of samples from different maternal donors at various ages in gestation.

3.5.1 *piggyBac Transposon* mediated iPS cells originating from human WGE (iPS WGE C9).

Following transfection of primary human WGE cells with the transposase and *piggyBac* transposon there appeared to be little cell death (Figure 3.3 A). After re-plating transfected human primary WGE on a MEF feeder plate the cells quickly started to clump (Figure 3.3 B), however at this stage, there were no iPS cell like-colonies to be observed. Around days 2-7, a small round patch of forming colonies emerged (Figure 3.3 C). The morphology of the gathering cells was different from the human WGE cells as previously observed at the earlier stage (Figure 3.3 A) with a clear change in the ratio of nucleus to cytoplasm, a morphology more in line with what is reported of ES cells.

Over a number of days most, but not all, of these cells continued to proliferate (Figure 3.3 C). The cells that did not proliferate were located around the edges of the newly formed clump and were more characteristic in morphology of the original starting material (Figure 3.3 C, arrow). The iPS cell colony gradually developed with a distinct border from the MEFs and had a rounded dome shape like appearance as the cells continued to divide (Figure 3.3 C, insert). Between days 7-14, the primary colonies were easily identified, they were larger in size thus making them accessible for selection and passaging (roughly 1.5-2.0 mm). iPS cell colonies were passaged as described in chapter 2. Interestingly, there were several clones that proliferated more vigorously compared to others. These clones used up the medium rapidly as evidenced by the yellowish color of the culture medium in comparison to other clones. In addition, the morphological appearance exhibited different to a typical ES colony. Therefore, the clones that were not characteristic of an expectant pluripotent cell colony were not selected to expand further as an iPS cell line.

After several passages, the iPS cells were seen to proliferate in a way that is comparable to ES cells and had a morphological appearance similar to a typical ES cell colony; rounded shape, distinct border and tightly compacted cells with a

nucleus dominant to the cytoplasm (Figure 3.3 D and inset). The iPS cell lines were expanded and collected for further analysis and study. This line is referred to as iPS WGE623 C9.

Transformation of the cellular morphologies and a high proliferation propensity may suggest that reprogramming has taken place. However, further investigation and evaluation of the pluripotent characteristics and gene expression pattern compared to human ES cells needs to be carried out before any conclusion can be made.

iPS WGE623 C9 generation.

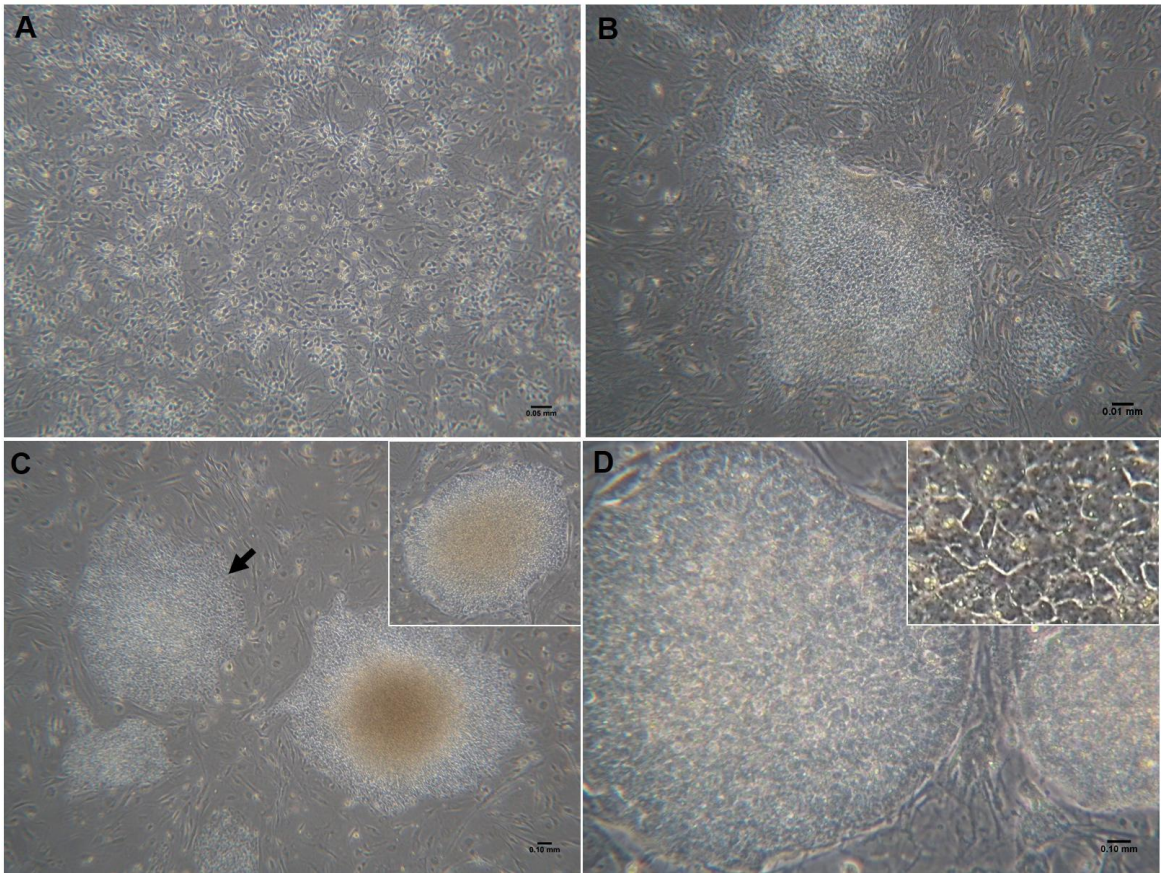

Figure 3.3 Generation of iPS cells from human primary WGE using *piggyBac* transposon. Bright-field images taken during the derivation of *piggyBac* transposon–mediated iPS cells. After 12-24 hours of gene delivery transduction with *piggyBac* transposon and transposase (pPB-CAG.OSKML-puΔtk and pCyL43), neural cells appeared healthy with no evidence of cell death (A). Transfected cells started to show signs of colony formation after re-plating on iMEFs and culturing in an ES cell environment (B). 2-7 day after re-plating they gradually formed ES-like colonies with high degree of proliferation in the middle of the accumulated patch of cells (C). Later on, morphological appearances continued to develop by appearing rounded in shape, presence of a sharp cell border, and proliferated up like a dome (C, inset). After passaging several times, the iPS colony continued to share a morphological appearance that was comparable to a typical ES colony (D) composed of nuclear-dominant cell population (insert). (Scale bar=0.01 mm A-B; scale bar=0.1 mm C-D)

3.5.2 *piggyBac Transposon* mediated iPS cells originating from human primary WGE, cortex, and HEFs.

As mentioned above the procedure was repeated on several samples from human fetal striatum (WGE SWIFT number 928, 949, 954), cortex (Ctx SWIFT number 962) and skin fibroblasts of different donors (SWIFT number 815 and 962). One fetal donor derived WGE sample was cultured as neurospheres for 7 days (SWIFT number 928). The *piggyBac transposon*- pPB-CAG.OSKML-puΔtk and transposase (pCyL43) were delivered to these cells in the same way as described above.

There was variability in the timing with which colonies were first observed; as early as 2-14 days after transfection in primary WGE, 7-14 days in cortex, and 14-21 days in skin fibroblasts (Figure 3.4 A, B, C respectively). WGE derived-iPS cell colonies continued to appear with time *in vitro*. Of the resulting colonies only 48 colonies were collected and expanded from the WGE cultures, 12 colonies were obtained from primary cortex and only 2-7 iPS colonies were propagated from skin fibroblasts (Table 3.2). Furthermore, subsequent culturing resulted in only one of the iPS cell lines derived from the fibroblasts being expanded as the other pre-iPS cell colonies did not proliferate or develop any further. The iPS cell colonies presented with morphological characteristics similar to a typical ES cell colony and had similar self-renewal features (Table 3.2).

The iPS cell lines were allowed to freely differentiate in ES/iPS cell medium without the addition of bFGF in a bacterial grade petri dish to look at the propensity of these cells to form EBs, which are differentiated multicellular aggregations of pluripotent cells (Figure 3.4 D).

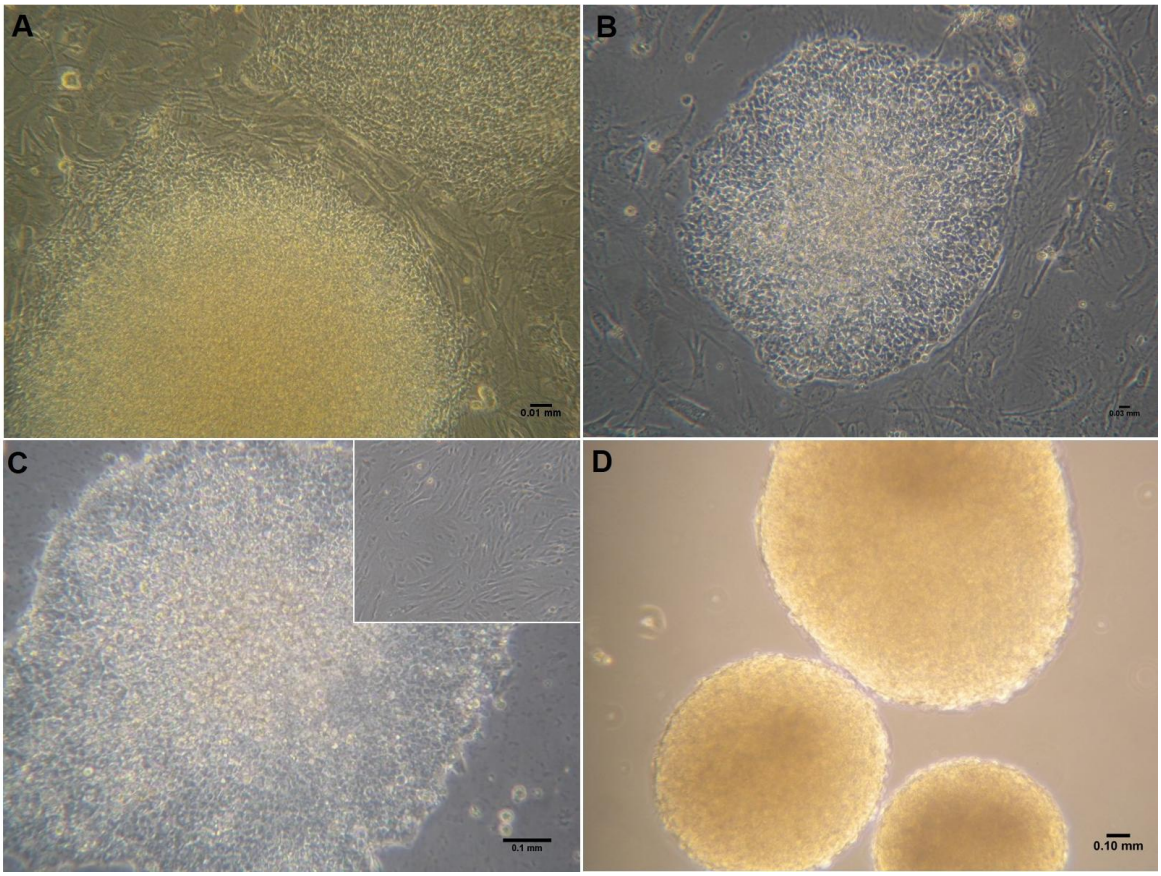

Figure 3.4 Morphological appearances of *piggyBac transposon* (PB) derived-iPS cells from human primary tissues. Developing primary colonies of PB transposon generated iPS cell from human primary WGE (SWIFT number 928) were recognized around 2-14 day after infection with *piggyBac transposon* and transposase (pPB-CAG.OSKML-puΔtk and pCyL43). The colonyborder was not defined at this stage and they needed around 5-7 days to be passaging; scale bar=0.01 mm (A). The colony which failed reprogramming to a pluripotent stage was exhibited as a patch of cells without a proliferating area (Figure A, upper right corner). The 2nd passage of iPS cell generated from cortex neurospheres demonstrating a more clearly defined border; scale bar=0.03 mm (B). A morphological comparison between iPS colonies and their original HEFs (C and inset respectively) (SWIFT number 962); iPS colonies propagated from HEFS at around passage 4-5 had similar features to typical ES colonies; sacle bar= 0.1 mm (C). The HEF iPS colony contained small tightly packed cells, with a proliferating area in the middle of colony, and distinctive colonyborder. All established iPS cell lines could generate multicellular aggregates called embryoid bodies (EBs) presenting as a ball shapes in ES medium without additional bFGF; scale bar=0.10 mm (D).

Original cell types	iPS cell lines	Number of iPS cell lines	Number of iPS cell lines applying to neural differentiation
1) Human WGE (NPC) SWIFT No.623	iPS WGE 623	28 iPS cell lines (C1-C28)	1
2) Human WGE (NPC) SWIFT No.928	iPS WGE 928	48 iPS cell lines (C1-C48)	4
3) Human WGE SWIFT No.949	iPS WGE 949	48+ iPS cell lines (C1-C48)	1
4) Human WGE SWIFT No.954	iPS WGE 954	48+ iPS cell lines (C1-C48)	1
6) Human embryonic fibroblasts SWIFT No.815	iPS HEF 815	2 iPS cell lines (C1-C2)	0
7) Human embryonic fibroblasts (HEF) and human embryo cortex (CTX) SWIFT No.962	iPS HEF 962 iPS CTX 962	7 iPS cell lines (C1-C7) 12 iPS cell lines (C1-C12)	1 0

Table 3.3 The table presents a summary of iPS cells generated using PB transposon based gene delivered system in distinct original cell phenotypes and donors as represented by the donor collection number (SWIFT number) and the approximate size (CRL) ranged from = 22-49 mm.

In summary, we were able to generate iPS cells from human fetal tissues using the *piggyBac* transposition system with 5 reprogramming factors (OSKLM) and transposase pCyL43. However, there appeared to be marked variability in the reprogramming efficiency and kinetics between the different donor tissues. Specifically, the WGE appeared to generate more clones with rapid kinetics than the cortical tissue or the HEF. The first iPS colony generating from human embryonic WGE was appeared within 2-7 days after transfection, while using CTX or HEF will need at least 14-21 days to obtain the first colony. In addition, the conversion efficiency appeared to be 4-5 times higher in WGE as an originated cell source in comparison to CTX and HEF respectively. (Table 3.3)

In the first instance all the cell lines generated were tested using immunocytochemistry for pluripotent markers. Due to the high expense and labour intensive nature of the work, it was only possible to take the first iPS cell line (iPS WGE623 C9) forward for full molecular, *in vitro* and *in vivo* validation of pluripotency.

3.5.3 *In vitro* Characterization of iPS cell line: iPS WGE623 C9.

Morphological characterization

The iPS cells (WGE623 C9) were similar in morphology to the the H9 human ES cell line as described above and seen in Fig 3.5.

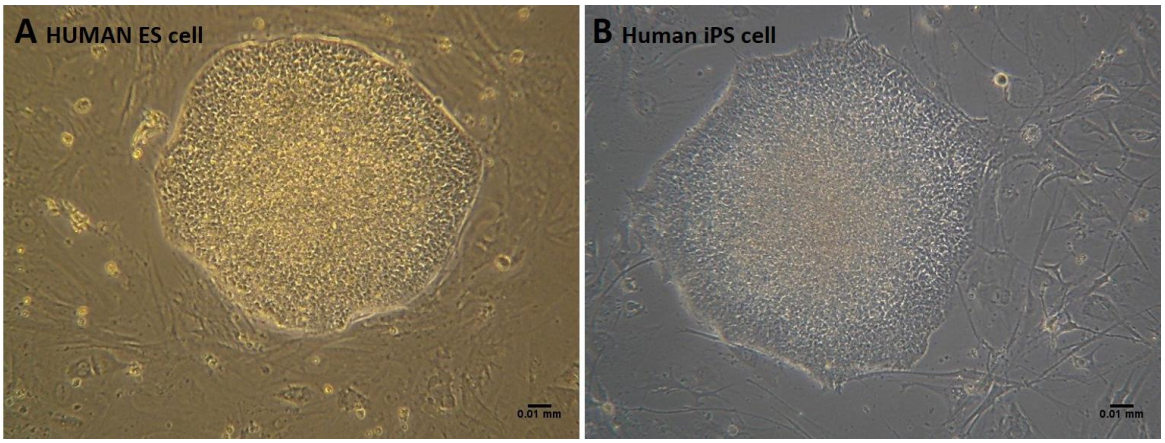

Figure 3.5 Comparison of the morphological appearance of a human ES colony (H9) (A) and a *piggyBac Transposon* mediated-iPS colony (B). Both ES and iPS colony are similar in terms of the morphological appearances—rounded shape, sharp border, tightly packed and nuclear dominant cells. (Scale bar = 0.01 mm)

Immunocytochemistry analysis for pluripotent markers.

Human ES cells (H9) were used as a positive control in this study. Immunofluorescence confirmed pluripotency in human ES cells (H9) and iPS cells for stem cell markers such as Oct4, SSEA4, Nanog and Tra-1-60. Fig 3.6 shows the positive expression of Tra-1-60 and Oct4 markers in H9 ES cells whilst Fig 3.7 confirms their expression in the WGE623 C9 iPS cell line and confirms the persistence of these markers with time in culture and passaging (passage 26 and 43) (Figure 3.7). In addition, our established iPS cell lines: iPS WGE 928, iPS WGE 949, and iPS HEF962 also expressed hallmark of pluripotent markers such as Oct4, Sox2, SSEA4, Nanog, and Tra-1-60 similar to ES cells (Figure 3.8-3.10, respectively).

Human ES cell (H9)

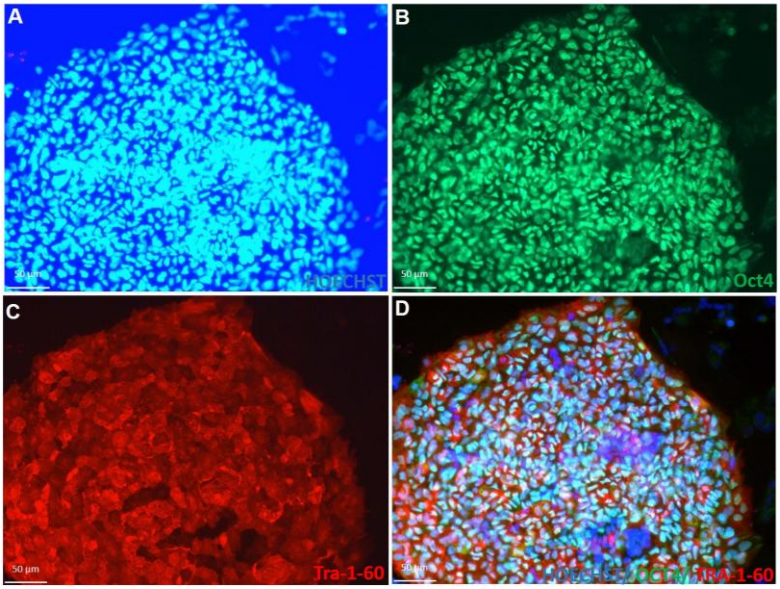

Figure 3.6 Characterization of human ES cell line H9. Immunofluorescence analysis of Hoechst staining (A). Expression of pluripotent markers **OCT4** (B), **TRA-1-60** (C), triple stained for **OCT4, TRA-1-60** and **Hoechst** (D). Scale bar=50 µm.

Human iPS cell from WGE (iPS WGE623 C9)

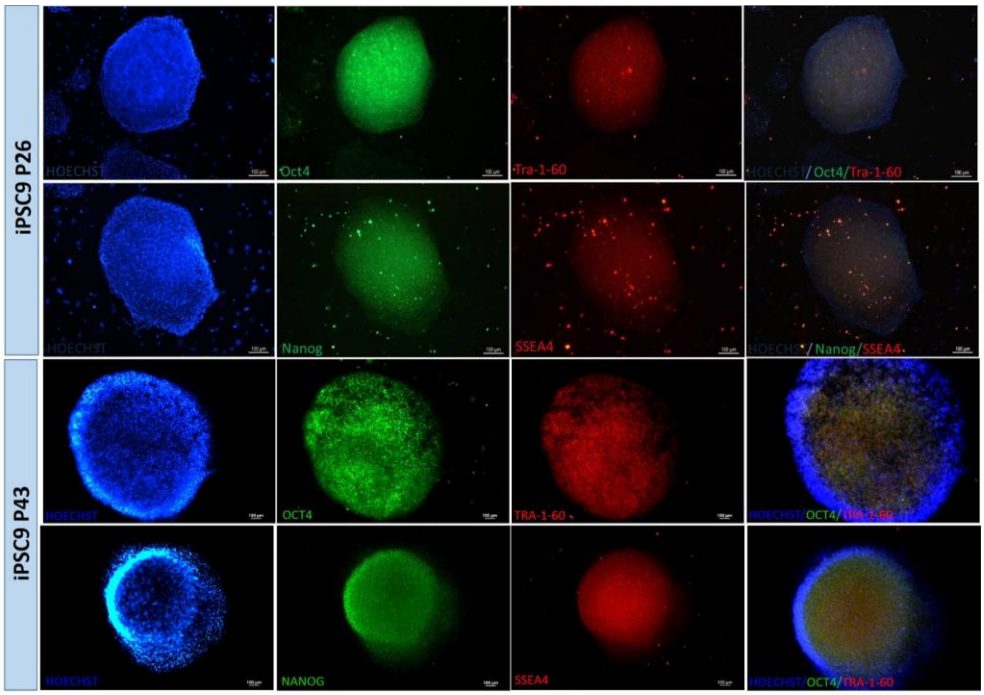

Figure 3.7 Characterization of iPS WGE623 C9 after continued passage. Immunofluorescence analysis of **OCT4**, **Nanog (column 2)**, **SSEA4** and **TRA-1-60** (column 3) expression in the *piggyBac Transposon* mediated - iPS cell line C9 at passage 26 and passage 43 which confirm the consistency in pluripotent genes expression of this iPS cell line over time (Scale bar=100 µm). Column 4 shows the merged images.

Human iPS cells from WGE SWIFT No. 928, 949 (iPS WGE 928 clone 5, 949 clone 5)

As mentioned above this process was carried out on a number of lines generated. Figure 3.8 and figure 3.9 are representative of two iPS cell lines where starting material was fetal WGE from two different maternal donors, showing positive expression for stem cell markers.

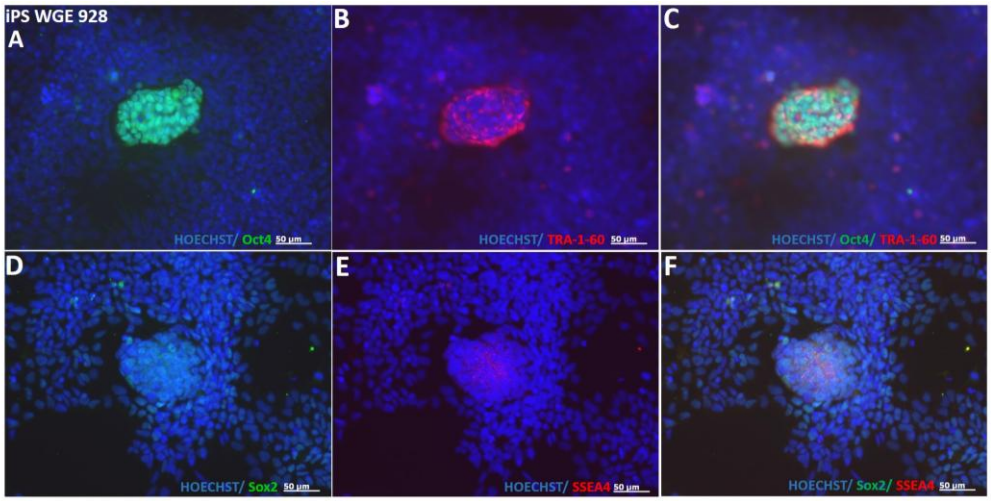

Figure 3.8 Characterization of iPS cells derived from human fetal WGE (SWIFT No. 928). Immunofluorescence analysis of genes expression **OCT4 (A)**, **TRA-1-60 (B),** **SOX2 (D)**, and **SSEA4 (E)** in the *piggyBac Transposon* mediated - iPS cell line (iPS WGE 928 clone 5). (C) and (F) show merged images.

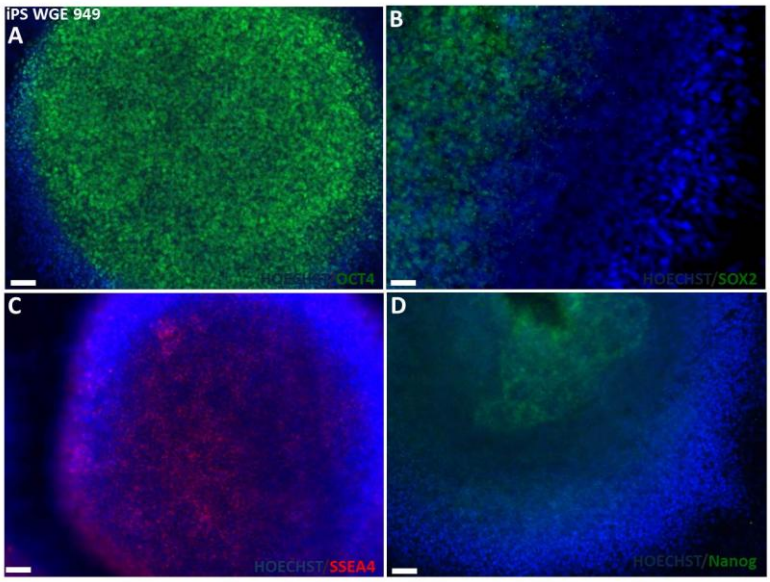

Figure 3.9 Characterization of iPS cells derivied from human fetal WGE from (SWIFT number 949). Immunofluorescence analysis of **OCT4 (A)**, **Sox2 (B)**, **SSEA4 (C)**, and **Nanog (D)**, in the *piggyBac Transposon* mediated - iPS cell line (iPS WGE 949 clone 5). Scale bars, 20 µm.

Human iPS cell from HEFs SWIFT No. 962 (iPS HEF 962 clone 2)

The HEF derived iPS cell line was also stained for expression of the pluripotency makers Oct4, Nanog, SSEA4, Sox2, and Tra-1-60 (Figure 3.10).

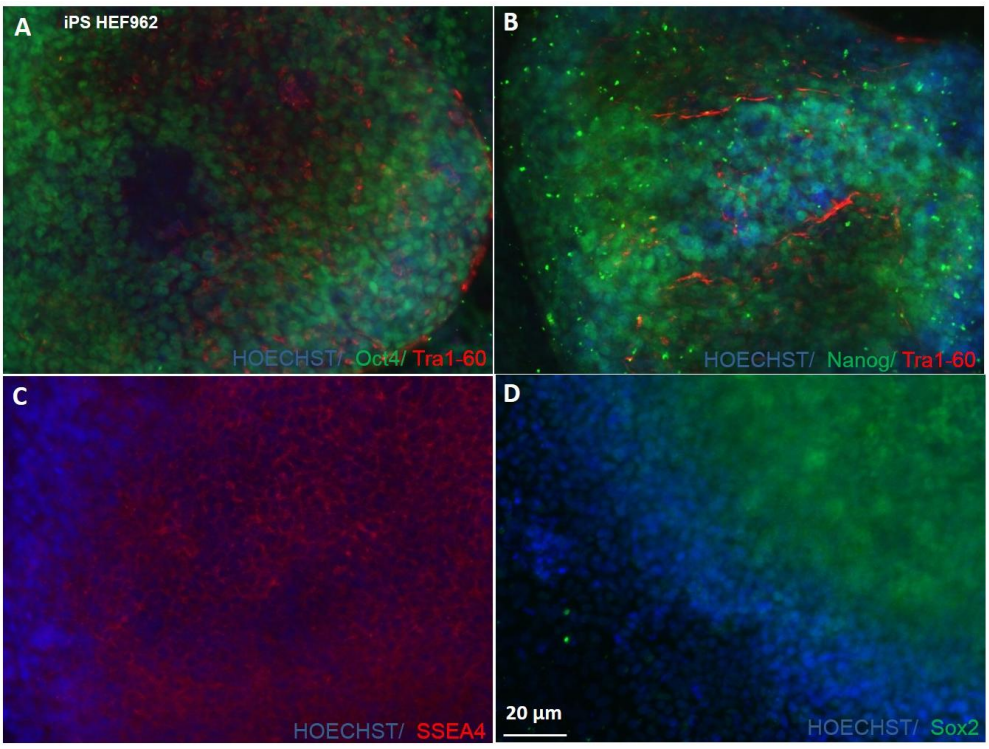

Figure 3.10 Characterization of the *piggyBac Transposon* mediated iPS cell line derived from HEFs (Swift number 962): iPS HEF 962 clone 2. Coexpression of the pluripotent markers **OCT4** in the nucleus and **TRA-1-60** in the cytoplasm (A), **Nanog** and **TRA-1-60** (B), **SSEA4** (C), and **Sox2** (D). Scale bars, 20 µm.

Spontaneous In vitro differentiation of iPS WGE623 C9.

The iPS cell line C9 was allowed to spontaneously differentiate on matrigel coated coverslips and cultured in ES medium without the addition of bFGF for 14-21 days. The results showed the differentiation of these cells into cells of all three germ layers: endoderm, mesoderm, and ectoderm (Figure 3.11 B, C, and D respectively). Immunocytochemistry was carried out on these cells to define the specific differentiated phenotypes. The expression of nestin and β-III tubulin represented the ectoderm lineage (Figure 3.12 A, B). The mesoderm phenotype was detected by the expression of Desmin, which represents intermediate filament in smooth muscle cells as well as expression of Alpha smooth muscle actin (α-SMA) (Figure 3.12 C, D). The hepatocellular marker Alpha- fetoprotein (AFP) and intermediate filament that is derived from mesenchymal cells, vimentin, were revealed confirming mesoderm derived cells (Figure 3.12 E, F). The expression of the three germ layer markers in these cultures of spontaneous *in vitro* differentiation further confirm the pluripotent properties of this iPS cell line. Furthermore, EBs were obtained when dissociated iPS WGE C9 cells were incubated with iPS cell medium in the absence of bFGF (Figure 3.11 A).

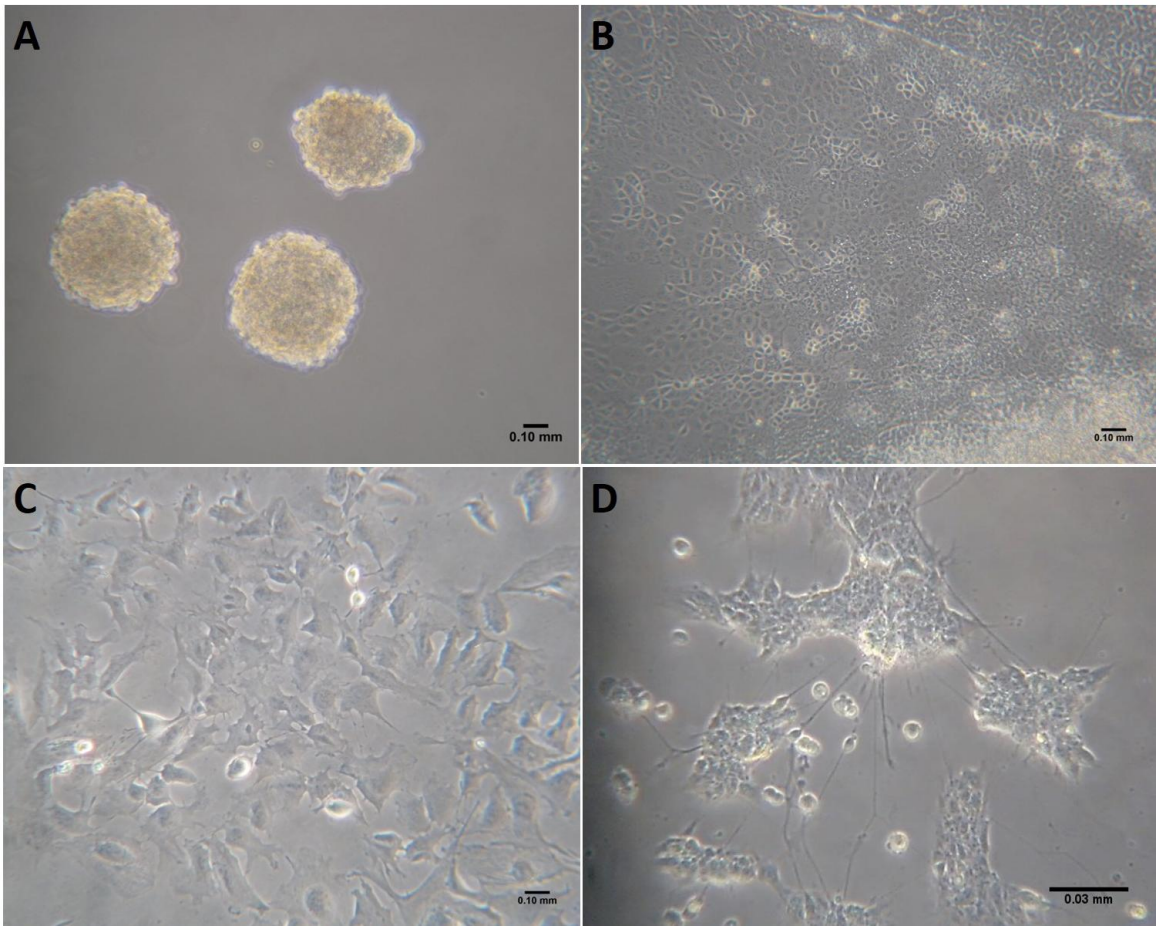

Figure 3.11 Bright field images presenting trigerminal differentiation *in vitro*. EB formation from the iPS cell lines (iPS WGE C9) in iPS medium without the additional of bFGF, cultured for 7 days (A). Morphology of endothelial cells (B), muscle cells (C), and neuronal cells (D) were observed following the spontaneous differentiation protocol (Scale bar=0.10 mm A-C; scale bar=0.03 mm D).

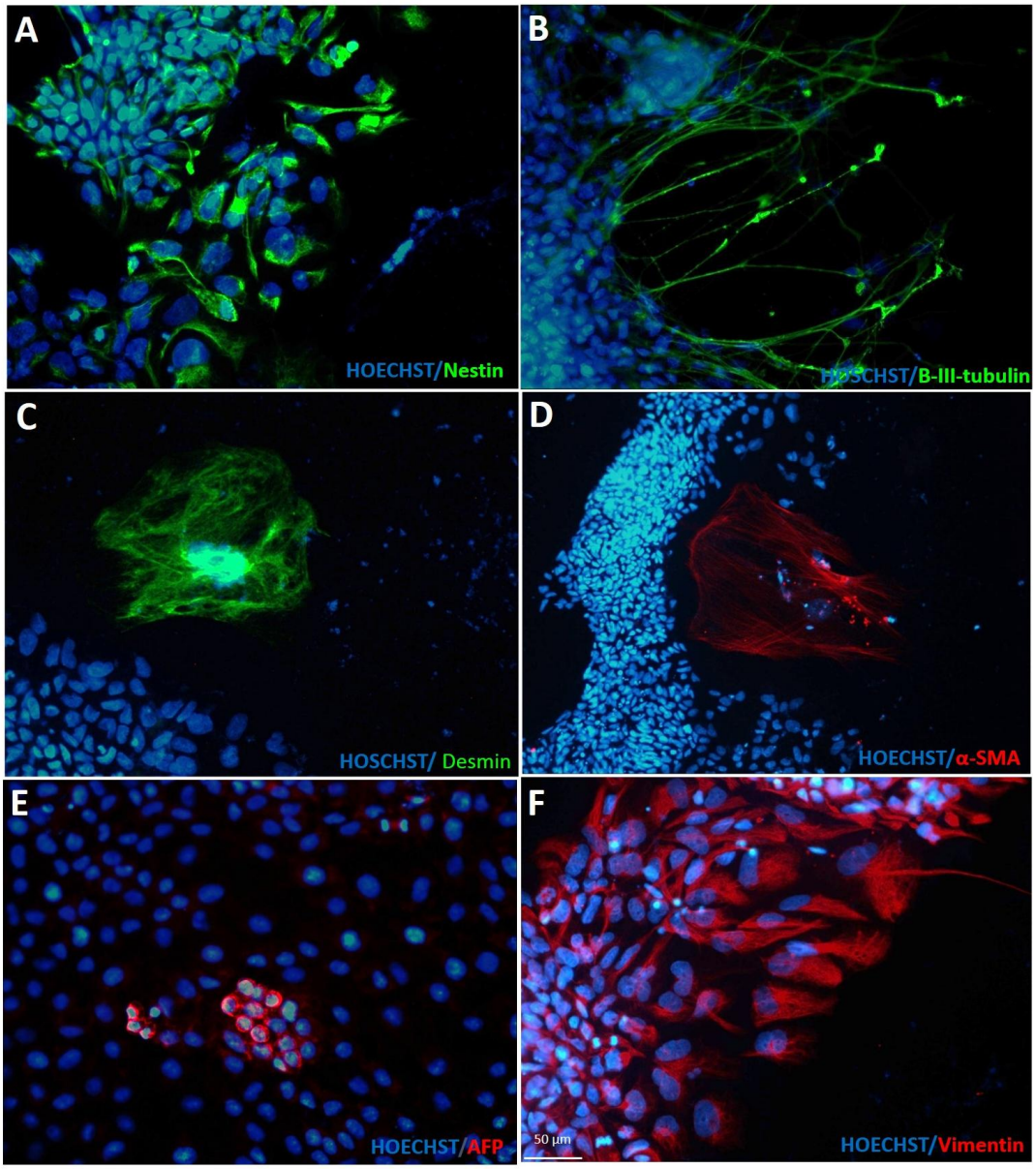

Figure 3.12 Characterisation of *In vitro* spontaneous differentiation of iPS cells derived from human WGE (iPS WGE C9). Immunofluorescence analysis of nestin and β-III Tubullin (A, B) representing ectoderm lineage, Desmin and α-SMA (C, D) representative of a mesoderm lineage, and AFP and Vimentin (E, F) showing endoderm lineage. Scale bars, 50 µm.

3.5.4 Molecular Analysis of iPS cells.

Reverse Transcriptase PCR (RT-PCR) analysis

Gene expression analysis was carried out on the iPS cell line C9 at various passages (P37, 38, 39 and 41) using RT-PCR analysis and pluripotent gene expression markers. The results confirmed the consistent expression of essential pluripotent transcription factors- Oct4, Sox2, Nanog, Lin28, c-Myc, and Klf4 (Figure 3.13).

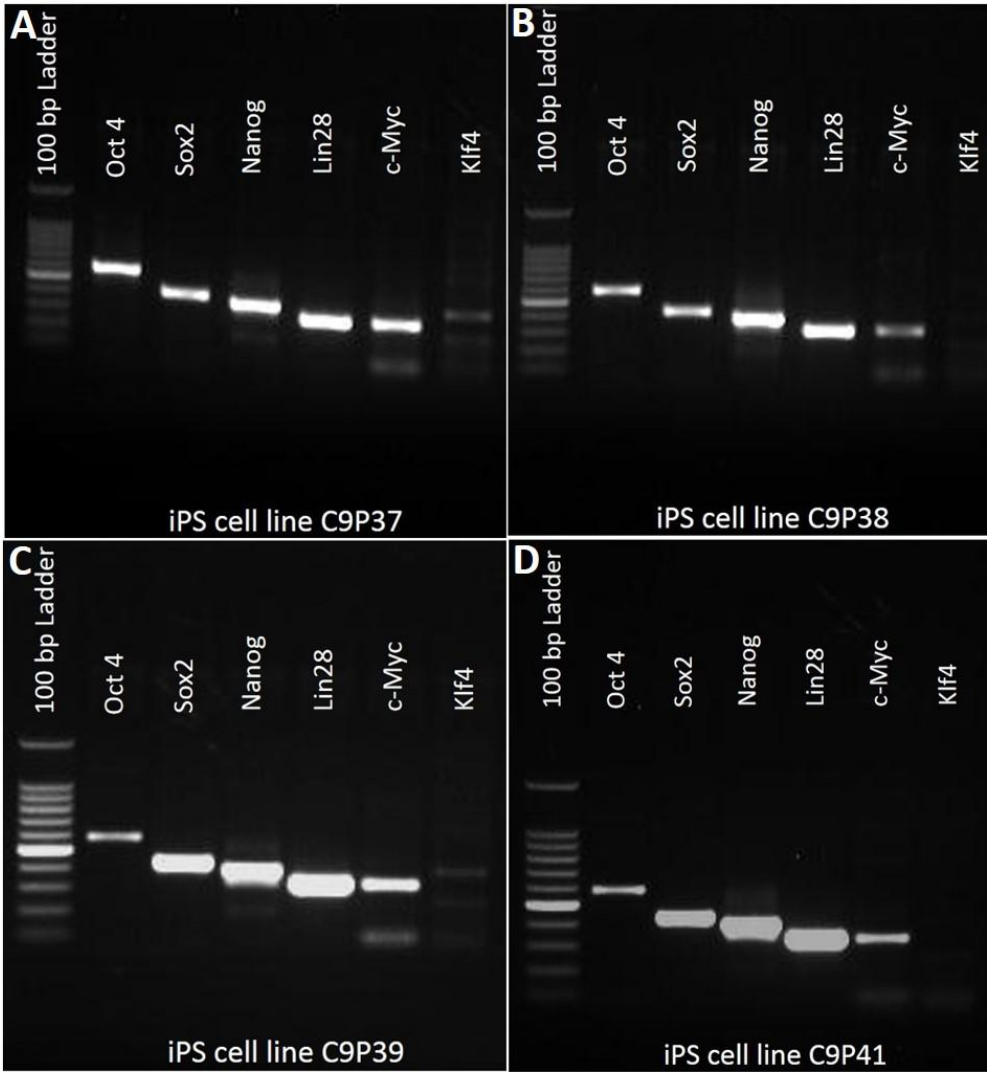

Figure 3.13 RT-PCR analysis of the pluripotent genes expression: Oct4 (573 bp), Nanog (391 bp) and Klf4 (397 bp), Sox2 (428 bp), Lin28 (323 bp) and c-Myc (328 bp) in the *piggyBac Transposon* –generated iPS cell line at different passages (C9 at P37, 38, 39, 41).

3.5.5 *In vivo* differentiation of iPS cell line (iPS WGE C9).

Further evidence of established iPS cell pluripotency can be shown following injection of these cells subcutaneously into immunodeficient mice (Figure 3.14 A). Tumour formation emerged within 8-10 weeks after iPS cells were injected (N=2) (Figure 3.14 A, B). The tumour was surgically dissected, fixed and processed for immuno-histochemistry using H&E staining to distinguish cells' component within the tumour (Figure 3.15). H&E stained sections (Figure 3.15) revealed components of all three germ layers thus confirming pluripotency of the established iPS cells.

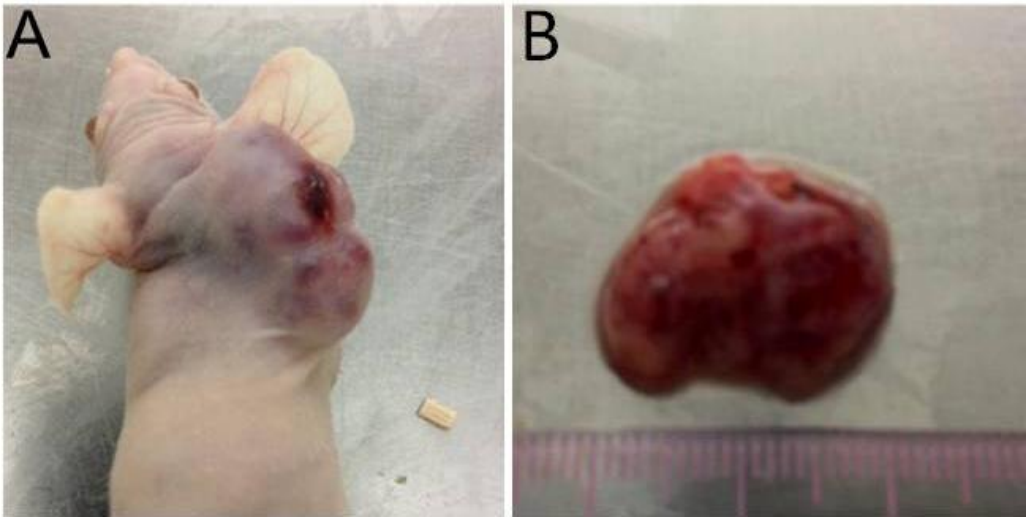

Figure 3.14 *In vivo* differentiation characterize pluripotency of iPS cells. At week 8, a tumour appeared after subcutaneous injection with iPS cells (iPS WGE623 C9) mixed 1:1 with matrigel (A). The tumour was 2 cm in size (B) and was surgically dissected from the animals.

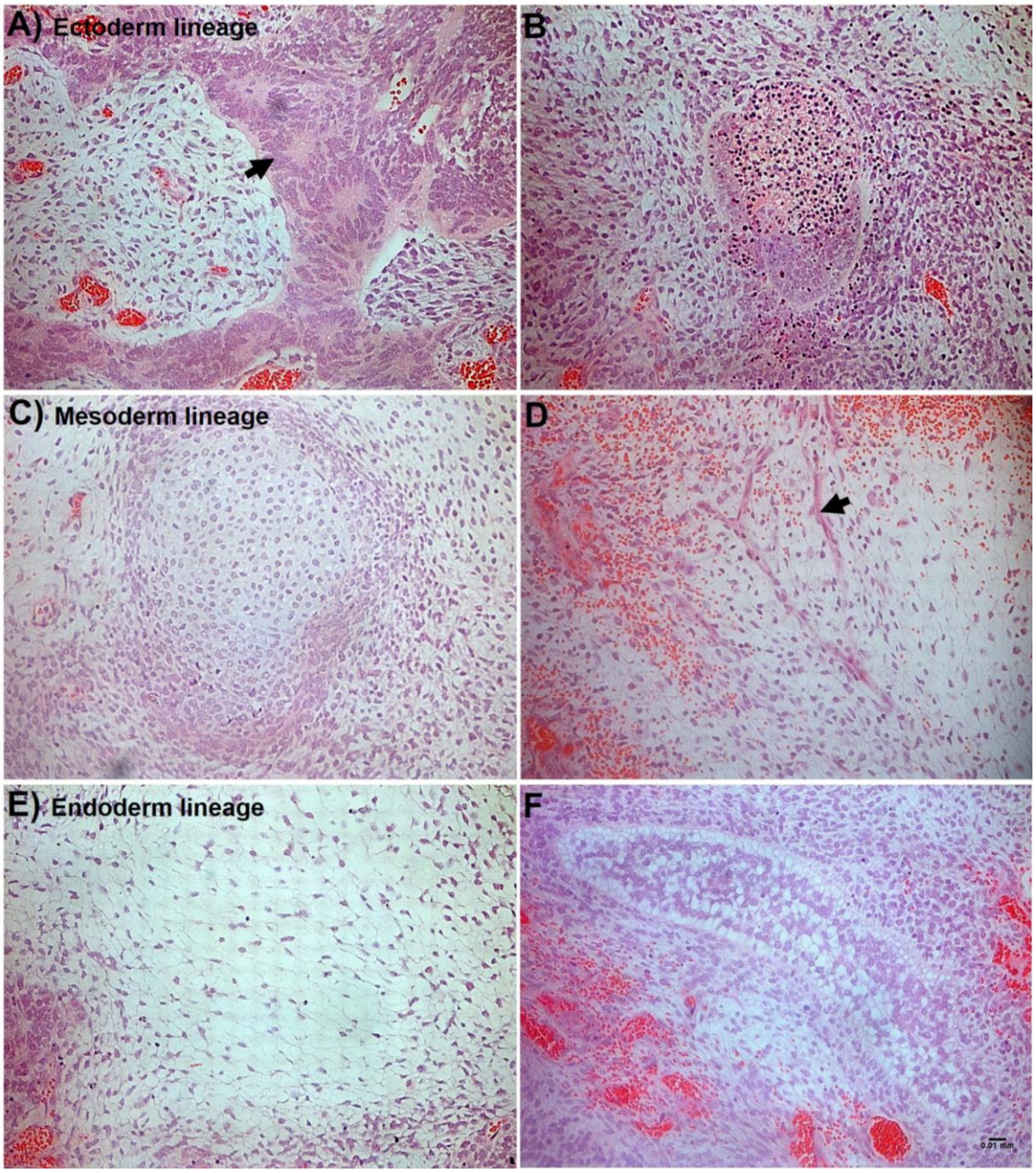

Figure 3.15 Teratomas generated from *piggyBac* transposon derived iPS cells showing differentiation to all three germ layers. An 8 week teratoma was processed and stained with H&E. The histological sections presented trigerminal differentiation of ectodermal cell neural rosette (A and arrow) and pigmented cells (B); mesodermal cells such as chondroblasts (C) and smooth muscle fiber (D and arrow); endodermal such as adipose tissue (E) and gland tissue (F). (Scale bar=0.01mm)

3.6 Discussion

The *piggyBac* transposon strategy provides an effective method to reprogramme somatic cells that is comparable in its efficiency to the viral vector approaches (Grabundzija et al., 2013). Moreover, different human tissue sources such as fibroblast, primary neural tissue, and some cell phenotypes that have been reported to be difficult to reprogram, such as T cells (Staerk et al., 2010), can be successfully reprogrammed to a pluripotent state using *piggyBac* (Yusa et al., 2009; Woltjen et al., 2009; Grabundzija et al., 2012). This may suggest a high efficiency of the *piggyBac* transposon gene deliver strategy. In this study, we could identify more than 48 ES cell-like colonies depending on the starting material used with WGE tissue resulting in the greatest number of clones. In addition, we observed the continued emergence of ES cell-like colonies in culture with a time line similar to that described by Woltjen et al (Woltjen et al., 2009). Whilst there was variability in the number of colonies formed depending on the tissue source (as few as 2-7 colonies from HEF compared to more than 48 colonies from WGE) it is clear that overall the *piggyBac transposon* method is efficient in generating pluripotent cell colonies from these tissue sources. It was not feasible to collect every colony that formed and thus up to 48 colonies were picked per condition.

Many studies have suggested that a higher number of reprogramming factors increased the efficiency of inducing a pluripotent state in differentiated cells (Woltjen et al., 2009, Muenthaisong et al., 2013). Woltjen and colleagues (2009) suggested a 4 times higher reprogramming efficiency when utilising 5 reprogramming factors (OSKML) compared to 4 factors (OSKM) (Woltjent et al., 2009). Recently, a similar trend was revealed by Grabundzija and team where using 5 factors (OSKML) not only increased the yield of iPS colonies but also shortened the time spent before the first colony was recognized when compared to the application of 4 factors (Grabundzija et al., 2013). Aasen and coworkers reported a significant conversion efficiency up to 100 folds higher and more rapid kinetics up to 2 folds when human keratinocytes were used as the originate cells comparing to human fibroblasts (Aasen et al., 2008). This may suggest a plasticity and feasibility differences among various cell types in order to generate iPS cell lines. In our study, we applied 5 reprogramming factors to various human primary tissues with the same gene delivery method *piggyBac* transposition. As mentioned

already the number of colonies generated varied, as did the time taken *in vitro* to observe the first iPS colony, which took 2-3 weeks longer in fibroblasts compared to neural tissue. This may associate with the idea that naturally high expression of the endogenous pluripotent gene Sox2 in human primary neural tissue may accelerate the efficiency of iPS cell generation (Kim JB et al., 2009). Compared to previous studies in which fibroblasts have been used and a similar strategy of transposon gene transporting system have been applied, we observed iPS cell colonies as early as 2-3 days after transfection. Furthermore, the plasticity in the different tissue donors may affect the reprogramming capacity as reported by Kim et al. (Kim J et al., 2011). In this study, postnatal cortex was unable to be reprogrammed to a pluripotent state with the original 4 factors of Oct4, Sox2, Klf-4, and c-Myc unless neuronal activation genes and p53 were suppressed (Kim J et al., 2011). Thus, this suggests that the human fetal neural tissues used in our study may be more plastic, which may then enhance the reprogramming efficiency resulting in a richness of iPS colonies without the need to repress the activity of neural genes.

Muenthaisong et al in 2013 reported the derivation of iPS cells from distinct genetic background mice (Muenthaisong et al., 2013). They suggested that the differences in genetic background had an effect relating to the efficiency in pluripotent state conversion as well as differentiation potential from each established iPS cell line. In agreement with these findings, we observed difficulties in reprogramming iPS cell from some donors such as HEFs from SWIFT number 815. Even though many attempts and optimized protocols were applied, iPS cell lines could not be propagated from this donor. Interestingly, iPS WGE623 C9, the first iPS cell line derived in our hands have struggled to differentiate thoroughly to a neural lineage and could not be differentiate into MSNs, in contrast to other established iPS lines derived in house (see chapter 4).

In the normal human genome it has been reported that there are 18 integrations sites available for transposons (Wilson et al., 2007). Using the *piggyBac* transposon method in HEK293 cells, it has been found that there are as many as 15 integrations in the cells genome (Wilson et al., 2007). Whilst this would be of great benefit for gene therapy, in this situation in which we aim to generate integration free cell lines, it poses a significant problem. This finding was in accordance with other studies such as that reported from Woltjen et al (2009)

which claimed to identify an average of 9 transgene integration sites in an iPS clone generated using the same system (Woltjen et al., 2009). At the same time, Yusa et al (2009) also suggested that a minimum requirement of 3 integration sites was needed for efficient reprogramming of differentiated cells (Yusa et al., 2009).

The number of integration sites in the cell lines generated here is unknown due to technical difficulties with the southern blot technique. However, in an attempt to address this we will be able to detect transgene insertions using specific reverse primers of as shown in table 3.2 to identify the presence of exogenous transgenes remaining in our iPS cells (Woltjen et al., 2009).

Davis et al (Davis et al 2013) stated that 2-3 integration sites were found in their iPS sub clones. Similarly Grabundzija and team (Grabundzija et al 2013), revealed at least 2 integration sites in the majority of their established iPS cell lines using the *Sleeping Beauty* (SB) transduction system; even though they reduced the DNA concentration of transposon used in the reprogramming process (Grabundzija et al., 2013). In addition, Davis and team also tested the method multiple times, but found re-insertion of the transgene into other integration sites after it was successfully removed from the initial integration site, thus failing to produce a transgene free iPS cell line (Davis et al., 2013).

In terms of taking these cells forward for clinical application, viral gene integration or the presence of residual transgenes in the donor cells is unlikely to be acceptable. Many reprogramming strategies have been developed; however, with non-integration methods the reprogramming efficiency is low. Here our aim was to use the *piggBac* method as a non-viral method to generate iPS cells and whilst we successfully generated iPS cell lines as validated by their pluripotency and ability to form teratoma's, these cells continued to express reprogramming factors that would inhibit their use clinically. This is a field that is progressing fast and it entirely possible that new methods will be identified sooner rather than later to overcome these issues.

Chapter 4

Human iPS cell derived GABAergic MSNs-liked cells using EBs-Based Method.

4.1 Introduction

Protocols for differentiating human PSCs towards MSNs have been refined from generating NPCs, to generating more specific phenotypes using ontological recapitulation of brain development (Song et al., 2007; Aubry et al., 2008; Li et al., 2009; Ma et al., 2012; Delli Carri et al., 2013).

Neuroepithelial cells have been generated from PSCs by different methods such as co-culture with stromal cells (Song et al., 2007; Aubry et al., 2008), multi-aggregate cells as EBs (Li et al., 2009; Ma et al. 2012), and adherent monolayer method (Nasokin et al., 2009; Delli Carri et al., 2013). One disadvantage of neural induction by co-culture for applications such as cell implantation is the safety concern of exposing the host to the stromal cells such as the murine stromal cell lines PA6 (Song et al. 2007) and MS 5 (Aubry et al., 2008). In addition, this is a time consuming method as it takes several weeks to initiate and obtain the neuro epithelial cells. Therefore, multi-cellular aggregation as differentiated EBs was developed, imitating the development of the three germ layers in an embryo. However, other non-neural cells differentiating within the EB may interfere with the efficiency of neural differentiation by secreting signals to direct cells to lineages other than the desired ones and changing the microenvironment of the whole culture (Li et al., 2009; Ma et al. 2012). More recently, an adherent monolayer based method, which was first introduced by Nasonkin and colleagues in 2009, reported success in the generation of ‘authentic DARPP-32 MSNs’ (Delli Carri et al., 2013).

Ontogeny recapitulation protocols have been considered, improved and applied to human PSCs. PSC-derived NPCs were manipulated by either SHH (Ma et al., 2012), or a combination of SHH with a Wnt signalling antagonist DKK-1 to acquire a ventral telencephalic phenotype before terminal differentiation both *in*

vitro and *in vivo* (Aubry et al., 2008; Li et al., 2009; Delli Carri et al., 2013). Further differentiation of committed ventral telencephalic precursors was assessed chronologically by immunocytochemistry, RT-PCR, and Q-PCR for neural precursor markers, ventral telencephalic precursors, and post mitotic MSNs (Aubry et al., 2008; Li et al., 2009; Ma et al., 2012, Delli Carri et al., 2013). The different protocols achieved varying amounts of striatal neurons: Aubry et al. reported 53% DARPP32 expression within the 32% of GABA positive cells (Aubry et al., 2008); Ma et al. claimed that there was up to 89% DARPP32 positive cells within the 90% of GABAergic cells (Ma et al., 2012). Recently, Delli Carri reported approximately 20% co-labelling of Ctip2 and DARPP32 as a percentage of all cells (Delli Carri et al., 2013).

Graft overgrowth was recognized in human PSC-derived striatal GABA positive grafts in the Aubry's study, while Ma and Delli Carri claimed an absence of teratoma or neuronal overgrowth in their studies. After implanting human PSC-derived MSNs like cells into the QA-lesioned rodent model of HD, improvements in behavioural tests, such as correction of locomotion deficits (Ma et al., 2012), and improved apomorphine induced rotations were reported, as well as an action potential firing pattern in these neurons (Delli Carri et al., 2013). Taken together, these studies show that human PSCs-derived MSNs are capable of providing large numbers of donor neurons with a variable proportion of these neurons having the sub-phenotype of MSN-like striatal projection neurons, potentially suitable for cell implantation therapy in HD.

However, despite this, the proportions of MSN-like cells is generally lower than that developing from primary fetal WGE, and moreover, the behavioural improvement following implantation into animal models of HD fails to demonstrate the full range of behavioural improvements seen following transplantation of primary fetal WGE (reviewed in Reddington et al 2014 Frontiers in cellular neuroscience 2014 8, article 398.). One explanation for this is that the differentiation protocols used directed cells towards a subtype that displays many features of an MSN, but is not a "genuine" MSN.

In this chapter, we attempted to produce MSNs from human WGE iPS cells using methods based on these studies with further optimisation as described further below.

4.2 Aims

In this chapter I hypothesise that (i) human iPS WGE cells can be differentiated to an MSN-like phenotype, both *in vitro* and after neural transplantation, and (ii) that epigenetic memory remaining in the iPS WGE cell lines may cause the cells to more readily differentiate into MSNs and may in addition enhance sub-type specific differentiation.

The first step was to establish an *in vitro* differentiation protocol for directing iPS cells toward a GABAergic MSN phenotype. The iPS cell lines used were derived from WGE (The C9 clone and SWIFT numbers 928, 949, and 954). We take advantage of the fact that the WGE iPS cell lines should already be primed to readily differentiate toward our desired MSN phenotype. A HEF line (SWIFT number 962), as described in detail previously in chapter 4, and an ES cell line (H9) were used for comparison. In addition, human primary fetal WGE was used as a source of “genuine” MSNs for comparison. iPS/ES cells underwent neuronal conversion protocols which comprised of 3 steps: neuronal induction, regional specification, and maturation. A combination of small molecules and morphogens were applied to the culture at specific time windows in order to produce projection GABAergic MSNs. The iPS derived-neurons were chronologically analysed with various methods such as RT-PCR, immunocytochemistry analysis so as to demonstrate neuronal markers related to MSNs induction. Finally, cells were transplanted into the QA-lesioned rat striatum and immunohistochemistry was used to analyse *in vivo* differentiation.

4.3 Experimental design

An EB based method was used to achieve striatal MSN differentiation. It can be described in 3 stages. First, we generated free floating multicellular aggregating cells or EBs from human iPS and ES cells and allowed them to proliferate and differentiate freely as described in the schematic in figure 4.1. (1). Second, neural induction was started by transferring these EBs into KSR medium (days 1-5) and N2/B27 medium (days 5-10) with a combination of selective molecules until rosette structures were recognized (2). Third, neuroepithelial cells from neural rosettes were subsequently pushed toward a ventral telencephalic phenotype generating committed regional specific telencephalic precursors using SHH and DKK-1. Following these three steps, these cells were terminally differentiated (methods described below) and maturated into striatal MSNs, confirmed by an expression of DARPP32 (3). Finally, iPS and ES derived MSN-like donor cells at 30 days (the early post mitotic stage of mature MSNs confirming by positive expression of DARPP32) were implanted into the QA-lesioned rat striatum, as an HD model, with the intention to allow them to differentiate *in vivo* for 7 and 20 weeks (although as explained below, both time points had to be brought forward) (4). The brains were collected and processed to analyse phenotypic characterization using various methodologies (5).

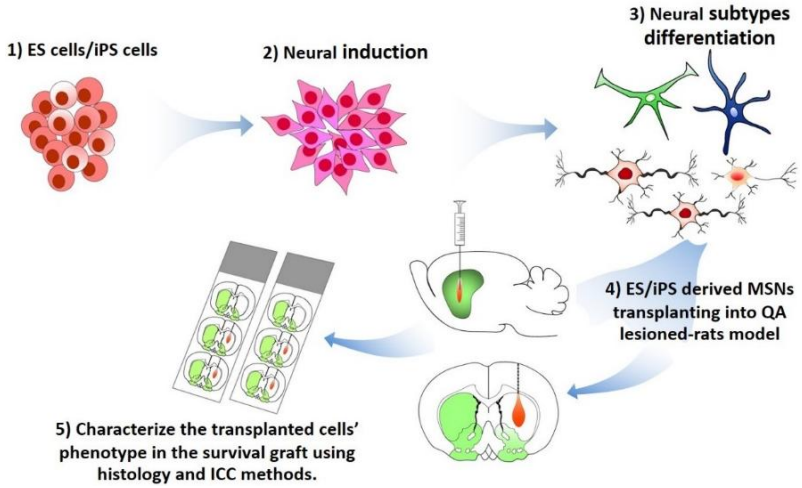

Figure 4.1 The schematic presents the experimental design for producing human iPS and ES derived GABAergic projection neurons (MSNs) using an EBs-based method to initiate neural induction in culture (1 and 2). A specific phenotype of MSNs-liked cells was generated using a combination of small molecules, morphogens, and growth factors supplement within N2/B27 medium (3). The **human iPS and ES** derived MSNs like cells were characterised by various methods (not shown on diagram) before being transplantation into a QA lesioned-rat model of HD (4). The surviving grafts were investigated by histology and immunohistochemistry (5).

4.4 Methods

4.4.1 Induction and differentiation of ventral telencephalon progenitors and GABAergic MSNs from human iPS cells lines

Two differentiation methods are described, Protocol 1 is taken directly from (Arber et al., submitted) and was used to differentiate the iPS WGE623 C9 line. Following the unsuccessful differentiation of this line, I modified the protocol and this is termed protocol 2 (currently unpublished). The second protocol was eventually also applied to iPS WGE623 C9.

Protocol 1

The whole EBs from iPS WGE623 C9 were re-plated onto a matrigel coated tissue culture plate. Neural induction was induced in this culture by supplementing KSR medium with dual SMAD inhibitors-SB431542 (10 µM) and Noggin (500 ng/ml) (Figure 4.2). From day 6-9, the KSR medium was substituted by N2B27 medium. The combination of exogenous signalling regulators (Noggin, Dorsomorphin (200 nM), Activin A (25 ng/ml), SHH (200 ng/ml)) was described as seen in figure 4.2. Neural progenitors were patterned further to a restricted region of ventral telencephalon by exposure to the morphogens SHH from 9 to 26 DIV. At 9 and 18 DIV, attached-EBs were detached, dissociated as single cell suspension using enzymatic digestion reagent Accutase® (1 Unit/ml) in N2B27 medium with the addition of ROCK inhibitor (Y-27632) and re-cultured on PLL-POL-Laminin treated coverslips. In terminal differentiation and maturation, cells were cultured with N2B27 medium supplemented with BDNF (10 µg/ml), GDNF (10 µg/ml), and ascorbic acid (200µM).

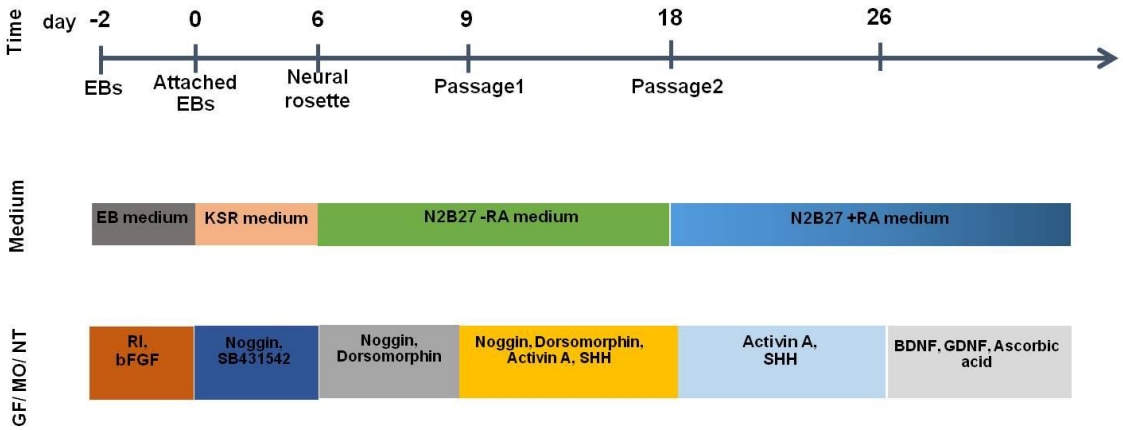

Figure 4.2 Protocol 1: The schematic shows the time line of human ES and iPS cells (iPS WGE C9) differentiation toward an MSN specific phenotype *in vitro* by using a chemical defined medium with exogenous signalling regulators as shown in the picture. (Arber et al., submitted)

Protocol 2

Human iPS cells (line 928, 949, 954, 962, and eventually C9) were maintained and expanded on an irradiated MEFs feeder layer as described by Thompson et al (Thomson et al., 1998). This protocol was improved and based on many previous published papers (Aubry et al., 2008; Chamber et al., 2009; Ma et al., 2012; Delli Carri et al., 2013; Arber et al., submitted). Firstly, neuronal induction was initiated by manually separating the iPS colonies into small clumps using a sterilized glass pipette. The tissues were then harvested and cultured in suspension as 'EBs' in human iPS medium without addition of bFGF for 2 days. From day 3-5, the EBs were transferred to culture in the presence of SB431542 (10 µM), Noggin (500 µg/ml), Dorsomorphin (200 µM), SHH (100 ng/ml), and DKK-1 (100 ng/ml) in KSR medium. At this stage, the iPS cells were allowed to differentiate freely as EBs, however, additional dual SMAD inhibitors (SB431542 and Noggin) were pushed the iPS cells toward ectodermal differentiation by inhibit BMP and Lefty/Activin/TGFβ pathways in order to obtain a higher yield of ectoderm lineage especially neural cells (Chamber et al., 2009). Moreover, dorsomorphin was supplemented in order to further inhibit BMP pathway as triple SMAD inhibitors (Arber et al., submitted). Regional differentiation toward ventral telencephalon by SHH and DKK-1 supplement were induced as early as in the neural induction stage.

Then, EBs were again placed in neural induction medium (N2/B27 medium) supplemented with the previously mentioned-combinations for up to 10 DIV in order to induce neuronal progenitor differentiation (Figure 4.3).

For regional patterning toward ventral telencephalon, neuronal precursor clusters were produced in 2 different ways. First, EBs were dissociated with Accutase® (1 Unit/ml) at 37°C for 5-7 minutes. Second, whole EBs were attached on matrigel coated tissue culture plate for several days before being dissociated with Accutase® as mentioned earlier. The cells were further separated into single cell suspension and placed onto PLL-POL-Laminin treated coverslips. Then the cells were cultured in neural precursors medium with SHH and DKK-1 supplemented up to 26 DIV. The combination of SHH and DKK-1 gave a synergetic effect incomparison to use only one factor of SHH (Delli Carri et al., 2013). Moreover, the most effective concentration SHH for LGE patterning was reported at 200 ng/ml (Ma et al., 2012). Therefore, in this experiment, we decided to add 100 ng/ml SHH incombination with 100 ng/ml DKK-1 in order to gain a benefit from the synergetic effect with the most effective LGE conversion efficiency. In addition, Activin A (25 ng/ml) was supplemented into the medium from day 22-30 so as to encourage neural telencephalic progenitors by promoting RA signalling pathway (Cambray et al., 2012). Moreover, Activin A was suggested to promote LGE precursor cells via SMAD 2/3 pathway, which further differentiate to mature MSNs (Arber et al., submitted).

Ventral progenitors were further persuaded to a maturation of GABAergic MSN subtype by using a group of trophic factors and small molecules Ascorbic acid (200 µg/ml), VPA (10mM/ml), BDNF (100 ng/ml), and GDNF (10 ng/ml). BDNF has been reported to get involve in adult neurogenesis, improve activities of GABAergic receptors (Waterhouse et al., 2012), and enhance GABAergic neuronal maturation, receptors and synapses (Yamada et al., 2002). Moreover, GDNF supplement has been suggested to accelerate branching and elongaging of neurites in primary cells cuture (Costantini and Isacson, 2000). From day 26-62, the cells were allowed to remain in culture in order to enable terminal differentiation and maturation (Figure 4.3).

From the previous study, Aubry and co-workers suggested an appropriate time window to harvest the cells for transplantation at around 35-45 DIV because at this stage, the ES cells derived neurons were situated between a late proliferative stage and early post mitotic stage (Aubry et al., 2008). This will enhance the graft survival and allow the cells proliferating a little bit further *in vivo* without an overgrowth of high proliferative transplated precursors (Aubry et al., 2008). In this study, *in vivo* differentiation within QA-lesioned rat model was performed by transplantation of iPS cell derived MSN-like precursors at 30 DIV, which DARPP32 positive cells were first recognized.

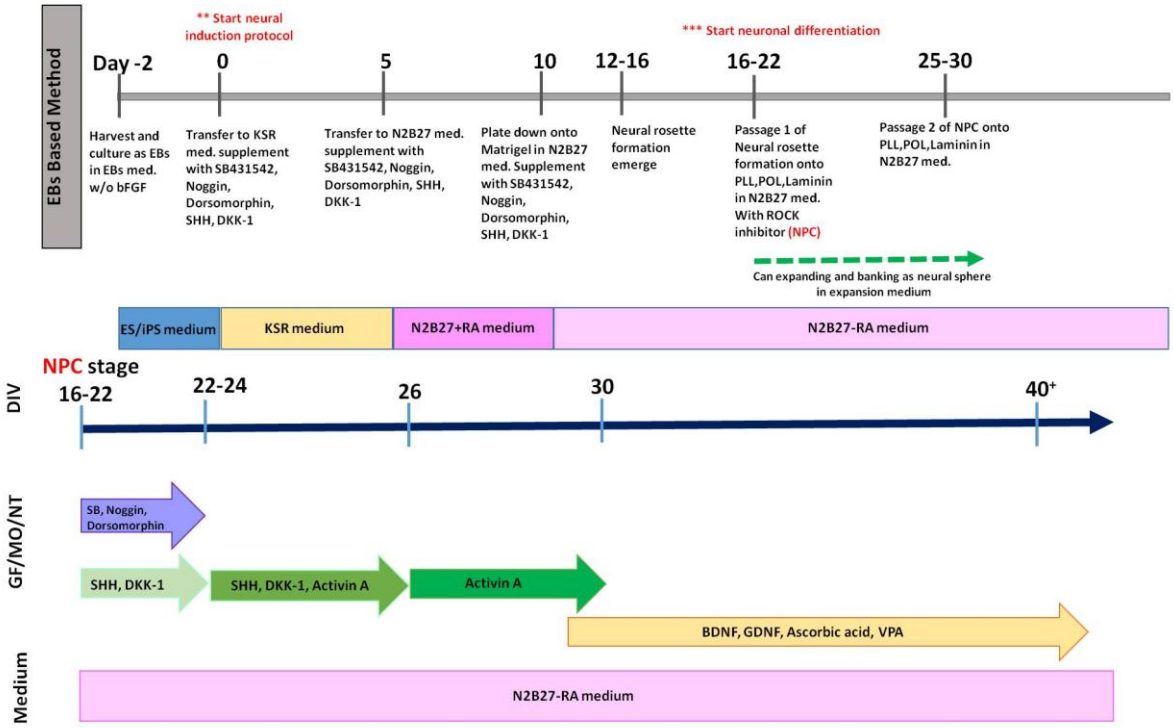

Figure 4.3 Protocol 2: Schematic of the time line for neural induction from PSC using EBs-Based method, which is described above. (EB= embryoid body, NI medium= neural induction medium, NPC= neural precursor cell)

4.4.2 Immunocytochemistry

Cells on the coated-coverslips were fixed in 4% PFA for 15 minutes at room temperature. Then 100% Ethanol was added to penetrate cells for 2 minutes. Blocking solution adding a suitable serum was applied at room temperature for 1 hour. Following this, the cells were incubated overnight at 4°C with a wide range of primary antibodies (for antibody details see table below). Alexaflour 488 and 594 appropriated with the primary antibodies were performed at room temperature up to 2 hours. Nuclei were stained with Hoechst for 5 minutes and washed with 1XPBS prior to coverslip onto glass slides.

Primary antibody	Isotope	Clonal Type	Concentration	Supplier	Code
1. Sox2	IgG	Rabbit	1:100	abcam	ab97959
2. PAX6	IgG	Rabbit	1:500	abcam	ab5790
3. Nestin	IgG	Rabbit	1:1000	Millipore	MAB5922
4. ZO-1	IgG1	Mouse	1:200-1:500	BD Bioscience	BD610966
5. FoxP1	IgG	Rabbit	1:500	abcam	ab16645
6. FoxP2	IgG	Rabbit	1:500	abcam	ab16046
7. Ctip2	IgG	Rat	1:200-1:500	abcam	ab18465
8. TTF1	IgG	Rabbit	1:200	abcam	ab40880
9. Islet1	IgG	Rabbit	1:200	abcam	ab20670
10. GSH2	IgG	Rabbit	1:200	abcam	ab26255
11. β-III tubullin	-	Rabbit	1:1000	Sigma	T2200
12. MAP2ab	IgG1	Mouse	1:200	abcam	ab36447
13. Dlx1	IgG2a	Mouse	1:200-1:500	abcam	ab54668
14. Dlx2	IgG	Rabbit	1:200-1:500	abcam	ab18188
15. DARPP32	IgG	Rabbit	1:200	Santa Cruz	SC11365
16. hDARPP32	IgG	Rabbit	1:1000	abcam	ab40802
17. FoxP1	IgG2a	Mouse	1:200-1:500	abcam	ab32010
18. Synaptophysin	IgG1	Mouse	1:100	abcam	ab8049
19. PSD95	IgG	Rabbit	1:100	abcam	ab18258
20. GFAP	IgG2b	Mouse	1:1000	abcam	ab10062
21. Otx2	-	Rabbit	1:500	Millipore	MAB9566
22. GABA	IgG	Rabbit	1:200-1:500	abcam	ab9446
23. Ki67	IgG1	Mouse	1:500	Dako	M7240
24. HuNu	IgG1	Rabbit	1:500	Millipore	MAB1281
25. β-III tubullin	IgG1	Mouse	1:1000	Sigma	T9026
26. GFAP	IgG	Rabbit	1:1000	Dako	ZO334

Table 4.1 Summary table of the primary antibodies used for immunocytochemistry and immunohistochemistry analysis both *in vitro* and *in vivo* studies.

4.4.3 Gene expression analysis

The RNA was purified from cultured cells using RNeasy kit from Qiagen the protocol as previous described in Chapter 2. cDNA were generate using SuperScript III reverse transcriptase and universal primers according to manufacturer's instructions (Invitrogen). RT-PCR of the involved expressing gene and primer sequences were described in the table below.

Genes	Primer sequences
Nestin	GGCAGCGTTGGAACAGAGGTTGGA CTCTAAACTGGAGTGGTCAGGGCT
PAX6	TACGAGACTGGCTCCATCAGACC GCAGCCATCTTGCGTAGGTTGCC
FoxP1	GCAGTTACAGCAGCAGCACCTCC CAGCCTGGCCACTTGCATACACC
FoxP2	GCTTCTCCAGATGCAACAACTCC ACTGAGCAGTGCTTCGGTCATCC
Dlx1	CAAGGCGGTGTTTATGGAGT CGGGCAACCTCACATAAGTT
Dlx2	TCACCCAGACTCAGGTCAAA CGGGGTAAGCAATGAGGATA
Gsh2	GTCGACTCGCTCATCATCAA ATGGTGAGGCAGTGGAATCT
Islet1	GTTACCAGCCACCTTGGAAA TTTTGCTGGAGCTCCTGTTT
Ctip2	CCATCCTCGAAGAAGACGAG AGCAGGAGAACATTGCAGGT
DARPP32	GCCAGTCCATCTTCCAGGCACCCAG CTGTGCCTACACACCACCTTC
GAPDH	AGAAGGCTGGGGCTCATTG AGGGGCCATCCACAGTCTTC

Table 4.2 Summary table of the primer sequences used for RT-PCR analysis of neural differentiation *in vitro* study from human PSCs derived MSN like-cells.

4.4.4 Striatal lesion and Transplantation

Adult male and female Spague-Dawley rats were used under local ethical guidelines and approved animal care according to the UK Animals (Scientific procedures) Act 1986. 7 days after unilateral QA-lesions to the right striatum (see chapter 2), rats were transplanted with 250,000 cells/µl (500,000 cells in total) of human iPS/ES cell derived-neuronal cells, prepared as a single cell suspension in DMEM/F12 medium. The transplantation side using stereotaxic coordinates was at +0.6 mm AP and -2.8 mm L from bregma, at two heights -5.0 mm and -4.0 mm below dura. Immunosuppression- Cyclosporin A was initiated (10 mg/kg) the day prior to transplantation and carried on daily until the end of the experiment. Rats were perfused at 4 and 7 weeks post transplantation (see Chapter 2 for details). Dr.Claire M. Kelly and Dr.Victoria Roberton, BRG, School of Bioscience, Cardiff University have done the work.

4.4.5 Immunodetection on brain tissue slices

At different time periods post transplantation, animals were sacrificed and the brains were processed as follow described. Rats were perfused with cold 4% PFA for 5 minutes. Then the brains were dissected and fixed in 4%PFA overnight on a shaker. The following day, the brains were incubated with 25% sucrose in prewash solution for 48 hours or until they sank. Brains were coronally sectioned at 40 µm thickness using a freezing microtome. Sections were stored in anti-freeze solution and stored at -20 degree. Free-floating immune- and DAB staining were as described in Chapter 2.

4.4.6 Microscopy and analysis

Cells were visualized under UV fluorescence and images were collected using an Axiocam microscope with Axiovision program and a Leica DMRBE microscope with LAS V3.8 program.

4.4.7 Quantitation of grafts.

Graft were visualized under the Leitz DRMB light microscope. Digitised images were visualized using a Hamamatsu C4752 video camera and NIH 1.55.2 image analysis software, and the area corresponding to grafted tissue in each section was traced around and measured. Graft volume was subsequently calculated to be:

$$V = \frac{\sum a.M}{f}$$

V = graft volume (mm^3)

a = area (mm^2)

M = section thickness (0.06/0.04 mm)

F = frequency of sampled sections (1:6)

Cell number was calculated in all cases by manually counting all cells from a 1:12 series.

The Abercrombie correction formula was the applied to calculate the total number of cells in the graft:

$$\text{Total number of cells} = \frac{F \times A \times M}{(D+M)}$$

F = frequency of section i.e. 1 in 6

A = cell counts for entire animal

M = section thickness

D = average cell diameter

4.5 Results

***In vitro* differentiation of human cell lines towards an MSN-like subtype: primary fetal WGE, iPS cells, and ES cells**

4.5.1 Human embryonic WGE differentiation *in vitro*.

Human primary WGE was used as the "gold standard" in this study. Human primary WGEs (SWIFT number 1006, 1037, 2073) (approximate crown rump length (CRL) 22-49 mm.) were dissected, dissociated and plated down for *in vitro* differentiation as single cells onto PLL coated-coverslips in N2B27 medium. Cultures were characterised using immunocytochemistry for markers of neurons and authentic MSNs at different times post plating (N=2 coverslips/condition). At 10 DIV, the cells showed neuronal morphology with processes, small cell bodies and nuclei on phase contrast microscopy (Figure 4.4 A). The cells were fixed and immunocytochemistry was employed at 14 DIV (Figure 4.4 B, D, F, and G) and at 22 DIV (Figure 4.4 E, H-L).

Comparison of cultures at 14 DIV and 22 DIV (Figure 4.4 B, C respectively) revealed that Ki67 appeared to be less widely expressed by 22 DIV. Ventral forebrain markers-Dlx1, FoxP1, Islet1 were present by 14 DIV and persisted and expression was still evident at 22 DIV (Figure 4.4 D-I-E). Interestingly, the expression of FoxP1 (Figure 4.4 D, E), Dlx1 (Figure 4.4 G, H) and Dlx2 (Figure 4.4 I) was presented in the cytoplasm at the earlier time point and then translocated to the nucleus with prolonged culture to 22 DIV. Expression of the terminally differentiated MSN marker, DARRP32, was recognized at 22 DIV co-labelled with Ctip2, an earlier marker of less mature MSNs (Figure 4.4 J). To elucidate functional neurons, PSD95 and synaptophysin markers involved in synaptic activity, were used and found to co-express with the neuronal markers Map2 and β-III tubulin at 22 DIV (Figure 4.4 K and L respectively).

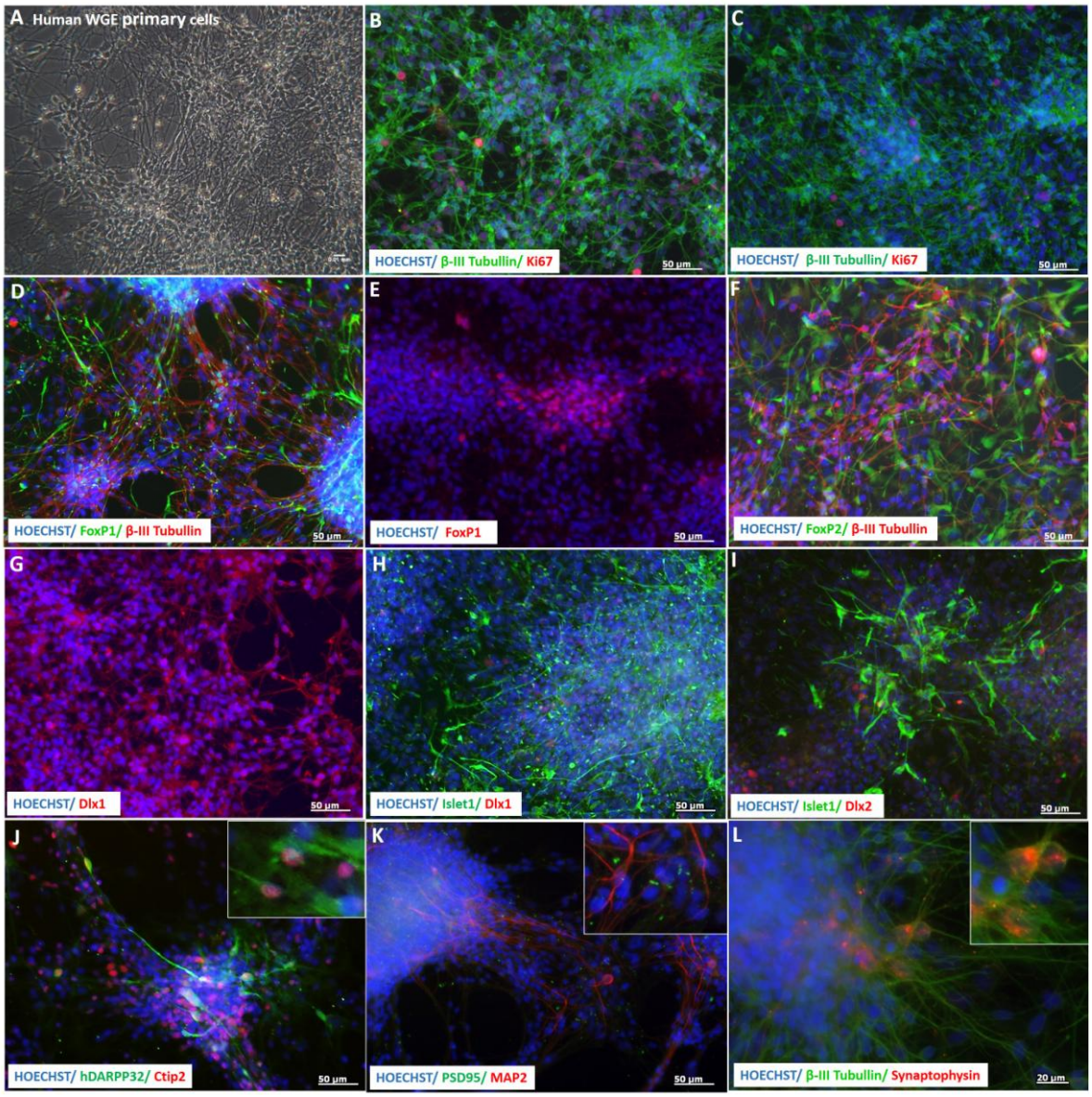

Figure 4.4 WGE differentiation cultures. Characterisation and phenotypic potential of human primary WGE. Representative phase contrast and immunocytochemistry photomicrographs of differentiated human primary WGE (CRL= 49 mm.). Neuronal morphology under phase contrast at 14 DIV (Scale bar = 0.01 mm) (A) and expression of neuronal marker β-III tubulin (B,C). At 14DIV, human primary WGE demonstrated higher expression of proliferative neural cells with Ki67 co-expressed with β-III tubullin (B) compared to 22 DIV (C). Region specific characterization of ventral telencephalic markers FoxP1 (D,E), FoxP2 (F), Dlx1 (G,H), and Islet1 (H,I). Expression of Dlx1 appeared in cytoplasm at 14 DIV (G), whereas at 22 DIV, its expression was present in the nuclei (H). A similar phenomena was seen for Dlx2 – nuclear staining only shown in I). At 22 DIV, encoded ventral telencephalic proteins FoxP1 (E) and Dlx1 (H) translocated into nuclei. MSN marker DARRP32 co-expressing with Ctip2 (J) and expression of markers suggesting neuronal activity PSD95 (K), and synaptophysin (L). Scale bars= 50 µm (B-K) and 20 µm (L).

4.5.2 iPS WGE623-derived MSNs: C9 clone (protocol 1).

For differentiation of human iPS WGE623 C9 towards striatal MSNs, we employed the Arber and Li protocol (submitted), which has successfully generated DARPP32 positive cells both *in vitro* and *in vivo*. The iPS cell line WGE623 C9, the first iPS cell line generated in this thesis as previously mentioned in chapter 4, was differentiated toward MSN-like cells following this protocol. The iPS cells were allowed to differentiate as EBs for 48 hours before re-plating onto a Matrigel coated culture plate. Neural rosette structures are represented by a group of radially elongated shaped cells arranged as a flower-like structure (Figure 4.5 A), appeared around 6 DIV after subsequently exchanging defined medium with a combination of small molecules, growth factors and morphogens.

Photomicrographs of human iPS WGE623 C9-derived neural cells were labelled for the neural progenitor marker nestin (Figure 4.5 B, C), and expression of zonula occludens-1 (ZO-1) a tight junction marker expressed by neuroepithelial cells during development of the neural plate, was also seen - figure 4.5 B. With time in vitro, ZO-1 expression gradually migrated towards the luminal area suggestive of formation of a neural tube-like structure as occurs in development (Figure 4.5 C). At 9 and 18 DIV, these cells were passaged and re-attached onto culture plates and coverslips with an exchange of N2B27 medium and chemical combinations as described in figure 4.3. Neuronal morphological appearances were obtained with expression by immuno fluorescence positive for β-III tubulin (Figure 4.5 D, E). The ventral telencephalic marker 'Islet1' was also identified in the culture at 25 DIV fixed cells (Figure 4.5 F).

After passage 2, around 20-24 DIV, small islands of ES-like cells emerged among the differentiated neural like-cells, later on taking over the whole culture (Figure 4.5 G). These aggregations of cells were immunopositive for the pluripotent markers Oct4 and SSEA4 (Figure 4.5 H and I). The protocol was then optimised to prolong the EB stage and extend time of SMAD inhibition in culture and the number of re-plated cells was optimized under different cell densities ($5x10^4$, $7.5x10^4$, $1x10^5$ cells/coverslips). However, the same situation with appearance of ES-like cells took place at similar time point (after passage 2 around 20-24 DIV). To try to address this, the iPS cell line WGE623 C9 underwent

second transfection of transposase enzyme in a further attempt to remove the residual transgenes.

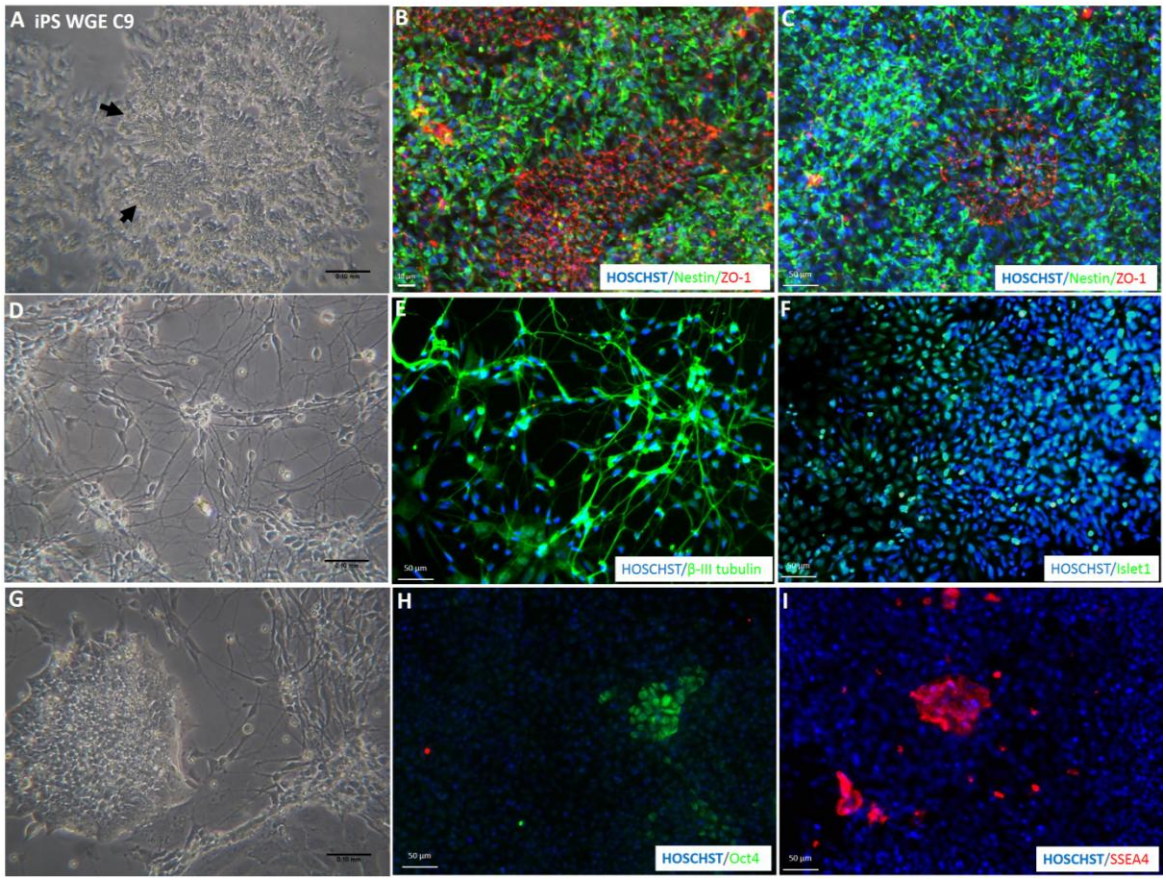

Figure 4.5 Photomicrographs presenting expression of neural marker series and pluripotent markers from iPS WGE623 C9 derived-MSNs study. Neural rosette formation emerged at around 6 DIV (A). By the first passage (9 DIV), the cells demonstrated expression of neural progenitor **nestin** with the cell adherent marker **ZO-1** (B). Initially, ZO-1 was expressed at the cell membrane surface (B) but with progression of neural rosette rearrangement the expression of ZO-1 became concentrated next to the luminal area (B, C, respectively). After passage 1, iPS cell derived-MSNs obtained neuronal morphological appearances as can be recognized by phase contrast (D) and demonstrated expression of the more mature neuronal marker β-III tubulin (E). Regional specification of the ventral telencephalic marker Islet1 was seen at 25 DIV (F). ES-like colonies emerged around 20-24 DIV after passage 2 and the same event kept repeating in other rounds of differentiation (G). The ES-like colonies expressed pluripotent markers of Oct4 and SSEA4 (H and I, respectively). (Scale bar= 0.10 mm A, D, G; Scale bar= 50 µm B, C, E, F, H, I)

EB-Based Method for differentiation of neurons from human iPS and ES cells (protocol 2).

4.5.3 Human iPS and ES derived MSNs-liked cells.

Following the problems differentiating the iPS WGE623 C9 clone, further iPS cell lines were generated, and the transgene inserts were attempted to remove before the iPS cells were differentiated toward neural lineage. In addition, I developed a novel neural differentiation protocol based on many previous published articles (Aubry et al., 2008; Chamber et al., 2009; Ma et al., 2012; Delli Carri et al., 2013; Arber et al., submitted) in order to obtain the desired MSN-like projection neurons suitable for cells therapy in HD (Figure 4.2). This was used to differentiate the various PSC lines including human ES cells (H9), iPS cell lines WGE623 C9, WGE 928, WGE 949, WGE 954, and HEF 962. All PSCs lines were able to form EB structures when detached from MEFs and clumps of PSC differentiated as multi-aggregated cells in ES medium without FGF2 supplement (figure 4.6 A-F). The generated-EBs did not appear different in their morphology when different cell lines were compared in this way. The EBs at 10 DIV were allowed to attach on matrigel coated-plates and were further cultured in defined chemical medium until neural rosette emerged over the next 2-6 day (Figure 4.6 G, H). Neural rosette structures were recognized by columnar epithelial cells arranged around luminal area in radius direction (Figure 4.6 G). Immunofluorescent Hoechst positive nuclei exemplified the structure of neural rosettes (Figure 4.6 H).

Neural rosettes were dissociated and re-attached onto PLL-POL-laminin coated culture vessels and coverslips in selective defined medium. The plated cell morphology at the earlier stage (12-16 DIV) of differentiation was observed as ovoid or elongated shaped cell bodies with short and fine processes comparable to neural precursor cells (Figure 4.7 A, C, E, G, I). In contrast to the differentiation of the iPS WGE623 C9 clone up to 25-30 DIV, these cells progressively obtained neuronal morphological appearances as described by smaller and tighter cells' bodies sending out thick and long neurites (Figure 4.7 B, D, F, H, J). Different human ES and iPS cell lines exhibited a similar pattern of *in vitro* differentiation

from neuroepithelial to neural precursor cell morphology and in becoming neuronal like-cells at a later stage.

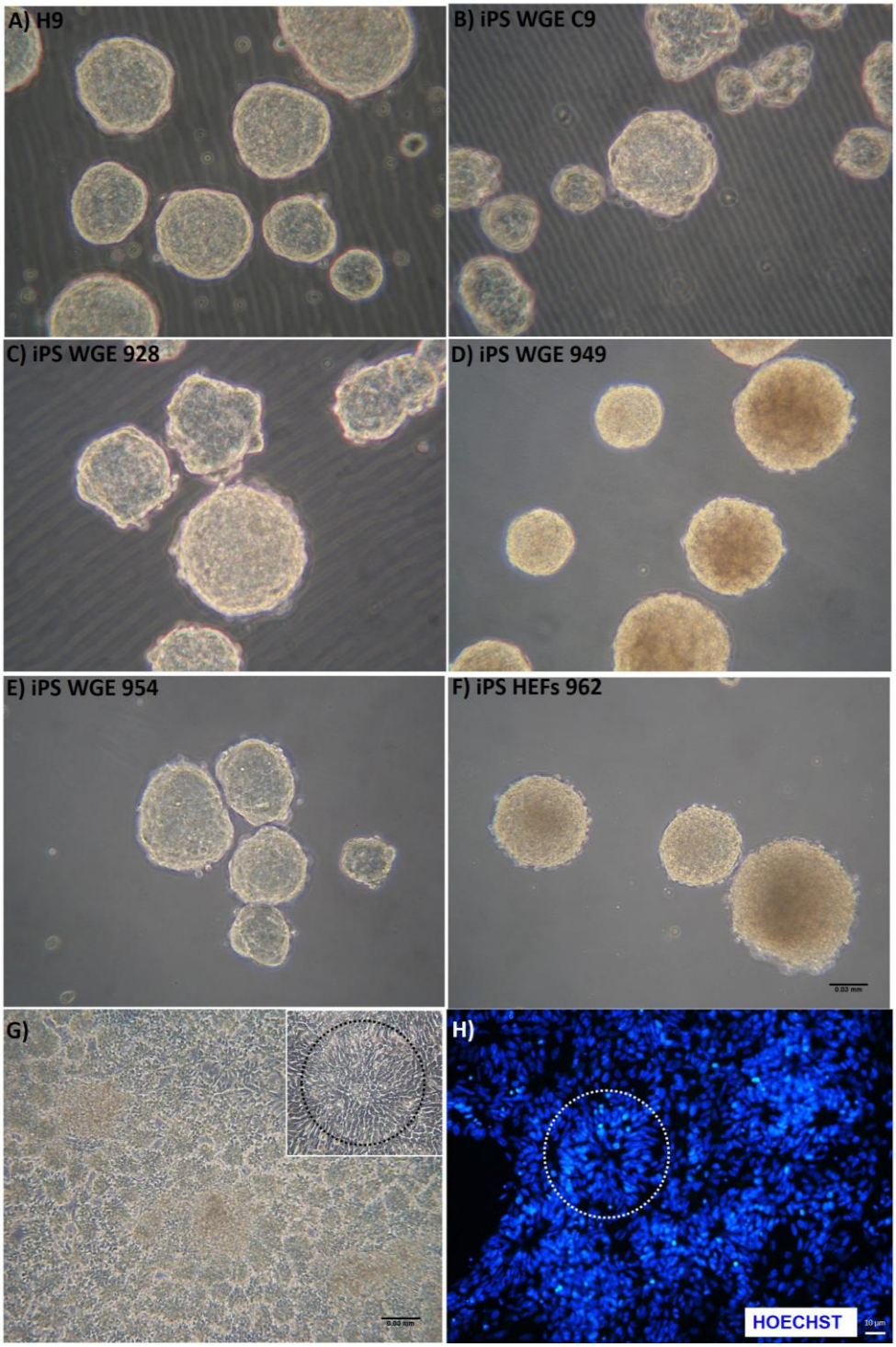

Figure 4.6 Photomicrographs of EBs formation generated from various human ES and iPS cells lines (A-F). Human ES cell (H9) and established iPS cells iPS WGE C9, WGE 928, WGE 949, WGE 954, and HEF 962 formed EBs after re-suspended in ES medium without bFGF supplement (A-F, respectively). Rosette structures appeared like a group of flowers in PSC differentiation, using the EBs based protocol when re-adhered to the culture plastic (G). A comparison of bright field photomicrograph and immuno-fluorescence of nuclei staining (**HOECHST**) illustrated the rosette structure (H). (Scale bar=0.03 mm (A-G); Scale bar= 10 µm H)

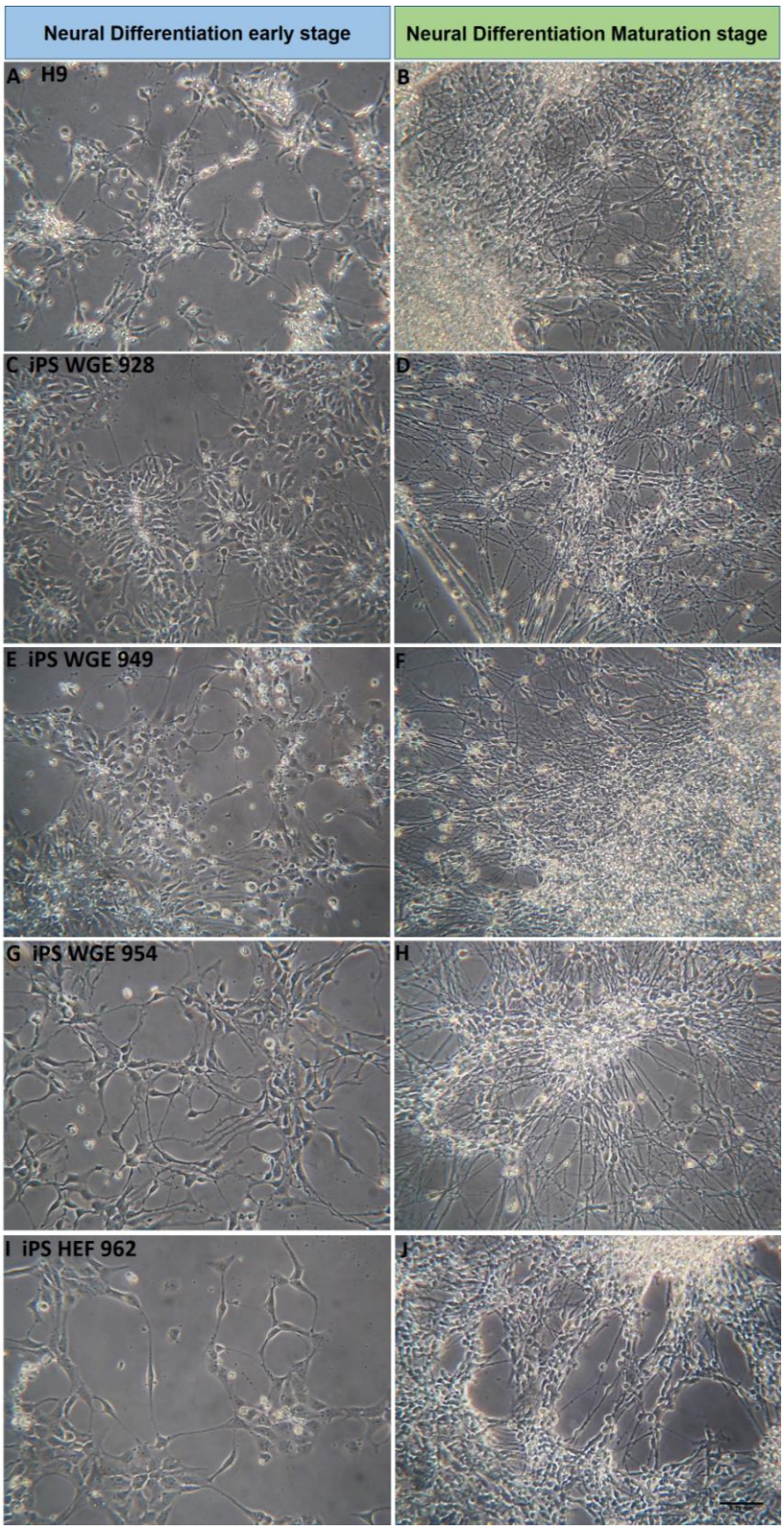

Figure 4.7 Photomicrographs showing the neuronal morphological appearances of neurally differentiated PSCs. An early stage of differentiation after passage 1 is shown in the left hand column (A= human ES cell, C= iPS WGE 928, E= iPS WGE 949, G= iPS WGE 954, I= iPS HEF 962). Following maturation in vitro, cells gained a morphology close to neuron like cells, with long neurites and small cell bodies (B= human ES cell, D= iPS WGE 928, F= iPS WGE 949, H= iPS WGE 954, J= iPS HEF 962) (Scale bar= 0.10 mm).

Characterisation of iPS cell lines following differentiation towards a striatal MSN phenotype.

To test our improved MSNs derived-protocol, 5 iPS cell lines (4 derived from WGE: 928, 949, 954, and WGE623 C9; and one HEF line: 962) and a standard human ES cell line (H9) were compared. Prior to differentiation, all iPS cell lines presented typical pluripotent properties by expressing a variety of pluripotent markers such as Oct4, Nanog, SSEA4, and Tra-1-60, with no differences between lines. In addition, they were indistinguishable in these respects from the standard human ES cell (Chapter 3).

4.5.4 iPS WGE 928 derived MSNs.

The iPS WGE 928 cell line was monitored from 0 to 62 DIV using immunocytochemistry and RT-PCR. The neural induction step used triple SMAD inhibition of SB431542, Noggin, and Dorsomorphin from day 0-22 (Figure 4.2). Neural rosettes were recognized as early as 2-6 DIV and progressively more were recognized around 6-9 DIV. Immuno-fluorescence staining indicated that at 7 DIV, the elongated shape of neuroepithelial cells demonstrated a homogeneity expressing neural precursor markers of nestin and Sox2 (Figure 4.8 A, B). After passage (passage 1) and re-plating as single cells, the dissociated cells were highly proliferative as demonstrated by the expression of Ki67 positive cells (Figure 4.8 C). ZO-1 expression was present at the luminal side of rosettes confirming generation of neural tube-like structures *in vitro* (Figure 4.8 A and B). In addition, subsequent passages were needed as the neural rosette structures continued to emerge up to 60 DIV. A heterogeneous population of immature and mature cells was illustrated by the expression of neurons with β-III tubulin confirming and neural precursors with nestin positive cells (Figure 4.8 D). At this stage, a lot of cell death was observed, probably resulting from the combination of defined culture medium, cytokines and morphogens. Cells that failed to differentiate along a neural lineage did not survive in this environment and dead cells were constantly discarded by exchanging the culture medium.

Regional specific commitment to ventral telencephalon fate was induced by SHH and DKK-1 applied into N2B27 medium supplement up to 26 DIV (see schematic Figure 5.2). The phenotype of ventral telencephalon identities was ensured by the expression of specific markers within this compartment such as FoxP2, GSH2, Dlx1, Dlx2, and Islet1 (Figure 4.8 E-H, respectively). Furthermore, the post mitotic neuronal marker microtubule-associated protein 2 (MAP2) was seen co-expressed with the LGE marker glutathione synthetase (GSH2) (Figure 4.8 F). In the maturation stage, the committed telencephalic precursors were persuaded toward post mitotic neurons with a striatal projection phenotype by subsequently separating and re-adhering on PLL-POL-laminin pre-treated tissue culture plates. Culture medium was supplemented with Fibronectin, Activin A, and VPA around DIV 16 to 26. Next, for terminal differentiation of MSN-like neurons, cells were cultured in N2B27 with addition of BDNF, GDNF, and ascorbic acid. Ctip2 is exclusively expressed by DARPP32 positive neurons within the striatum, was clearly elucidated in high intensity with a nuclear stain of HOECHST around 25-30 DIV while there was a small number of DARRP32 positive cells at this stage (Figure 4.8 I and inset).

Between 30 DIV and 62 DIV, there was an increase of presumed post mitotic MSNs as recognised by DARPP32 expression compared to 30 DIV (Figure 4.8 J). Moreover, co-expression of Ctip2 with DARPP32 positive cells was seen at this time point (Figure 4.8 J and K).

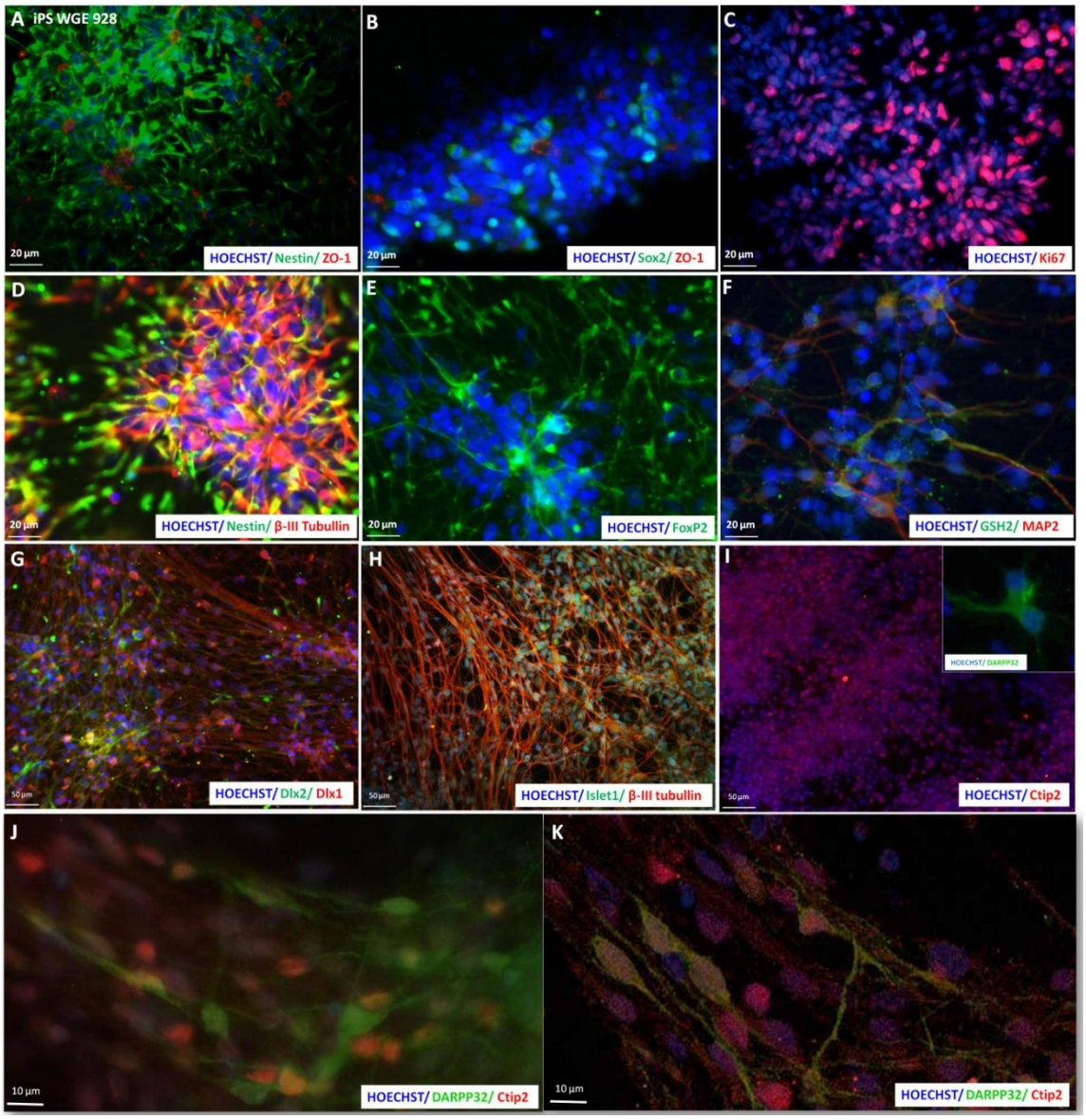

Figure 4.8 Phenotypic characterisation of striatal progenitors and MSN-like striatal projection neurons derived from iPS WGE 928 line. Typical neural rosette structure demonstrated proliferative properties by expressing neural precursor markers nestin and Sox2 with the proliferative marker Ki67 (A-C). Within the culture, heterogeneous populations of neural precursors with more mature neurons expressed nestin and β-III tubulin (D). Committed ventral telencephalic phenotypes were confirmed with positive immune-reactivity of FoxP2, GSH2, Dlx1, Dlx2, and Islet1 (E-H). Ctip2, a marker of post mitotic MSNs, was expressed with high intensity (I) concomitant with DARPP32 expression at later time in culture (inset). DARPP32 expression was intense in cells' body area and its expression was increased over time (J). A confocal reconstruction confirmed that human iPS cells derived from the WGE co-expressed DARPP32 and Ctip2, typical of a striatal projection neuron (MSN-like cells) (K). (Scale bar= 20 µm A-F; Scale bar= 50 µm G-I; Scale bar= 10 µm J,K)

Testing the reproducibility of the differentiation protocol in differentiating iPS cell lines towards striatal MSNs.

4.5.5 iPS WGE 949 derived MSNs.

To evaluate the efficiency and consistency of the differentiation results, the protocol was applied to other PSC lines. The WGE 949 line, which was produced in a similar way to 928 (ie from the induction of early neural spheres) achieved similar results to the iPS WGE 928 line. Neuroepithelial cells generated from rosette structures were present in a conventional rosette construction with expression of stage-matched markers of Sox2 and ZO-1 (Figure 4.9 (A)). Chronological expression of neural markers from neural precursors to regional ventral telencephalic precursors were revealed over time in *in vitro* differentiation (Figure 4.9). Nestin positive cells were seen promptly after passage 1 (11 DIV) (Figure 4.9 B), while later on these cells acquired immune-reactivity against β-III tubullin and MAP2 indicating post mitotic neuronal identity (Figure 4.9 C, D). Committed ventral telencephalic phenotypes were revealed by Dlx1 which co-expressed with Otx2 (a rostral regional marker) around 20-25 DIV, while striatal precursors were labelled with FoxP2 expressing cells throughout differentiation (Figure 4.9 E and G, respectively). At a later time in culture, glia cells emerged confirmed by expression of GFAP marker (Figure 4.9 F). The early post mitotic MSN precursor marker Ctip2 was abundantly observed in culture, and over time cells maturated into terminally differentiated MSNs with an increase in DARPP32 expression coinciding with Ctip2 (Figure 4.9 H, I and inset).

In contrast to the iPS WGE 928 cell line, the iPS WGE 949 cell line seemed to have a lower proliferation capacity as observed during *in vitro* differentiation. This cell line could subsequently be passaged several times before acquiring a mature neuronal morphology around 30-40 DIV, whereas neural rosette structures were persistently recognized and need to be passaged after 60 DIV in iPS WGE 928.

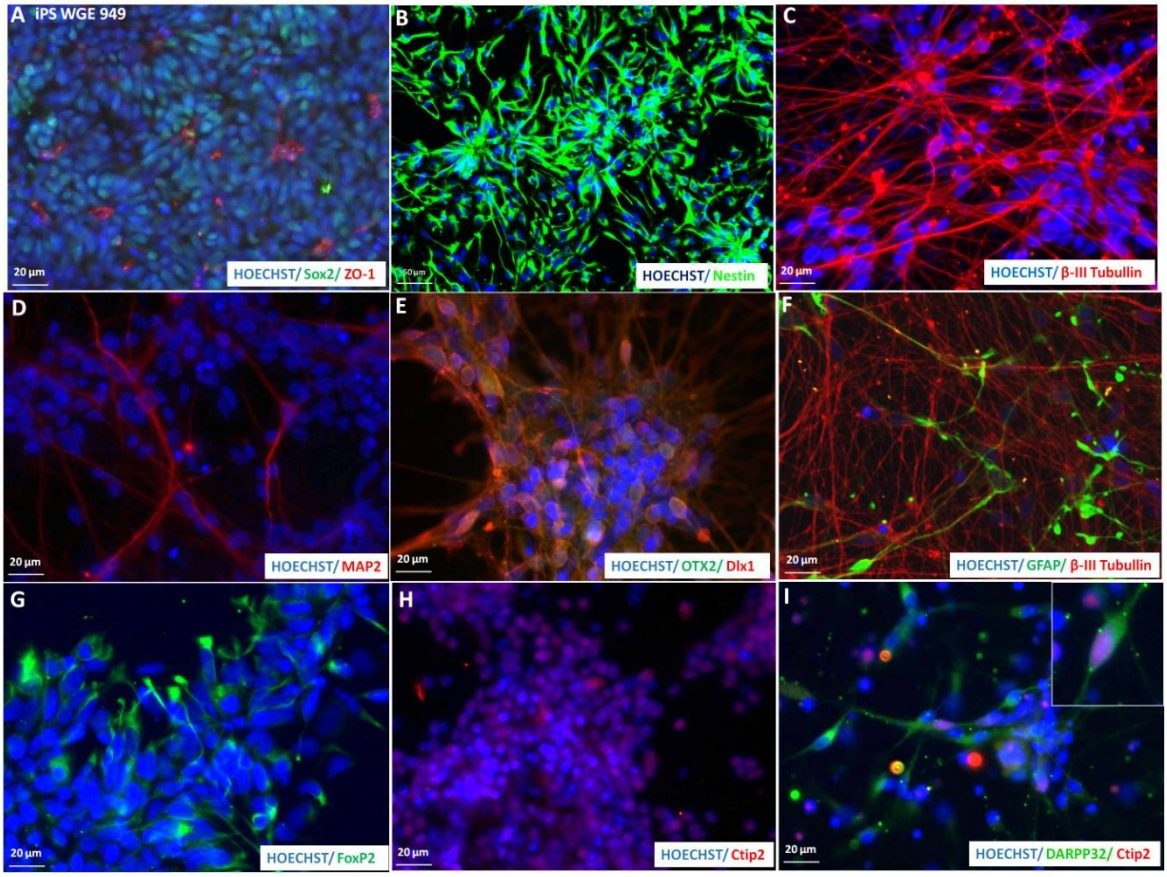

Figure 4.9 Phenotypic identification of *in vitro* differentiation from the iPS WGE 949 cell line. Sox2 is accompanied by ZO-1 at the luminal surface of rosette formation (A). Expression of stage specific markers of neural lineage nestin, β-III tubulin, MAP2 (B-D), regional committed ventral telencephalic precursor such as Dlx1 and FoxP2 expressed in response to SHH and DKK-1 (E, G). MSNs precursor marker Ctip2 and terminally differentiated MSN marker DARPP32 were revealed co-labelling within the nuclei and cytoplasmic area respectively (H, I and inset). (Scale bar= 20 µm)

4.5.6 iPS WGE 954 derived MSNs.

The iPS WGE 954 cell line was generated differently from WGE 928 as the original cells were human primary WGE, rather than neural spheres obtained from human primary WGE. Again, the improved protocol was applied to this line to test the reliability of differentiation into MSN-like cells.

The panel of immuno-micrographs revealed stage-specific gene expression from the beginning as NPC differentiated to terminal post mitotic DARPP32 expressing neurons (Figure 4.10). Expression of nestin was seen in almost all cells in the culture (Figure 4.10 A). Over time, their appearance changed and they gained morphological features similar to neuronal cells with expression of β-III tubulin (Figure 4.10 C). Ventral telencephalic fate was demonstrated by the presence of Dlx1 and Dlx2 expression (Figure 4.10 B). The regional specific LGE marker FoxP2 was also present in a subset of cells expressing β-III tubulin (Figure 4.10 C). Glial cells emerged around 28-30 DIV with prolonged *in vitro* differentiation. Glial-like cells were seen as a monolayer sheet spread underneath extensive neurite processes and neuronal like-cells which expressed β-III tubullin (Figure 4.10 D). Expression of Ctip2 gradually increased over time *in vitro* (Figure 4.10 E). Around 30 DIV, DARPP32 expressing cells were found predominantly in cells bodies and were observed co-labelling with Ctip2 positive cells (Figure 4.10 F and inset).

Of note, the iPS WGE 954 cell line exhibited a lower proliferation rate in comparison to the iPS WGE 928 and 949 cell lines. NPCs propagated from this iPS cell line proliferated in a similar ratio to the human ES cell (H9), which is further described in 4.5.8. After the second passage, iPS WGE 954 was cultured through to terminal differentiation and derived MSN-like cells without subsequent passages, similar to human ES cells. This was in contrast to iPS WGE 928 and 949, which exhibited a sub population of neural progenitor cells and needed many subsequent rounds of passaging. Furthermore, only neural phenotypes were recognized uniformly in cultures of iPS WGE 954 after subsequent passage. In addition, pluripotent cell clusters were not latterly seen in this culture.

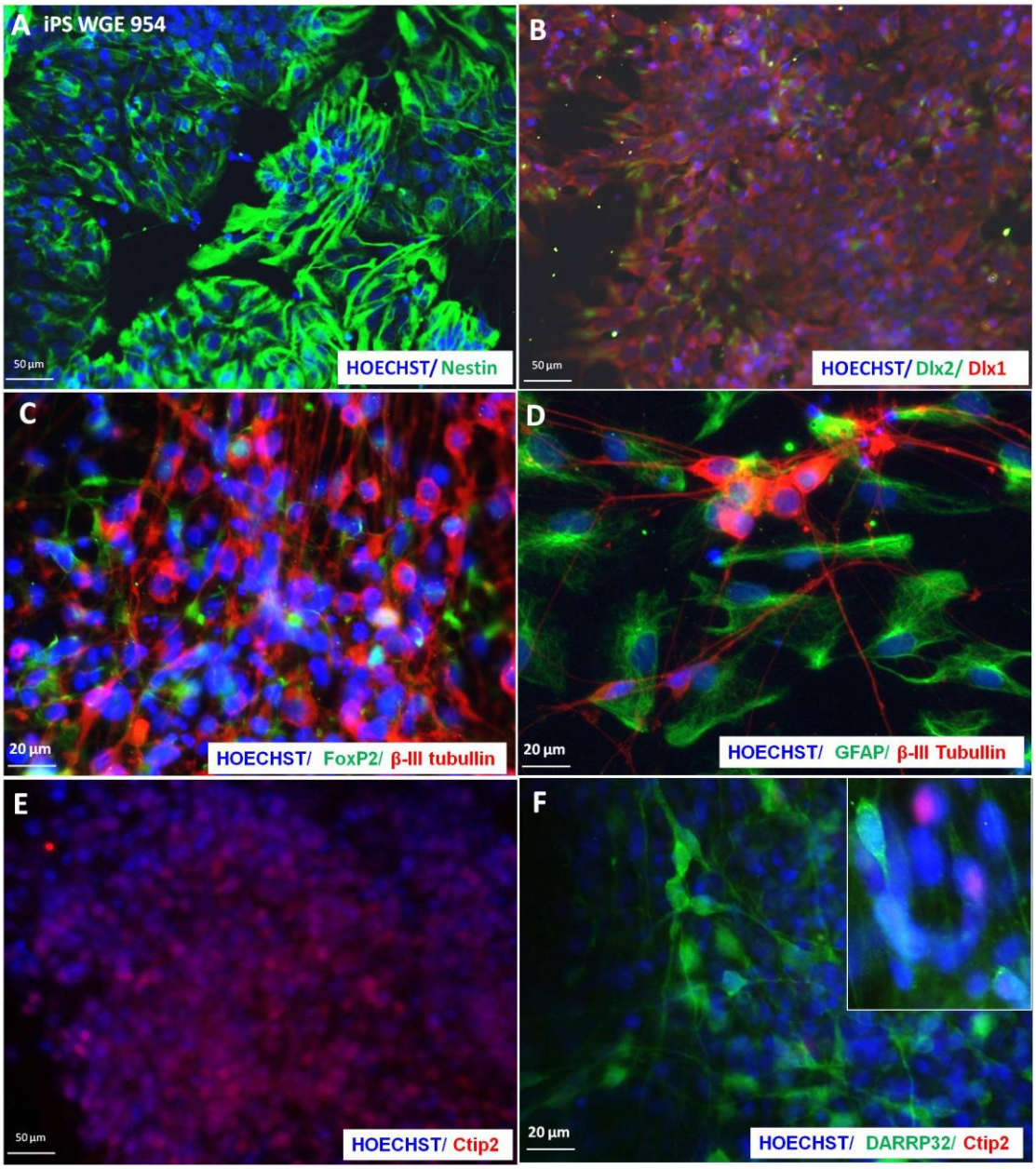

Figure 4.10 Phenotypic characterization of *in vitro* differentiation of the iPS WGE 954 cell line. A sequential expression of time specific markers from early neuron- nestin expressing cells (A), to progressive increase of expression of sub regional ventral telencephalic markers Dlx1, Dlx2, and FoxP2 (B-C). With long term culture, gial cells were detected by the presence of GFAP (D). An increase in DARPP32 expression was seen coinciding with Ctip2 expression around 30 DIV. (Scale bar= 20 µm C-E, Scale bar= 50 µm A,B,F)

4.5.7 iPS HEF 962 derived neural cells.

In a parallel, a comparison was made with, an iPS cell line generated from HEFs using the afore-described differentiation method.

Following *in vitro* differentiation around 13-18 DIV, cells with a distinctive appearance similar to fibroblast-like cells were recognizable among the population. For neural induction, neural rosettes were formed within EBs in the free-floating differentiation process around 5-6 DIV. After re-plating EBs on matrigel coated culture plate for 24 hours, definitive neuroepithelial cells were indicated by nestin expression. In addition, some cells were characteristic of neurons, with extended neurites and positive staining with β-III tubulin (Figure 4.11 A). It was noticeable that cells expressing more mature differentiation markers (β-III tubullin in this case) were mostly situated at the periphery of EB formation (Figure 4.11 A). After passage 1 (around 16-22 DIV), cells which were re-plated as a monolayer acquired a neural phenotype with evidence of immuno fluorescent positivity for nestin (Figure 4.11 B). These cells obtained a post mitotic neuronal phenotype at a later time point in culture (around 25-28 DIV), confirmed by Map2 expression (Figure 4.11 C). Moreover, characteristics of early LGE cells and ventral telencephalic phenotypes were revealed by expression of FoxP2, Dlx1, Dlx2, and Iselt1 (Figure 4.11 D-F). Unfortunately, the differentiating cultures became infected around day 28, therefore iPS cell line HEF962 have not been fully characterised because it was not possible to obtain results for DARPP32 immunohistochemistry.

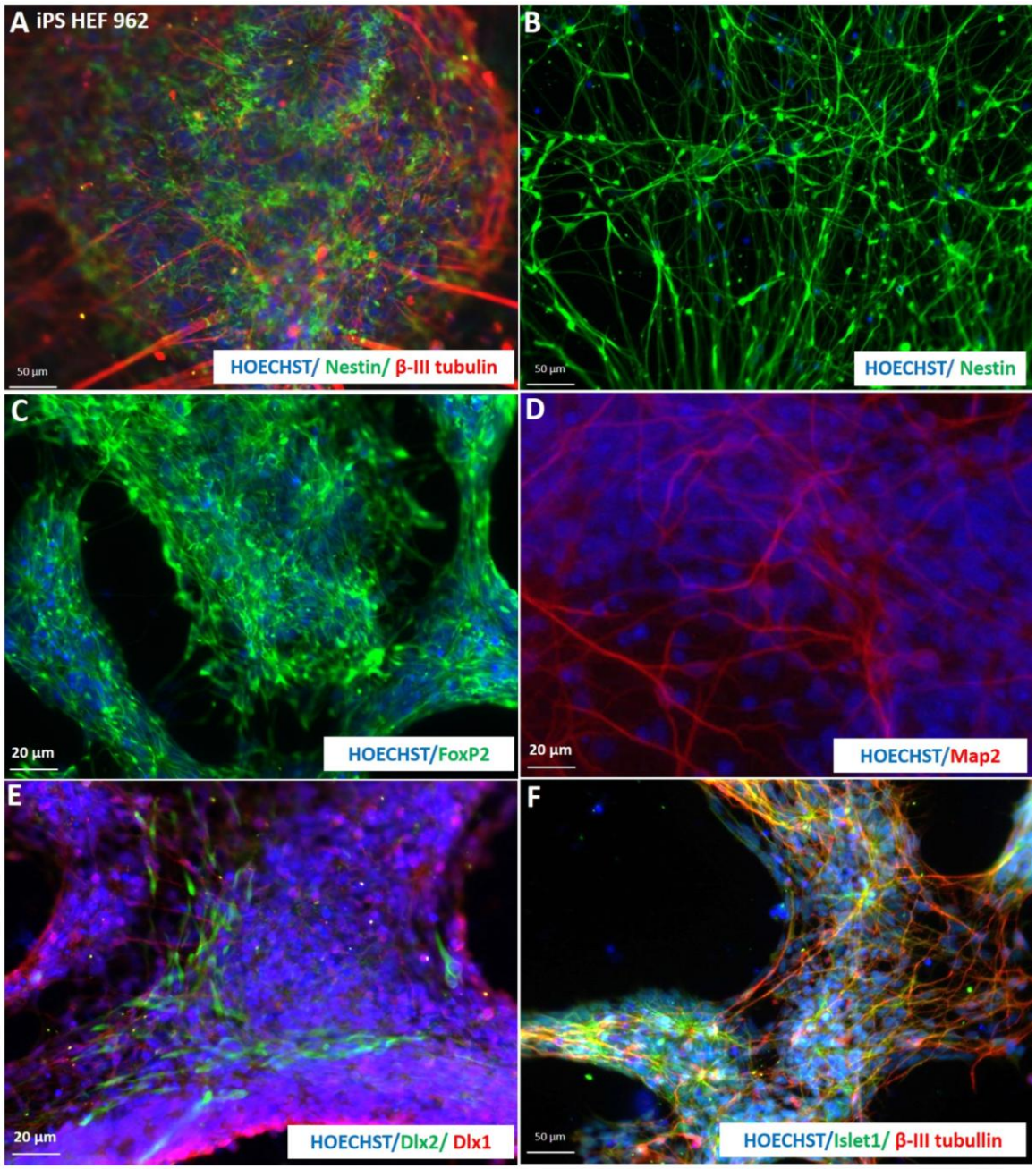

Figure 4.11 Phenotypic verification of *in vitro* differentiation from the iPS HEF 962 cell line. adherent-EBs demonstrated Cellular heterogeneity with neural precursors and more mature neuronal phenotypes is demonstrated within an adherent EB by the presence of nestin and β-III tubullin respectively (A). Subsequent in vitro culture revealed much progress in terms of maturation as indicated by Map2 positive cells (C) and cell fate restriction to ventral telencephalic by (Islet1 expression) (F) with more specific LGE structures (FoxP2, Dlx1 and 2 expression) (D-E). (Scale bar= 50 µm A, B, F; Scale bar= 20 µm C-E)

4.5.8 Human ES (H9) derived MSNs-liked cells.

The H9 human ES cell line was used in this study for comparison with our newly generated iPS cell lines. At 20-25 DIV, pluripotent markers of undifferentiated stem cells Oct4 and Tra-1-60 were not recognized in culture (Figure 4.12 A). Neuroepithelial propagation was again demonstrated via neural rosette formation expressing nestin positive cells (Figure 4.12 B). In addition, there was expression of proliferative cells expressing the nuclear proliferating marker-Ki67 and co-labelling with neuronal cells with β-III tubullin expression (Figure 4.12 C). Expression of Ki67 decreased over time in culture. In contrast, specific brain region markers representing ventral telencephalon, particularly the LGE, increased in expression under SHH and DKK-1 supplement over time, for example FoxP1, FoxP2, Islet1, and Dlx2 (Figure 4.12 D-F). At 30 DIV, a subset of glial cells with GFAP positive expression were detected among post mitotic differentiated neurons of Map2 (Figure 4.12 G). Striatal projection neurons were seen, as indicated by the expression of their precursor marker Ctip2 and DARPP32 (Figure 4.12 H), and the co-expression of, DARPP32 with the post mitotic neuronal marker Map2 were observed (Figure 4.12 I). Notably, DARPP32 positive neurons were often recognized as a group rather than standing alone. This was not only observed in human ES cells derived-MSNs but the same phenomenon was also identified in human WGE primary cell culture and human iPS cells derived MSNs.

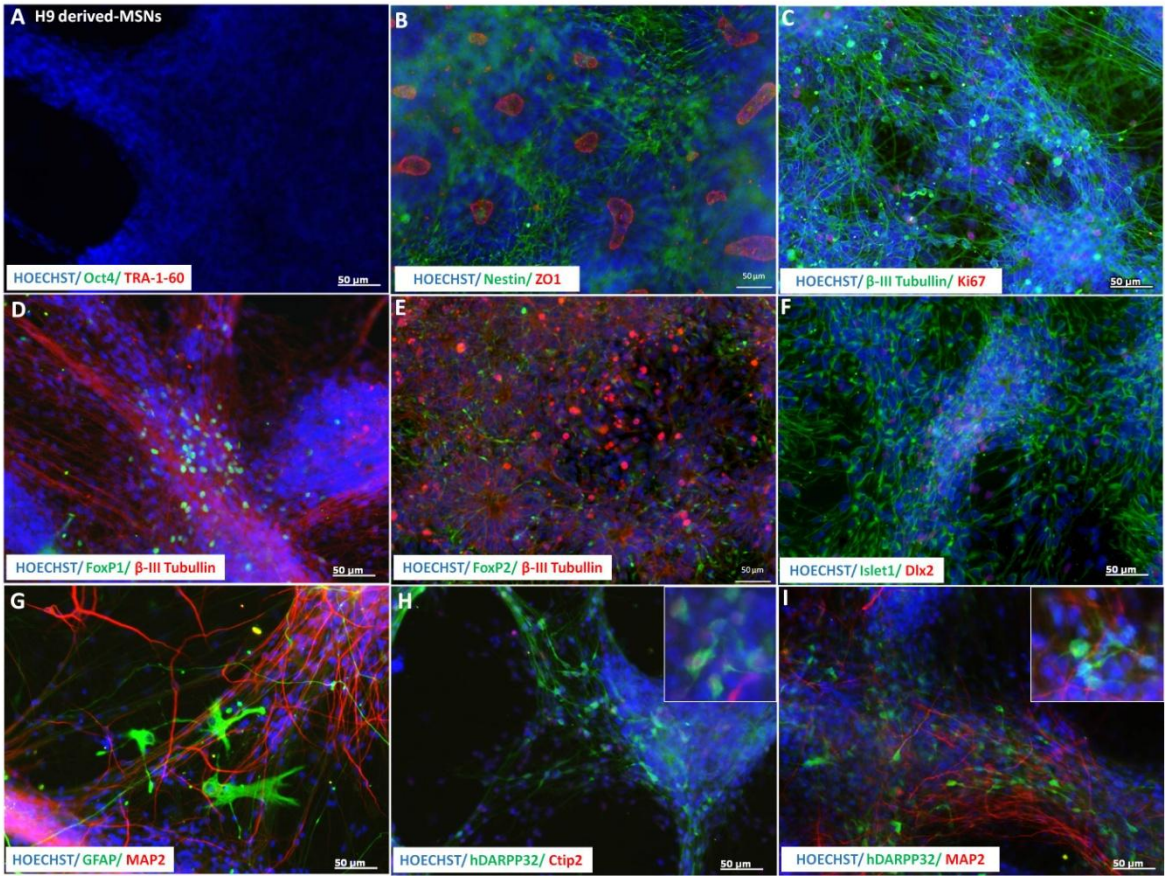

Figure 4.12 Phenotypic analysis of *in vitro* differentiation from human ES cell line (H9). No expression of the pluripotent genes Oct4 and Tra-1-60 (A). Stage-specific gene expression indicated neural rosette structures with expression of the neural precursor marker nestin and cell adherent molecule ZO-1 co-expressed in a typical rosette appearance (B). Proliferating neuronal cells were still present at 20 DIV as indicated by Ki-67, a neuronal proliferation marker, however the expression was reduced over time in prolonged culture (C). In the presence of exogenous SHH and DKK-1, a ventral telencephalic phenotype was present as evidenced by FoxP1, FoxP2, Islet1, and Dlx2 positive cells (D-F). Around 30 DIV, bona fide MSNs with DARPP32 expression were enriched in the culture and co-labelled with Ctip2 (H) and Map2 (I) markers. (Scale bar= 50 µm)

4.5.9 iPS WGE623 C9 derived MSNs-liked cells: application of modified differentiation protocol (protocol 2).

Next, I decided to apply the modified EB-based protocol to iPS WGE623 C9, which was previously unable to generate MSNs-liked cells, in order to probe whether the efficiency of the protocol or a general property of the iPS cell line was a hurdle for neuronal differentiation. Classical rosette structures were identified around 17 DIV after dissociation of adherent EBs and re-plating onto a PLL-POL-Laminin coated vessel (Figure 4.13 A). Similar to the previous studies in all established iPS cell lines, nestin positive cells were abundantly recognized on neuroepithelial precursors whereas in contrast ZO-1 was demonstrated at the centre point (Figure 4.13 B). These NPCs exhibited Ki-67 expression along with a high demand for subsequent passaging (Figure 4.13 D).

Once again, pluripotent clusters emerged as in previous observations (4.5.2); even though we applied a double round of transgene removal process to this iPS cell line. Oct4 and Tra-1-60 positive cells were present after passage 2 around 20-24 DIV, which corresponded to the previous studies (Figure 4.13 D).

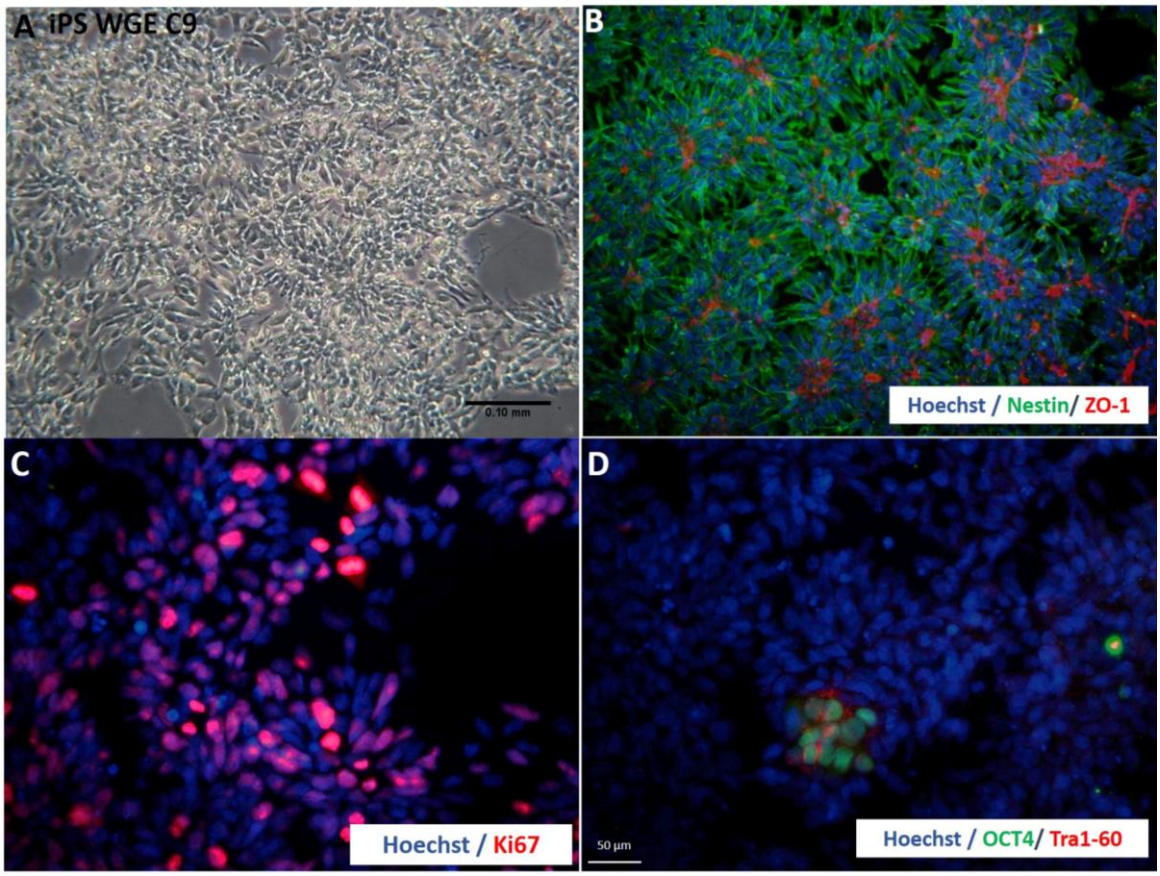

Figure 4.13 Phenotypic analysis of *in vitro* differentiation from iPS WGE623 C9 cell line. Phase contrast micrograph presenting neural precursors after replating onto PLL-POL-Laminin coated coverslips in N2B27 at 17 DIV (A). These cells reorganized and formed rosette structures identified by a typical appearance along with immune-reactivity against the neural precursor-nestin and the membrane marker-ZO-1 (B). High levels of proliferation were revealed by Ki-67 expressing cells (C). Stem cell-liked colonies subsequently emerged with prolonged culture, which can be recognized by their morphology as well as by immune-staining for pluripotent gene expression Oct4 and Tra-1-60 (D).(Scale bar= 50 µm)

In summary, 3 out of 5 established iPS cell lines and human ES cell line (H9) were shown to differentiate into DARPP32 positive cells and expressed the hallmark of neural/MSNs markers such as nestin, β-III tubulin, Map2, FoxP1, FoxP2, Dlx1, Dlx2, Islet1, GFAP and Ctip2. The iPS HEF 962 line could not be tested for DARPP32 expression due to the unexpected infection as outlined above, but using the improved protocol there was promising evidence that supported the differentiation of this iPS cell line toward a MSN phenotype as indicated by the expression of FoxP1, FoxP2, Dlx1, Dlx2, and Islet1. It is noteworthy that iPS HEF962 derived MSN experiment was unable to provide a fully diffetentiate results, therefore this may not a fair comparison between iPS WGE and iPS HEF cell lines derived MSNs in order to clarify benefits of epigenetic memories remain in different originated cells will provide an ease for MSN differentiation

A comparison of neural/MSN marker expression between the PSC lines during *in vitro* differentiation toward MSNs was shown in table 4.3.

Markers	DIV	H9	iPS WGE C9	iPS WGE 928	iPS WGE 949	iPS WGE 954	iPS HEF 962
Oct4	20	-	++	-	-	-	-
Nestin	2-14	++++	++++	++++	++++	++++	+++
B-III Tubullin	25-30	++++	+++	++++	++++	++++	+++
Ctip2	25-30	+++	N/A	+++	+++	+++	N/A
DARPP32	30+	++	N/A	+	+	++	N/A

Table 4.3 Summary table of neural/MSNs markers expression using immunocytochemistry analysis from 5 established iPS cell lines and human ES cell line (H9) during *in vitro* differentiation using a protocol designed to encourage MSN differentiation. (++++ = 75-90% of total Hoechst cells, +++ = 50-75% of Hoechst cells, ++ = 25-50% of Hoechst cells, + = 1-25% of Hoechst cells, - = no expression, N/A = Not available)

4.5.10 Expression of neural genes in iPS WGE 928 at the point of neural transplantation.

Cells need to be transplanted at a slightly earlier stage in their differentiation than those matured *in vitro* for immunocytochemical analysis, as described above. iPS WGE 928 cells prepared for neural transplantation were assessed by RT-PCR to assess neural conversion. The house keeping gene-GAPDH was used as a control (Figure 4.14 A).

The gene expression profile confirmed transformation of neural precursors to regional specific progenitors and importantly indicated that the cells carry an LGE-like identify. By 24 DIV, the early neural genes nestin and Pax6 were seen along with GSH2, FoxP1 and FoxP2, the latter appearing to produce a more intense band by 35 DIV. Dlx1, known to be related to early LGE generation, was weak at 24 DIV and stronger by 35 DIV. DARPP32 was seen by 35 DIV only, (Figure 4.14 G and H, respectively), corresponding to the emergence of DARPP32 positive neurons only after 30 DIV in the immunocytochemical analysis above. Exogenous transgene expression was tracked from 17 to 44 DIV.

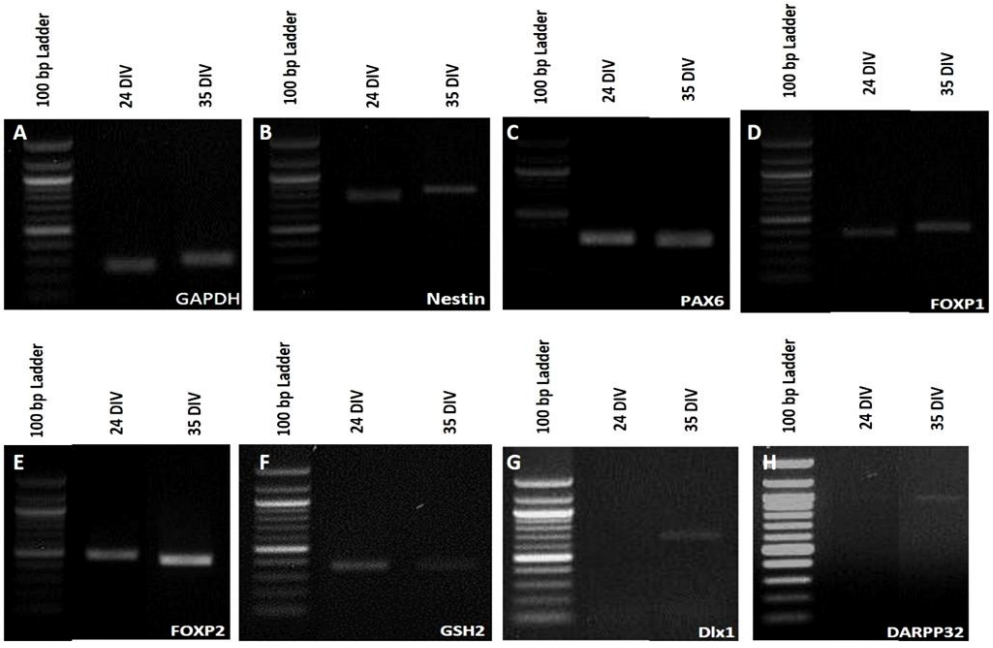

Figure 4.14 Gene expression profile observed in neural conversion from iPS WGE 928 cell line. Phase contrast micrographs showing gene expression at 24 and 35 DIV using RT PCR. Shown are: GAPDH (A), Nestin (B), Pax6 (C), FoxP1 (D), FoxP2 (E), GSH2 (F), Dlx1 (G), DARPP32 (H).

Transplantation into the quinolinic acid-lesioned rat striatum

In order to test the capacity of the iPS cells to differentiate into MSN-like cells following transplantation into the adult brain, one of the lines, iPS WGE 928, was directed in vitro to an MSN progenitor fate and then transplanted into the quinolinic-lesioned rat striatum. The grafts were compared to H9 cells, similarly differentiated, and human primary WGE (the "gold standard").

4.5.11 Analysis of iPS WGE 928 grafts.

Although the initial intention had been to examine the grafts at 7 and 20 weeks post transplantation, due to the appearance of ill health in some animals that may have been potentially due to graft overgrowth, the animals were sacrificed 4 and 7 weeks post transplantation for analysis.

Graft survival was demonstrated in all animals at 4 weeks (Figure 4.15 A-D, N=4) and 7 weeks (Figure 4.15 E-H, N=16) as revealed by HuNu positive staining. Grafted cells were seen to be contained within the lesioned striatum at 4 weeks, while by 7 weeks grafts had expanded further and invaded into the adjacent cortex (Figure 4.15). Around 6 weeks post-transplantation, we observed an obvious tumour emerging at the implantation side in one animal. In addition, the animal showed signs of ill health and thus the experiment was terminated at 7 weeks with all animals being sacrificed. Within the total number of 20 animals, there were 7 animals containing invasive tumours, whereas the remaining 13 animals revealed good graft survival with no signs of overgrowth. Representative composite images of all the grafts at 4 and 7 weeks post transplantation is demonstrated in figure 4.15 I and J. In addition, the grafted cells appeared to migrate out of the striatum into the adjacent cortex.

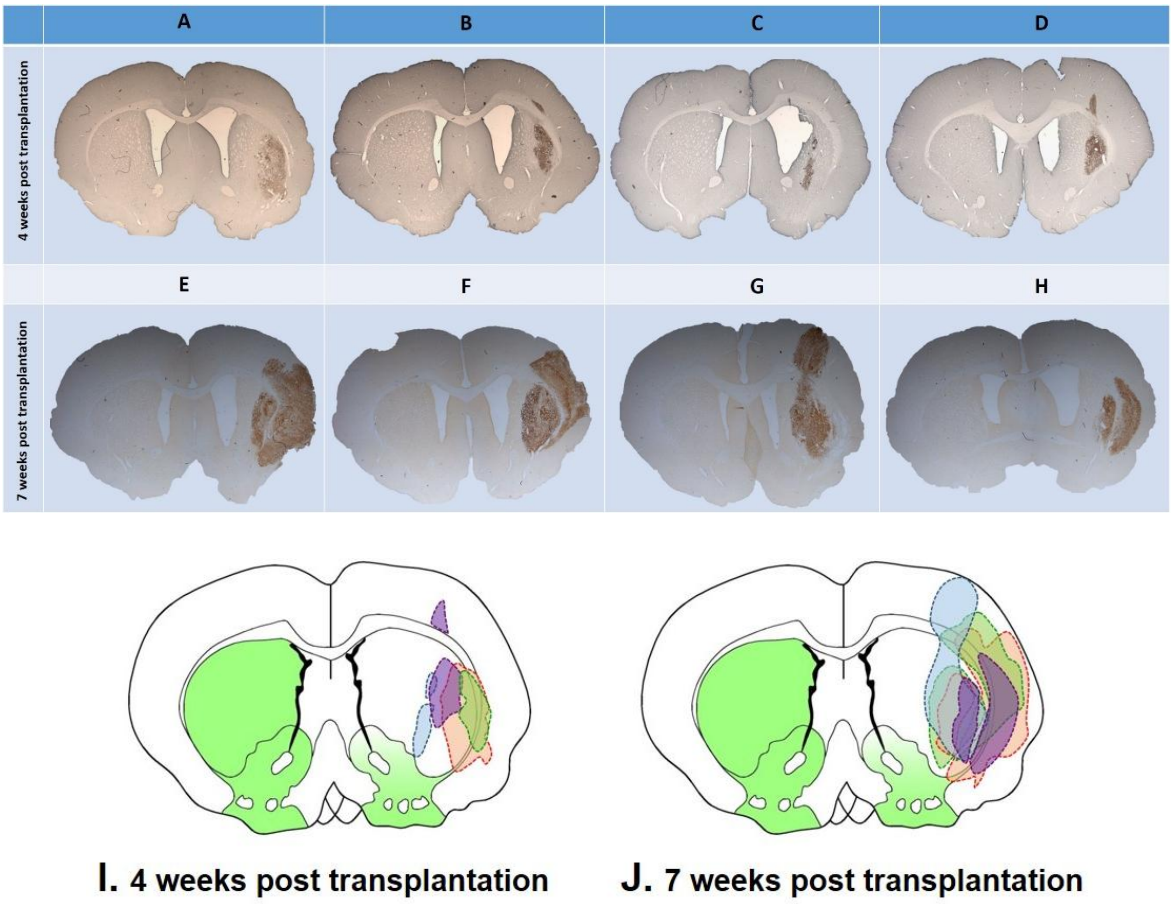

Figure 4.15 A representative 1:12 series of DAB staining showing graft morphology post transplantation. Surviving grafts were identified by HuNu positive cells which were largely restricted to the striatum at 4 weeks post implantation (A-D, N=4), but by 7 weeks had almost doubled in size suggesting continued proliferation of the grafted cells (E-H, N=4). Schematic comparison of graft borders from all transplanted animals is shown in I for 4 weeks (N=4) and J for 7 weeks (N=4).

At 4 weeks post transplantation, HuNu positive cells were distributed in the lesioned striatum along with fine processes of nestin positive cells (Figure 4.16 (A-D, N=4)). Nestin expression appeared limited to the graft area. At 7 weeks post transplantation (Figure 4.16 (E-H), one animal presented with some cells of a larger size situated in less dense areas (Figure 4.16 G and inset). The identity of these particular cells is currently unclear.

Overall 7 out of 20 animals had brain tumours after transplantation. Six animals had extensive tumours identified in the cortex, while one animal had a tumour within the striatum (Figure 4.17 A, C). The brain tumours had defined borders, were not well integrated into the host brain, and easily fell out during brain dissection. Furthermore, the tumour itself was fragile many not surviving the ICC process. Haematoxicillin and Eosin (H&E) staining revealed a heterogenous population of cells within the area of overgrowth (Figure 4.17). Neural-rosette like structures within the graft were observed as epithelial cells with luminal structures (Figure 4.17 B and inset). Immunocytochemistry analysis revealed the tumour to contain proliferating graft-derived cells as confirmed by co-expression of HuNu and Ki-67 (Figure 4.17 C, D). In addition, there were some DARPP32 expressing cells in a subset of the grafted population.

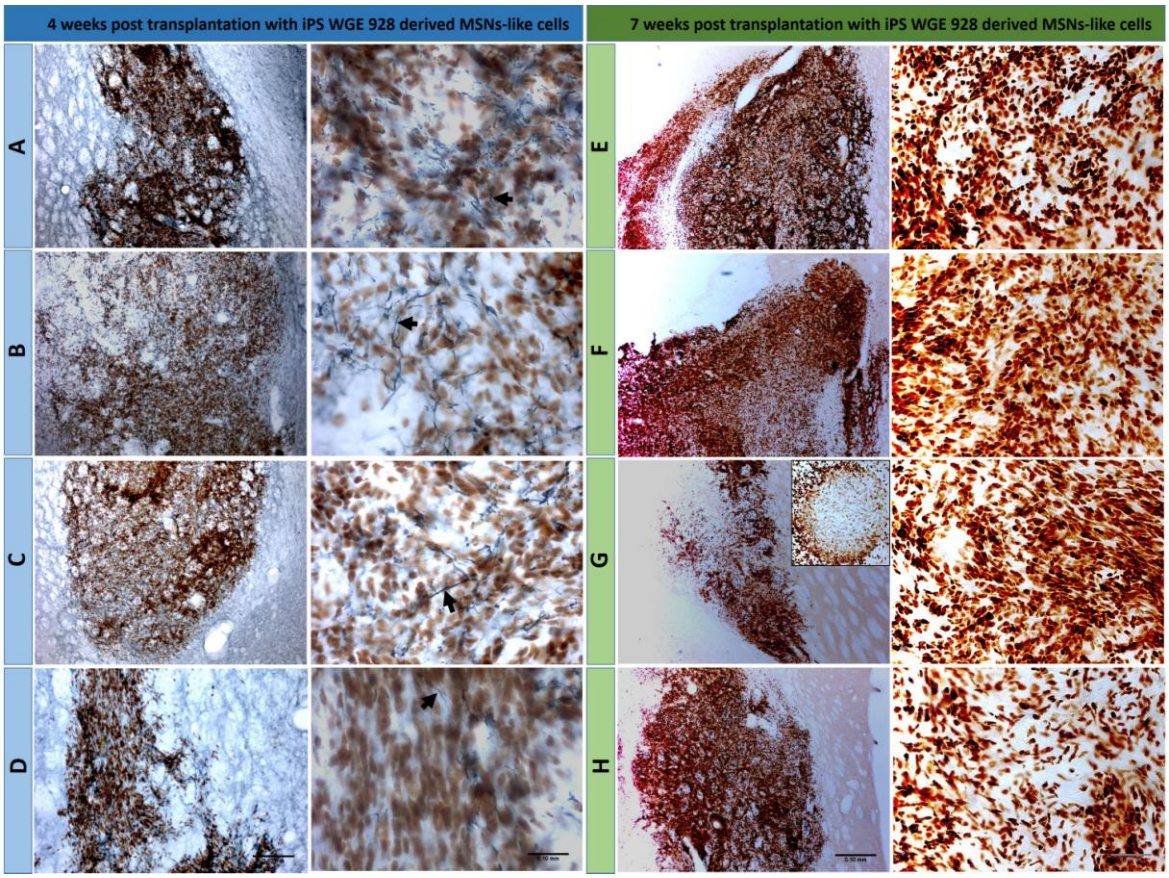

Figure 4.16 Panel of representative photomicrographs showing grafts at 4 weeks (N=4) and 7 weeks (N=16) post engraftment. The left panel (A-D) demonstrates 4 weeks post transplantation, human grafted cells labelled by HuNu in brown together with nestin positive fibers (arrow head) in deep blue which are restricted to the grafts area. The right panel (E-H) revealed survival of grafts at 7 weeks post transplantation demonstrated by HuNu expressing cells showing that the grafts have breached the striatal borders (E-H). One animal presented with a morphology different to the other animals with pockets of larger unidentified cells within the graft G and higher power insert representing one of these pockets of cells. (Scale bar= 0.10 mm)

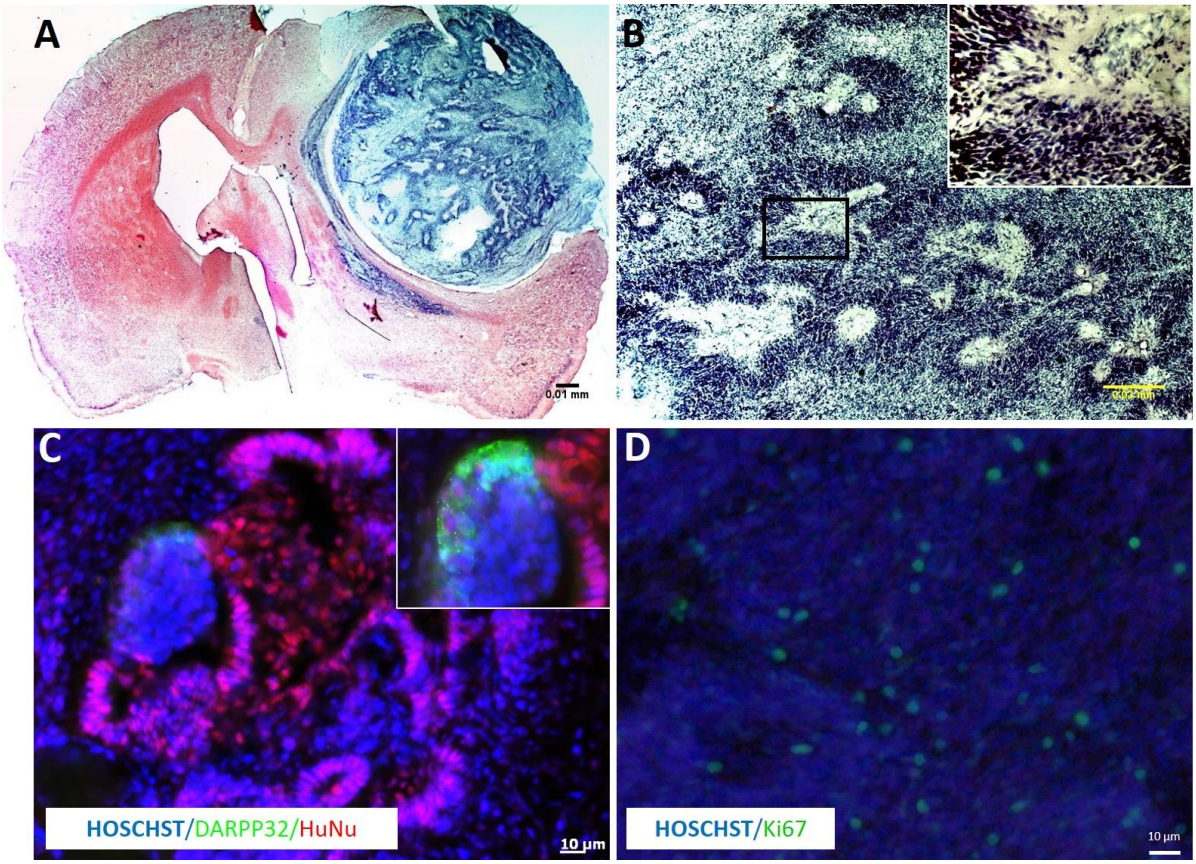

Figure 4.17 Characterization of iPS cell derived-tumour formation. The obvious disruption of striatum and cortex was revealed by H&E staining (A) scale bar = 0.01 mm. A large proportion of the graft contained neuroepithelial cells presented as neural rosette structures as seen in higher magnification; insert (B) scale bar = 0.03 mm. The cells within the tumour were positive for HuNu, indicating that they were graft-derived (C). MSN-like neurons were indicated by human specific DARPP32 expressing cells in a sub population of grafted cells (C (inset)). The proliferating nuclei marker Ki-67 was seen within the grafted region (D).

Grafts were assessed for the expression of general neuronal markers and sub-type specific/MSN markers by immuno-histochemical analysis.

At 7 weeks post transplantation, there was still evidence of proliferating cells within the grafts, shown by expression of Ki-67 (Figure 4.18 B). Ventral telencephalic precursors were as indicated by immuno-fluorescence reactivity against Gsh2 (Figure 4.18 A). In addition, β-III tubulin positive cell bodies and processes were seen co-labelled with the striatal MSN precursor marker FoxP1 (figure 4.18 C). Grafted cells expressed markers characteristic of striatal projection neurons including GABA and DARPP32 (Figure 4.18 D and E, F, respectively).

Human specific DARPP32 positive cells exhibiting typical neuronal morphologies were seen in the graft (Figure 4.18 E and F). Moreover, confocal analysis confirmed colabelling of DARPP32 with HuNu (Figure 4.19 A to D). Confocal microscopy was performed in 4 of the 9 surviving grafts without tumours; the other 5 brains were not suitable for high quality analysis as there was significant auto fluorescence from these sections. Fluorescent microscopy demonstrated that the DARPP32 cells co-labelled with NeuN. An additional observation was that the DARPP32 expressing cells accumulated as groups rather than single dispersed neurons, as previously mentioned in the *in vitro* study.

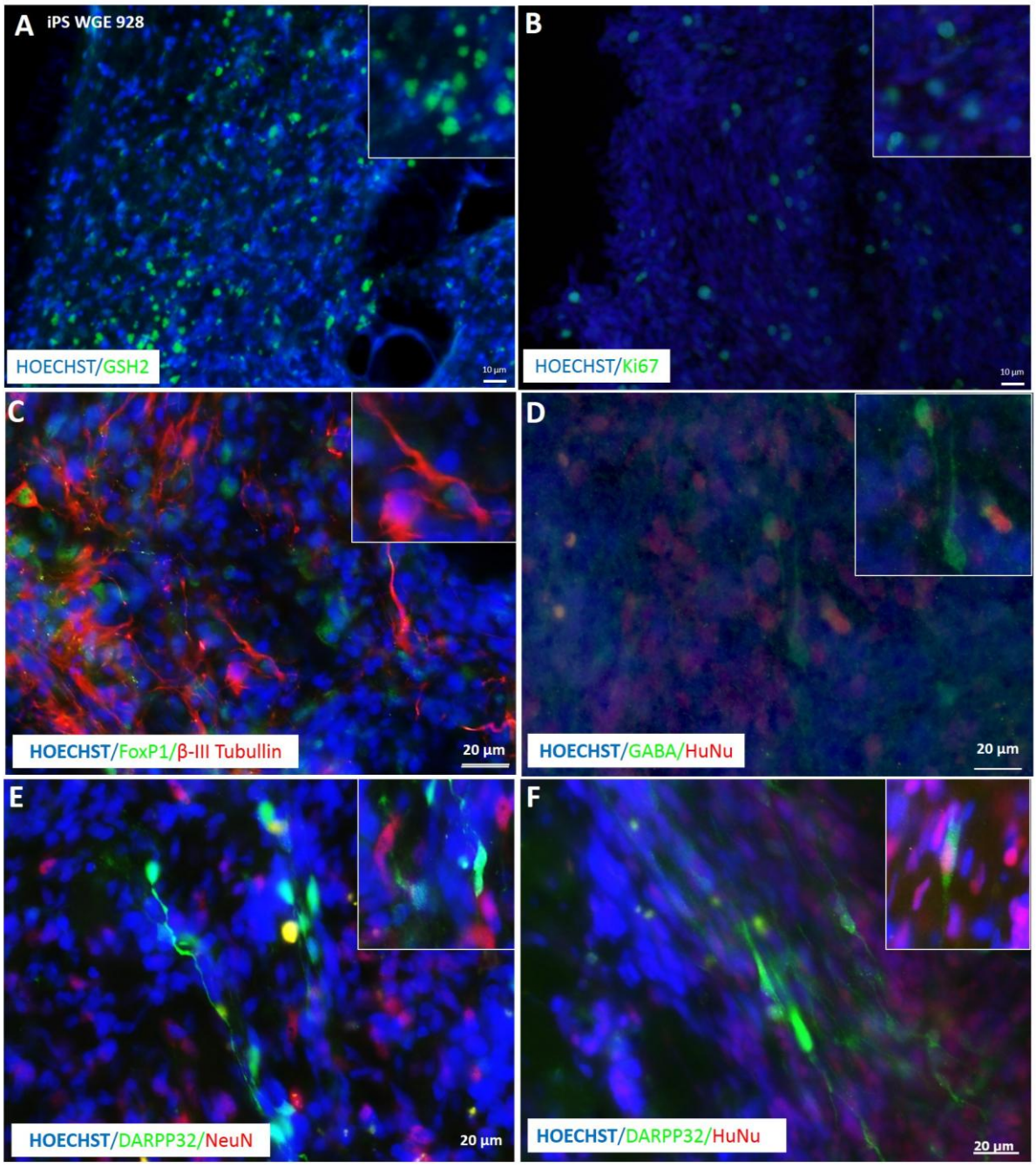

Figure 4.18 Phenotypic characterization of iPS WGE 928 derived MSNs-liked cells at 7 weeks post transplantation. A ventral telencephalic precursor identity was indicated by the presence of GSH2 expressing cells (A). However, the graft still contained proliferating cells represented by Ki-67 (B). β-III tubullin positive neurons were present, co-labelling with FoxP1, indicating an LGE-like patterning of neuronal progenitors (C). GABAergic striatal projection neurons were indicated by GABA positive cells co-expressing with HuNu (D). DARPP32, a typical post mitotic MSNs marker, was observed co-labelling with NeuN (E) and HuNu (F).

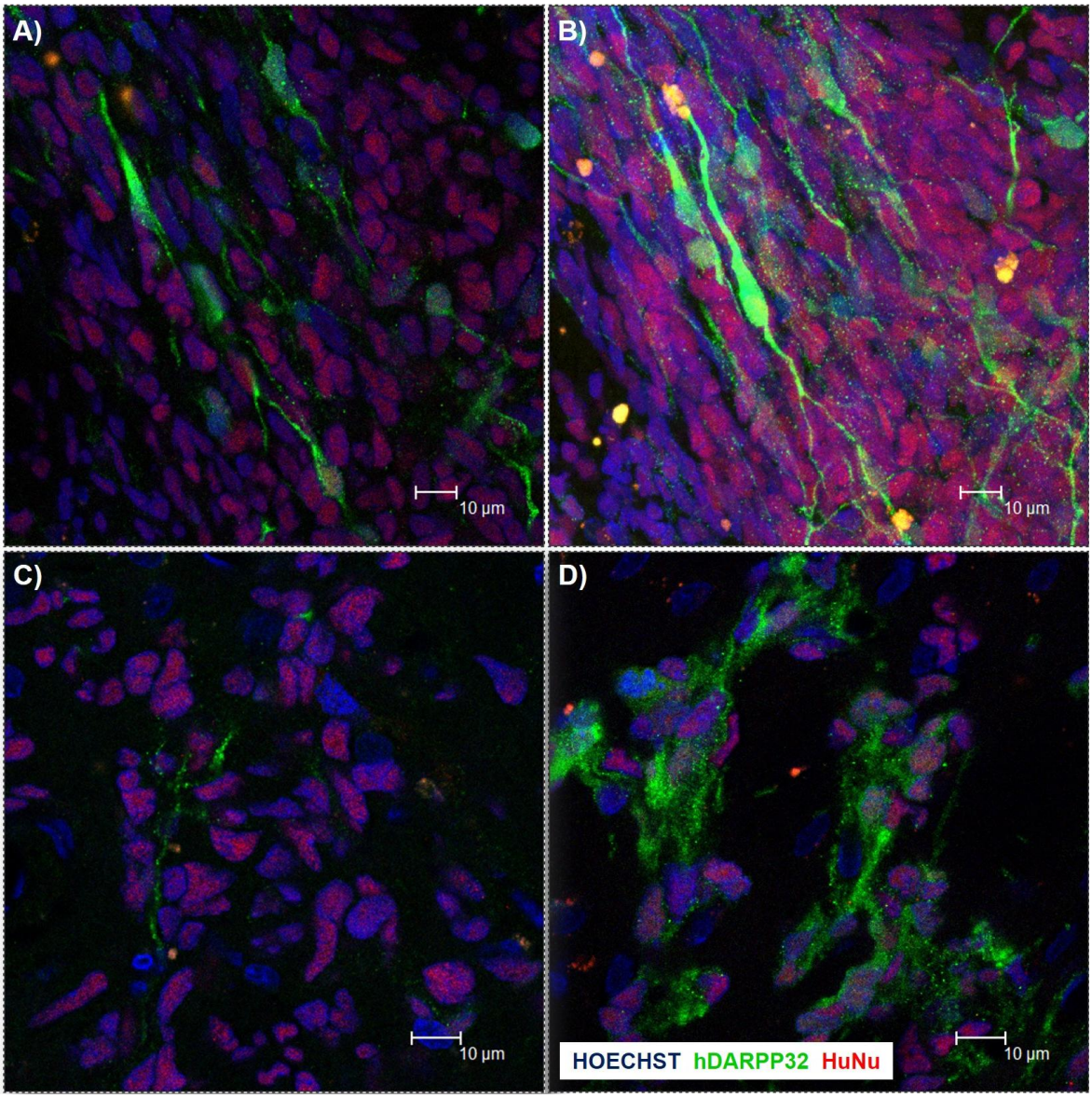

Figure 4.19 Immuno-photomicrographs using confocal analysis showing expression of DARPP32 and HuNu in grafts at 7 weeks post transplantation. The co-labelling of DARPP32 and HuNu was demonstrated in the grafts of all animals analysed (N=4) (A-D). DARPP32 positive cells were generally identified as a group of cells within graft area rather than as single neurons dispersed throughout the graft.

4.5.12 Analysis of Human ES (H9) grafts.

Although the initial intention had been to sacrifice the animals at 7 and 20 weeks post transplantation, we observed 2 out of 3 animals had signs of tumour development at 7 weeks. Therefore, the remaining animals were also sacrificed at 7 weeks before the brains were collected and analysed. Overall, 2 out of 6 animals developed tumour at 7 weeks post transplantation with ES cell derived MSN-like cells.

Graft survival was recognized in all 6 animals. However, in the 2 animals that developed tumours, the brains were deformed and the tumour was too fragile for processing with immunohistochemistry. Although, the remnant of grafts were recognized in the intact brain area. There were differences in grafts size among the transplanted animals as exhibited by HuNu positive cells. In addition, all surviving grafts were situated in the striatal region and were not distributed throughout the cortex (N=4, excluding the 2 animals with tumours) (Figure 4.20).

Immunohistochemical analysis revealed DARPP32 expression in all surviving grafts (Figure 4.21). Co-expression of human specific DARPP32 with HuNu positive cells confirmed the presence of graft derived MSNs (Figure 4.21, inset). It is noteworthy that, as mentioned above for the iPS derived grafts, the DARPP32 positive cells were identified as an accumulation/group of cells in both human primary WGE (Figure 4.21, A) and human ES derived grafts (Figure 4.21, B-F).

The number of DARPP32 positive cells were assessed at 7 weeks post transplantation in both iPS (N=4) and ES (N=3) cells derived MSNs. A significantly higher number DARPP32 expressing neurons was obtained from iPS cells derived MSNs, $p<0.001$ (Figure 4.22). This was also reflected in the graft volume with there being a significantly higher graft volume from the iPS derived grafts than the ES cell derived grafts, $p<0.05$ (Figure 4.23).

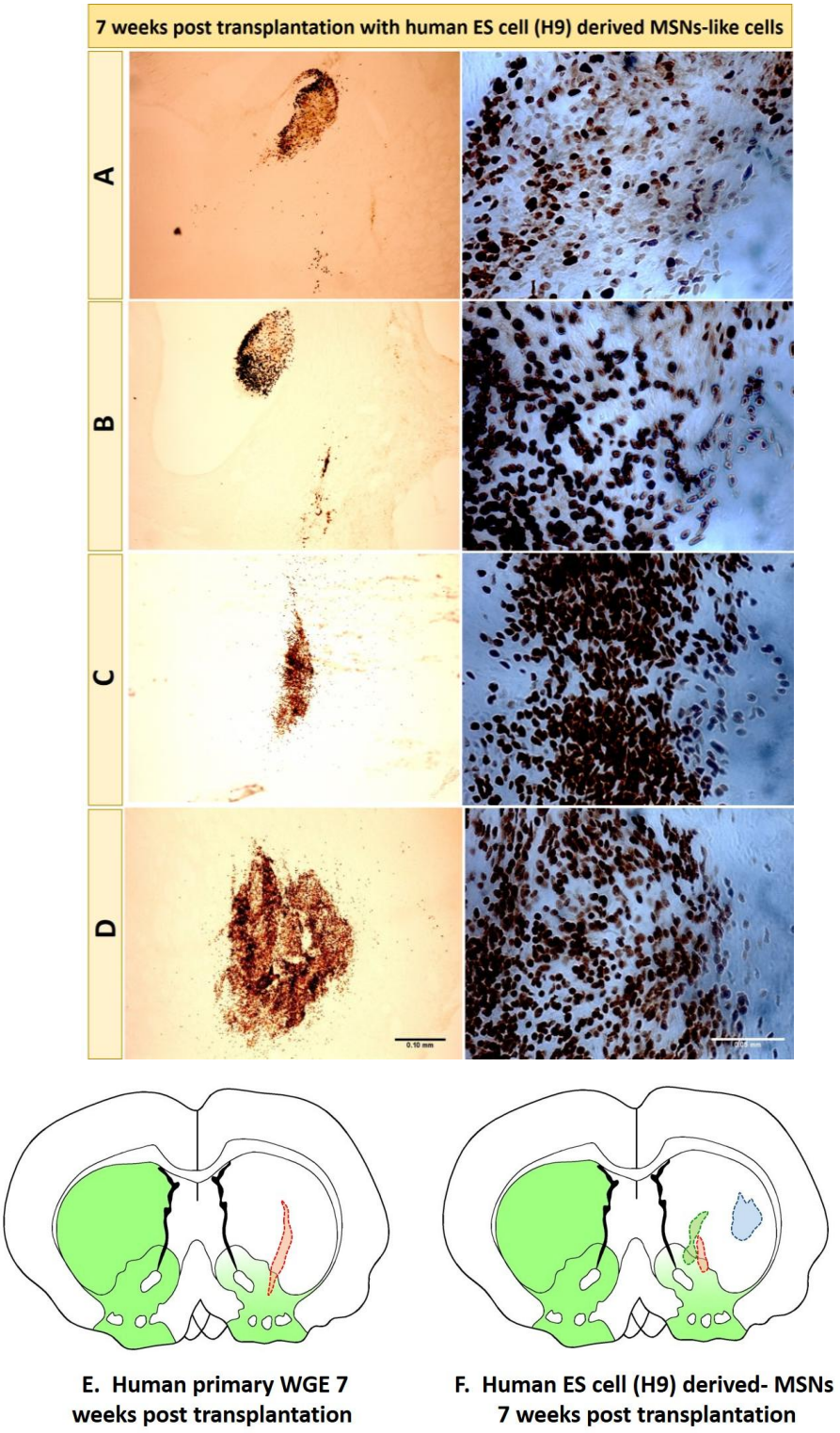

Figure 4.20 Panel of representative photomicrographs showing H9-derived grafts at 7 weeks (N=4) post engraftment. The left panel (A-D) demonstrates 7 weeks post transplantation N=4 (Scale bar= 0.10 mm) and the right panel at higher magnification (Scale bar= 0.05 mm), human grafted cells labelled by HuNu in brown which are restricted to the striatal area. Schematic comparison of graft borders from all transplanted animals is shown in E for human primary WGE transplanted brain as a control (N=1) and F for human ES-derived MSNs grafts (N=6; transplanted after 30 DIV)

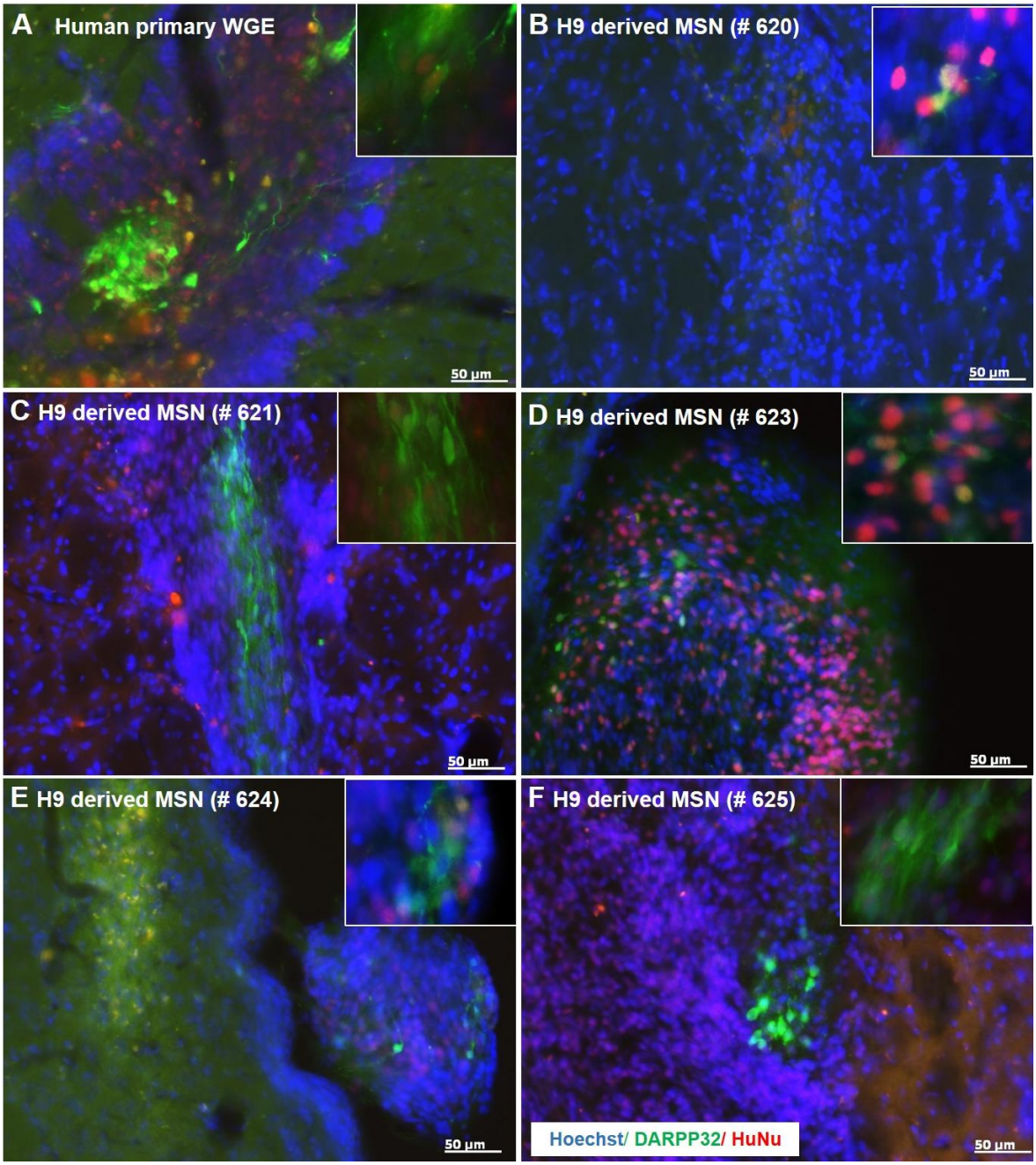

Figure 4.21 Immuno-photomicrographs using confocal analysis showing expression of DARPP32 and HuNu in grafts at 7 weeks post transplantation. The co-labelling of DARPP32 and HuNu was demonstrated in the grafts of all animals analysed (N=4) (A-D). DARPP32 positive cells were generally identified as a cluster of cells within graft area rather than as individual neurons dispersed throughout the graft.

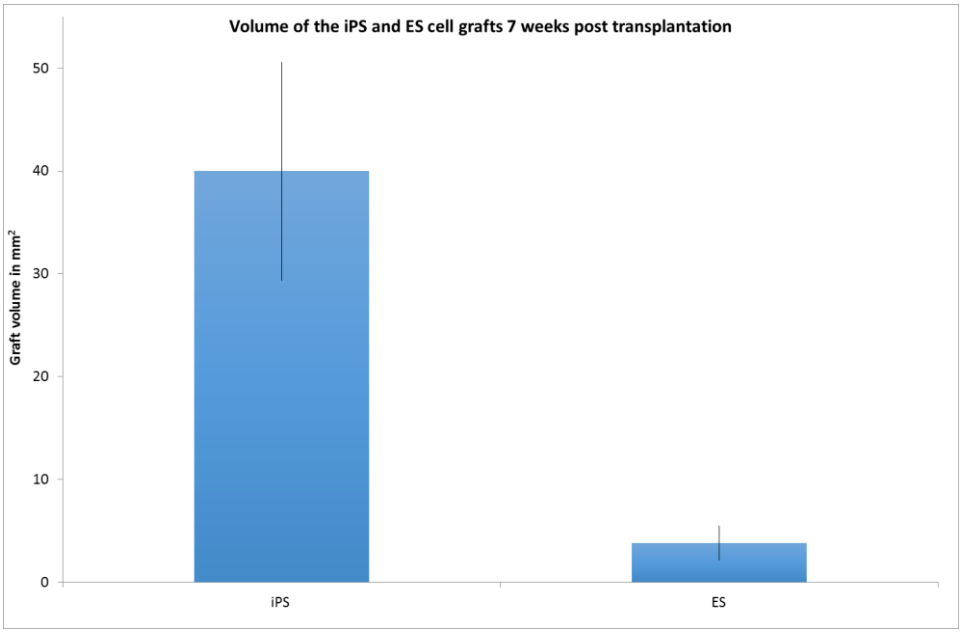

Figure 4.22 Graph presenting the total Graft volume of both the iPS (N=4) and ES (N=3) cell derived grafts at 7 weeks post transplantation. Statistical analysis using a standard t-test showed there to be a significant difference between the two graft groups, $p<0.05$.

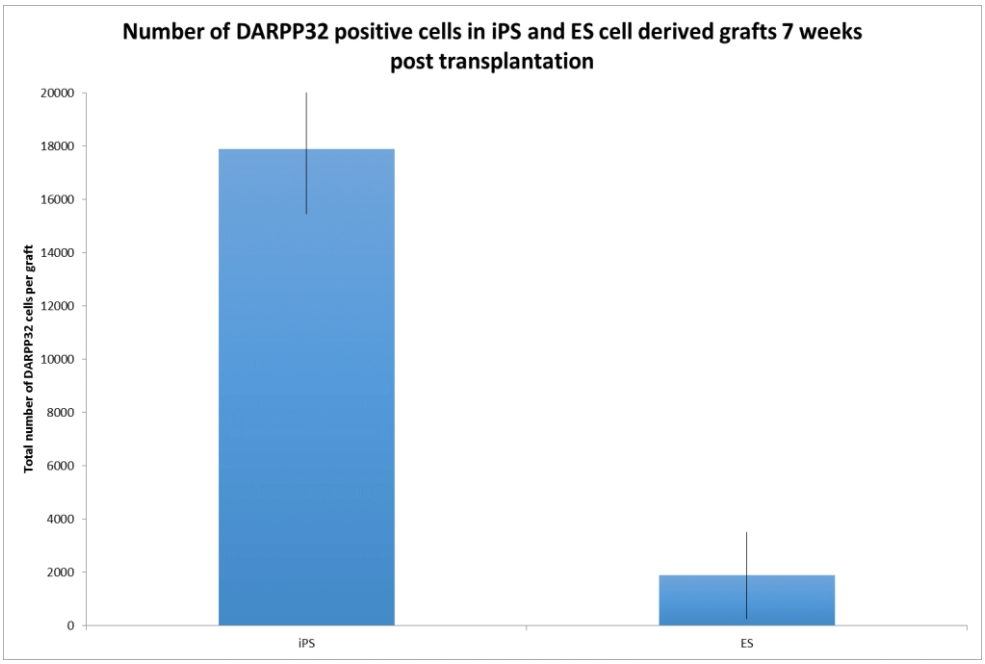

Figure 4.23 Graph presenting the total number of DARPP32 positive cells per graft in both the iPS (N=4) and ES (N=3) cell derived grafts at 7 weeks post transplantation. Statistical analysis using a standard t-test showed there to be a highly significant difference between the iPS and ES derived grafts, $p<0.001$.

4.5.13 Comparison of these results with the previous studies.

The schematic below summarizes the protocols for the generation of PSC derived-MSNs that have been published in the literature to date, Aubry et al. (2008), Ma et al. (2012), and Delli Carri et al. (2013) in comparison to the modified protocol we used in our study (Figure 4.24).

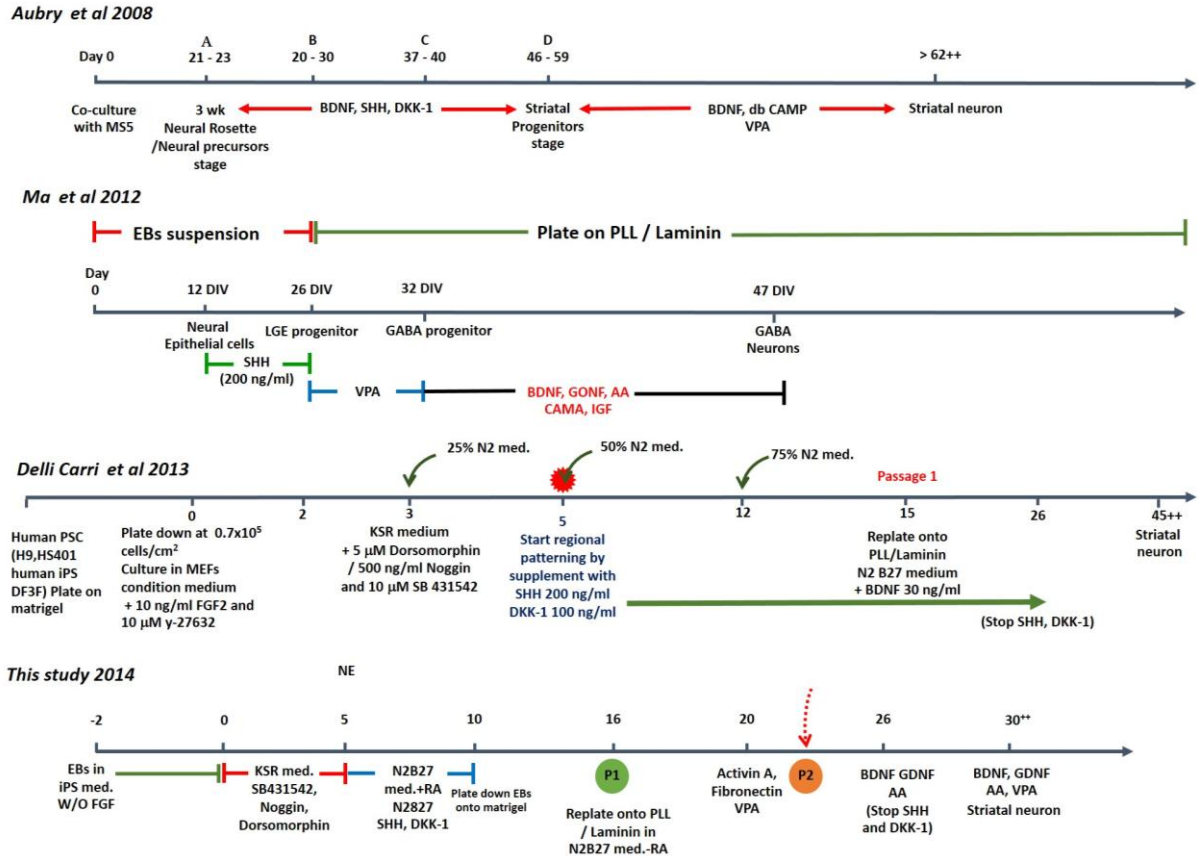

Figure 4.24 Schematic of different protocols for deriving MSNs from PSCs reported in previous studies and this study. 3 different methods have been reported for MSNs differentiation from PSCs: co-culture with stromal cells (Aubry et al., 2008), EBs method (Ma et al., 2012 and this study), monolayer based method (Delli Carri et al., 2013 and this study. Differences in combination of small molecules, growth factors, and morphogens presented in separate differentiation time lines.

As shown in table 4.4, it is demonstrated using our established iPS cell lines derived from human primary WGE, that we are able to differentiate these cells toward a neural lineage. In addition, sub type specific-MSN like-cells can be derived from these iPS cell lines using this modified protocol both *in vitro* and *in vivo* as confirmed by DARPP32 positive cells. Furthermore, in our study, the differentiation time line from neural induction to neuronal maturation of DARPP32

positive cells was shortened compared to previous studies. LGE-like progenitors were expressed around 13-17 DIV as indicated by GSX positive cells. In addition, cells expressing Ctip2 were identified around 25-28 DIV compared to 45 DIV in Delli Carri et al. (2013). These findings are in accordance with the expression of the MSN standard marker-DARPP32, which can be seen around 30 DIV in our study, 2 weeks earlier than the 45 DIV reported by Delli Carri et al. (2013).

PSCs derived MSN-like cells studies	Aubry et al 2008	Ma et al 2012	Delli Carri et al 2013	This study iPS WGE 928
LGE marker expression (DIV) (GSX)	29-30	26	15-25	13-17
Ctip2 marker expression (DIV)	N/A	N/A	45	25-28
DARPP32 marker expression (DIV)	67-72	47	45+	30+
DARPP32 generation efficiency	20% (In vivo)	89% (In vivo)	20% (In vitro)	N/A
In vivo differentiation in QA lesioned rodent model	Cells expanded to 45/56 DIV ; resulted in overgrowth	Cells expanded to 40 DIV ; claimed no overgrowth	Cells expanded to 30 DIV; claimed no overgrowth	Cells expanded 30 DIV, resulted in overgrowth found 7 from 20 animals (iPS derived-MSNs); 2 from 6 animals (ES cell derived-MSNs)

Table 4.4 Table summarises both in vitro and post transplantation results from the previous published studies of PSCs conversion to an MSN neuronal subtype. ES/iPS differentiation to striatal MSNs from Aubry et al. (2008), Ma et al., (2012), and Delli Carri et al., (2013) and the present study presented in categories of markers expression, differentiation efficiency, and evidence of tumour formation post transplantation.

4.6 Discussion

4.6.1 Generation of Neural Progenitor cells and Neurons from Transposon-mediated iPS cell.

The methodology for generation of iPS cells has been reported to play an important role in the distinctive properties of those iPS cell lines, which may be important for downstream application, for example it may influence their subsequent neural induction and neuronal differentiation. Ma and collaborators demonstrated that by using the same donor somatic cells and generating iPS cells using 2 different methods i) a nuclear transfer method and ii) the iPS cells generated from over expression of pluripotent transcription factors, that the reprogrammed cells had DNA methylation and transcriptome profiles that were characteristic of the starting somatic cells, thus suggesting this epigenetic memory may be advantageous to subsequent differentiation (Ma et al., 2014).

In addition, it has been reported that, even though there is an alteration in genomic structure during the reprogramming process, this is not powerful enough to get rid of all the epigenetic memories (Blelloch et al., 2006; Ng and Gurdon, 2005 and Ng and Gurdon, 2008). In this study, we hypothesised first, that iPS cells derived from fetal WGE could be differentiated to an MSN phenotype, and second that epigenetic memory remaining in the iPS cell lines could enhance sub-type specific differentiation to the desired MSN-like cells. Interestingly, it was suggested that correct functional cardiomyocytes can be better propagated from an iPS cell line generated from donor cardiomyocytes, rather than from donor cardiac fibroblasts (Rizzi et al., 2012). Therefore, we have generated iPS cell lines from human primary fetal WGE, cortex, and fibroblasts, and compared them, with respect to neural induction and neuronal differentiation specifically towards striatal MSNs.

Our *piggyBac* transposon derived-neural progenitor cells produced a high number of nestin positive cells in all established iPS cell lines. Indeed, comparable expression of nestin positive cells was identified across all lines, 5 iPS cell lines (iPS WGE623 C9, iPS WGE 928, iPS WGE 949, iPS WGE 954, iPS HEF962) and

1 human ES cell line (H9) (as illustrated in table 5.3). In addition, we were successful in repeatedly generating NPCs from the different cell lines, whether they were ES or iPS cells, using the defined chemical combination method and these cells responded to stimuli using the same pathway. Thus confirming the efficiency of our neural induction protocol toward neural lineages.

This contrasts to a study of 'The Sleeping Beauty' transposon mediated iPS cells, where the expression of nestin was 16 fold higher in ES-derived neuronal precursors (Klincumhom et al., 2012). Therefore, even though we use a similar strategy to generate iPS cells, a substantial increase in the proportion of nestin expressing cells was seen in our study. A direct comparison with the Sleeping Beauty approach would be required for confirmation and to explore this further.

There are studies suggesting that epigenetic or a remnant of transcriptional memories being retained in donor tissue may be responsible for iPS cells showing a preference to differentiate down particular lineages (Bar-Nur et al., 2011; Ohi et al., 2011). In our study, using iPS HEF 962 cells we observed a recognizable amount of fibroblast-like cells upon neural differentiation. Likewise, when differentiating WGE derived iPS cells a similar level of spontaneous differentiation was observed in all cell lines tested, thus suggesting that these iPS cells have a component of an epigenetic memory remaining, which results in them having a tendency to spontaneously differentiate back to the original cell phenotypes.

In the Klincumhom study mentioned above, donor mouse fibroblasts were used to generate iPS cell lines, whereas in our study, the iPS cells were generated from human primary neural tissue (WGE and cortex) thus the high yield of NPCs produced in our study may in part be due to the original starting material used to create our iPS cell lines. This favourable potential to generate specific lineages may offer advantages in sub-phenotypic neural differentiation in our study, which will be further described.

There is increasing evidence of differences in the potential to generate NPCs from PSCs. This has recently been reported, not only between distinctive PSC lines, but also among different clones from the same cell line (Martinez et al., 2011, Klincumhom et al., 2012). In addition, more recently, Salewski and team

reported a difference in the potential of NPCs derived from ES cells and PB-iPS (*piggyBac)* cells. They pin point an intrinsic distinction within ES versus PB-iPS cells in order to generate definitive neural spheres (Salewski et al., 2013). In our study, even though MSN-like cells, as determined by DARPP32 positive expression, were produced from 3 iPS WGE cell lines (excluding C9) and human ES cell line, there were differences with respect to their proliferation capacity, neural conversion efficiency, and ease of deriving post mitotic DARPP32 expressing neurons.

Out of the iPS WGE lines produced in this study, iPS WGE 954 performed most similarly to H9, in terms of the in vitro differentiation time lines and the expression of DARPP32. Interestingly, in iPS cell culture, higher proliferation was observed in all lines compared to H9 with repeated passaging being required. In addition, neural rosette structures were observed at 62 DIV in the iPS WGE 928 cell line at a time when a more mature phenotype was being observed in the other cell lines. This may stem from the reprogramming process which normally requires more than 3 copies of pluripotent transgenes to be inserted into the host genome, as previously reported in 2009 (Kaji et al., 2009).

In stark contrast to the lines just described, the iPS WGE623 C9 cell line could not be differentiated beyond the NPC stage, expressing Oct4 and Tra-1-60. Even though 2 different protocols (Arber et al., and our protocol) were used to differentiate this iPS cell line toward neural lineage, the expression of Oct4 and Tra-1-60 continually reappeared in the culture. This is in line with a study from Rhee et al which suggested that residual or reactivation of exogenous pluripotent genes may alter the terminal differentiation of these cells toward certain lineages (Rhee YH et al., 2011). In addition, Rhee also claimed that there was no evidence of any remaining transgene within their iPS cell lines which were generated using the protein based method when compared to reactivation of exogenous pluripotent genes that was found in their lentivirus based iPS cells (Rhee YH et al., 2011). This may suggest that the remnants of exogenous pluripotent transgenes in our cell lines could be a hurdle to complete neural differentiation.

In addition, it is well accepted that ES and iPS cells are not identical. Whilst they share the characteristics of pluripotency and self-renewal there are reports of variability at the genomic level (Hu et al., 2010, Feng et al., 2010, Narsinh et al., 2011, Bock et al., 2011). Thus, there is a strong likelihood that a 'one fits all' approach may not work with these cells, especially in terms of specific protocols for their directed differentiation down particular lineages. Therefore, reprogramming strategies need to be improved in order to generate single copy transgene iPS cells, and also exogenous transgenes need to be removed before further application can be performed. Moreover, an important point is to clarify the inherent distinction of genetic and epigenetic profiles among PSC lines before translation to other applications.

It is noteworthy, that all our iPS cell lines reported here are capable of generating nerosphere-like structures when cultured in neural expansion medium with FGF2 supplementation. The neurosphere-like structures can also be expanded further (for more than 4 passages). The pattern of proliferation and differentiation seen in these iPS-generated NPCs is in accordance with what is seen with human primary neural tissue derived neurospheres. Overall, there was a considerable level of homogeneity across the cell lines produced here in terms of their proliferation and differentiation probably due to the efficiency of the protocol itself and this could be directly compared to the primary starting material.

4.6.2 *In vitro* and *in vivo* differentiation of human PSCs to a DARPP32 positive MSN-like phenotype using an EB-Based method.

Primary human embryonic WGE is considered as the 'gold standard" donor tissue for cell therapy in HD. This donor source was used for the 'proof of principle' donor source for transplantation in HD patients (Kelly et al., 2009). Development of protocols for deriving MSNs from human PSCs have been improved since 2008 when Aubry and colleagues first reported generating striatal projection neurons/MSNs from human ES cells (Aubry et al., 2008). In their study, the neural induction stage was performed using murine stromal co-culture, which poses safety concerns for clinical translation. In addition, co-culture with stromal cells is a

time consuming process as it takes several weeks before neural epithelial structures can be identified (Song et al., 2007; Aubry et al., 2008). In 2012, Ma introduced a multi-aggregated cell method called 'EB' formation that recapitulates the 3 germ layer differentiation in embryogenesis (Ma et al., 2012). Nevertheless, there are drawbacks to the EB method such as heterogeneity of the cell population within and among EBs (Kilncumhom et al., 2012), persistent and higher expression of pluripotent genes, and contamination of other cell lineages (Salewski et al., 2013). Addition of BMP inhibitors such as Noggin, NOTCH signalling molecule such as Delta-like ligand 4 (DLL4), and small molecule SB431542 and Dorsomorphin have been reported to improve neural conversion from human PSC (Chamber et al., 2009; Sally et al., 2012; Salewski et al., 2013; Delli Carri et a., 2013).

In our study, we applied the EB-based method with Noggin along with small molecules SB431542 and Dorsomorphin in order to push the cells down the ectoderm lineage, generate neural epithelial cells and improve homogeneity of neural precursors (Delli Carri et al., 2013). Here, we succeeded in generating neuroepithelial cells as demonstrated by typical rosette formations in vitro, giving rise to a high proportion of neural precursors confirmed by gene expression and immunopositivity of cells for nestin, PAX6, and Sox2. However, non-neural cell types and/or pluripotent cells were still observed in our cultures following the neural induction phase.

In addition, heterogeneous populations, including a mixture of neural rosette formation and mature neurons bearing neurites, were observed in several lines at a later neuronal differentiation stage (beyond 25 DIV). This raised the issue about the accuracy and efficiency of the differentiation protocol. Therefore, we looked to enhance neural induction by subjecting our iPS cell lines and human ES cell line to a monolayer-based strategy. This is part of ongoing work as the time constraints of this thesis didn't allow completion in time for submission. However, the data to date is presented as part of Appendix A. The cell adherent method as a monolayer allows fairly even exposure to exogenous signalling molecules in defined medium, which results in starting material being at the same stage of differentiation and more homogeneity of the cell population as neural

precursors in the neural induction stage (Nasonkin et al, 2009; Chamber et al., 2009; Delli Carri et al., 2013). Overall, human ES cell (H9) with a monolayer-based method offer a more uniform cell population with no expression of pluripotent markers Oct4 and Tra-1-60. In addition, MSN-like cells with DARPP32 immuno-positive expression has been recognized when supplemented with the same combination of chemical defined factors.

The established iPS cell lines exhibit high proliferation rates, as evidenced by Ki67 staining. Therefore, it was necessary to perform more passages of EBs and neuroepithelial cells during the neural induction process. However, when these cells were transferred to neural progenitor expansion medium with the addition of FGF2, neural spheres-liked structures emerged with multipotent properties to generate neural progeny over many passages. Subsequent passaging of neurospheres with FGF2 supplement improved the quality from primitive to definitive neurospheres in a study by Salewski et al. and in addition, this method helps to reduce gene expression of pluripotent and contaminating cell types (Salewski et al., 2013). Furthermore, a similar strategy was applied to monolayer based method to generate ‘long term, self-renewing neuroepithelial stem cell population from ‘hESCs’ called ‘lt-hESNSCs’ from Koch and colleague in 2008 (Koch et al., 2008). This provided extensive proliferation of neural precursors which could differentiate into any specific sub-phenotypes.

In our monolayer-based method, we obtained homogenous and proliferative naive NPCs which were able to differentiate further to DARPP32 positive expressing cells when exposed to distinct combinations of cytokines. These cells were able to generate neurons, up to 6-12 fold from the starting NPC (Appendix A).

Regarding sub-phenotypic differentiation, we applied SHH and DKK-1 in order to manipulate neuroepithelial cells to cells characteristic of the ventral telencephalon sub-region. The combination of SHH and DKK-1 provides a synergistic effect and is more effective than when supplementing with SHH alone (Aubry et al., 2008, Li et al., 2009; Delli Carri et al., 2013). In 2008, Schwartz and colleagues suggested that PSC may maintain low levels of a wide range of

transcription factors which can be triggered or repressed by exogenous signalling and that this is important for the emergence of differentiated phenotypes (Schwartz et al., 2008). Therefore, in contrast to previous studies, combinations of developmental factors were applied at the beginning of the neural conversion process from day 3 to day 26 (see fig 4.25), even though the appropriate time points at which to apply factors to trigger sub-type specific transcription factors has not yet been identified. We proposed that our iPS cell lines may be already primed to a specific lineage, which are ready to be initiated by the right signals. However, SHH and DKK-1 were not provided after 26 DIV as over-expression or prolonged presence of SHH supplement can result in cortical or motor neuron phenotypes (Li et al., 2009, Danjo et al., 2011; Ma et al., 2012). The observed expression of Dlx1, Dlx2, Islet1, FoxP1, FoxP2, and Ctip2 suggest successful to commitment of the NPCs to a ventral telencephalic phenotype; in particular the LGE structure.

These results match the previous studies which characterise the progression of developing MSNs and identify the emergence of LGE markers at 15-25 DIV (Delli Carri et al., 2013), 26 DIV (Ma et al., 2012) and 29-30 DIV (Aubry et al., 2008). However, the finding of our current studies do not match the previous studies with regard to a time line of LGE markers expression, which emerged as early as day 13-17 (see table 4.4) and appeared to increase over time *in vitro*. It seems possible that these results are due to epigenetic memories being retained within our founded cell lines, accelerating LGE phenotypic development. In accordance with this, human primary WGE exhibit those LGE markers by 7-10 DIV but expression of the more mature MSN markers Ctip2 and DARPP32 is not seen until 18 and 20 DIV respectively.

Ctip2 is crucial in the differentiation of striatal MSNs. It has also been reported to govern and organize a cellular architecture in the striatum. In addition, Ctip2 is expressed in all DARPP32 positive cells and is restricted to projection neurons and not interneurons in the striatum. The absence of Ctip2 results in drastic reduction of the expression of MSN genes (Arlotta et al., 2008). The results of our study indicated high expression of Ctip2 by ICC analysis around 25-28 DIV and co-expression with DARPP32 by 30-32 DIV. As shown in table 5.4, this finding occurs earlier than the previous study by Delli Carri and team which first

identify Ctip2 expression at 45 DIV (Delli Carri et al., 2013). The expression of DARPP32 has been reported from 45 (Delli Carri et al., 2013), 47 (Ma et al., 2012), 60-72 DIV (Aubry et al., 2008). However, in our control study, human primary WGE demonstrated abundant Ctip2 positive cells by 18 DIV and co-labelled with DARPP32 by 20 DIV. This finding is consistent with the ideas of Halley-Stott and Gurdon (2013), who suggested that epigenetics governs a particular cell's phenotype pattern and can also be passed on to the progeny. Rather than changing the DNA sequences, epigenetic memory control genes functions (Halley-Stott & Gurdon, 2013).

Although epigenetic memory has been reported to be retained in human PSCs after multiple passages (Halley-Stott & Gurdon, 2013, Lu et al., 2013), sub-clonal PSCs shows signs of the emergence of genetic variation over time in culture (Hussein et al., 2011; Gore et al., 2011), and exposure to mechanical or chemical stimulation can provoke such genomic alterations. Therefore, we limited our starting material to much earlier passages in order to avoid the genome alteration and minimize unpredictable results. Successful human PSC-derived DARPP32 cells expression has been reported from 12-89% among different research teams (Aubry et al., 2008; Ma et al., 2012; Delli Carri et al., 2013) as illustrated in table 5.4. We observe repetitive enriched Ctip2 and DARPP32 expression in our in vitro studies.

Immuno-fluorescence expression over time from neural precursors to MSN-like cells and RT-PCR of gene expression profiles suggest successful derivation of striatal projection neurons from our established cell line as compared to that recently reported by Delli Carri and co-worker in 2013 (Delli Carri et al., 2013). The results illustrate the efficiency of our differentiation protocol to differentiate cells from a distinct background toward striatal MSNs.

Following characterisation of *in vitro* differentiation, *in vivo* differentiation was performed following transplantation into the QA lesioned rat striatum to compare our iPS WGE 928 derived MSNs and human ES cell (H9) derived MSNs using the same EBs-based differentiation method. These cells had been previously differentiated for approximately 30 DIV, and expressed LGE markers

and Ctip2. In our study, 7 animals generated tumours post transplantation with iPS derived MSNs, compared to, 3 out of 6 animals transplanted with human ES (H9) derived MSNs after 7 weeks post transplantation. Our results agree with the findings of Aubry et al. (2008) which reported overgrowth of human ES derived striatal progenitors at 8 weeks post transplantation in the QA lesion HD model (Aubry et al., 2008).

In addition, Aubry characterised tumour compartments, which generated from transplanted cells differentiated for 21-23 DIV (neural precursors stage), 29-30 DIV, 37-40 DIV, and 45-59 DIV (striatal progenitors stage). Aubry suggested that the content within the grafts depended on DIV of transplanted cells. Teratroma-like regions and neural rosette structures were observed when transplanting with neural precursor cells whereas transplantation with more mature neurons generated fully committed neural lineage grafts with absence of teratoma like areas (Aubry et al., 2008). In our study at 7 weeks H&E staining revealed rosette structures of neural epithelial like cells with an absence of other cell phenotypes. However, pluripotent markers such as Oct4 and Tra-1-60 needed to be performed to identify undifferentiated cells within the grafts. This may be due to the heterogenous population of transplanted LGE precursors along with the remnants of neural precursor cells in our differentiation culture. Mixed populations of neural precursors and more mature neurons may give rise to distinct combination among our grafts (N=20, brain with tumour formation=7).

Interestingly, the tumours generated from our iPS derived-MSNs behaved differently from those in Aubry et al. (2008). We observed the migration of transplanted cells from striatal area to cortex with independent tumours compressing the striatum and ventricle (5 out of 6 animals with tumour formation) which have not been reported in previous studies. This finding is a rather different pattern to that seen in Aubry et al where the overgrown cells remained in the area of the striatum and compressed the lateral ventricle. In addition, the tumour separated from the intact brain, thus making it impossible to perform further analysis of the cells component within our tumours.

Another reason for graft overgrowth in our study may be the relatively large number of transplanted cells ($5x10^5$ cells per animal) in comparison to Aubry et al. ($5x10^4$ – $2x10^5$ cells) and Ma et al. ($5x10^4$ cells) (Aubry et al., 2008; Ma et al., 2012). Therefore, if we reduce the number of transplanted cells to $5x10^4$ cells per animal, tumours may not develop. Furthermore, we explored a monolayer based method of deriving MSNs using the same chemical defined factors and medium as the EBs-based method reported earlier (results in Appendix A). Interestingly, 7 weeks after transplanting with $5x10^5$ human ES derived-LGE precursor cells (prepared at 30 DIV) no tumour formation was identified in any transplanted animals (N=7). There was also 100% graft survival, confirmed by HuNu positive cells (data not shown). This corresponds to the work of Delli Carri et al. (2013) which claimed an absence of graft overgrowth or tumour formation using the same cell numbers and the same methodology of monolayer differentiation method (Delli Carri et al., 2013). However, the images presented in the manuscript of Delli Carri would suggest the likelihood of overgrowth and it must be highlighted that only 3 animals were used in that study. Thus, differentiation methods may affect differentiation efficiency and the ability of cells to terminally differentiate to the desired phenotypes. We hypothesise that using monolayer-based method, where there is no bias of cells within the population being exposed to exogenous signalling, leads to homogeneity in the cell population and more complete differentiation toward the desired lineages.

It is noteworthy, that we observed other features corresponding to previous reports from Aubry et al. First, DARPP32 positive cells were identified as groups/clusters of cells rather than standing alone both *in vitro* and *in vivo*. This may support the idea that cell-cell interactions are essential for a maturation of striatal projection neurons/MSNs. This idea was also supported by Fraichard et al. (1995) who suggested that striatal MSNs need to associate as groups of cells in order to mature, which is different to the maturation requirements of dopaminergic neurons (Fraichard et al. 1995). In addition, similar to Aubry's study, bipolar neuronal morphology with medium sized cell bodies were identified after 7 weeks in the grafts, both for human ES and our established iPS cell donors. Second, despite the obvious overgrowth we observed no migration of neuronal cells

beyond the graft border in our EBs-based experiment (N=7), whereas in monolayer-based method, albeit in only one animal, we identified grafted cells starting to migrate into across the graft host border. Interestingly, a control group of grafted human primary WGE cells migrated and distributed evenly in the host striatal area at the similar time point (7 weeks post transplantation). This may suggest that PSC derived-neuronal cells need longer time in vivo to integrate into the host genome and reconstruct the neuronal circuit.

It will be important to clarify the cell components within our tumour, as this may affect the solution. For example, if undifferentiated cells were identified efficient transgene removal strategies could be implemented, whereas if graft overgrowth is due to high proliferation of more mature neural precursors, longer periods of in vitro differentiation may be required, or even reduced numbers of transplanted cells. Once the tumour issue is overcome other assessments such as electrophysiology and behavioural studies will be more meaningful.

Finally, assessment of DARPP-32 expression in grafts revealed a significantly higher number of DARPP32 expressing cells from iPS WGE derived-MSNs compared to human ES cell (H9). Furthermore, the graft volume was also significantly greater in the iPS derived grafts than in the ES cell grafts at this time point. At this stage this is a preliminary result as the numbers of grafted animals assessed was small (iPS group N= 4; ES group N= 3) and thus more extensive quantitative assessments will be necessary. However, despite being preliminary, this result supports the notion that it may be possible to take advantage of epigenetic memory to generate cell sources with a propensity to differentiate into specific desired cellular phenotypes.

Chapter 5

General Discussion

5.1 The challenges of iPS cell line generation

The discovery of methodology to generate iPS cells has paved the way to produce unlimited numbers of almost any kind of cells with many potential applications, including disease modeling, drug screening and regenerative medicine. There are some distinct advantages of using iPS cells in regenerative medicine in terms of avoiding some of the ethical issues associated with primary fetal tissue and ES cells and avoiding some of the problems of immune rejection. Since 2006, when Yamanaka and team first reported the generation of iPS cells, there have been many attempts to generate them from various types of cells such as fibroblast, adipose tissue, urine and menstrual tissue (Meissner et al., 2007, Chen MJ 2014, Xue Y et al., 2013, Li Y et al., 2013), and technological advancements are continuing to improve and simplify the method of production. However, iPS cells are not free of all ethical concerns as they raise some novel concerns related to human cloning (Lo B et al., 2010) and furthermore there is no international committee or restriction agreement between countries. In addition, there is still controversy about what iPS cells are: what the biological processes are underlying the reprogramming; whether they are really indistinguishable from ES cells; and concerns about their safety, with some scientists having referred to iPS cells as ‘man made cancer stem cells’ and thus questioning their suitability for clinical usage (Liu et al., 2008, Sipp D., 2010).

Despite these ongoing concerns, we cannot deny the potential of iPS cells to provide insight into the developmental, pathological, and toxicological studies, and the possibilities they present for regenerative medicine. However, it is important to bear in mind that even though iPS and ES cells share many similarities, they cannot necessarily be considered as identical, and many of the hidden mysteries of these cells need to be better understood before jumping on the iPS bandwagon. Furthermore, with regard to clinical translation, extensive and

vigorous *in vitro* and *in vivo* experiments will need to be performed to ensure the safety of these cells before pursuing their application in cell replacement therapy.

In this thesis, I am ultimately interested in producing striatal MSNs for cell replacement therapy and have attempted to generate iPS cells from tissue containing MSN progenitors in the hope that iPS cells from this source will be more easily differentiated back to an MSN phenotype due to retention of an 'epigenetic memory'. There have been previous attempts to directly proliferate such progenitors *in vitro* as neurospheres and as monolayers, but it proved impossible to cause them to proliferate beyond one passage without losing their capacity to differentiate back to MSNs (Anderson et al., 2007; Zietlow et al., 2012). There have been many reports related to the epigenetic memories retained in iPS cells, which is sometimes seen as a disadvantage, but may also make iPS cells more attractive in terms of their accurate differentiation to specific phenotypes such as the MSNs (Shtrichman R et al., 2013, Sullivan GJ et al., 2010, Kim K et al., 2010). For example it has been shown that iPS cells derived directly from blood cells more readily formed haematopoietic colonies in culture when directly compared to iPS cells derived from fibroblasts in the mouse (Kim et al 2010). Furthermore it was highlighted that neural derived iPS cells have the propensity to retain residual methylation sites that may be important when directing the differentiation of these cells. Therefore, considering generating iPS cells from the target cell type may offer advantages. However, it is likely that other pluripotent properties should equate closely to the standard ES cell in order to propagate a stable and faithful iPS cell line.

In this study, I started by attempting to generate a viral-free iPS cell line using CPP methodologies as described in Chapter 3. However, it became evident that this approach was not a viable means to generating iPS cells due to the technical difficulties in getting the plasmid into the cells along with the reprogramming factors. Despite many attempts to overcome these difficulties I was unsuccessful in generating an iPS cell line. Thus it was decided to explore a different method that had at the time just been published, the *piggyBac* method. Chapter 4 describes how this approach was utilized to generate iPS cell lines from human fetal striatal tissues. Whilst iPS cell lines were successfully generated it

was not without issues. The *piggyBac* method suggests that the reprogramming transgenes can be removed from the established iPS cells, thus making an integration free cell line. Despite exposing the cell lines generated in this thesis to the protocols for removing the transgene it was found that complete removal was not achievable with variability seen in the level of residual transgene expression between different iPS cell lines. Even though the *piggyBac* transposon is an efficient method, however, our downstream application is for cell replacement therapy; therefore pluripotent transgenes must be removed. Chapter 4 looked to direct the differentiation of the established iPS cell lines generated in chapter 3 specifically into MSNs using previously described protocols as well as a new protocol devised in house. Subsequently the cells were transplanted into an animal model of HD as this was the ultimate goal to generate a cell line for cell replacement therapy in HD. I successfully generated DARPP32 positive neurons from iPS cell lines and the efficiency of this method was considerable with a large proportion of positive cells identified both *in vitro* and *in vivo.*

Since the start of this thesis, integration free methods of re-programming have been improved and include strategies such as miRNA, synthetic modified mRNA, and Sendai virus (Fusaki et al., 2009; Warren et al., 2010; Anokye-Danso et al., 2011). The reprogramming efficiency using viral free methods has been improved from a general figure of around 0.001 up to 10% and so the possibility of incorporating these protocols along with the understanding that neural tissues contain a high level of endogenous Sox2 may be a way forward when generating iPS cells from fetal neural tissue specifically WGE or Cortex. The drive to optimize the production protocol for generating integration viral free methods for reprogramming has resulted in a significant amount of experimental data and literature being published. However, at the time of writing the most promising approach would appear to be the Sendai virus method. This approach has been used on human cells and works to a high degree of efficiency (Fusaki N 2009). However, as is the case with all methods described to date it has not been possible to completely remove the vector from the iPS cells generated using this approach. Thus moving forward the aim would be to develop a protocol that would allow complete removal of the reprogramming factors before these cells could be considered for clinical application. However, the cell lines generated using the

current methods are important as they can be used for preclinical experimental analysis.

Producing cell systems for clinical application, however, requires consideration of aspects beyond the efficiency and safety concerns associated with iPS cell production as described above. For example, it may not sufficient to select the primary clones by their morphological similarity to ES cells. Therefore, it will be important to consider using live AP or Tra-1-80 pluripotent markers in cell culture to facilitate selecting the right iPS colonies. This strategy is likely to increase the chance of obtaining a reliable cell line. Moreover, the epigenetic and genomic profiles should have been observed and monitored from the starting material to the established iPS cell line and also the later subsequent progeny of the iPS cells in comparison to human ES cells.

Another consideration is the system used for iPS cell propagation. We considered transferring our iPS cells to a feeder free and animal free culture system because of the eventual aim of designing such cells for clinical application. These refinements would get rid of the problem of contaminating feeder cells and facilitate the selection of more uniform populations of cells for further passaging (Amit et al., 2006). As described in Chapter 5 it was found that using the EB method for directed differentiation of the iPS cells and ES cells, there was the propensity of these cells to form tumours following neural transplantation. Thus an alternative method was explored and I have also been successful in deriving MSNs form human ES cells using monolayer neural differentiation protocol (see appendix A), whilst using the same exogenous signaling molecules as were used in the EBs-based method. As mentioned in the literature reviews, the neural induction stage and regional patterning are separate stages, therefore subjecting the cells to a monolayer-based method should not affect the competence of subtype specification from our chemical defined combination (Delli Carri et al., 2013). In addition, monolayer-based methods allow the exogenous signaling molecules easier and more equal access to the cells, ultimately leading to more cell homogeneity in terms of differentiation. This may lead to improvements in the differentiation of cells within a graft and may help to reduce tumour formation as we would have more control over the lineage specification of the transplanted

cells. Preliminary results have shown this method to produce a homogenous neural population, an ease to manipulate into neural lineages and an absence of pluripotent cells or tumour formation *in vitro* and *in vivo* following directed differentiation. Therefore, the monolayer differentiation strategy may enhance the quality and quantity of our MSNs-like cells. However, this data is part of ongoing work and at the time of completion of this thesis there were still animals alive that had received transplants and were awaiting analysis. Following on from the positive outcomes with human ES cells, iPS cells will be exposed to this monolayer protocol and transplanted for *in vivo* analysis.

5.2 In vitro study of human iPS/ ES derived-MSNs.

In cell differentiation experiments such as those reported in this thesis, it is crucial to perform close and careful observation, tracking the cells from the pluripotent stage through to terminally differentiated cells. In our study, the specific time points for collection of samples for ICC and RT-PCR were taken from the obvious changes in the differentiation phases, such as the neural rosette stage, neural precursor stage, the appearance of LGE progenitors, and terminal neuronal differentiation. However, there are gaps between each time point where we may miss out on important information. In addition, although RT-PCR provides useful information about the presence or absence of the expression of genes of interest, it is limited in that it does not produce accurate information about levels of expression. It would have been useful to have been able to use Q-PCR to observe up- and down- regulation of the expression of genes of interest, from the pluripotent stages through to the differentiated MSN phenotype. This would set a solid framework and would allow cross reference to other characterization strategies such as ICC, electrophysiology, and cross comparison of *in vitro* to *in vivo* differentiation.

We were fortunate in these studies to have access to human fetal WGE, which provided a supply of “genuine’ MSN progenitors. It would have been useful to apply Q-PCR to assess their gene expression profile too as this would have provided a standard profile of neural differentiation with which to compare the iPS

cells. This would likely help to accelerate improvement of the neural conversion protocol by addition or withdrawal of the supporter/repressor signaling in a more accurate time frame as seen in the gene expression patters of primary WGE differentiation.

As discussed in this thesis, to date only a small number of protocols to differentiate MSNs from human PSCs have been reported and there is still much work ongoing to improve such protocols. Of the reports to date, there are huge differences between studies in terms of their efficiency in producing DARPP32 positive neurons, ranging from only 20% up to 89% (although direct comparison is complicated by the fact that the studies use different methods of estimating the efficiency). Thus, specific, reliable, and stable conditions need to be improved to optimize and standardize the differentiation protocol. In Chapter 4, we reported a failure to achieve stable neural conversion in our iPS cell line WGE623 C9; even though, we used a protocol which has been reported to successfully generate MSNs from human ES cells (Arber et al submitted to Development). There are a number of reasons why this might have occurred, and one that was discussed in chapter 4 was the possibility that the transposons had been inadequately removed. However, it is also possible that the differences between PSC lines is such that translation of a protocol from one line to another is not straight forward. Further careful controlled observations are needed to probe and characterize the differences between various cell lines. Indeed as highlighted in Chapter 4 it was possible using our newly devised protocol to silence the expression of the endogenous transgenes in some cell lines and this is something that may be of great importance if methods can't be identified to generate completely transgene free iPS cells albeit with variability across cell lines. The detailed mechanisms whereby the silencing occurred have not been investigated here and why it worked for some cell lines and not others is unknown but raises important questions for further investigation.

In our studies, we were able to convert several iPS cell lines and a human ES line to MSN-like cells, as indicated by their gene expression and antibody staining for specific markers. However, there is a room for improvement in our studies in which we could further test our hypothesis and enhance the current

protocols reported here. As described in Chapter 4 and above, an EBs-based protocol was used to derive MSN-like cells, but this presented some problems including disorganized aggregation, heterogeneity of the differentiated population, persistence of pluripotent cells and possibly also for the differentiation of non-neural lineages within EBs. And as said above, we are exploring the monolayer approach and this is the subject of ongoing work. As aforementioned, in our studies we have chronologically observed the specific stages of differentiation using gene expression markers such as ICC and RT-PCR. However, this passive characterization may not be sufficiently effective to detect small errors within the experiment, such as subset of pluripotent cells amongst the differentiated cells. One way to overcome this could be the integration of reporter genes to allow the identification of expression of key genes. As an active characterization strategy, the expression of reporter genes may act to confirm the cells characteristic *in vitro*, thus allowing the grafting of cells at specific stages of differentiation and allowing purification of cells using technologies such as FACS sorting. The importance of grafting cells at specific stages of differentiation has been previously noted and related to tumour formation or hyper proliferation of the grafted cells (Aubry et al., 2008; Ma et al., 2009; Seminatore et al., 2011). The best estimate to date of the most suitable stage for grafting has been reported to be around the proneuronal stage up to the early post mitotic stage; therefore the reporter genes for our MSN-like cells should be expressed within this time window (Fricker-Gates RA et al., 2004).

Cell transplantation in HD aims to reconstruct the damaged neuronal circuits of the striatum. Thus, being able to demonstrate appropriate function of PSC derived MSNs after transplantation into the striatum in animal models of HD is an important step. Furthermore, this is the ultimate test that the PSC derived MSNs are fully functional. As discussed in Chapter 5, there is limited improvement in the behavioral outcomes reported in the previous studies in which human PSC-derived MSNs are transplanted into HD animal models (Aubrey et al., 2008; Ma et al., 2012; Delli Carri et al., 2013), despite the fact that such cells appeared to possess the markers expected of MSNs in the in vitro studies. This raises two issues: first, are there better *in vitro* culture systems for assessing the

differentiation of PSCs; and secondly, why is it that the PSC-derived MSNs so far reported in the literature appear to function less well than their WGE counterparts?

To first consider the suitability of the culture system: a two dimensional culture system is not ideal when compared to the natural environment of neural cells, and this may be one of the reasons why neurons produced within culture do not show full function post transplantation. A 3D culture system may be preferable, in which cells can differentiate, migrate, and connect in a manner that is closer to what they would do in the brain (Ortinau et al., 2010), and this in itself may promote differentiation and accelerate phenotypic maturation (Thonhoff et al., 2008; Holmes et al., 2000; Taraballi et al., 2010; Ortinau et al., 2010).

In tissue engineering, biomaterial scaffolds have been introduced and used to aid differentiation of various cell types for regenerative medicine, such as spinal cord injury (Ortinau et al., 2010; Li et al., 2012; Binan et al., 2014). Ortinau et al. (2010) reported a higher survival rate of human neural progenitor cells and fewer dead cells over time when cells were cultured in a 3D, rather than a 2D culture system (Ortinau et al., 2010). In addition, this correlated to the number of β-III tubulin expressing neurons which is higher in 3D culture. However, it would be necessary to optimize any biomatrix in terms of composition, concentration, and functionalization if such a 3D system were to be applied in our study.

It is not only the spatial dimension that is different between *in vitro* and *in vivo* differentiation; the cellular microenvironment within those two conditions are also distinct. In the natural CNS environment, there are many signaling pathways, both stimulators and inhibitors, coming from every direction. In addition, other neural cell types, such as surrounding, astrocytes, oligodendrocytes, and interneurons, which may secrete various factors, such as neurotrophic factors, that may influence the developing neural cells in a variety of ways (Ruiz et al., 2012; Perucho et al., 2013). Therefore, co-culture with gial cells derived from human WGE, or their conditioned media, may increase phenotypic differentiation, improve postmitotic maturation, and enhance the appropriate function of MSN-like cells produced from our iPS cells.

From our data it can be seen that the expression of DARPP32 was confirmed much earlier than in other reported protocols. This is suggestive of the role of the importance of the 'epigenetic memory' in affecting the differentiation potential of our iPS cells. Whilst we can't say this for certain as further investigations are required to confirm this there is strong evidence to suggest its significance. Further work would require epigenetic screening of both the DARPP32 positive cells from the iPS cells and the donor derived tissues. Interestingly the expression of DARPP32 was also seen at this earlier time point in ES derived neural cells using the same protocol, albeit at a lower level. At this point detailed quantification has not been carried out to be able to directly compare between the two cell types but initial analysis would suggest that there are differences between the two cell types *in vitro* and *in vivo*.

5.3 In vivo study of human iPS/ES derived-MSNs.

As discussed in Chapter 5, tumour formation was reported at 6-7 weeks post transplantation in a proportion of animals having received iPS cell derived neural grafts and also human ES cell derived neural grafts, although they were less common in the latter. The tumours appeared to contain areas of hyperproliferation activity of neural epithelial cells and/or neural precursors. Similar structures were observed and reported in 2008 by Aubry and team (Aubry et al., 2008). H&E staining of the grafts where significant overgrowth was seen would suggest that the tumour like structure in the graft area is the result of neural precursor overgrowth rather than teratoma formation based on the absence of mesoderm and endoderm type cells based on morphology alone. This is an important finding as it validates the neural induction protocol used but highlights the need for some refinements to prevent future overgrowths occurring. Interestingly, graft overgrowth in primary cells transplanted into the rat striatum has been reported from time to time (Geny et al., 1994).

There are a number of ways to overcome this issue including, as mentioned above, looking at transplanting the cells at different stages in the differentiation protocol. Another way to overcome this obstacle is to apply DAPT 4-5 days *in vitro*

culture prior to harvesting the cells for transplantation. As previous study from Kirkeby and colleague (2012) suggested that DAPT, which is Notch signaling pathway inhibitor and γ-secretase inhibitor, accelerates neural cells commitment and decreases the proliferation property (Kirk et al., 2011; Kirkeby et al., 2012). In addition, good graft survival without tumour formation was obtained when transplanted with DAPT treated human PSC-derived neuronal cells (Kirkeby et al., 2012). FACS sorting is another option to select particular cells types within a population. This method offers the opportunity to pick up stage-specific cells, and avoid transplanting pluripotent or highly proliferative cells. However, the viability of sorted cells may decrease due to various disturbing processes associated with the procedure itself. Therefore, we could consider re-plating the FACS sorted cells and transplanting the cells after a recovery period. Which method will be employed will be determined based on further understanding of the nature of the tumour itself.

An additional problem related to the final distribution of the grafted cells in the brain is that some grafted cells were observed within the needle tract suggesting backflow of cells up the needle during surgery. This may have contributed to the grafted cells reaching the cortex. One potential method to address this would be to implant the cells within a hydrogel matrix. Hydrogels have been suggested to promote cell viability, reduce scar formation, and improve grafted cell implantation in stroke models (Chai et al., 2007; Potter et al., 2008; Zhong et al., 2010). Many gels contain hyaluronan, which is an extracellular matrix component, and the viscoelastic and mechanical characters of this hydrogel is similar to the extracellular matrix of the brain (Zhong et al., 2010). These properties appear to encourage cell differentiation and allow neurite extension without encouraging scar formation and may help to maintain transplanted cells within the graft region. Furthermore, neurotrophic factors can be incorporated into the hydrogel to support the grafted neurons. Thus, I would be interested in transplanting our iPS/ES-derived MSNs within a hydrogel composing of hyaluronan+heparin+collagen with BDNF, GDNF, and Rock inhibitor supplement (Zhong et al., 2010).

In this study, we transplanted iPS cells derived MSN-like cells into the QA-lesioned rat model using a xenograft paradigm (human-to-rat) cross-comparing to human ES derived MSN-like cells and human primary WGE. This model allows us to investigate graft survival, grafted cells differentiation and integration into host tissue, reconstruction of neural circuits, and eventually, correction of symptom deficits via behavioral studies. However, immune suppression is needed in xenograft transplantation; as a result the transplanted animal will inevitably become sick and will need to be scarified around 20 weeks post implantation. Therefore, this model may not permit us to validate terminally differentiated grafted cells *in vivo* which is essential in preclinical PSC transplantation studies. As extensive *in vivo* differentiation is needed, desensitization of the host animal with the xenogeneic donor tissue at neonatal stage is an alternative choice to escape immune reactivity problems (Kelly et al., 2009). This strategy would allow the transplanted cells to terminally differentiate longer term *post transplantation*. In addition, repeated behavioral studies can be performed to investigate the beneficial effect from grafting cells at alleviating deficits in the diseased model. Furthermore, extensive long-term differentiation is important for more comprehensive recognition of tumour formation at later time in the study because tumour production can take time to emerge.

The hypothesis behind the work carried out in this thesis was that the iPS cells generated from fetal derived WGE would have an epigenetic memory of their origin thus facilitating their differentiation into mature MSNs in vitro. The data presented here, whilst not confirming this, suggest the possibility that this may be the case. Due to time constraints it was not possible to carry out a detailed epigenetic screen of our iPS cells and to compare this to our starting material however, future work would look to prioritize this experiment. Moreover, we would not only compare the WGE derived iPS cells to WGE primary tissue but would also include ES derived MSNs as well as cortex and fibroblast derived iPS cells in the analysis.

5.4 Functional characterization of iPS/ES derived-MSNs

As aforementioned, the ultimate aim of the work described in this study is to produce cells that are suitable to reconstruct the neural network in the damaged striatum. Therefore, it is crucial to ensure appropriate functional properties from these MSN like-cells before and after implanting into the host brain. First of all in vitro studies were performed measuring: the expression of markers such as synaptophysin, demonstrating synaptic transmission activities; GAD65/67 identifying GABA synthesizing enzymes which provide an indicator that the cells may be functional neurons; and PSD95 presenting post synaptic protein with varying expression seen between ES and iPS derived neurons. Expression of these markers also needs to be analysed in graft sections. Neuro-electrophysiology should be performed in culture at chronological time point so as to monitor the functional maturation and their firing pattern over time *in vitro*. In addition, the same strategy should be applied on to human primary WGE at a similar time window for comparison with 'natural' MSN development. Moreover, neuro-electrophysiological on brain slices would allow us to record the action potential of the grafted neurons and monitor their function in the normal brain environment.

The ultimate test of whether the iPS and ES derived MSNs are functional is to transplant them into animal models of HD to see whether they are capable of repairing the damaged neural circuitry. Our initial studies looking at this have found that both the iPS and ES derived neurons had the ability to differentiate into mature MSN-like cells expressing DARPP32 in vivo 7 weeks post transplantation. However, the presence of tumours in these animals is a major concern and will need to be rectified before further in vivo experiments can be carried out. Future studies would first look to incorporate anterograde and retrograde labelling to allow us to examine neuronal connectivity between grafted-host tissues (reviewed in Sanberg et al., 1989) and to further understand the potential of these cells to reform connections in the brain. In addition detailed behavioral characterization at a motor and cognitive level should be investigated. Various tasks can be assessed such as spontaneous/amphetamine induce hyperactivities, haloperidol induced catalepsy, asymmetry rotation on a motor level, whilst cognitive deficits can be

assessed using conditioned behavior such as delay alteration tasks (Nakao and Itakura, 1999). However, the HD rodent model may not be the most effective model to assess such aspects of the disease as the psychiatric component, and it may eventually be necessary to consider using non-human primate models (Nakao and Itakura, 1999).

Concluding remarks

iPS cells technology provides us with a powerful tool to understand biological development from its origin and can be applied in various branches of knowledge including cell replacement therapy. However, all PSC derived donors must be vigorously tested in every aspect in order to ensure safety when considering using such cells in patients. Absolute requirements for neural cell replacement therapy are that the desired specific subtypes can be efficiently and effectively produced, that they are functional, that non-target cell types are kept to an acceptable minimum, and that cells with significant proliferative properties (in particular, pluripotent cells) are eliminated. The efficient and reliable generation of sufficient numbers of genuine functional MSNs for cell therapy in HD is challenging, and there are many issues to take into consideration, such as genetic and epigenetic alteration, teratoma formation, and immuno-reactivity.

In this thesis some challenges of iPS cell generation are highlighted and iPS cells generated using *piggyBac* technology are characterized and found to be capable of differentiating into MSNs, although the issue of tumour formation remains problematic. It appears that our modifications of pre-existing differentiation protocols may be more efficient at generating MSNs and that MSNs generated from human WGE may be more ready to differentiate into MSNs than cells from other sources, although further work will be needed to confirm this. Ultimately, quantitative assessment, and an array of characterization and behavioral studies need to be undertaken in order to complete this work. The drive to establish an efficient protocol for the generation of iPS cells is ongoing and it is important that we keep abreast of this literature as more efficient methods may become available for generating these cells thus overcoming some of the issues highlighted with the current protocol.

Bibliography

Amit, M., Carpenter, M.K., Inokuma, M.S., Chiu, C.-P., Harris, C.P., Waknitz, M.A., Itskovitz-Eldor, J., Thomson, J.A., 2000. Clonally derived human embryonic stem cell lines maintain pluripotency and proliferative potential for prolonged periods of culture. *Developmental Biology*, 227 (2), pp.271-278.

Amit, M., Itskovitz-Eldor, J., 2006. Feeder-free culture of human embryonic stem cells. *Methods Enzymol*, 420, pp.37–49.

Anderson, S.A., Qiu, M., Bulfone, A. et al., 1997. Mutations of the homeobox genes Dlx-1 and Dlx-2 disrupt the striatal subventricular zone and differentiation of late born striatal neurons. *Neuron*, 19(1), pp.27-37.

Anderson, L., Burnstein, R.M., He, X., Luce, R., Furlong, R., Foltynie, T., Sykacek, P., Menon, D.K. & Caldwell, M.A., 2007. Gene expression changes in long term expanded human neural progenitor cells passaged by chopping lead to loss of neurogenic potential in vivo. *Experimental Neurology*, 204(2), pp.512–524.

Androutsellis-Theotokis, A., R.R., Leker, F., Soldner, D.J., Hoeppner, R., Ravin, S.W., Poser, M.A., Rueger, S.K., Bae, R., Kittappa and R.D. McKay., 2006. Notch signalling regulates stem cell numbers in vitro and in vivo. *Nature*, 442, pp.823-826.

Anokye-Danso, F. et al., 2011. Highly efficient miRNA-mediated reprogramming of mouse and human somatic cells to pluripotency. *Cell stem cell*, 8(4), pp.376–388.

Aoi, T., 2008. Advance in study of induced pluripotent stem cells (iPS cells). *Nippon Rinsho*, 66(5), pp.850-856.

Aoi, T. et al., 2008. Generation of pluripotent stem cells from adult mouse liver and stomach cells. *Science*, 321(5889), pp.699-702.

Arlotta, P., et al., 2008. Ctip2 controls the differentiation of medium spiny neurons and the establishment of the cellular architecture of the striatum. *The Journal of neuroscience : the official journal of the Society for Neuroscience*, 28(3), pp.622–632.

Armstrong, R.J., Watts, C., Svendsen, C.N., Dunnett, S.B., & Rossor, A.E., 2000. Survival, neuronal differentiation, and fiber outgrowth of propagated human neural precursor grafts in an animal model of Huntington's disease. *Cell Transplantation*, 9(1), pp.55-64.

Atkin, N.B., Baker, M.C., Robinson, R., Gaze, S.E., 1974. Chromosome studies on 14 near-diploid carcinomas of the ovary. *Eur. J. Cancer*, 10, pp.144–146.

Aubry, L. et al., 2008. Striatal progenitors derived from human ES cells mature into DARPP32 neurons in vitro and in quinolinic acid-lesioned rats. *Proceedings of the National Academy of Sciences of the United States of America*, 105(43), pp.16707–16712.

Bachoud-Lévi, a et al., 2000. Safety and tolerability assessment of intrastriatal neural allografts in five patients with Huntington's disease. *Experimental neurology*, 161(1), pp.194–202.

Bachoud-Levi, A.C., Gaura, V., Brugieres, P. et al., 2006. Effect of fetal neural transplants in patients with Huntington's disease 6 years after surgery: a long-term follow-up study. *Lancet Neurol*, 5, pp.303-309.

Bain, G., Kitchens, D., Yao, M. et al., 1995. Embryonic stem cells express neuronal properties in vitro. *Dev Biol*, 168 (2), pp.342-357.

Bain, G., Bain, W.J., Ray, M., Yao, D.I., Gottlieb, et al., 1996. Retinoic acid promotes neural and represses mesodermal gene expression in mouse embryonic stem cells in culture Biochem. Biophys. *Res. Commun*., 223, pp.691–694.

Ban, H., Nishishita, N., Fusaki, N., Tabata, T., Saeki, K. et al., 2011. Efficient generation of transgene-free human induced pluripotent stem cells (iPSCs) by temperature-sensitive Sendai virus vectors. *Proc Natl Acad Sci USA* 108, pp.14234-14239.

Bar-Nur, O., Russ, H.A,, Efrat, S., Benvenisty, N., 2011. Epigenetic memory and preferential lineage-specific differentiation in induced pluripotent stem cells derived from human pancreatic islet beta cells. *Cell Stem Cell*, 9, pp.17-23.

Binan, L. et al., 2014. Differentiation of neuronal stem cells into motor neurons using electrospun poly-L-lactic acid/gelatin scaffold. *Biomaterials*, 35(2), pp.664–674.

Bissonnette, C.J., Lyass, L., Bhattacharyya, B.J., Belmadani, A., Miller, R.J., & Kessler, J. A., 2011. The controlled generation of functional basal forebrain cholinergic neurons from human embryonic stem cells. *Stem cells*, 29, pp.802-811.

Blelloch, R., 2006. Reprogramming efficiency following somatic cell nuclear transfer is influenced by the differentiation and methylation state of the donor nucleus. *Stem Cells*, 24, pp. 2007-2013.

Bock, C., Kiskinis, E., Verstappen, G., Gu, H., Boulting, G., Smith, Z.D. et al., 2011. Reference maps of human ES and iPS cell variation enable high-throughput characterization of pluripotent cell lines. *Cell*, 144, pp.439–452.

Bradley, A., Evans, M., Kaufman, M.H., Robertson, E., 1984. Formation of germ-line chimaeras from embryo-derived teratocarcinoma cell lines. *Nature*, 309 (5965), pp.255-256.

Brambrink, T. et al. 2008. Sequential expression of pluripotency markers during direct reprogramming of mouse somatic cells. *Cell Stem Cell* 2(2), pp.151-159.

Brinster, R.L., 1974. The effect of cells transferred into the mouse blastocyst on subsequent development. *J. Exp. Med.*,140, pp.1049–1056.

Brueckner, B., Kuck, D. & Lyko, F., 2007. DNA methyltransferase inhibitors for cancer therapy. *Cancer J*., 13, pp.17-22.

Carri, A.D. et al., 2013. Developmentally coordinated extrinsic signals drive human pluripotent stem cell differentiation toward authentic DARPP-32+ medium-sized spiny neurons. *Development (Cambridge, England)*,140(2), pp.301–312.

Cambray S, Arber C, Little G, Dougalis AG, de Paola V, Ungless MA, et al. Activin induces cortical interneuron identity and differentiation in embryonic stem cell-derived telencephalic neural precursors. Nat Commun. 2012;3: 841

Campbell, K. et al., 1993. Characterization of GABA release from intrastriatal striatal transplants: dependence on host-derived afferents. *Neuroscience*, 53(2), pp.403–415.

Campbell, K., Olsson, M. and Bjorklund, A., 1995. Regional incorporation and site-specific differentiation of striatal precursors transplanted to the embryonic forebrain ventricle. *Neuron*, 15(6), pp.1259-1273.

Campbell, K., 2003a. Dorsal-ventral patterning in the mammalian telencephalon. *Current Opinion in Neurobiology*, 13(1), pp.50–56.

Carey, B. W. et al., 2009. Reprogramming of murine and human somatic cells using a single polycistronic vector. *Proc Natl Acad Sci U S A*., 106(1), pp.157-162.

Cary, L.C., Goebel, M., Corsaro, B.G., Wang, H.G., Rosen, E., Fraser, M.J., 1989. Transposon mutagenesis of baculoviruses: Analysis of Trichoplusia ni transposon IFP2 insertions within the FP-locus of nuclear polyhedrosis viruses. *Virology*, 172, pp.156–169.

Chai, C., Leong, K.W., 2007. Biomaterials approach to expand and direct differentiation of stem cells. *Mol. Ther*., 15(3), pp.467-480.

Chambers, S.M., Fasano, C. A, et al., 2009. Highly efficient neural conversion of human ES and iPS cells by dual inhibition of SMAD signaling. *Nature biotechnology*, 27(3), pp.275–280.

Chen, Z.-Y. et al., 2003. Minicircle DNA vectors devoid of bacterial DNA result in persistent and high-level transgene expression in vivo. *Mol. Ther.*, 8, pp.495-500.

Chen, Z.Y., He, C.Y. & Kay, M.A., 2005. Improved production and purificataion of minicircle DNA vector free of plasmid bacterial sequences and capable of persistent transgene expression in vivo. Hum. *Gene Ther.*, 16, pp.126-131.

Chin, M.H., Mason, M.J., Xie, W., Volinia, S., Singer, M., Peterson, C., Ambartsumyan, G., Aimiuwu, O., Richter, L., Zhang, J. et al., 2009. Induced pluripotent stem cells and embryonic stem cells are distinguished by gene expression signatures. *Cell Stem Cell*, 5, pp.111-123.

Cowan, C.A., Atienza, J., Melton, D.A., Eggan K., 2005. Nuclear reprogramming of somatic cells after fusion with human embryonic stem cells. *Sicence* , 309, pp.1369-1373.

Costantini L.C. and Isacson O., 2000. Immunophilin ligands and GDNF enhance neurite branching or elongation from developing dopamine neurons in culture. Exp. Neurol., 164, pp.60-70

Daheron, L., Opitz, S.L., Zaehres, H., Lensch, M.W., Andrews, P.W., Itskovitz-Eldor, J., 2004. Daley G.Q. LIF/STAT3 signaling fails to maintain self-renewal of human embryonic stem cells. *Stem Cells*, 22, pp.770–778.

Danjo, T., Eiraku, M., Muguruma, K. et al., 2011. Subregional specification of embryonic stem cell-derived ventral telencephalic tissues by timed and combinatory treatment with extrinsic signals. *J Neurosci*, 31, pp.1919-1933.

Davis, R.P. et al., 2013a. Generation of induced pluripotent stem cells from human foetal fibroblasts using the Sleeping Beauty transposon gene delivery system. *Differentiation; research in biological diversity*, 86(1-2), pp.30–37.

Dinsmore, J., Ratliff, J., Deacon, T. et al., 1996. Embryonic stem cells differentiated in vitro as a novel source of cells for transplantation. *Cell Transplantation*, 5 (2), pp.131-143.

Dong, F.L., Kaleri, H.A., Lu, Y.D., Song, C.L., Jiang, B.C. et al., 2012. Generation of induced pluripotent mouse stem cells in an indirect co-culture system. *Genet Mol Res*, 11, pp.4179–86

Dunnett, S.B. et al., 1998. Striatal transplantation in a transgenic mouse model of Huntington's disease. *Experimental neurology*, 154(1), pp.31–40.

Dunnett, S.B., 2000. Functional analysis of fronto-striatal reconstruction by striatal grafts, in *Neural Transplantation in Neurodegenerative Disease: Current Status and New Directions*, No.231, eds D. J. Chadwick and J. A. Goode (London: Wiley), pp.21–42.

Dunnett, S.B. and Rosser, A.E., 2011. Clinical translation of cell transplantation in the brain. *Current Opinion in Organ Transplantation*, 16(6), pp.632-639.

Dunnett, S.B. and Rosser, A.E., 2011. Cell-based treatments for Huntington's disease. *International Review of Neurobiology*, 98, pp.483-508.

Dunnett, S.B. and Rosser, A.E., 2014. Challenges for taking primary and stem cell therapies into clinical trials for neurodegenerative disease. *Neurobiology of Disease*, 61, pp.79–89.

Eisenstat, D.D., Liu, J.K., Mione, M., Zhong, W., Yu, G., Anderson, S.A., Ghattas, I., Puelles, L., Rubenstein, J.L., 1999. DLX-1, DLX-2, and DLX-5 expression define distinct stages of basal forebrain differentiation. *J Comp Neurol*, 414, pp.217-237.

El-Sayed, W.A., Rashad, A.E., Awad, S.M., Ali, M.M., 2009. Synthesis and in vitro antitumor activity of new substituted thiopyrimidine acyclic nucleosides and their thioglycoside analogs. *Nucleosides Nucleotides Nucleic Acids*, 28(4), pp.261-74.

El-Sayed, A., Futaki, S., Harashima, H., 2009. Delivery of Macromolecules Using Arginine-Rich Cell-Penetrating Peptides: Ways to Overcome Endosomal Entrapment. Aaps J.

Elkabetz, Y. et al., 2008. Human ES cell-derived neural rosettes reveal a functionally distinct early neural stem cell stage. *Genes & development*, 22(2), pp.152–165.

Elkabetz, Y. & Studer, L., 2008. Human ESC-derived neural rosettes and neural stem cell progression. *Cold Spring Harbor symposia on quantitative biology*, 73, pp.377–387.

Eminli, S., Utikal, J., Arnold, K., Jaenisch, R., Hochedlinger, K., 2008. Reprogramming of neural progenitor cells into induced pluripotent stem cells in the absence of exogenous Sox2 expression. *Stem Cells*, 26, pp.101-106.

Erceg, S. et al., 2008. Differentiation of human embryonic stem cells to regional specific neural precursors in chemically defined medium conditions. *PloS one*, 3(5), p.e2122.

Ericson, J., Muhr, J., Placzek, M., Lints, T., Jessell, T.M., Edlund, T., 1995. Sonic hedgehog induced the differentiation of ventral forebrain neurons: a common signal for ventral patterning within the neural tube. Cell, 81, pp.747-756.

Evans, M.J., and Kaufman, M.H., 1981. Establishment in culture of pluripotential cells from mouse embryos*. Nature*, 292, pp.154-156.

Evans, a E. et al., 2012. Molecular regulation of striatal development: a review. *Anatomy research international*, p.106529.

Feng, B., Jiang, J., Kraus, P. et al., 2009. Reprogramming of fibroblasts into induced pluripotent stem cells with orphan nuclear receptor Esrrb. *Nat Cell Biol*, 11, pp.197-203.

Feng, Q., Lu, S.J., Klimanskaya, I., Gomes, I., Kim, D., Chung, Y. et al., 2010. Hemangioblastic derivatives from human induced pluripotent stem cells exhibit limited expansion and early senescence. *Stem Cells*, 28, pp.704–712.

Ferrari, D., Sanchez-Pernaute, R., Lee, H., Studer, L., Isacson, O., 2006. Transplanted dopamine neurons derived from primate ES cells preferentially innervate DARPP32 striatal progenitors within the graft. *Eur J Neurosci*, 24, pp.1885-1896.

Ferrari, S., Griesenbach, U., Iida, A., Farley, R., Wright, A.M., Zhu, J. et al., 2007. Sendai virus-mediated CFTR gene transfer to the airway epithelium. *Gene Ther*., 14, pp.1371-1379.

Foster, K.W. et al., 2005. Induction of KLF4 in basal keratinocytes blocks the proliferation-differantiation switch and initiates squamous epithelial dysplasia. *Oncogene*, 24, pp.1491-1500.

Fraichard, A., Chassande, O., Bilbaut, G., Dehay, C., Savatier, P. & Samarut, J., 1995. In vitro differentiation of embryonic stem cells into glial cells and functional neurons. *Journal of Cell Science*, 108 (Pt 10), pp.3181-3188.

Fraser, M.J., Ciszczon, T., Elick, T. & Bauser, C.,1996. Precise excision of TTAA-specific lepidopteran transposons piggyBac (IFP2) and tagalong (TFP3) from the baculovirus genome in cell lines from two species of Lepidoptera. *Insect Mol. Biol*. 5, pp.141-151.

Fricker-Gates, R.A., White, A., Gates, M.A., Dunnett, S.B., 2004. Striatal neurons in striatal grafts are derived from both post-mitotic cells and dividing progenitors. *Eur J Neurosci*, 19, pp.513-520.

Fu, W., Wang, S.J., Zhou, G.D., Liu, W., Cao, Y. and Zhang, W.J., 2012. Residual undifferentiated cells during differentiation of induced pluripotent stem cells *in vitro* and *in vivo*. *Stem Cells Dev*, 21, pp.521.

Fusaki, N. et al., 2009. Efficient induction of transgene-free human pluripotent stem cells using a vector based on Sendai virus, an RNA virus that does not integrate into the host

genome. *Proceedings of the Japan Academy. Series B, Physical and biological sciences*, 85(8), pp.348–362.

Gachelin, G., Kemler, R., Kelly, F., Jacob, F., 1977. PCC4, a new cell surface antigen common to multipotential embryonal carcinoma cells, spermatozoa, and mouse early embryos. *Dev. Biol*, 57, pp.199–209.

Gaspard, N. & Vanderhaeghen, P., 2010. Mechanisms of neural specification from embryonic stem cells. *Current opinion in neurobiology*, 20(1), pp.37–43.

Geny, C. et al.,1994. Long-term delayed vascularization of human neural transplants to the rat brain. *J Neurosci*, 14, pp.7553–7562.

Gerrard, L., Rodgers, L. & Cui, W., 2005. Differentiation of human embryonic stem cells to neural lineages in adherent culture by blocking bone morphogenetic protein signaling. *Stem cells (Dayton, Ohio)*, 23(9), pp.1234–1241.

Ghosh, Z., Wilson, K.D., Wu, Y., Hu, S., Quertermous, T., Wu, J.C., 2010. Persistent donor cell gene expression among human induced pluripotent stem cells contributes to differences with human embryonic stem cells. *PLoS ONE*., 5, e8975.

Giorgetti, A. et al., 2009. Generation of induced pluripotent stem cells from human cord blood using OCT4 and SOX2. *Cell Stem Cell*, 5, pp.353-357.

Goldman, S., 2005. Stem and progenitor cell-based therapy of the human central nervous system. *Nat Biotechnol*, 23, pp.862-871.

Gonzalez, F., Boue, S., Izpisua Belmonte, J.C., 2011. Methods for making induced pluripotent stem cells: reprogramming a la carte. *Nat Rev Genet*, 12, pp.231-242.

Gorbin, J.G., Gaiano, N., Machold, R.P., Langston, A. and Fishell, G., 2000. The Gsh2 homeodoomain gene controls multiple aspects of telencephalic development. *Development*, 127(20), pp.5007-5020.

Gore, A., Li, Z., Fung, H.L., Young, J.E., Agarwal, S., Antosiewicz-Bourget, J., Canto, I., Giorgetti, A., Israel, M.A., Kiskinis, E., Lee, J.H., Loh, Y.H., Manos, P.D., Montserrat, N., Panopoulos, A.D., Ruiz, S., Wilbert, M.L., Yu, J., Kirkness, E.F., Izpisua, Belmonte, J.C., Rossi ,D.J., Thomson, J.A., Eggan, K., Daley, G.Q., Goldstein, L.S. and Zhang, K., 2011. Somatic coding mutations in human induced pluripotent stem cells. *Nature*, 2011 Mar 3, 471(7336), pp.63-67.

Grabundzija, I. et al., 2013. Sleeping Beauty transposon-based system for cellular reprogramming and targeted gene insertion in induced pluripotent stem cells. *Nucleic acids research*, 41(3), pp.1829–1847.

Gratsch, T.E., O'Shea, K.S., 2002. Noggin and chordin have distinct activities in promoting lineage commitment of mouse embryonic stem (ES) cells. *Dev Biol*., 245(1), pp.83-94.

Gurdon, J.B., Wilmut, I., 2011. Nuclear transfer to eggs and oocytes. *Cold Spring Harb Perspect Biol.*, 3.

Halley-Stott, R.P. & Gurdon, J.B., 2013. Epigenetic memory in the context of nuclear reprogramming and cancer. *Briefings in functional genomics*, 12(3), pp.164–173.

Hanna, J. et al. 2007. Treatment of sickle cell anemia mouse model with iPS cells generated from autologous skin. *Science*, 318(5858), pp.1920-1923.

Harreither, E. et al., 2014. Characterization of a novel cell penetrating peptide derived from human Oct4. *Cell regeneration (London, England)*, 3(1), p.2.

Haskell, G.T. and LaMantia, A.S., 2005. Retinoic acid signaling identified a distinct precursor population in the developing and adult forebrain. Journal of Neuroscience, 25(33), pp.7636-7647.

Hauser, R.A., Furtado, S., Cimino, C. R., Delgado, H., Eichler, S., Schwartz, S. et al., 2002. Bilateral human fetal striatal transplantation in Huntington‘s disease. *Neurology*, 58, pp.687–695 10.1212/WNL.58.5.687

Hochedlinger, K. et al., 2005. Ectopic expression of Oct-4 blocks progenitor-cell differentiation and causes dysplasia in epithelial tissues. *Cell* 121, pp.465-477.

Hogan, B., Fellous, M., Avner, P., Jacob, F., 1977. Isolation of a human teratoma cell line which expresses F9 antigen. *Nature*, 270, pp.515–518.

Holmes, T.C., de Lacalle, S., Su, X., Liu, G., Rich, A., Zhang, S., 2000. Extensive neurite outgrowth and active synapse formation on self-assembling peptide scaffolds. *Proc Natl Acad Sci USA.*, 97, pp.6728–6733.

Hu, B.Y., Du, Z.W., Li, X.J., Ayala, M. and Zhang, S.C., 2009. Human oligodendrocytes from embryonic stem cells: conserved SHH signalling networks and divergent FGF effects. *Development*, 136, pp.1443-1452.

Hu, B.Y., Weick, J.P., Yu, J., Ma, L.X., Zhang, X.Q., Thomson, J.A. et al., 2010. Neural differentiation of human induced pluripotent stem cells follows developmental principles but with variable potency. *Proc Natl Acad Sci USA*., 107, pp.4335–4340.

Huangfu, D. et al., 2008. Induction of pluripotent stem cells from primary human fibroblasts with only Oct4 and Sox2. *Nature biotechnology*, 26(11), pp.1269–1275.

Humphrey, R.K., Beattie, G.M., Lopez, A.D., Bucay, N., King, C.C., Firpo, M.T., Rose-John, S., Hayek, A., 2004. Maintenance of pluripotency in human embryonic stem cells is STAT3 independent*. Stem Cells*, 22, pp.522–530.

Huntington, G., 1872. On chorea. In The Medical and Surgical Reporter. *A Weekly Journal, (ed. Butler SW)*, pp.317–321. Philadelphia.

Hussein, S.M. et al., 2011. Copy number variation and selection during reprogramming to pluripotency. *Nature*, 471(7336), pp.58–62.

Imarisio, S., Carmichael, J., Korolchuk, V., Chen, C.W., Saiki, S., Rose, C., Krishna, G., Davies, J.E., Ttofi, E., Underwood, B.R., et al., 2008. Huntington’s disease: from pathology and genetics to potential therapies. *Biochem J*., 412, pp.191–209.

Ivics, Z., Li, M.A., Mates, L., Boeke, J.D., Nagy, A., Bradley, A. And Izsvak, Z., 2009. Transposon-mediated genome manipulation in vertebrates. *Nat. Methods*, 6, pp.415-422.

Jin, C.H. et al., 2003. Recombinant Sendai virus provides a highly efficient gene transfer into human cord blood-derived hematopoietic stem cells. *Gene Ther*., 10, pp.272-277.

Joannides, A.J. et al., 2007. Environmental signals regulate lineage choice and temporal maturation of neural stem cells from human embryonic stem cells. *Brain : a journal of neurology*, 130(Pt 5), pp.1263–1275.

Kahan, B.W., Ephrussi, B., 1970. Developmental potentialities of clonal in vitro cultures of mouse testicular teratoma. *Journal of the National Cancer Institute*, 44 (5), pp.1015-1036.

Kaji, K. et al., 2009. Virus-free induction of pluripotency and subsequent excision of reprogramming factors. *Nature*, 458(7239), pp.771–775.

Kelly, C.M., Dunnett, S.B., Rosser, A.E., 2009. Medium spiny neurons for transplantation in Huntington's disease. *Biochem Soc Trans,* 37(pt 1), pp.323–328.

Kim, J.B. et al., 2008. Pluripotent stem cells induced from adult neural stem cells by reprogramming with two factors. *Nature*, 454, (7204), pp.646-650.

Kim, D. et al., 2009. Generation of human induced pluripotent stem cells by direct delivery of reprogramming proteins. *Cell stem cell*, 4(6), pp.472–476.

Kim, J.B., Greber, B. et al., 2009. Direct reprogramming of human neural stem cells by OCT4. *Nature*, 461(7264), pp.649–653.

Kim, J.B., Sebastiano, V. et al., 2009. Oct4-induced pluripotency in adult neural stem cells. *Cell*, 136(3), pp.411–419.

Kim, J.B. et al., 2009. Generation of induced pluripotent stem cells from neural stem cells. *Nat Protoc*, 4(10), pp.1464-1470.

Kim, J., Efe, J.A., Zhu, S., Talantova, M., Yuan, X., Wang, S. & Lipton, S.A., 2011. Direct reprogramming of mouse fi broblasts to neural progenitors. , pp.1–6.

Kim, J., Efe, J.A., Zhu, S., Talantova, M., Yuan, X., Wang, S., Lipton, S.A. et al., 2011. Direct reprogramming of mouse fibroblasts to neural progenitors. *Proceedings of the National Academy of Sciences of the United States of America*, 108(19), pp.7838–7843.

Kirkeby, A., Kirkeby, S., Grealish, D.A., Wolf, J., Nelander, J., Wood, M., Lundblad, O., Lindvall, M., Parmar, et al., 2012. Generation of Regionally Specified Neural Progenitors and Functional Neurons from Human Embryonic Stem Cells under Defined Conditions Cell. *Reprogram*, 1, pp.703–714.

Kleinsmith, L.J., Pierce Jr., G.B., 1964. Multipotentiality of single embryonal carcinoma cells. *Cancer Res*., 24, pp.1544–1551.

Klincumhom, N., Pirity, M.K., Berzsenyi, S. et al., 2012. Generation of neuronal progenitor cells and neurons from mouse sleeping beauty transposon-generated induced pluripotent stem cells. *Cell Reprogram*, 14, pp.390–397.

Knoepfler, P.S., Zhang, X.Y., Cheng, P.F., Gafken, P.R., McMahon, S.B., Eisenman R.N., 2006. Myc influences global chromatin structure. *EMBO J*, 25, pp.2723-2734.

Koch, P. et al., 2009. A rosette-type, self-renewing human ES cell-derived neural stem cell with potential for in vitro instruction and synaptic integration. *Proceedings of the National Academy of Sciences of the United States of America*, 106(9), pp.3225–3230.

Koehler, K.R. et al., 2012. Extended passaging increases the efficiency of neural differentiation from induced pluripotent stem cells. *BMC Neurosci*, 12, pp.82.

Kohtz, J.D., Baker, D.P., Corte, G., Fishell, G., 1998. Regionalization within the mammalian telencephalon is mediated by changes in responsiveness to Sonic Hedgehog. *Development*, 125, pp.5079-5089.

Kriks, S., Shim, J.W., Piao, J., Ganat, Y.M., Wakeman, D.R., Xie, Z., Carrillo-Reid, L., Auyeung, G., Antonacci, C., Buch, A. et al., 2011. Dopamine neurons derivedfrom human ES cells efficiently engraft inanimal modelsof Parkinson's disease. *Nature*, 480, pp.547–551.

Kunath, T. et al., 2007. FGF stimulation of the Erk1/2 signalling cascade triggers transition of pluripotent embryonic stem cells from self-renewal to lineage commitment. *Development*, 134, pp.2895-2902.

Labosky, P.A. et al., 1994. Mouse embryonic germ (EG) cell lines: transmission through the germline and differences in the methylation imprint of insulin-like growth factor 2 receptor (Igf2r) gene compared with embryonic stem (ES) cell lines. *Development*, 120, pp. 3197-3204.

Lafevre-Bernt, M., Wu, S., Lin, X., 2008. Recombinant, refolded tetrameric p53 and gonadotropin-releasing hormone-p53 slow proliferation and induce apoptosis in p53-deficient cancer cells. *Mol Cancer Ther*., 7(6), pp.1420-1429.

Lai, W.H., Ho, J.C., Lee, Y.K., Ng, K.M., Au, K.W., Chan, Y.C., Lau, C.P., Tse, H.F., Siu, C.W., 2010. ROCK inhibition facilitates the generation of human-induced pluripotent stem cells in a defined, feeder-, and serum-free system. *Cell Reprogram*, 12, pp.641–653.

Lamb, R.A., Kolakofsky, D., 1996. Paramyxoviridae: The viruses and their replication. Fields Virology, eds Fields BN, Knipe DM, Howley PM (Lippincott- Raven, Philadelphia). *3rd Ed*, pp.1177-1204.

Lang, K.J.D. et al., 2004. Differentiation of embryonic stem cells to a neural fate: a route to re-building the nervous system? *Journal of neuroscience research*, 76(2), pp.184–192.

Li, M. et al., 1998. Generation of purified neural precursors from embryonic stem cells by lineage selection. *Current Biology*, 8(17), pp.971–S2.

Li, H.-O., Zhu, Y.-F., Asakawa, M., Kuma, H., Hirata, T., Ueda, Y. et al., 2000. A cytoplasmic RNA vector derived from nontransmissible Sendai virus with efficient gene transfer and expression. *J. Virol*., 74, pp.6564-9569.

Li, S.-H. and Li, X.-J., 2004. Huntingtin-protein interactions and the pathogenesis of Huntington's disease. *Trends in Genetics*, 20(3), pp.146-154.

Li, W. and Ding, S., Small molecules that modulate embryonic stem cell fate and somatic cell reprogramming. *Trends Pharmacol Sci*, 31(1), pp.36-45.

Li, X.J., Hu, B.Y., Jones, S.A., Zhang, Y.S., Lavaute, T., Du, Z.W., and Zhang, S.C., 2008. Directed differentiation of ventral spinal progenitors and motor neurons from human embryonic stem cells by small molecules. *Stem Cells*, 26, pp.886-893.

Li, X. et al., 2009. ROCK inhibitor improves survival of cryopreserved serum/feeder-free single human embryonic stem cells. *Human reproduction (Oxford, England)*, 24(3), pp.580–589.

Li, X.-J. et al., 2009. Coordination of sonic hedgehog and Wnt signaling determines ventral and dorsal telencephalic neuron types from human embryonic stem cells. *Development (Cambridge, England)*, 136(23), pp.4055–4063.

Li, H., Wijekoon, A. & Leipzig, N.D., 2012. 3D differentiation of neural stem cells in macroporous photopolymerizable hydrogel scaffolds. *PloS one*, 7(11), p.e48824.

Lim, D.A. et al., 2000. Noggin antagonizes BMP signalling to create a niche for adult neurogenesis. *Neuron*, 28(3), pp.713-726. [PubMed: 11163261]

Lister, R., Pelizzola, M., Kida, Y.S., Hawkins, R.D., Nery, J.R., Hon, G., Antosiewicz-Bourget J., O'Malley, R., Castanon, R., Klugman, S., Downes, M., Yu, R., Stewart, R., Ren, B., Thomson, J.A., Evans, R.M. and Ecker, J.R., 2011. Hotspots of aberrant epigenomic reprogramming in human induced pluripotent stem cells. *Nature*, 471(7336), pp.68-73.

Liu, X. et al., 2008. Yamanaka factors critically regulate the developmental signaling network in mouse embryonic stem cells. *Cell Res* 18(12), pp.1177-1189.

Liu, Y. and Labosky, P.A., 2008. Regulation of embryonic stem cell self-renewal and pluripotency by Foxd3. *Stem Cells*, 26(10), pp.2475-2484.

Liu, H. and Zhang, S.C., 2011. Specification of neuronal and glial subtypes from human pluripotent stem cells. *Cell. Mol. Life Sci.* 68, pp.3995-4008.

Löhle, M. et al., 2012. Differentiation efficiency of induced pluripotent stem cells depends on the number of reprogramming factors. *Stem cells (Dayton, Ohio)*, 30(3), pp.570–579.

Louvi, A. and S. Artavanis-Tsakonas., 2006. Notch signalling in vertebrate neural development. *Nat Rev Neurosci* 7, pp.93-102.

Lowry, W. E. et al., 2008. Generation of human induced pluripotent stem cells from dermal fibroblasts. *Proc Natl Acad Sci U S A*., 105(8), pp.2883-2888.

Lu, J., Liu, H., Huang, C.T.-L., Chen, H., Du, Z., Liu, Y., Sherafat, M.A., Zhang, S.-C., 2013. Generation of integration-free and region-specific neural progenitors from primate fibroblasts. *Cell reports*.

Lupo, G., Harris, W.A., Lewia, K.E., 2006. Mechanisms of ventral patterning in the vertebrate nervous system. *Nat Rev Neurosci*, 7, pp.103-114.

Ma, L., Baoyang, H., Liu, Y., Vermilyea, S.C., Liu, H., Gao, L., Sun, Y., Zhang, X. and Zhang, S.C., 2012. Human Embryonic Stem Cell-Derived GABA Neurons Correct Locomotion Deficits in Quinolinic Acid-Lesioned Mice. *Cell Stem Cell,* 10, pp.455-464.

Ma, H., Morey, R., O'Neil, R.C., He, Y., Daughtry, B., Schultz, M.D., Hariharan, M., Nery, J.R., Castanon, R., Sabatini, K., 2014. Abnormalities in human pluripotent cells due to reprogramming mechanisms. *Nature*, 511, pp.177-183.

Maherali, N., 2007. Directly reprogrammed fibroblasts show global epigenetic remodeling and widespread tissue contribution. *Cell Stem Cell,* 1, pp.55-70.

Manuel, M., Martynoga, B., Yu, T., West, J.D., Mason, J.O. and Price, D.J., 2010. The transcription factor Foxg1 regulates the competence of telencephalic cells to adopt subpallial fates in mice. Development, 137(3), pp.487-497.

Marchetto, M.C., Yeo, G.W., Kainohana, O., Marsala, M., Gage, F.H., Muotri, A.R., 2009. Transcriptional signature and memory retention of human-induced pluripotent stem cells. *PLoS ONE*, 4, pp.e7076.

Marklund, M., Sjodal, M., Beehler, B.C., Jessell, T.M., Edlund, T. and Gunhaga, L., 2004. Retinoic acid signaling specifies intermediate character in the developing telencephalon. *Development*, 131(17), pp.4323-4332.

Martin, G.R., 1981. Isolation of a pluripotent cell line from early mouse embryos cultured in medium conditioned by teratocarcinoma stem cells. *Proc. Natl. Acad. Sci. USA*, 78, pp.7634-7638.

Martinez-Fernandez, A., Nelson, T.J. & Terzic, A., 2011. Nuclear reprogramming strategy modulates differentiation potential of induced pluripotent stem cells. *Journal of cardiovascular translational research*, 4(2), pp.131–137.

Masaki, I., Yonemitsu, Y., Komori, K., Ueno, H., Nakashima, Y., Nakagawa, K. et al., 2001. Recombinant Sendai virus-mediated gene transfer to vaculature: a new class of efficient gene transfer vector to the vascular system. *FASEB J*., 15, pp.1294-1296.

Matsui, Y., Zsebo, K. and Hogan, B.L.M., 1992. Derivation of pluripotential embryonic stem cells from murine primordial germ cells in culture. *Cell*, 70, pp.841-847.

Meissner, A. et al., 2007. Direct reprogramming of genetically unmodified fibroblasts into pluripotent stem cells. *Nat Biotech* 25(10), pp.1177-1181.

Mikkelsen, T.S., Ku, M., Jaffe, D.B., Issac, B., Lieberman, E., Giannoukos, G., Alvarez, P., Brockman, W., Kim, T.K.,Koche, R.P., et al., 2007. Genome-wide maps of chromatin state in pluripotent and lineage-committed cells. *Nature*, 448, pp.553-560.

Mikkelsen, T.S. et al., 2008. Dissecting direct reprogramming through integrative genomic analysis. *Nature*, 454(7200), pp.49-55.

Miller, R.A., Ruddle, F.H., 1976. Pluripotent teratocarcinoma-thymus somatic cell hybrids. *Cell*, 9, pp.45-55.

Mitsui, K., 2003. The homeoprotein Nanog is required for maintenance of pluripotency in mouse epiblast and ES cells. *Cell*, 113, pp.631-642.

Miura, K. et al., 2009. Variation in the safety of induced pluripotent stem cell lines. *Nat Biotechnol*, 27(8), pp.743-745.

Muenthaisong, S. et al., 2012. Generation of mouse induced pluripotent stem cells from different genetic backgrounds using Sleeping beauty transposon mediated gene transfer. *Experimental cell research*, 318(19), pp.2482–2489.

Nagy, K., Sung, H.K., Zhang, P., Laflamme, S., Vincent, P., Agha-Mohammadi, S., Woltjen, K., Monetti, C., Michael, I.P., Smith, L.C., and Nagy, A., 2011. Induced pluripotent stem cell lines divered from equine fibroblasts. *Stem cell Rev*. 7, pp.693-702.

Nakagawa, M. et al., 2008. Generation of induced pluripotent stem cells without Myc from mouse and human fibroblasts. *Nat Biotechnol*, 26(1), pp.101-106.

Nakatake, Y., Fukui, N., Iwamatsu, Y., Masui, S., Takahashi, K., Yagi, R., Yagi, K., Miyazaki, J., Matoba, R., Ko, M.S. et al., 2006. Klf4 cooperates with Oct3/4 and Sox2 to activate the Lefty1 core promoter in embryonic stem cells. *Mol Cell Biol*, 26, pp.7772-7782.

Narsinh, K.H., Sun, N., Sanchez-Freire, V., Lee, A.S., Almeida, P., Hu, S. et al., 2011. Single cell transcriptional profiling reveals heterogeneity of human induced pluripotent stem cells. J Clin Invest; e-pub ahead of print 7 February 2011

Nasonkin, I. et al., 2009. Long-term, stable differentiation of human embryonic stem cell-derived neural precursors grafted into the adult mammalian neostriatum. *Stem cells (Dayton, Ohio)*, 27(10), pp.2414–2426.
Ng, R.K. and Gurdon, J.B., 2005. Epigenetic memory of active gene transcription is inherited through somatic cell nuclear transfer. *Proc. Natl. Acad. Sci. USA*., 102, pp.1957-1962.

Ng, R.K. and Gurdon, J.B., 2008. Epigenetic memory of an active gene state depends on histone H3.3 incorporation into chromatin in the absence of transcription. *Nat. Cell Biol*., 10, pp.102-109.

Niwa, H., 2007. How is pluripotency determined and maintained? *Development*, 134, pp.635-646.

Niwa, H., 2011. Wnt: what's needed to maintain pluripotency? *Nat Cell Biol*, 13, pp.1024-1026.

Ohi, Y., Qin, H., Hong, C. et al., 2011. Incomplete DNA methylation underlies a transcriptional memory of somatic cells in human iPS cells. *Nat Cell Biol*, 13, pp.541-549.

Okabe, S. et al., 1996. Development of neuronal precursor cells and functional postmitotic neurons from embryonic stem cells in vitro. *Mechanisms of Development*, 59(1), pp.89–102.

Okita, K. et al. Generation of mouse-induced pluripotent stem cells with plasmid vectors. *Nat. Protocols*, 5(3), pp.418-428.

Okita, K. et al., 2007. Generation of germline-competent induced pluripotent stem cells. *Nature*, 448(7151), pp.313-317.

Okita, K., Nakagawa, M., Hyenjong, H., Ichisaka, T. & Yamanaka, S., 2008. Generation of mouse induced pluripotent stem cells without viral vectors. *Science*, 322, pp.949-953.

Olsson, M., Bjorklund, A., Campbell, K., 1998. Early specification of striatal projection neurons and interneuronal subtypes in the lateral and medial ganglionic eminence. *Neuroscience*, 84, pp.867-876.

O' Rahilly, R. and Muller, F., 1999. The Embryonic Human Brain. An Atlas of Development Stages, Wiely-Liss, New York, NY, USA.

Ortinau, S. et al., 2010. Effect of 3D-scaffold formation on differentiation and survival in human neural progenitor cells. *Biomedical engineering online*, 9(1), p.70.

Ouimet, C.C., Langley-Gullion, K.C., Greengard, P., 1998. Quantitative immunocytochemistry of DARPP-32-expressing neurons in the rat caudaltoputamen. *Brain Res*., 808, pp.8-12.

Pankratz, M.T. et al., 2007. Directed neural differentiation of human embryonic stem cells via an obligated primitive anterior stage. *Stem cells (Dayton, Ohio)*, 25(6), pp.1511–1520.

Park, I.H., Zhao, R., West, J.A., Yabuuchi, A., Huo, H., Ince, T.A., Lerou, P.H., Lensch, M.W., Daley, G.Q., 2007. Reprogramming of human somatic cells to pluripotency with defined factors. *Nature*, 451, pp.141-146.

Park, I.H. et al., 2008. Reprogramming of human somatic cells to pluripotency with defined factors. *Nature*, 451(7175), pp.141-U141.

Pauly, M.C., Dobrossy, M.D., Nikkhah, G., Winkler, C., and Piroth, T., 2014. Organization of the human fetal subpallium. *Front. Neuroanat,* 7, p.54.

Perucho, J., Casarejos, M.J., Gómez, A., Ruíz, C., Fernández-Estevez, M.Á., Muñoz, M.P., de Yébenes, J.G., Mena, M.Á., eCollection, 2013. Striatal infusion of glial conditioned medium diminishes huntingtin pathology in r6/1 mice. 12, 8(9), e73120.

Polkinghorne, J., London: Her Majesty's Stationary Office, 1989. Review of the Guidance on the Research Use of Fetuses and Fetal Material.

Potter, W., Kalil, R. E., Kao, W. J., 2008. Biomimetic material systems for neural progenitor cell-based therapy. Front. Biosci., 13, pp.806–821.

Puelles, L., Kuwana, E., Puelles, E., Bulfone, A., Shimamura, K., Keleher, J., Smiga, S., and Rubenstein, J.L., 2000. Pallial and subpallial derivatives in the embryonic chick and mouse telencephalon, traced by the expression of the genes Dix-2, Emx-1, Nkx-2.1, Pax-6, and Tbr-1. J. Comp. *Neurol*. 424, pp.409-438.

Resnick, J.L., Bixler, L.S., Cheng, L. and Donovan, P.J., 1992. Long-term proliferation of mouse primordial germ cells in culture. *Nature*, 359, pp.550-551.

Rhee, Y.H., Ko, J.Y., Chang, M.Y., Yi, S.H., Kim, D. et al., 2011. Protein-based human iPS cells efficiently generate functional dopamine neurons and can treat a rat model of Parkinson disease. *J Clin Invest*, 121, pp.2326–2335.

Rizzi, R., Di Pasquale, E., Portararo, P., Papait, R., Cattaneo, P., et al., 2012. Post-natal cardiomyocytes can generate iPS cells with an enhanced capacity toward cardiomyogenic re-differentation. *Cell Death Differ*.

Rosser, A.E., Barker, R.A., Harrower, T. et al., 2002. Unilateral transplantation of human primary fetal tissue in four patients with Huntington's disease: NEST-UK safety report ISRCTN no 36485475. *J Neuol Neurosurg Psychiatry*, 73, pp.678-685.

Rosser, A. E. and Svendsen, C. N., 2014. Stem cells for cell replacement therapy: A therapeutic strategy for HD?. *Movement Disorders*, 29(11), pp.1446-1454.

Rowland, J.W., Lee, J.J., Salewski, R.P., Eftekharpour, E., van der Kooy, D. and Fehlings, M.G., 2011. Generation of neural stem cells from embryonic stem cells using the default mechanism: in vivo and in vivo characterization. *Stem Cells Dev*. 20, pp.1829-1845.

Roy, N.S., Cleren, C., Singh, S.K., Yang, L., Beal, M.F., and Goldman, S.A., 2006. Functional engraftment of human ES cell-derived dopaminergic neurons enriched by coculture with telomerase-immortalized midbrain astrocytes. *Nat. Med*., 12, pp.1259-1268.

Roy, S., Gascard, P., Dumont, N., Zhao, J., Pan, D., Petrie, S., Margeta, M., Tlsty, T.D., 2013. Rare somatic cells from human breast tissue exhibit extensive lineage plasticity. *Proc Natl Acad Sci USA.*, 110, pp.4598-4603.

Rubenstein, J.L.R., Shimamura, K., Martinez, S. and Pulles, L., 1998. Regionalization of the prosencephalic neural plate. *Annual Review of Neuroscience,* 21, pp.445-477.

Ruiz, C., Casarejos. M.J., Gomez,A., Solano, R., de Yebenes, J.G. et al., 2012. Protection by glia-conditioned medium in a cell model of Huntington disease. *PLoS Curr*, 4, e4fbca54a2028b.

S. Chambers, C. Fasano, E. Papapetrou, M. Tomishima, M. Sadelain, L. Studer. Highly efficient neural conversion of human ES and iPS cells by dual inhibition of Smad signaling. Nat Biotechnol, 27 (2009), pp. 275–280

S.B. Dunnett, A. Björklund (Eds.), 1992. Neural Transplantation: A Practical Approach, IRL Press, Oxford, pp.1–19.

Salewski, R.P. et al., 2013. The generation of definitive neural stem cells from PiggyBac transposon-induced pluripotent stem cells can be enhanced by induction of the NOTCH signaling pathway. *Stem Cells Dev*, 22, pp.383–396.

Schneider, R.A., Hu, D., Rubenstein, J.L.R., Maden, M. and Helms, J.A., 2001. Local retinoid signaling coordinates forebrain and facial morphogenesis by maintaining FGF8 and SHH. *Development*, 128(14), pp.2755-2767.

Schulz, T.C., Palmarini, G.M., Noggle, S.A. et al., 2003. Directed neuronals differentiation of human embryonic stem cells. *BMC Neurosci*, 4, p.27.

Schwartz, P.H. et al., 2008. Differentiation of neural lineage cells from human pluripotent stem cells. *Methods (San Diego, Calif.)*, 45(2), pp.142–158.

Schwartz, S.C. and Schwarz, J. 2010. Translation of stem cell therapy for neurological diseases. *Transl. Res.* 156, pp.155-160.

Seki, T. et al., 2010. Generation of induced pluripotent stem cells from human terminally differentiated circulating T cells. *Cell Stem Cell* 7, pp.11-14.

Seminatore, C. et al., 2010. The postischemic environment differentially impacts teratoma or tumor formation after transplantation of human embryonic stem cell-derived neural progenitors. *Stroke*, 41(1), pp.153–159.

Shamblott, M.J., Axelman, J., Wang, S., Bugg, E.M., Littlefield, J.W., Donovan, P.J., Blumenthal, P.D., Huggins, G.R., Gearhart, J.D., 1998. Derivation of pluripotent stem cells from cultured human primordial germ cells. *Proceedings of the National Academy of Sciences of the United States of America*, 95 (23), pp.13726-13731.

Shi, Y., Kirwan, P., Smith, J., Robinson, H. P., & Livesey, F.J., 2012. Human cerebral cortex development from pluripotent stem cells to functional excitatory synapses. *Nature Neuroscience*, 15(S1), pp.477-486.

Shin, K., Lee, J., Guo, N., Kim, J., Lim, A., Qu, L., Mysorekar I.U., Beachy, P.A., 2011. Hedgehog/Wnt feedback supports regenerative proliferation of epithelial stem cells in bladder. *Nature*., Apr 7,472(7341), pp.110-114.

Si-Tayeb, K. et al., 2010. Generation of human induced pluripotent stem cells by simple transient transfection of plasmid DNA encoding reprogramming factors. *BMC developmental biology*, 10, p.81.

S.K. Mak, Y.A. Huang, S. Iranmanesh, M. Vangipuram, R. Sundararajan, L. Nguyen, J.W. Langston and B. Schule, 2012. Small molecules greatly improve conversion of human-induced pluripotent stem cells to the neuronal lineage. *Stem Cells Int*., 140427.

Smith, A.G., Health, J.K., Donaldson, D.D., Wong, G.G., Moreau, J., Stahl, M., and Rogers, D., 1988. Inhibition of pluripotential embryonic stem cell differentiation by purified polypeptides. *Nature*, 336, pp.688-690.

Smith-Fernandez, A., Pieau, C., Reperant, J., Boncinelli, E., Wassef, M., 1998. Expression of the Emx-1 and Dlx-1 homeobox genes define three molecularly distinct domains in the telencephalon of mouse, chick, turtle and frog embryos: implications for the evolution of telencephalic subdivisions in amniotes. *Development*, 125, pp.2099–2111.

Smith, K.P. et al., 2009. Pluripotency: toward a gold standard for human ES and iPS cells. *J Cell Physiol*, 220(1), pp.21-29.

Soldner, F. et al., 2009. Parkinson's disease patient-derived induced pluripotent stem cells free of viral reprogramming factors. *Cell*, 136, pp.964-977.

Sommer, C.A. et al., 2008. iPS cell generation using a single lentiviral stem cell cassette. *Stem Cells doi*, 10.1634/*stemcells*, pp.2008-1075.

Sommer, C.A. et al., 2009. Excision of Reprogramming Transgenes Improves the Differentiation Potential of iPS Cells Generated with a Single Excisable Vector. *Stem Cells*.

Sommer, C. a & Mostoslavsky, G., 2010. Experimental approaches for the generation of induced pluripotent stem cells. *Stem cell research & therapy*, 1(3), p.26.

Song, J. et al., 2007a. Human embryonic stem cell-derived neural precursor transplants attenuate apomorphine-induced rotational behavior in rats with unilateral quinolinic acid lesions. *Neuroscience Letters*, 423(1), pp.58–61.

Solter, D., Skreb, N., Damjanov, I., 1970. Extrauterine growth of mouse egg-cylinders results in malignant teratoma. *Nature*, 227, pp.503–504.

Solter, D., Knowles, B.B., 1978. Monoclonal antibody defining a stage-specific mouse embryonic antigen (SSEA-1) Proc. *Natl. Acad. Sci*., 75, pp.5565–5569.

Stadtfeld, M., Nagaya, M., Utikal, J., Weir, G. & Hochedlinger, K., 2008. Induced pluripotent stem cells generated without viral integration. *Science*, 322, pp.954-949.

Staerk, J., Dawlaty, M.M., Gao, Q., Maetzel, D., Hanna, J., Sommer, C.A., Mostoslavsky, G., Jaenisch, R., 2010. Reprogramming of human peripheral blood cells to induced pluripotent stem cells. *Cell Stem Cell*, 7, pp.20-24.

Stenman, J., Toresson, H., Campbell, K., 2003. Identification of two distinct progenitor populations in the lateral ganglionic eminence: implications for striatal and olfactory bulb neurogenesis. *J Neurosci*, 23(1), pp.167-174.

Stevens, L.C., 1970. The development of transplantable teratocarcinomas from intratesticular grafts of pre- and postimplantation mouse embryos Source of the Document Developmental Biology, 21(3), pp.364-382.

Stewart, C.L., Gadi, I., Bhatt, H., 1994. Stem cells from primordial germ cells can reenter the germ line. *Dev. Biol*., 161, pp.626-628.

Stoykova, A., Fritsch, R., Walther, C. and Gruss, P., 1996. Forebrain patterning defects in Small eye mutant mice. *Development*, 122, pp.3453-3465.

Tada, M., Tada, T., Lefebvre, L., Barton, S.C., Surani, M.A., 1997. Embryonic germ cells induce epigenetic reprogramming of somatic nucleus in hybrid cells. *EMBO J*.,16, pp.6510–6520.

Takahashi, K. and Yamanaka, S., 2006. Induction of pluripotent stem cells from mouse embryonic and adult fibroblast cultures by defined factors. *Cell*, 126(4), pp.663-676.

Takahashi, K. et al., 2007. Induction of pluripotent stem cells from fibroblast cultures. *Nat Protoc*, 2(12), pp.3081-3089.

Takahashi, K. et al., 2007. Induction of pluripotent stem cells from adult human fibroblasts by defined factors. *Cell* 131(5), pp.861-872.

Takeda, A., Igarashi, H., Kawada, M., Tsukamoto, T., Yamamoto, H., Inoue, M. et al., 2008. Evaluation of the immunogenicity of replication-competent V-Knocked-out and replication-defective F-deleted Sendai virus vector-based vaccines in macaques. *Vaccine*, 26, pp.6839-6843.

Takenaka, C., Nishishita, N., Takada, N., Jakt, L.M., Kawamata, S., 2010. Effective generation of iPS cells from $CD34^+$ cord blood cells by inhibition of p53. *Exp Hematol* 38, pp.154-162.

Tamura, S., Morikawa, Y., Iwanishi, H., Hisaoka, T. and Senba, E., 2004. Foxp1 gene expression in projection neurons of the mouse striatum. *Neuroscience*, 124, pp.261–267.

Taraballi, F., Natalello, A., Campione, M. et al., 2010. Glycine-spacers influence functional motifs exposure and self-assembling propensity of functionalized substrates tailored for neural stem cell cultures. *Front Neuroeng*, 3(1).

The Huntington's Disease Collaborative Research Group, 1993. A novel gene containing a trinucleotide repeat that is expanded and unstable on Huntington's disease chromosomes. *Cell*, 72, pp.971-983.

Thomson, J.A., et al., 1998. Embryonic stem cell lines derived from human blastocysts. *Science*, 282(5391), pp.1145-1147.

Thonhoff, J.R., Lou, D.I., Jordan, P.M., Zhao, X., Wu, P., 2008. Compatibility of human fetal neural stem cells with hydrogel biomaterials *in vitro. Brain Res.*, 1187, pp.42–51.

Tokusumi, T., Iida, A., Hirata, T., Kato, A., Nagai, Y. and Hasegawa, M., 2002. Recombinant Sendai viruses expressing different levels of a foreign reporter gene. *Virus Res*. 86, pp.33-38.

Tokuzawa, Y., Kaiho, E., Maruyama, M., Takahashi, K., Mitsui, K., Maeda, M., Niwa, H., Yamanaka, S., 2003. Fbx15 is a novel target of Oct3/4 but is dispensable for embryonic stem cell self-renewal and mouse development. *Mol Cell Biol*, 23, pp.2699-2708.

Toresson, H., De Urquiza, A.M., Fagerstrom, C., Perlman, T. and Campbell, K., 1999. Retinoids are produced by glia in the lateral ganglionic eminence and regulate striatal neuron differentiation. *Development,* 126(6), pp.1317-1326.

Toresson, H., Potter, S.S., Campbell, K., 2000. Genetic control of dorsal-ventral identity in the telencephalon: opposing roles for Pax6 and Gsh2. *Development*, 127, pp.4361-4371.

Turnpenny, L., Brickwood, S., Spalluto, C.M., Piper, K., Cameron, I.T., Wilson, D.I., Hanley, N.A., 2003. Derivation of Human Embryonic Germ Cells: An Alternative Source of Pluripotent Stem Cells. *Stem Cells*, 21(5), pp.598-609.

Vierbuchen, T., Ostermeier, A., Pang, Z.P., Kokubu, Y., Sudhof, T.C., Wernig, M., 2010. Direct conversion of fibroblasts to functional neurons by defined factors. *Nature*, 463(7284), pp.1035-1041.

Wang, W. et al., 2008. Chromosomal transposition of PiggyBac in mouse embryonic stem cells. *Proceedings of the National Academy of Sciences of the United States of America*, 105(27), pp.9290–9295.

Warren, L., Manos, P.D., Ahfeldt, T., Loh, Y. et al., 2010. Highly Efficient Reprogramming to Pluripotency and Directed Differentiation of Human Cells with Synthetic Modified mRNA., pp.618–630.

Watanabe, K. et al., 2005. Directed differentiation of telencephalic precursors from embryonic stem cells. *Nature neuroscience*, 8(3), pp.288–296.

Watanabe, K. et al., 2007. A ROCK inhibitor permits survival of dissociated human embryonic stem cells. *Nat Biotech*, 25(6), pp.681–686.

Waterhouse E.G., An J.J, Orefice L.L., Baydyuk M., Liao G.Y., Zheng K., et al., 2012. BDNF promotes differentiation and maturation of adult-born neurons through GABAergic transmission, *Journal of Neuroscience*, 32 (41), pp. 14318-14330

Welstead, G.G. et al., 2008. Generating iPS cells from MEFS through forced expression of Sox-2, Oct-4, c-Myc, and Klf4. *J Vis Exp*, (14), pii.734.

Welstead, G.G., Schorderet, P. & Boyer, L.A., 2008. The reprogramming language of pluripotency. *Current opinion in genetics & development*, 18(2), pp.123–129.

Wernig, M., 2007. In vitro reprogramming of fibroblasts into a pluripotent ES-cell-like state. *Nature*, 448, pp.318-324.

Wernig, M. et al., 2008. A drug-inducible transgenic system for direct reprogramming of multiple somatic cell types. *Nat Biotechnol*, 26(8), pp.916-924.

Wernig, M. et al. 2008. Neurons derived from reprogrammed fibroblasts functionally integrate into the fetal brain and improve symptoms of rats with Parkinson's disease. *Proc Natl Acad Sci U S A*., 105(15), pp. 5856-5861.

Williams, R.L., Hilton, D.J., Pease, S., Wilson, T.A., Stewart, C.L., Gearing, D.P., Wagner, E.F., Metcalf, D., Nicola, N.A., Gough, N.M., 1988. Myeloid leukaemia inhibitory factor maintains the developmental potential of embryonic stem cells. *Nature*, 336 (6200), pp.684-687.

Wilmut, I., Schnieke, A.E., McWhir, J., Kind, A.J., and Campbell, K.H.,1997. Viable offspring derived from fetal and adult mammalian cells. *Nature*, 385, pp.810-813.

Wilson, S.W. and Houar, C., 2004. Early steps in the development of the forebrain. *Development Cell*, 6(2), pp.167-181.

Wilson, M.H., Coates, C.J., George, A.L., 2007. Jr PiggyBac Transposon-mediated Gene Transfer in Human Cells. *Mol Ther*., 15, pp.139–145.

Woltjen, K. et al., 2009. piggyBac transposition reprograms fibroblasts to induced pluripotent stem cells. *Nature*, 458(7239), pp.766-770.

Yamada MK., Nakanishi K., Ohba S., Nakamura T., Ikegaya Y., Nishiyama N., Matsuki N., 2002. Brain-derived neurotrophic factor promotes the maturation of GABAergic mechanism in cultured hippocampal neurons. *J Neurosci*, 22, pp.7580-7585

Yonemitsu, Y., Kitson, C., Ferrari, S., Farley, R., Griesenbach, U., Judd, D. et al., 2000. Efficient gene transfer to airway epithelium using recombinant Sendai virus. *Nat. Biotechnol,* 18, pp.970-973.

Yoon, K. and N. Gaiano., 2005. Notch signalling in the mammalian central nervous system: insights from mouse mutants. *Nat Neurosci,* 8, pp.709-715.

Yu, J., Vodyanik, M.A., He, P., Slukvin, I.I., and Thomson, J.A., 2006. Human embryonic stem cells reprogram myeloid precursors following cell-cell fusion. *Stem Cells*, 24, pp.168-176.

Yu, J., Vodyanik, M.A., Smuga-Otto, K., Antosiewicz-Bourget, J., Frane, J.L., Tian, S., Nie, J., Jonsdottir, G.A., Ruotti, V., Stewart, R., Slukvin, I.I., Thomson, J.A. et al., 2007. Induced pluripotent stem cell lines derived from human somatic cells. *Science (New York, N.Y.)*, 318(5858), pp.1917–1920.

Yu, J., Hu, K., Smuga-Otto, K., Tian, S., Stewart, R., Slukvin, I.I., Thomson, J.A. et al., 2009. Human induced pluripotent stem cells free of vector and transgene sequences. *Science (New York, N.Y.)*, 324(5928), pp.797–801.

Yun, K., Potter, S. and Rubenstein J.L.R., 2001. Gsh2 and Pax6 play complementary roles in dorsoventral patterning of the mammalian telencephalon. *Development*, 128(2), pp.193-205.

Yusa, K. et al., 2009b. Generation of transgene-free induced pluripotent mouse stem cells by the piggyBac transposon. *Nature methods*, 6(5), pp.363–369.

Zhang, S.C. et al., 2001. In vitro differentiation of transplantable neural precursors from human embryonic stem cells. *Nature biotechnology*, 19(12), pp.1129–1133.

Zhang, S.C., 2006. Neural subtype specification from embryonic stem cells. *Brain Pathol*, 16, pp.132–142.

Zhang, S.-C. et al., 2008. Human embryonic stem cells for brain repair? *Philosophical transactions of the Royal Society of London. Series B, Biological sciences*, 363(1489), pp.87–99.

Zhang, J., Lian, Q., Zhu, G. et al., 2010. A Human iPSC model of Hutchinson Gilford progeria reveals vascular smooth muscle and mesenchymal stem cell defects. *Cell Stem Cell*.

Zhang, N., An, M.C., Montoro, D. and Ellerby, L.M., 2010. Characterization of human Huntington's disease cell model from induced pluripotent stem cells. *PLoS Curr 2*, RRN1193.

Zhao, T. et al., 2011. Immunogenicity of induced pluripotent stem cells. *Nature*, 474(7350), pp.212–215.

Zhong, J., Chan, A., Morad, L., Kornblum, H.I., Guoping, Fan Carmichael, S.T., Hydrogel, 2010. Matrix to Support Stem Cell Survival After Brain Transplantation in Stroke. *Neurorehabil Neural Repair*, 24, pp.636–644.

Zhou, H., Wu, S., Joo, J.Y., Zhu, S., Han, D.W., Lin, T., Trauger, S., Bien, G., Yao, S., Zhu, Y. et al., 2009. Generation of induced pluripotent stem cells using recombinant proteins. *Cell Stem Cell*, 4, pp.381-384.

Zhou, W., Freed C.R., 2009. Adenoviral gene delivery can reprogram human fibroblasts to induced pluripotent stem cells. *Stem cells (Dayton, Ohio)*, 27(11), pp.2667-2674.

Zhou, J., Su, P., Li, D., Tsang, S., Duan, E. and Wang, F., 2010. High-efficiency induction of neural conversion in human ESCs and human induced pluripotent stem cells with a sigle chemical inhibitor of transforming growth factor beta superfamily receptors. *Stem Cells*, 28, pp.1741-1750.

Zhou, T. et al., 2011. Generation of induced pluripotent stem cells from urine. *Journal of the American Society of Nephrology : JASN*, 22(7), pp.1221–1228.

Ziegler, A., Nervi, P., Durrenberger, M., Seelig, J., 2005. The cationic cell-penetrating peptide CPP(TAT) derived from the HIV-1 protein TAT is rapidly transported into living fibroblasts: optical, biophysical, and metabolic evidence. *Biochemistry*, 44, pp.138–148.

Zietlow, R., Precious, S.V., Kelly, C.M., Dunnett S.B., Rosser, A.E., 2012. Long-term expansion of human foetal neural progenitors leads to reduced graft viability in the neonatal rat brain. *Exp Neurol*., 235(2), pp.563-573.

Appendix A

Human ES cell (H9) derived MSN-like cells mono-layer based method.

Neural induction Monolayer-Based Method.

(this is ongoing work that was incomplete at the time of submission of this thesis but is relevant for consideration and discussion)

Human ES/iPS cells at 70-80% confluency were passaged as cell clumps and redistributed from 1 well of a 6 well-plate in 1:3 ratio (~20-25% each well) into Geltrax® matrix (Life Technologies®) coated 6 well-plate and cultured in ES/iPS medium. The day after, medium was changed to neural induction medium (NI medium, Gibco®, Paisley, Scotland, UK). Full medium changes were performed every other day for 7 days until the cells reached 80-90% confluence. Cells were passaged (passage 1) as a single cell suspension by incubating with 1 ml Accutase® for 5-7 minutes. NI medium 9 ml was added; cells were passed through the cell strainer and centrifuged at 86.64 g for 3 minutes. Cells were cultured in NI medium and adhered onto Geltrax® coated tissue culture dish at 2.5-3.0x10^5 cells/well of 6-well plate. Between days 10-14, cells were dissociated again (passage 2) (using the previously described method). Cells were passaged again (passage 3) between days 16-22, when they were plated onto PLL-POL-Laminin pre-treated tissue culture plates/coverslips in neural expansion medium (1:1 ration NI medium and Advanced™ DMEM/F12). From this stage cells were be able to be expanded and banked as NPCs. (Figure 1)

Neural induction was as per shown in Figure 1 below (lower panel). The cells were exposed to SB431542, dorsomorphin and noggin from days 16-22 DIV as well as SHH, DKK1 and Activin A from day 16 to 26 DIV. From day 28 as well as Activin A, GDNF, BDNF, ascorbic acid and VPA were also added to the culture for maturation of the neural precurosor population.

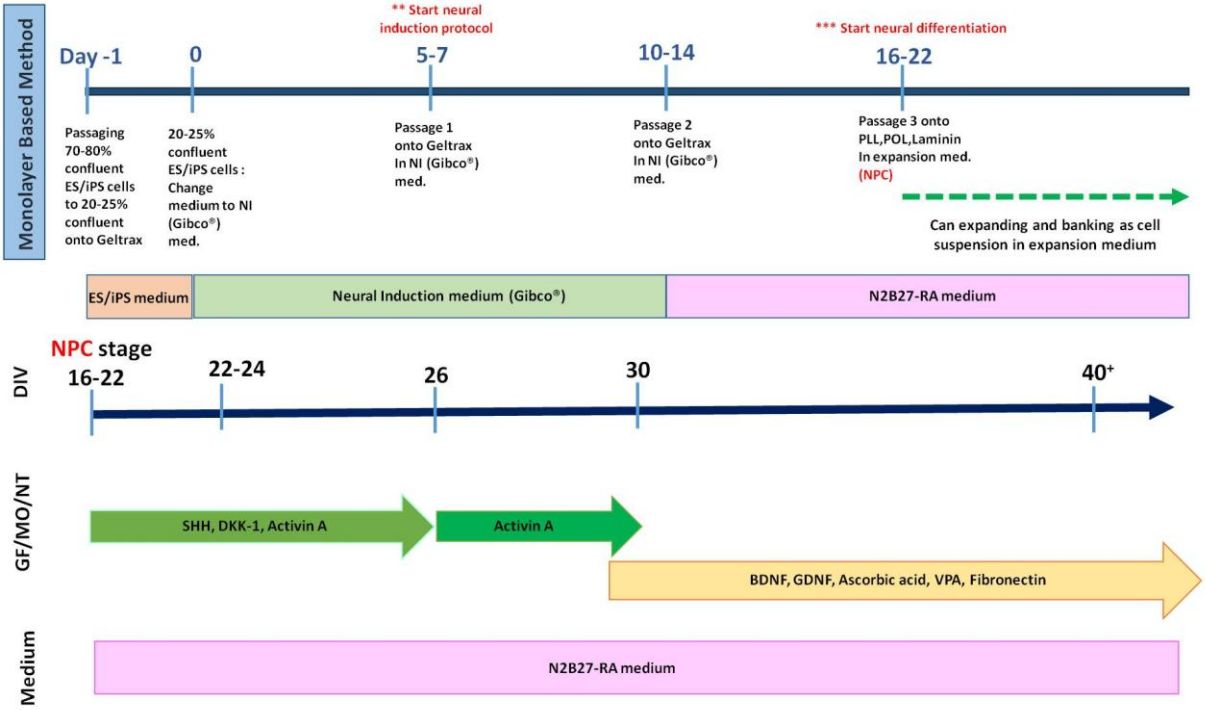

Figure 1. Schematic of the time line for neural induction and neuronal differentiation from PSCs using Monolayer-Based method (as described above).

In vitro differentiation to MSN-like cells.

7 days after passage 2, neural induction medium was changed to N2B27 medium with supplementation with the chemical combinations as described above. Cells started to form 2D rosette structures (Figure 1 A). Later on in culture, cells transformed to neural like morphology with short and fine processes (Figure 1 B). Cells progressively obtained a neuronal morphology with small and tight cell bodies, thickening and long neurites (day 28, Figure 1 C). Gial cells were identified in prolonged culture around day 28 as a carpet underlying the neuronal layer (Figure 1 D). There was an absence of other non-neural cell phenotypes or pluripotent like cells.

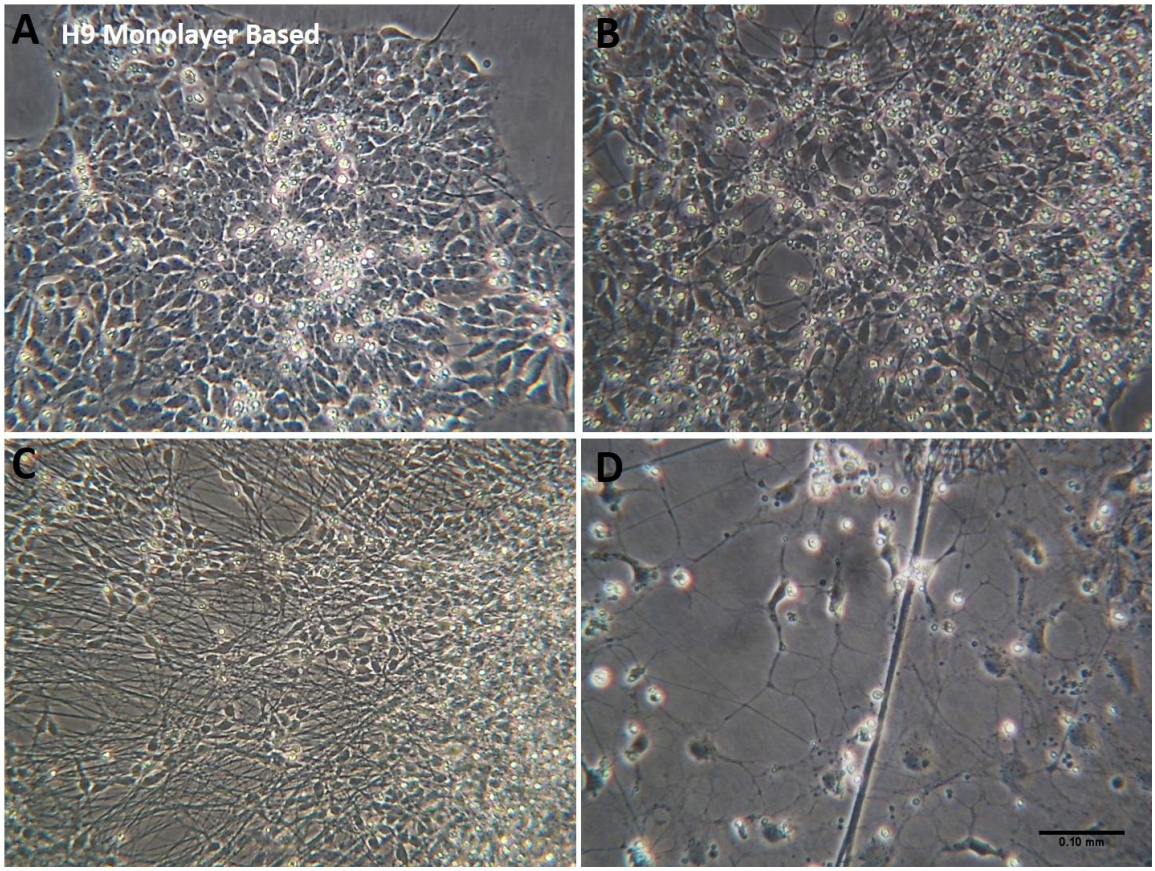

Figure 2. Phase contrast micrographs of human ES (H9) derived MSN like cells using monolayer-based method. Neural rosette structures were identified 3 day after changing to N2B27 medium (A). After passage 3, cultured with N2B27 and a combination of small molecules, morphogens, and growth factors designed to encourage differentiation to an LGE progenitor phenotype, cells gradually changed their morphology to resemble neuronal cells with short and fine processes (B). The cells' maturated appearance was similar to neurons with small and tight cell bodies; thick and long connecting neurites were identified (C). Glia cells emerged later, forming a carpet underneath the neuronal cells (D). Scale bar = 0.10 mm.

In vitro Analysis of H9 derived MSN-like cells.

Immunocytochemistry was performed at different time point during *in vitro* differentiation followed the previous study in Chapter 5. Neural precursors were identified with Nestin (Figure 3 A) around day 7 after passage 2 (Figure 1). At a later time in culture, cells with long processes were identified by more the neuronal marker of β-III tubulin and post mitotic neuronal marker, Map2 (Figure 3 B and C). LGE progenitors were identified by the hall mark markers such as FoxP1 and FoxP2, co-expressed with the less mature MSNs marker Ctip2 (Figure 3 D and E). GFAP positive glial cells emerged at later time in culture (Figure 3 F). Around 28-32 DIV, DARPP32 positive cells were recognized as groups of cells co-localizing with Ctip2 (Figure 3 G and insert, H). The postsynaptic NMDA receptor PSD-95 was also recognized from around day 30 onwards (Figure 3 I).

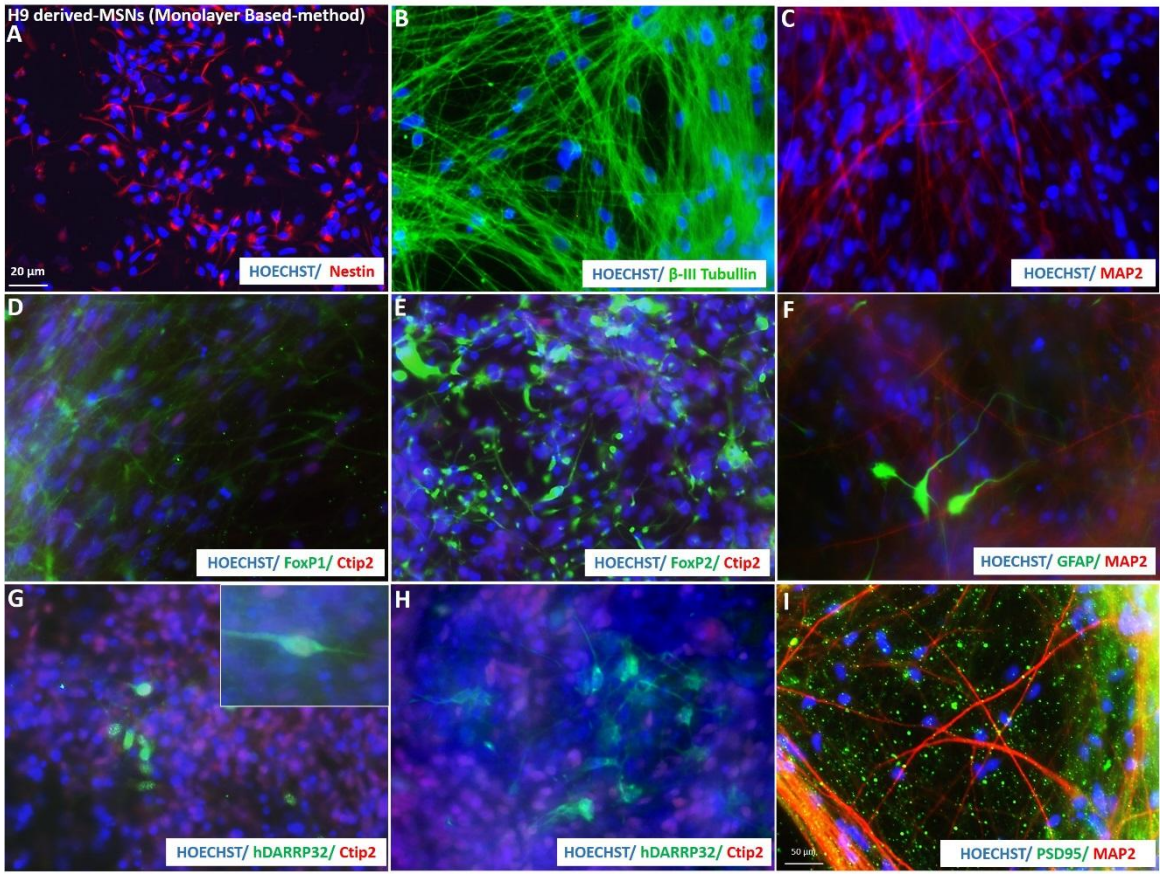

Figure 3. Immunocytofluorescence micrographs of the phenotypic characterization of striatal progenitors and neurons generated from human ES (H9) cells using a monolayer-based method. Neural maturation is indicated by the neural progenitor marker, Nestin (A) through to a more mature neuron marker, β-III Tubullin (B), and post mitotic neurons Map2 (C). FoxP1 and FoxP2 were present throughout differentiation (D, E), whereas Ctip 2 appeared around day 20-25 with increasing expression over time in culture (D, E, G). From 30 DIV, DARPP32 with Ctip2 co-labelling were identified (G and insert, H). GFAP, representing glia cells, was identified in a prolonged culture at later time in differentiation (F). A synaptic marker PSD-95 was also recognized in this study (I).

In vivo differentiation to MSN-like cells.

Cells at 30 DIV were transplanted into the QA-lesioned rat striatum (HD model) at $5x10^5$ cells per animal. At 7 and 20 weeks post-surgery, animals were sacrificed and their brains were collected for immunohistochemistry analysis as described in Chapter 2. Graft survival was identified in all animals with expression of HuNu positive cells. No tumour formation/graft overgrowth were found in any transplanted animals (N=7). Migration of transplanted cells across the graft host border within the striatum showed integration of the grafted cells in 1 out of 7 animals (data not shown). The surviving grafts (N=7) were situated in the striatal area and are illustrated in a schematic in figure 4, A. Immunohistochemistry was performed, DARPP32 expressing cells with HuNu co-labelling confirmed *in vivo* differentiation of human ES (H9) derived MSNs (Figure 4, B).

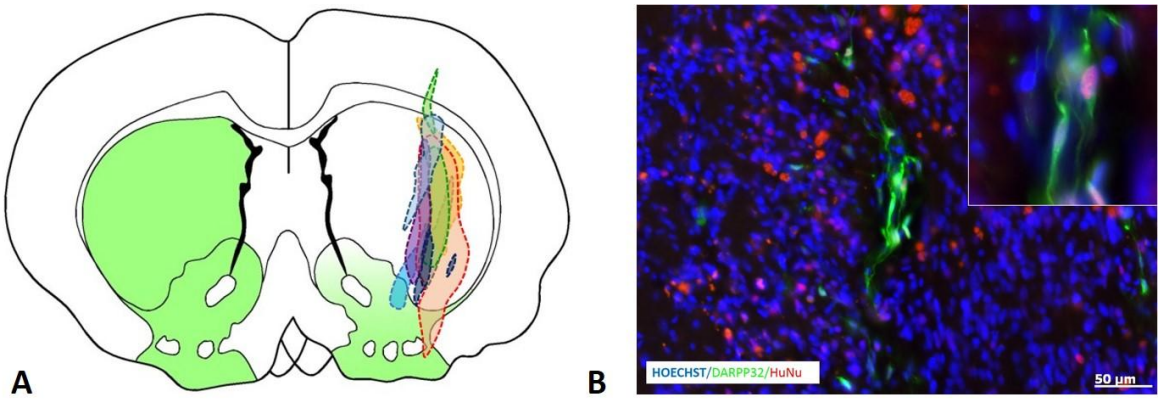

Figure 4. Schematic of surviving grafts of human ES (H9) derived MSN like-cells post transplantation 7 weeks (N=7) (A). Surviving grafts were recognized by HuNu positive cells in the striatal area with absences of tumour formation or neural epithelial overgrowth. Immunofluorescence was performed on the brain sections, DARPP32 expressing cells revealed the presence of human ES (H9) derived MSNs *in vivo* (B). HuNu positive cells co-labelled with DARPP32-expressing cells indicated graft-derived MSNs.

In summary, we demonstrate that human ES (H9) cells can be differentiated towards MSNs phenotype using our revised protocol. This revised protocol was the one used (the same chemical combinations) in EBs-based differentiation presented in chapter 5. This suggested an efficient protocol which could be applied to various PSC lines in adapted culture conditions. Importantly, no tumour formation was identified at this stage (7 weeks) post transplantation. However, this is only a preliminary study, due to time constraints, and is ongoing with more animals waiting to be sacrificed and analyzed.

Appendix B

Materials and Suppliers

Materials	Suppliers	Location
Accutase	PAA Labs	Farnborough, Hampshire, UK
Activin A	R&D	
Advanced DMEM/F12	Gibco	Paisley, Scotland, UK
Agarose electrophoresis grade	Invitrogen	Paisley, USA
Age I	Promega	
AhD I	NEB	
Ampicillin	DIFCO	
Ascorbic acid		
B27	Gibco	Paisley, Scotland
BDNF	Peprotech	
bFGF	invitrogen	
Biotin-High Prime	Roche	
B-mercaptoethanol	Sigma	Poole, Dorset, UK
BSA	Sigma	
Cyclopamine	Calbiochem	Hull, UK
Difco™ LB AGAR	BD	Claix, France
Difco™ LB BROTH	BD	
Dispase Solution	STEMCELL technologies	
DKK1	R&D Systems	Abingdon, Oxfordshire, UK
DMEM/F12	Gibco	
DMSO	Sigma	Poole, Dorset, UK
DNase	Sigma	Poole, Dorset, UK
Dorsomorphin	Tocris	
EGF	Sigma	Poole, Dorset, UK
FCS	Gibco	Paisley, Scotland
FGF2	R&D Systems	

Materials	Suppliers	Location
FIAU	TCI	Tokyo, Japan
Fibronectin	Sigma	
Fugene®6 Transfection Ragent	Promega	
GDNF	Tocris	
Gelatin	Chemicon	Chandlers Ford, Southampton, UK
HBSS^{--} Solution	Gibco	Paisley, Scotland
Hoechst	Fisher	Loughborough, Leicestershire, UK
HyClone®	Thermo Scientific	USA
IMDM	Gibco	
Insulin	Sigma	
KSR	Gibco	
Laminin	Sigma	
L-Glutamine	Gibco	Paisley, Scotland
Lipid concentrate	Gibco	
Lipofectamine	Invitrogen	Paisley, USA
LookOut® Mycoplasma PCR detection kit	Sigma	Poole, Dorset, UK
Matrigel	BD	
MyTaq™	Bioline	
Neon™ transfection system	Invitrogen	Paisley, USA
Neurobasal	Gibco	
NGS	Dako	Glostrup, Denmark
Noggin	R&D	
Non-essential amino acids (MEM)	Gibco	
Nuclease free water	Ambion	
Opti-MEM® I reduce serum	Invitrogen	
Paraformaldehyde	Fisher Scientific	
PBS	Gibco	
pcDNA3.1(+)/myc-HisA	Invitrogen	

Materials	Suppliers	Location
PD0325901	Sigma	
pDsRed-Express-N1	Clonetech	
Penicillin Streptomycin	Gibco	Paisley, Scotland
Plasmid Mini-prep	Qiagen	
PLL	Sigma	Poole, Dorset, UK
Primate ES Cell medium	ReproCELL	Japan
Proteinase K	Gibco	
PSF	Gibco	
Purmorphamine	Calbiochem	
QIAquick Gel Extraction Kit	Qiagen	
QIAquick PCR Purification Kit	Qiagen	
QIAprep Spin Miniprep Kit	Qiagen	
RA	Sigma	
SafeView	Biolabs	
SB431542	Tocris	
SHH	R&D	
SK-4700 Kit	Vector® SG	
SOC media	Invitrogen	Paisley, USA
SuperScript™ II Reverse Transcriptase	invitrogen	
SYBR Green	Bioline	
TOP10	Invitrogen	Paisley, USA
Transferrin	Sigma	
Tryphan blue	Sigma	
Trypsin	Worthington Biochemical Corporation	Freehold, New Jersey, USA
Trypsin/EDTA	Gibco	
Trypsin inhibitor	Sigma	
β-mercaptoethanol	Sigma	Gillingham, Dorset, UK
1 kb DNA Ladder	Biolabs	
10X BSA	Promega	
100 bp DNA Ladder	Biolabs	

Appendix C

Antibodies for immunofluorescence

Primary antibody	Isotope	Clonal Type	Concentration	Supplier	Code
1. Sox2	IgG	Rabbit	1:100	abcam	ab97959
2. PAX6	IgG	Rabbit	1:500	abcam	ab5790
3. Nestin	IgG	Rabbit	1:1000	Millipore	MAB5922
4. ZO-1	IgG1	Mouse	1:200-1:500	BD Bioscience	BD610966
5. FoxP1	IgG	Rabbit	1:500	abcam	ab16645
6. FoxP2	IgG	Rabbit	1:500	abcam	ab16046
7. Ctip2	IgG	Rat	1:200-1:500	abcam	ab18465
8. TTF1	IgG	Rabbit	1:200	abcam	ab40880
9. Islet1	IgG	Rabbit	1:200	abcam	ab20670
10. GSH2	IgG	Rabbit	1:200	abcam	ab26255
11. β-III tubullin	-	Rabbit	1:1000	Sigma	T2200
12. MAP2ab	IgG1	Mouse	1:200	abcam	ab36447
13. Dlx1	IgG2a	Mouse	1:200-1:500	abcam	ab54668
14. Dlx2	IgG	Rabbit	1:200-1:500	abcam	ab18188
15. DARPP32	IgG	Rabbit	1:200	Santa Cruz	SC11365
16. hDARPP32	IgG	Rabbit	1:1000	abcam	ab40802
17. FoxP1	IgG2a	Mouse	1:200-1:500	abcam	ab32010
18. Synaptophysin	IgG1	Mouse	1:100	abcam	ab8049
19. PSD95	IgG	Rabbit	1:100	abcam	ab18258
20. GFAP	IgG2b	Mouse	1:1000	abcam	ab10062
21. Otx2	-	Rabbit	1:500	Millipore	MAB9566
22. GABA	IgG	Rabbit	1:200-1:500	abcam	ab9446
23. Ki67	IgG1	Mouse	1:500	Dako	M7240
24. HuNu	IgG1	Rabbit	1:500	Millipore	MAB1281
25. β-III tubullin	IgG1	Mouse	1:1000	Sigma	T9026
26. GFAP	IgG	Rabbit	1:1000	Dako	ZO334
27. Oct4	IgG	Rabbit	1:1000	abcam	ab18976
28. Tra-1-60	IgM	Rabbit	1:1000	abcam	ab16288
29. Nanog	IgG	Rabbit	1:500-1:1000	abcam	ab80892
30. SSEA4	IgG3	Mouse	1:500-1:1000	abcam	ab16287
31. AFP	IgG1	Mouse	1:500-1:1000	Santa Cruz	SC166335
32. SMA	IgG2a	Mouse	1:500-1:1000	abcam	ab7817
33. Vimentin	IgG2a	Mouse	1:500-1:1000	DAKO	M7020

Appendix D

Solutions

1. **Culture Media:**
- Dulbecco's modified eagle medium (Standard Medium) 500 ml
- 1% PSF (Penicillin, Streptomycin, and Fungizone) 5 ml

2. **Neural Differentiation Media:**
- DMEM/F12
- 1% PS 50 ml
- 1% Fetal Calf Serum (FCS) 500 µl
- 2% B27 1 ml

3. **MEF Media: expansion (4°C)**
- DMEM 450 ml
- FBS(Fetal Bovine Serum) 50 ml
- Penicillin or Streptomycin 5 ml
- L-Glutamine 5 ml

Mix thoroughly, expiry date within one month from formulation

4. **MEF Media: derivation (4°C)**
- DMEM 450 ml
- FBS(Fetal Bovine Serum) 50 ml
- Antibiotic, Antimycotic or MYKOKILL 5 ml
- L-Glutamine 5 ml

Mix thoroughly, expiry date within one month from formulation

5. **MEF Freezing Media (4°C)**
- MEF media (expansion) 45 ml
- DMSO 5 ml

Mix thoroughly, expiry date within one month from formulation

6. **Trypsin solution:**
- 0.1% Trypsin
- 0.05% DNase
- HBSS

7. **DNase solution:**
- 0.05% DNase
- Dissection medium

8. **Phosphate Buffered Saline (PBS):**
- Sodium Chloride ($NaCl_2$) 8.5 gm
- Dihydrogen Sodium Phosphate 0.4 gm
- Disodium Hydrogen Phosphate 1 gm
- Distilled water up to 1,000 ml

The pH 7.4, was adjusted using Hydrochloric acid

9. TRIS-BORATE EDTA (5XTBE):
- Tris Base 54 gm
- Boric acid 27.5 gm
- EDTA (0.5M) 20 ml
- Distilled water up to 1,000 ml

Working concentration 0.5XTBE: 5XTBE 100 ml add distilled water up to 1,000 ml

10. 1% Agarose Gel (for 400 ml)
- Agarose powder 4 gm
- 0.5X TBE add up to 400 ml
- Put on microwave for 2 min and shake well until dissolved, keep in the oven

11. Formalin 4% (for 50 ml)
- 38%(V/W) ~ 40% Formalin 5 ml
- 1X PBS add up to 50 ml

12. Poly-L-Lysine (PLL)
- Aliquot Poly-L-Lysine 5 ml
- Add distilled water 45 ml

13. Proliferation Media
- DMEM/F12
- 1% PS 50 ml
- 2% B27 1 ml

Growth factor:
- FGE-2 20 ng/ml
- EGF 20 ng/ml

14. LB AGAR
- Difco LB AGAR 16 gm
- Add distilled water up to 400 ml
- Before use add Ampicillin 1:1,000 (400 µl), IPTG 1:1,000 (400 µl), and XGAL (Stock concentration 20 mg/ml, Working concentration 40 µg/ml) (800 µl)

15. Difco LB BROTH Medium
- Difco LB Broth Medium 16 gm
- Add distilled water up to 400 ml
- Before use: add Ampicillin 1:1,000 (400 µl)

16. Human ES cell culture medium
- Knock out DMEM 160 ml
- Knock out serum replacement 40 ml
- 2 ml L-Glutamine/β-mercaptoethanol solution
- 2 ml 100X non-essential amino acid solution
- 400 µl of 2 µg/ml bFGF stock
- Filter and store at 4°C and use within two weeks

17. Human basic FGF
- 0.1%BSA in PBS (without Ca^{+}, Mg^{++}) 5 ml
- Human bFGF 10 µg
- Aliquot into 400 µl lots and stored at -20°C

18. Collagenase IV solution
- Collagenase Type IV 50 mg
- DMEM/F12 50 ml
- Sterile with a 0.2 micron acetate filter and store at 4°C
- Use within two weeks

19. Cryopreservation Medium
- Defined FBS 6 ml
- hES cell culture medium 2 ml
- Filter sterile with a 50 ml filter unit and then add
- DMSO 2 ml
- Make the medium fresh and keep it on ice.

20. KSR medium
- K/O DMEM 87 ml
- K/O Serum Replacement 10 ml
- L-glutamine (200 mM) 1 ml
- Non-essential amino acid 1 ml
- B-mercaptoethanol (50 mM) 100 µl
- Penicillin/Streptomycin 1 ml

21. N2B27 with RA
- Advanced DMEM/F12 60 ml
- Neurobasal medium 30 ml
- N2 (1:150) 600 µl
- B27 with RA (1:150) 600 µl

22. N2B27 without RA
- Advanced DMEM/F12 60 ml
- Neurobasal medium 30 ml
- N2 (1:150) 600 µl
- B27 with RA (1:150) 600 µl

23. Human fifroblast medium
- MEM α medium+Glutamax 160 ml
- FBS 40 ml
- Non-essential amino acid 2 ml
- Penicillin/Streptomycin 2 ml
- Filter and store at 4˚C up to 1 month.

24. Tris non saline (TNS) Buffer
- TRIS 6.0 g.
- Distilled water 1 litre
- Adjust to pH 7.4 with HCl

25. Pre-wash (0.1 M PBS)
- Di- Sodium hydrogen phosphate (dehydrate) 18 g.
- Sodium chloride 9 g.
- Make up to 1 litre with distilled water

26. 1.5% Paraformaldehyde solution (PFA)
- Paraformaldehyde (granulated) 15 g.
- Make up to 1 litre with Pre-wash 1 litre
  (Dissolve with heat on the stirring (50-60°C) for 3 hours, then turn off the heat and leave stirring overnight at room temperature. Check the pH and adjust to pH 7.3 with either sodium hydroxide or orthophosphoric acid.)

27. 4.0% Paraformaldehyde solution (PFA)
- Paraformaldehyde (granulated) 200 g.
- Di- Sodium hydrogen phosphate (dehydrate) 90 g.
- Sodium chloride 45 g.
- Make up to 5 litre with distilled water
- (Dissolve with heat on the stirring (50-60°C) for 3 hours, then turn off the heat and leave stirring overnight at room temperature. Check the pH and adjust to pH 7.3 with either sodium hydroxide or orthophosphoric acid.)

28. Sucrose 25%
- Sucrose 250 g.
- Make up to 1 litre with Pre-wash, mix well and adjust pH to 7.3 if necessary.

29. DAB stock solution
- DAB 1 g.
- Mix with TNS 100 ml.
- Dissolve and divide into 2 ml aliquots in small bijou pots. Freeze the aliquots as quickly as possible after dissolving the DAB.

30. DAB solution
- DAB 20 mg.
- Buffer solution 40 ml.
- 30% Hydrogen peroxide 12 µl
- This solution can be diluted 2-5 times in TNS before use. This slows the reaction down without affecting the quality of the reaction.

31. Antifreeze Solution
- Di-sodium hydrogen orthophosphate 5.45 g.
- Sodium di-hydrogen orthophosphate 1.57 g.
- Distilled water 400 ml.
- Dissolve fully, adjust pH to 7.3-7.4 then add:
- Ethylene Glycol 300 ml.
- Glycerol 300 ml.
- Store solution in the fridge